A PHOTOCHEMICAL STUDY OF CRYSTALLINE DIBENZOBARRELENE DIESTERS: THE DI-π-METHANE PHOTOREARRANGEMENT IN THE SOLID STATE.

By

Miguel Angel García Garibay

B.Sc., Universidad Michoacana, Mexico, 1982

A THESIS SUBMITTED IN PARTIAL FULFILMENT OF

THE REQUIREMENTS FOR THE DEGREE OF

DOCTOR OF PHILOSOPHY

in

THE FACULTY OF GRADUATE STUDIES

(DEPARTMENT OF CHEMISTRY)

We accept this thesis as conforming

to the required standard

THE UNIVERSITY OF BRITISH COLUMBIA

October 1988

© Miguel Angel García Garibay, 1988

In presenting this thesis in partial fulfilment of the requirements for an advanced degree at the University of British Columbia, I agree that the Library shall make it freely available for reference and study. I further agree that permission for extensive copying of this thesis for scholarly purposes may be granted by the head of my department or by his or her representatives. It is understood that copying or publication of this thesis for financial gain shall not be allowed without my written permission.

Department of CHEMISTRY

The University of British Columbia
Vancouver, Canada

Date Dec 1, 1988

DE-6 (2/88)

ABSTRACT

The di-π-methane photorearrangement has been investigated for the first time in the solid state. A series of symmetric ($-CO_2R_1 = -CO_2R_2$) and mixed ($-CO_2R_1 \neq -CO_2R_2$) 11,12-dibenzobarrelene diesters, used as the model substrates, reacted in the solid state with efficiencies that are similar to those observed in solution.

Photolysis of symmetric diesters in solution and in the solid state gave a single dibenzosemibullvalene photoproduct. Two diesters ($R_1 = R_2 =$ Et and $R_1 = R_2 =$ iPr) turned out to be dimorphic with one of their crystal modifications having the chiral space group $P2_12_12_1$. Photolysis of the chiral crystals resulted in absolute asymmetric syntheses with quantitative (iPr) and near quantitative (80%, Et) enantiomeric yields. The absolute configuration of the starting material and photoproduct was obtained in the case of the isopropyl compounds by X-ray anomalous dispersion analysis. The stereochemical correlation and the X-ray crystallographic results indicated an extremely high stereoselectivity where only one of the four degenerate solution pathways seems to be followed in the solid state.

Mixed diesters gave upon photolysis two regioisomeric photoproducts that formed in nearly equal amounts in solution media. The solid state regioselectivity varied from moderate to high with no apparent correlation between the nature of the ester substituent and the photochemical results. X-ray structural information was used to analyze the effect of the ene-dioate conformation on the solid state regioselectivity. The radical delocalizing ability of the carbonyl groups, which is expected to depend

on the degree of conjugation with the central vinyl bond, does not seem to play an important role in determining the solid state results. An excellent correlation was found between solid state steric factors and the photochemical results. In general, the reaction occurred at the least tightly packed vinyl carbon.

Chiral dibenzobarrelene diesters containing sec-butyl groups were studied in optically active and racemic forms. Crystals of the sec-butyl/isopropyl compound were found to form a solid solution of the enantiomers that is isomorphous with the chiral crystals of the diisopropyl compound. A third example of absolute asymmetric synthesis in the solid state was discovered when photolysis of the racemate generated optically active products with very high enantiomeric yields. Photochemical and spectroscopic results from the methyl/sec-butyl compound indicated a second example of solid solution of the enantiomers, but this time with a racemic space group. Lack of diastereoslectivity in the solid state reaction of the latter compound was rationalized in terms of efficient steric control in the solid state reaction but inefficient steric control during the crystallization process.

An unusual solid state luminescence of the 11,12-diesters was noted and analyzed in terms of the biradical intermediates postulated along the di-π-methane rearrangement pathway. Finally, the solution and solid state photochemical results from dibenzobarrelenes bearing an ester group at the bridgehead position are analyzed.

TABLE OF CONTENTS

page

ABSTRACT ii

LIST OF TABLES ix

LIST OF FIGURES xi

ACKNOWLEDGMENTS xix

INTRODUCTION 1

The Topochemical Postulate 2

Solid State Chemical Reactivity 5

1. Number of Components 6

2. Thermodynamic Factors 11

3. Kinetic Requirements 13

Photochemical Reactions in Molecular Crystals . . . 20

Excited State Partitioning 22

The Di-π-Methane Rearrangement 26

The Regioselectivity of the Di-π-Methane Rearrangement 32

Objectives of Present Research and Outline of the Thesis 34

RESULTS AND DISCUSSION 41

Preparation of Substrates 42

11,12-Dibenzobarrelene Diesters 42

10,11- and 9,11-Dibenzobarrelene Diesters 46

PART I. THE DI-π-METHANE REARRANGEMENT IN THE SOLID STATE 49

On the True Solid State Nature of the Rearrangement 52

The Limiting Conversion on the Solid State Reaction of Diester Me/Me-**18** 55

Perturbations of the Excited State Decay Channels of Crystalline **18** by Accumulation of Photoproduct 56

a) Luminescence Measurements 60

b) Conversion Dependence of the Relative Quantum Yields of Reaction of **18** 64

Mechanical Effects and Limiting Conversion . . . 67

The Crystal and Molecular Structure of Diester **18** 70

PART II. STUDIES ON SYMMETRIC DIBENZOBARRELENE DIESTERS 72

Photochemistry in Solution 74

Photochemistry in the Solid State 75

The Solid State Molecular Structures of the Diethyl Diester **21** 75

The Solid State Molecular Structure of the Di-n-Propyl Diester **22** 79

The Solid State Molecular Structure of the Diisopropyl Diester **23** 80

Conformational Polymorphism 83

Spectral Differences Between the Dimorphs of Diesters Et/Et-**21** and iPr/iPr-**23** 85

Diethyl Diester **21**
1) Solid State FTIR Spectra 85

2) Solid State CPMAS ^{13}C NMR Spectra 89

Diisopropyl Diester **23**

1) Solid State FTIR Spectra 91

2) Solid State CPMAS ^{13}C NMR Spectra 93

Differences in Reactivity between Dimorphs . . . 95

Molecular and Crystal Chirality 101

Absolute Asymmetric Synthesis 103

Asymmetric Synthesis by Reaction of Diethyl Ester **21** 108

Asymmetric Synthesis by Reaction of Diester **23** . . 111

Mechanistic Implications of the Solid State Asymmetric Synthesis 115

Correlation of the Absolute Stereochemistry of the Crystalline Diisopropyl Diester pro-(-)-**23** ($P2_12_12_1$ Form) and its Optically Pure Photoproduct (-)-Dibenzosemibullvalene **57** 116

Studies on the Spontaneous Resolution of Diester **23** 120

1) Enantiomorphism of Chiral Crystals of Diester **23** from Ethanol Solution 121

2) Enantiomorphism of Chiral Crystals of Diester **23** Grown from the Melt in Open Containers 123

3) Enantiomorphism in Crystals of Diester **23** Grown from the Melt in a Sealed Container . . . 124

4) Enantiomorphism in Crystals of Diester **23** Grown from the Melt in a Sealed Container (B) . . 125

PART III. THE REGIOSELECTIVITY OF THE DI-π-METHANE REARRANGEMENT IN THE SOLID STATE 129

Compounds Studied and Identification of Photoproduct Stereochemistry 129

Photolysis of Mixed Diesters in Solution and in the Solid State 140

Analysis of the Solution Regioselectivity 142

A Primary Steric Effect? 142

A Secondary Steric Effect? 147

The Regioselectivity in the Solid State 157

Stereoelectronic Factors in the Solid State 158

Solid State Primary Steric Effects.
Steric Compression 164

Regioselectivity in Chiral Crystals
of Diester iPr/iPr-23 172

The Solid State Results at Large 173

PART IV. STUDIES ON CHIRAL MIXED
DIESTERS 176

Photochemistry in Solution 178

Studies in the Solid State 186

Crystallization of Chiral Compounds 186

The Solid State Properties and Photochemistry
of Diester 42 195

Photochemistry of the Optically Pure
Crystalline Material 201

Photochemistry of the Racemate of Compound 42 . . 205

Asymmetric Synthesis by Solid State Reaction
of the Racemate of 42 206

Extent of Asymmetric Induction in Chiral
Crystals of the Racemate 209

On the Reaction Diastereoselectivity 211

The Solid State Properties and Photochemistry
of Diesters Me/sBu-31 217

The Solid State Properties and Photochemistry
of Diester 39 229

Concluding Remarks 229

PART V. LUMINESCENCE STUDIES ON THE DIMETHYL DIESTER **18** 232

General Observations 234

Observations at Different Temperatures 237

Excitation Spectrum of the Red-Emitting Species 238

Observations at Different Wavelengths 241

What is the Precursor of the Red-Emitting Species? 242

Is the RE Produced by an Impurity? 243

What is the RE Species? 248

The Identity of Species **X** and **Y** 256

PART VI STUDIES ON 9-SUBSTITUTED DIBENZOBARRELENES 265

Photolysis of Diester 10-iPr/11-Me-**44** 267

Photolysis of Diester 9-iPr/11-Me-**45** 279

EXPERIMENTAL 283

REFERENCES 348

LIST OF TABLES

Table	Caption	Page
I	Dibenzobarrelene Diesters Prepared by Stepwise Esterification of Diacid **19**	45
II	Analytical Photolysis of **18** in Solution and in the Solid State	54
III	Symmetrically Substituted Dibenzobarrelene Diesters	73
IV	Relative Reaction Efficiencies of Crystalline Dibenzobarrelene Diesters	96
V	Solid State Induced Optical Activity in Crystals of **21**	109
VI	Solid State Induced Optical Activity in Single Crystals of **23**	112
VII	Photolysis of Single Crystals of **23** from Batch 3	122
VIII	Photolysis of Chiral Crystals of **23** from Batch Melt I	123
IX	Photolysis of Chiral Crystals of **23** from Batch Melt II	124
X	Photolysis of Chiral Crystals of **23** from Batch Melt III	126
XI	Glc and ^{1}H NMR Results from Solution Photolysis of Mixed Dibenzobarrelene Diesters	132
XII	High Mass Fragmentation of the Dibenzosemibullvalene Diesters	139
XIII	Glc Analysis of the Photoproducts of Diesters Me/sBu-**31**, Et/sBu-**39** and iPr/sBu-**42**	179
XIV	Selected Fragment-Ions from Photoproducts of Diester **42**	181
XV	The ^{1}H NMR Resonances of H(8d) and H(4b) from Products of Diester iPr/sBu-**42** as a Function of Four Different Solvents	183

XVI Relative Yields Of Photoproducts from Diester iPr/sBu-**42** 184

XVII Lattice Parameters of $P2_12_12_1$ Crystals of Compounds **23**, (S)-(+)-**42** and (R,S)-**42** 198

XVIII Conformation of the Ene-Dioate System in Diesters **23**, (S)-(+)-**42** and (R,S)-**42** 199

XIX Melting Points of Mixed Crystals of Diester **42** . . . 200

XX Solid State Stereoselectivity from Compound **42** . . . 201

XXI Solid State Induced Optical Activity by Photolysis of Crystals of the Racemate of Diester **42** 208

XXII Relative Solid State Stereoselectivity from Crystals of Compound Me/sBu-**31** 219

XXIII Proposed Occupancies in the Isomorphous Crystal Structures of Diesters **30** and **31** (optically pure and Racemic) 228

XXIV Relative Solid State Stereoselectivity from Crystals of Compound Et/sBu-**39** 229

LIST OF FIGURES

Figure	Caption	Page
1	Examples of Compounds Displaying Different Solution and Solid State reactivity	1
2	The Polymorphic trans-Cinnamic Acids and their Solution and Solid State Reactivity	4
3	The Dimerization of Benzylidenecyclopentanone	8
4	An Example of a Solid State Chemical Reaction in an Inclusion Compound	10
5	Some Examples of Gas-Solid Reactions	11
6	Differences in the Reaction Coordinate between Solution and Solid State Reactivity	13
7	Differences in Number of Available States and Reaction Pathways Between Fluid Media and Solid State	16
8	Representation of: (a) Allowed and (b) Disallowed Solid State Reactions in the Reaction Cavity	18
9	Reaction Inhibition by Steric Compression Control	19
10	Jablonski Diagram	23
11	The Di-π-Methane Reaction Mechanism Represented in 1,4-Pentadiene and Allyl Benzene	27
12	The Multiplicity-Dependent Photochemistry of Barrelene	28
13	Examples of Substrates that Undergo Reactions Other than the Di-π-Methane Rearrangement from the Singlet Excited State	30
14	Dienes that Undergo Double Bond Isomerization Instead of the Di-π-Methane Rearrangement from The Triplet Excited State	31

15 Examples of Regioselective Di-π-Methane Rearrangements 33

16 The Di-π-Methane Rearrangement of Dibenzobarrelene Diesters 35

17 The four Di-π-Methane Systems in the Dibenzobarrelene Skeleton 37

18 Regioisomeric Products from "Mixed" Dibenzobarrelene Diesters 38

19 Di-π-Methane Rearrangement of 10,11- and 9,11-Dibenzobarrelene Diesters 40

20 Synthesis of Dibenzobarrelene Diesters by Diels-Alder Reaction 42

21 Acid Catalyzed Transesterification of Diester **18** . . . 43

22 Preparation of 9-Anthracenecarboxylate Derivatives . . 46

23 Preparation of 10,11- and 9,11-Dibenzobarrelene Diesters 47

24 Partial ^{1}H NMR of: (A) 10-Isopropyl-11-methyl- and (B) 9-Isopropyl-11-methyl-dibenzobarrelene Diesters 48

25 The Di-π-Methane Rearrangement of the Dimethyl Diester **18** 50

26 Derivatization of Partially Reacted Diester **18** with Diazomethane to Yield the Chromatographically Separable Adduct **53** 51

27 Photochemical Activation and Decay Processes Available to Crystals of Reactant **18** 59

28 Uncorrected Fluorescence and Phosphorescence Spectra of Polycrystalline **18** at 77K (a) Before and (b) After Irradiation with the Nitrogen Laser 63

29 Consumption of Diester **18** as a Function of Photolysis Time. Variations in the Reaction Quantum Yield as a Function of Conversion 66

30 Photographs of a Single Crystal of Diisopropyl Diester **23** (Pbca Modification) Before (top) and After Photolysis (bottom) 69

31 Stereoview of the Molecular Structure of the Dimethyl Diester **18** 71

32 Stereoviews of the Molecular Structures of the Diethyl Dibenzobarrelene Diester **21** in (a) the $P2_1/c$ and (b) $P2_12_12_1$ Modifications 78

33 Stereoview of the Molecular Structure of the Di-n-propyl Diester **22** (Space group P1) 79

34 Stereoviews of the Molecular Structures of the Diisopropyl Diester **23** in its (a) $P2_12_12_1$ and (b) Pbca Modifications 82

35 The Molecular Structure of Lepidopterane 83

36 Solid State FTIR Spectra of Diester Et/Et-**21** in its $P2_12_12_1$ (top) and $P2_1/c$ Modifications (bottom) . 86

37 CPMAS ^{13}C NMR Spectra of Et/Et-**21** in its (a) $P2_12_12_1$ and (b) $P2_1/c$ Modifications 90

38 Solid State FTIR Spectra of Diester **23** in its (A) $P2_12_12_1$ and (B) Pbca Modifications 92

39 CPMAS ^{13}C NMR Spectra of iPr/iPr-**23** in its (A) Pbca and (B) $P2_12_12_1$ Modifications 94

40 Solution and Solid State Photochemistry of Azobisisobutyronitrile 98

41 Solution and Solid State Photochemistry of α-adamantyl-p-chloro-acetophenone 99

42 The Four Reaction Pathways of Symmetrically Substituted Dibenzobarrelene Diesters 101

43 Solid State Photochemistry of Chiral Crystals of Pure and Mixed Aryl Butadienes 107

44 Asymmetric Synthesis by Reaction of Unsymmetrically Substituted Vinyl Diacrylates 107

45 The Four Non-Equivalent Protons in the Methylene Groups the Diethyl Dibenzosemibullvalene Diester **55** 110

46 Partial ^1H NMR Spectra (300 MHz) of Racemic (top) and Optically Active (bottom) Diester **57** after Addition of 1 eq of $Eu(hfc)_3$ 114

47 Absolute Configuration of Diester (-)-**57** 117

48 Sterodiagrams with Absolute Configuration of: (a) Diester **23** in pro-(-) Enatiomorph, (b) Local Environment of Diester **23** and (c) Diisopropyl Dibenzosemibullvalene (-)-**57** 118

49 Possible Reaction Pathways of Diester **23** that Account for the Observed Absolute Configuration . . . 119

50 Spontaneous Resolution of Ethyl-Allyl-Anilinium Iodide 127

51 Mixed Diesters Used in the Study of the Regioselectivity of the Di-π-Methane Rearrangement 129

52 Products from the Di-π-Methane Rearrangement of Mixed Dibenzobarrelene Diesters 131

53 Independent Synthesis of Photoproduct **63A** 133

54 ^{1}H NMR Spectra of Dibenzosemibullvalenes **63A** (top) and **63B** (bottom) 134

55 Stereospecific Electron Impact Induced Fragmentation of Dibenzosemibullvalene Diesters . . . 138

56 Comparison Between the Solution and Solid State Regioselectivity of Compounds **28** to **39** 141

57 Radical Center Stabilization by Bridgehead (R) Substituents in **BR-2** 143

58 The Involvement of a Primary Steric Effect on the Regioselectivity of the Di-π-Methane Rearrangement of 9-substituted Dibenzobarrelenes . . 145

59 Possible Relief of the Steric Interactions by Bond Formation at the Carbon Attached to the Bulkier Substituent 146

60 Variations of the Resonance Energy of an α,β-unsaturated Carbonyl System as a Function of the Torsion Angle (θ) Between the Mean Planes of Two π-Systems 148

61 The Triplet Excited State of Dibenzobarrelenes as a 1,2-Biradical 149

62 Free Radical Rearrangement of Dibenzobarrelenes . . . 150

63 Regioselectivity of Dibenzobarrelene Monoesters . . . 150

64 Effect of the Alkyl Substituents on the Carbonyl Absorption Frequency of Alkyl Benzoates 152

65 Gas Phase Conformation of Dibenzobarrelene Diesters Obtained from Molecular Mechanics (MMP2) . . 156

66 Stereoelectronic Effects of the Carbonyl Groups on the Predicted and Observed Regioselectivity from the Di-π-Methane Rearrangement of Some Dibenzobarrelene Diesters 160

67 Photochemical Differences between the Conjugated and Non-Conjugated Rotamers of Benzoyl Naphthobarrelene **73** 162

68 Displacement of the Vinyl-Attached Substituent During the Benzo-Vinyl Bridging Step on Vinyl Disubstituted Dibenzobarrelenes 165

69 Lattice Environment Around the Vinyl Substituents of the Diesters Me/iPr-**30** and Me/Ph-**37** 166

70 Simulation of the Aryl-Vinyl Bridging Step in the Di-π-Methane Rearrangement of Dibenzobarrelenes 169

71 Plots of the Change in Packing Potential Energy during the First Step of the Di-π-Methane Rearrangement of Dibenzobarrelenes Me/iPr-**30** and Me/Ph-**37** 171

72 Changes in the PPE during the First Step of the Di-π-Methane Rearrangement of Diester iPr/iPr-**23** . . 173

73 The Di-π-Methane Rearrangement of Chiral Mixed Diesters 177

74 Mass Spectrometric Fragmentation of the Photoproducts from Sec-butyl Containing Dibenzobarrelene Diesters 180

75 Regioselective Preparation of Dibenzosemibullvalenes **75I**/**75II** and **74I**/**74II** 182

76 Binary Phase Diagrams of (a) the Racemic Mixture, (b) the Racemic Compound and, (c) Solid Solutions (Mixed Crystals) of the Enantiomers 188

77 Solid Solution with Statistical Disorder 192

78 Solid Solution with Short Range Order 193

79 Solid Solution with Non-Statistical Inverse Symmetry Order 193

80 Solid State FTIR Spectra of Chiral $P2_12_12_1$ Crystals of Diester iPr/sBu-**42**: (a) Racemic and (b) Optically Active 196

81 Conversion of the Photoproducts from (S)-(+)-**42** into the Dimethyl Dibenzosemibullvalene (+)-**52** . . . 203

82 Formation of Dibenzosemibullvalenes **75I** and **75II** from (S)-(+)-**42** 204

83 Structural Possibilities for the Photoproducts from Diester (±)-sBu/iPr-**42** 206

84 ^{1}H NMR Spectra of Racemic (top) and Optically Active (bottom) Dibenzosemibullvalene **52** after Addition of 1 eq of $Eu(hfc)_3$ 210

85 The Four Modes of Isomorphous Replacement of Diester **23** by Diester **42** 213

86 Loss of Diastereomeric Control in the Product Stereochemistry by Means of Occupancy of the Same Chiral Lattice Site by Two Different Enantiomers . . 215

87 Loss of Regioisomeric Control by Means of Positional Disorder in the Crystal Lattice of (R,S)-**42** 216

87A Solid State FTIR Spectra of (a) Racemic and (b) Optically Pure Diester Me/sBu-**31** 218

88 Hypothetical Reaction of Diester **31** to Give the Two Diastereomers **64A** as a Result of a Lack of Lattice Control on the Face-Selectivity of the Rearrangement 220

89 Hypothetical Reaction of One Enantiomer of **31** at Two Enantiomeric Crystal Lattice Sites 222

90 Hypothetical Reaction of Two Enantiomers at Two Enantiomeric Crystal Sites 223

91 Reaction of Two Enantiomers at Equivalent Reaction Sites Through Equivalent Reaction Pathways 224

92 Comparison between (R)- and (S)-**31** in Order to Determine their Coefficient of Geometrical Similarity (ϵ) 227

93 Asymmetric Synthesis in Crystals of Vinyl Diacryates **76** 231

94 Uncorrected Emission of Crystals of Diester Me/Me-**18** Irradiated at 337 nm 236

95 Corrected Excitation Spectrum of the Red-Emitting Species (**X**) in Crystalline Samples of Diester **18** . . 240

96 Possible Formation Pathways for the Red-Emitting Species **X** and Biphotonic Mechanism for the Appearance of the Red-Emission 243

97 Fluorescence Excitation (a) and Emission (b) of Anthracene Impurity in Crystals of Diester Me/Me-**18** 245

98 Formation of Anthracene Sandwich Pairs and their Red Excimer Emission 246

99 Hypothetical Formation of Anthracene Red Excimer Emission in Crystals of Diester **18** 247

100 Thermal Decay of the Red-Emitting Species and Appearance of New Species **Y** 249

101 Luminescence Excitation (a) and Emission (b) Spectra of Species **Y** 250

102 Singlet State Reactivity of Dibenzobarrelenes . . . 252

103 The Di-π-Methane Rearrangement as a Possible Explanation for the Luminescence of Crystalline Dibenzobarrelene Diesters 254

104 The Intermediates in the Di-π-Methane Rearrangement of Naphthobarrelene **73** 257

105 The Two Radical Fragments of **BR-1** 259

106 (a) The Neophyl Rearrangement of the Spiro-cyclooctadienyl Radical **87-R** and (b) Absorption Spectrum of **87-R** 261

107 (a) Comparison between **BR-2** and the Benzyl Radical, (b) Structure of the Dibezocycloheptadienyl Radical **88**, and (c) Excitation and Emission Spectra of the Benzyl Radical 263

108 Photochemistry of Dibenzobarrelene Monoesters . . . 265

109 Photochemistry of 9-Carbomethoxy-Dibenzobarrelenes . 266

110 The 10,11- and 9,11-Dibenzobarrelene Diesters **44** and **45** 267

111 Photochemistry of Diester **44** 269

112 Stern-Volmer Plot for Diester **44** 271

113 Dibenzobarrelenes That Display Singlet State Reactivity 274

114 Stereoviews of the Packing Diagram and Molecular Structure of Diester **44** 278

115 Reaction of Diester **45** 280

116 Stereoview of the Molecular and Packing Structures of Diester **45** 282

ACKNOWLEDGEMENTS

I would like to express my most sincere thanks to Professor John Scheffer for his valuable guidance and tremendous support throughout the progress of the present work. He does not spare interest and advice that go well beyond chemistry and I have been very fortunate to learn from such an enthusiastic and knowledgeable man.

Lab 346 has been a place of wonderful learning and sharing experiences. I will always be indebted to the members of the group, past and present, for keeping such a fresh and friendly environment. Phani Raj Pokkuluri and Graham Rattray deserve special thanks as they proofread the entire manuscript. Thanks are also due to Professor J. Trotter and the members of his group for all their assistance and continuous advice. I am specially grateful to Fred Wireko who did all the crystallographic work reported in this thesis.

Financial support from the University of British Columbia in the form of a University Graduate Fellowship is also gratefully acknowledged.

Last but not least I would like to say: gracias a Mama, Papa, los Garcia Garibay y anexas por haberme dado tanto apoyo. Los Mendoza han sido un gran ejemplo que siempre apreciare. Gracias a Bety y a Ingrid por ser fuente de continuo amor e inspiracion.

INTRODUCTION.

The study of organic chemical reactions in crystalline solids is a rapidly developing area of organic chemistry.[1] It is now recognized that molecular crystals can modify the "intrinsic" or solution phase chemical reactivity in a manner that depends deeply on the structural properties of the crystal. Many examples are known of reactions that occur in a completely different manner when carried out in solution or in the solid state. A set of representative examples where these differences can be illustrated is shown in Figure 1 below.

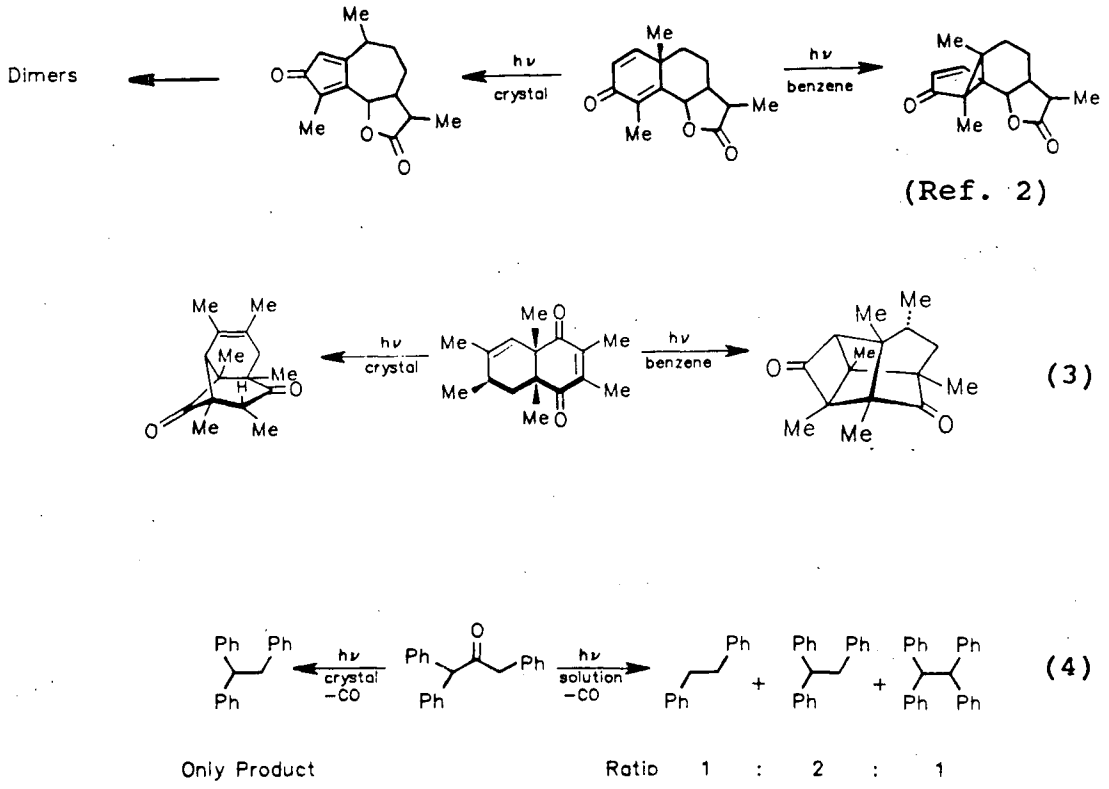

Figure 1. Examples of Compounds Displaying Different Solution and Solid State Reactivity.

Solid state organic chemistry is an area that very closely reflects the understanding that organic chemists have of the structural details of the mechanistic aspects of organic chemistry and of the nature and properties of molecular crystals. It is for these reasons that some of the most impressive demonstrations of the scope of solid state organic chemistry have been discovered only during the last twenty five years.[1]

It has been speculated[1d] that Wohler in 1828 may have been the first scientist to study an organic solid state chemical reaction while synthesizing urea from solid ammonium cyanate.[5] Sporadic reports of organic solid state reactivity can be found throughout the literature with a period of increased activity during the late nineteenth and early twentieth centuries.[6] It seems that at these times the experimental and conceptual difficulties in studying chemical reactivity in the liquid, gas and solid states might have been comparable. Practical considerations and stronger theoretical models, however, led to a gap between the understanding of solution and gas phase reactivities on the one hand and solid state reactivity on the other. Fluid phase organic chemists, the immense majority, took the responsibility for developing the experimental, analytical and theoretical aspects of the field.

The Topochemical Postulate.[7]

In the early 1960s X-ray crystallography had been firmly established as the most important solid state analytical tool and many structural concepts were developed therefrom. The crystalline state had become the

preferred medium for structural studies, whereas much accumulated experience maintained the liquid state as the primary medium for the study of organic chemical reactivity. It was at that time that Gerhard Schmidt executed a brilliant idea he probably conceived during the mid 1940s.[7] Schmidt restudied some of the solid state reactions known since the last century, especially the photochemical ones, with the application of X-ray analytical techniques.[1a] By studying primarily the $2\pi + 2\pi$ cyclodimerization of many crystalline olefins, Schmidt put on a firm basis the most general and intuitive concept evolved in the early days of solid state organic chemistry, the topochemical postulate.

The topochemical postulate as first enunciated by Kohlschutter[8] in 1918 stated that reactions in solids are controlled by the three dimensional arrangement of the molecules in the crystals. Schmidt put the topochemical postulate on a strong experimental basis and refined it by stating that reactions in crystals occur with a minimum of atomic and molecular motion.[9] Schmidt recognized that one of the implications of the postulate is that solid state reactions are controlled by the relatively fixed distances and orientations between the potentially reacting centers.[9] The behavior of the different crystal forms of trans cinnamic acids towards photochemical dimerization served him to illustrate these points in the most elegant manner[10] (Figure 2).

The trans cinnamic acids (1) crystallize in one of three different crystal modifications known as α, β and γ. A fundamental difference between the three types of packing is given by the manner in which molecular pairs can be related (Figure 2). The key finding in Schmidt's study was that this intermolecular geometry determines not only the

absence or presence of reactivity but also the product stereochemistry.[10] The centrosymmetric intermolecular arrangement in the α type led to the centrosymmetric α-truxilic acids (2). The parallel translational arrangement shown to exist in the β form gave the mirror-symmetric β-truxinic acids (3) and finally the γ form, characterized by a long translational axis and a poorly overlapped arrangement between the two double bonds, was found to be unreactive. Interestingly, trans-cinnamic acid in solution simply undergoes trans-to-cis isomerization.

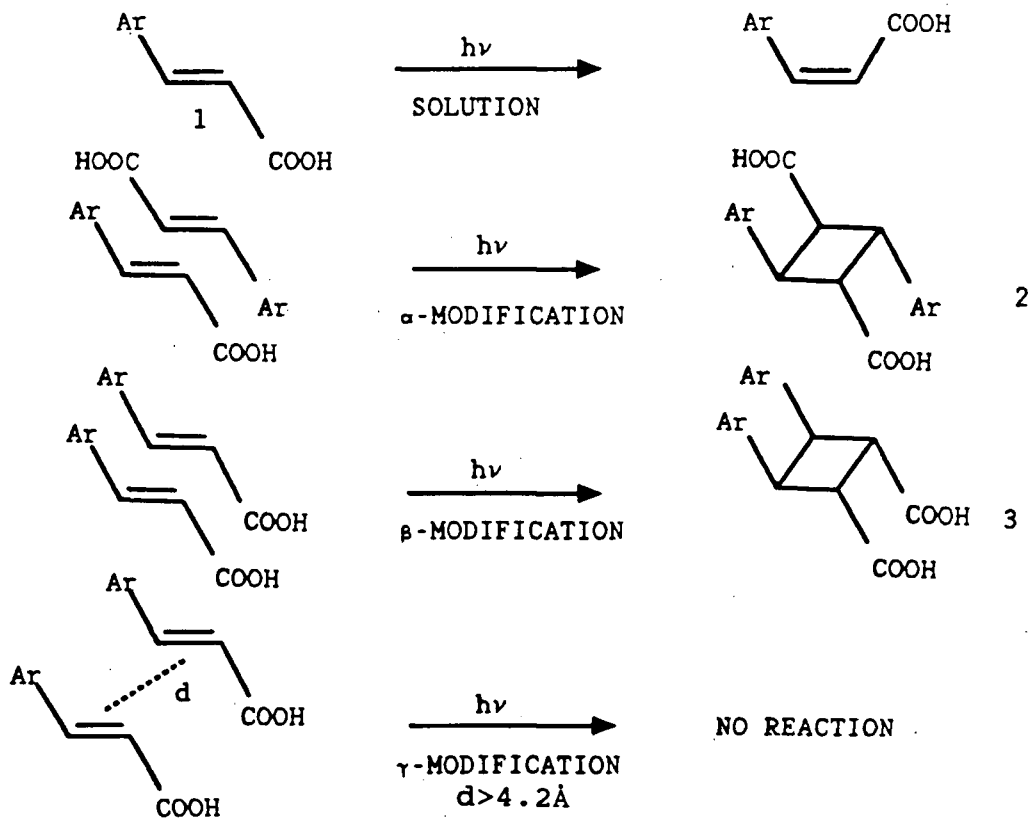

Figure 2. The Polymorphic trans-Cinnamic Acids and their Solution and Solid State Reactivity.

The results obtained with the cinnamic acids and other olefinic compounds led Schmidt to suggest that for each reaction type there should exist an upper limit beyond which reaction can no longer occur.[1a] In the case of the cinnamic acids it was found that the center-to-center distance between the two reacting olefinic double bonds of the α and β modification was within 3.6 to 4.1 Å. Schmidt suggested that a distance shorter than approximately 4.2 Å and a parallel arrangement between the reacting double bonds was required for $2\pi + 2\pi$ dimerization to occur. These requirements are not fulfilled by the unreactive γ-modification, which has center-to-center distances between 4.7 and 5.1 Å and non-parallel olefin arrangements. Despite some apparent exceptions,[1b] Schmidt's proposals have been often cited with the authority of a fundamental law of nature.

Solid State Chemical Reactivity.

In spite of the early reports of solid state reactivity, the crystalline phase of organic compounds was for a long time considered nothing more than a convenient resort for easy handling and purification. The concept that molecular freedom was a prerequisite for chemical reactivity evolved from studies in fluid media and led to the intuitively incorrect concept that all organic solids should be unreactive.[11] While unreactivity may be common to many crystalline compounds, it is far from being a general phenomenon. The most interesting aspects of solid state reactivity come from the fact that reactions occur under conditions where most molecular motions are disallowed.[8,9] Topochemical

reactions tend to occur through a continuous structural similarity between the reactants, intermediates and products. Large amounts of mechanistic information can sometimes be inferred from the X-ray structures of the reactants.[1]

It is known that three general factors will determine the chemical reactivity to be observed in a given system.[12] These factors relate to: 1) the number of components present in the reaction medium, 2) the thermodynamic factors determined by the free energy changes involved during the reaction, and, 3) the kinetic factors determined by the free energy of the transition states. Due to the restricted composition and to the rigid and ordered molecular arrangement present in the crystalline state, the above factors play their roles in a different manner in the solid state and in isotropic solution media.

1. Number of Components.

The first and main limitation to the general occurrence of solid state reactivity relates to the number of components allowed in the reaction medium. While the number of components in a solution reaction is only seldom limited by solubility problems, it is known that homogeneous crystalline phases are rarely composed of more than one component. Most solid state reactions, whether unimolecular or bimolecular, are expected to be homomolecular. At the present time most solid state research work is carried out in molecular crystals with a single component. It seems, however, that the impact that solid state chemistry will have on other areas will depend largely on our ability to

manipulate multicomponent crystalline samples. Fortunately, additional reaction components can be considered in some circumstances.[13-16] These situations may occur and have sometimes been used with advantage in the case of mixed molecular crystals.[13] Substitutional solid solutions and molecular complexes (also called molecular compounds, intermetallic compounds and chemical compounds) are the most important cases to consider.

Substitutional solid solutions are characterized by incorporation of foreign "solute" molecules into the spaces otherwise reserved for the molecules of the "solvent" crystal.[13] The solubility that two organic compounds can display in the solid state can range from no solubility at all to the much rarer cases of continuous solubility. The importance of solid solubility between different reactants is easy to recognize but difficult to bring into practice. A large amount of chemical and structural information could also be obtained by having a compound reacting while dissolved in several different crystalline environments. It should also be recognized that a partially reacted crystal is a mixed crystal. The solubility that the product will display in the crystal lattice of the starting material will determine the extent of conversion and the integrity of the crystal lattice as a function of reaction progress.[17] Reactions where a sample preserves its crystallinity during the entire conversion of starting material into product are called <u>topotactic</u> or single crystal-to-single crystal transformations.[18] These reactions are characterized by a remarkable structural similarity between the reactants and the products, which allows for continuous solid solubility. Topotactic transformations offer the possibility of

monitoring the reaction through X-ray crystallography. Few examples of topotactic reactions are known. One the best studied systems is represented by the benzylidenecyclopentanones (4) and their photodimers (5) studied by Jones and Thomas[19] (Figure 3). The structural similarity between the two symmetry related monomers and the centrosymmetric dimer is evident in the same figure.

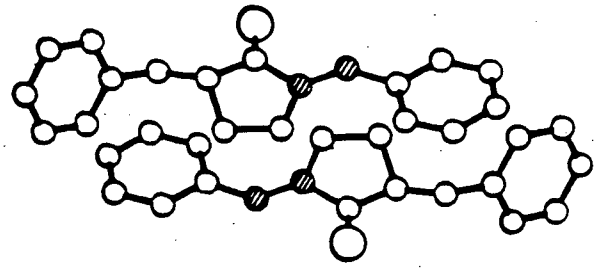

4

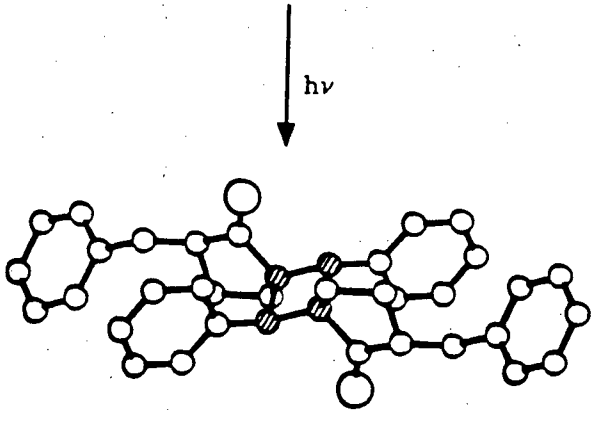

5

Figure 3. The Dimerization of Benzylidenecyclopentanone.

Some of the most interesting two component solid systems, the molecular complexes,[13-16] are primarily classified[13] according to the forces responsible for their existence as: i) electron transfer complexes, and, ii) packing complexes. Included in the second category, (also called guest-host complexes) are some of the multicomponent solid state systems currently under more active investigation. Clathrates[14] and inclusion compounds with intermolecular and intramolecular cavities[13,15,16] belong to this category. Very often, however, the host components play a passive, organizing role, and do not participate in the chemical reactivity of the included compounds or solutes. Exceptions to this have been found in the photochemical reactivity of deoxycholic acid-ketone complexes[20] (Figure 4). When the complexes are photolyzed for long periods of time a hydrogen is abstracted from the deoxycholic acid host by the photoexcited ketone guest. A radical pair is formed which then collapses to form an aryl derivatized steroid[20] (Figure 4).

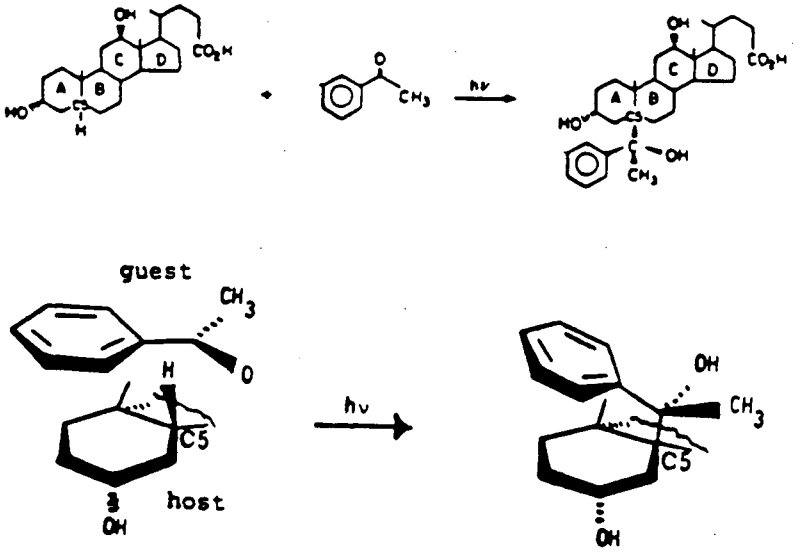

Figure 4. An example of a Solid State Chemical Reaction in an Inclusion Compound.

Additional reagents can also sometimes be considered for solid state reactions when they are allowed to diffuse into the crystal lattice.[21] This is precisely the case for some known gas-solid reactions where diffusion is, however, severely limited to relatively small molecules (Br_2, O_2, CO_2, NH_3, etc.).[21-22] Some interesting examples falling in this category are shown in Figure 5.

Other heterogeneous reactions may take place at crystal surfaces, and several gas-solid,[23] liquid-solid[24] and solid-solid[25] reactions are known.

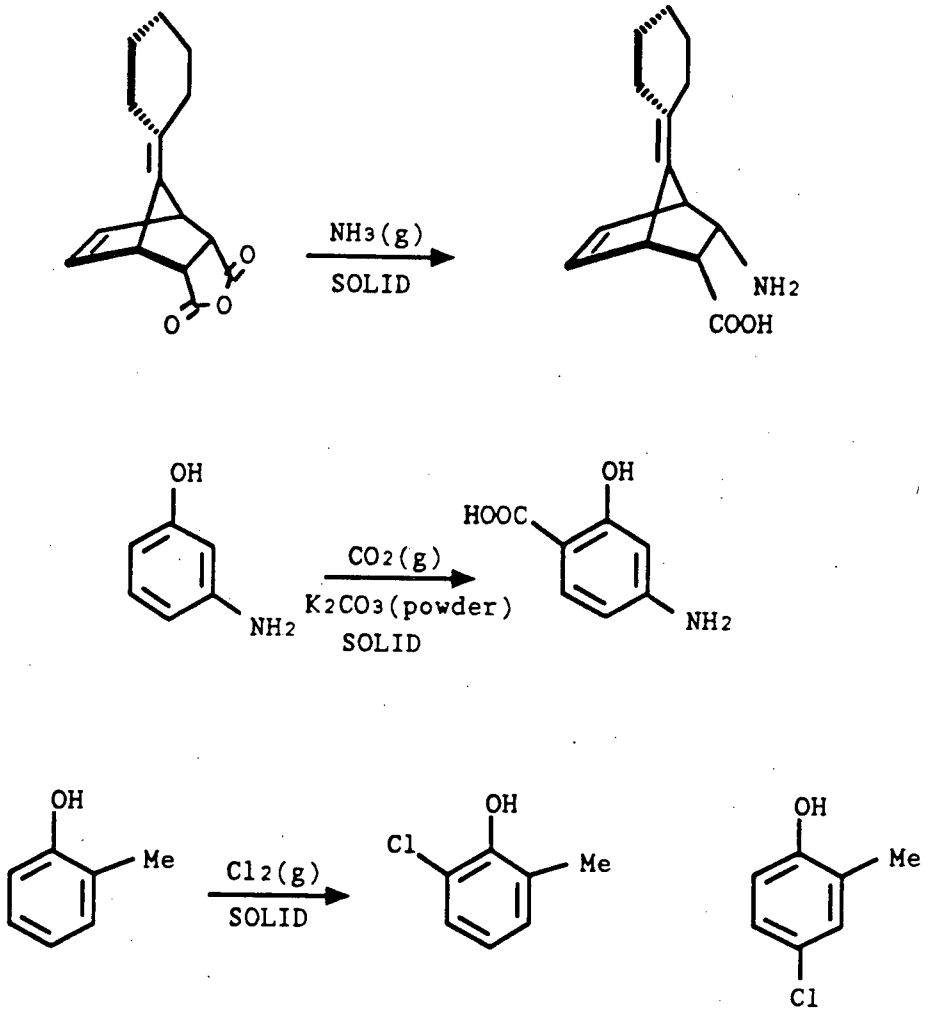

Figure 5. Some Examples of Gas-Solid Reactions.[26-28]

2. Thermodynamic Factors.

It has been recently argued by S.K. Kearsley[29] that solid state reactions, in general, are not as thermodynamically viable as reactions in fluid media. Kearsley suggested that the enthalpies of the initial and final states of a solid state reaction are respectively lower and

higher with respect to values observed in fluid solution media (Figure 6). The lower energy in the initial state of solid state reactions can be understood as arising from the additional stabilization energy gained by the molecules in the crystallization process.[30] It is known that organic compounds tend to crystallize in their minimum energy conformations[31] and with the most favorable intermolecular arrangement. In the final state, the higher enthalpy of the solid state reactions comes from the energy required by the product molecules to adjust into the rigid environment of the starting material.[32] Perturbations to and from the medium are expected to play a very important role. First of all, the formation of a product molecule in the space that was originally occupied by and tailor made for the starting material will be the source of additional energy to the final state. The larger the structural difference between reactant and product the more energy would be required to locate the product in the space otherwise reserved for the starting material. This energy increase can be identified with the steric energy arising from unfavorable product-lattice interactions and is undoubtedly a source of internal stress.[33] It is known that the mechanical relaxation that follows this stress may play a very important role in determining the integrity of the lattice at the later stages of the reaction.[33]

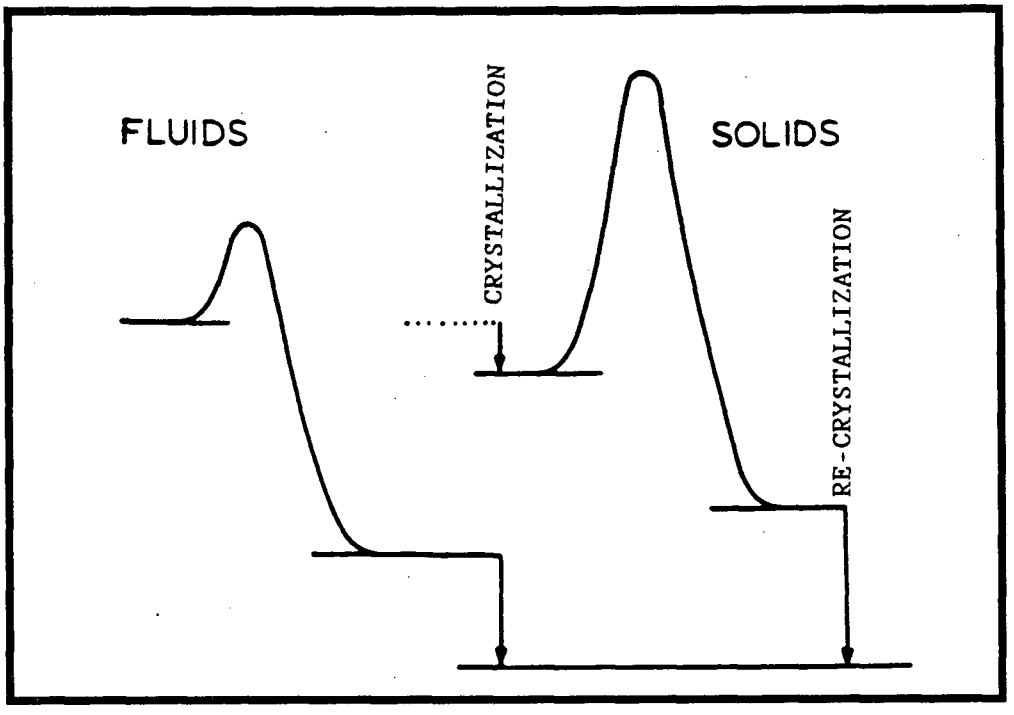

Figure 6. Difference in the Reaction Coordinate Between Solution and Solid State Reactivity (From Reference 29).

3. Kinetic Requirements.

The kinetic requirements for a reaction to occur refer to the necessity for part of the reactants to acquire the free energy of activation required to overcome the energetic barriers that separate the starting materials and the products along the reaction coordinate.[12] The

kinetic barriers of solution and gas phase reactions are mainly determined by the high enthalpic and low entropic contents of the species defined by the transition state, or activated complex. It seems reasonable that the enthalpy of the transition state, as shown in Figure 6, should also be higher in the solid than in the fluid states.[29] This is expected because the rigid environment of molecular crystals will resist the motions required to reach the transition state more than the solution environment would. At the same time the structure of the activated complex should be accommodated in a restricted space to which it does not ideally belong to. A critical difference between the two media, that may sometimes favor solid state versus solution reactivity, concerns to the entropy of activation. The entropy of activation is the entropy difference between the transition state and the reactants.[12]

The reactants in the fluid media exist in a large number of dynamically equilibrated states (n_i, Figure 7) defined by their molecular conformations, interactions with the solvent, vibrational states, etc. The large number of energetically different (and degenerate) alternatives given to the reactants makes their entropy content very large. If E_i is the energy of the state n_i and P_i the fraction of the system with energy E_i we have that the entropy is given by:

$$S = k \, \Sigma P_i \ln P_i$$

where k is the Boltzmann constant and the summation is carried over all the states that describe the system.

Since most organic reactions occur through highly defined transition states, the number of different states ($n^{\neq}$) available to the activated complex will be very small. Many organic reactions, for instance, occur through only few well defined conformations, while the reactant has a much larger number of conformational states. Not only conformational properties, however, may determine the occurrence of a chemical reaction and the properties of an activated complex. Suppose that there are only two states for two different activated complexes, A and B, available to a given substrate. In fluid solution the number of different states, n_i, is very large compared to the number of states (two in Figure 7) possessing the requirements for reactions to occur. The two activated complexes $n^{\neq}_A$ and $n^{\neq}_B$ for reactions A and B respectively (Figure 7) can be reached through the starting material states n_1 and n_4 respectively. Due to the translational and vibrational freedom, there are many collisional and vibrational modes that may put the reactants in the configuration required for reaction ($n_1=n_2=n_3=$etc.). The probability for reaction, or ratio of productive to non-productive collisions or vibrations, can sometimes be very similar for many alternative reactions with the result that several reactions can simultaneously occur. Both reactions, A and B, as indicated schematically in Figure 7, would occur.

In the solid state, on the other hand, the reacting molecules exist already with a very low entropy. The molecules in the crystal will possess few vibrational and rotational modes while translation will normally not be allowed. We can illustrate this by representing only one state (n_4) for a reactant in the solid state. The molecules in the state n_4 will react, given enough enthalpy of activation, if there is a

large resemblance between the structure of the starting material and of the activated complex. In Figure 7, a reaction in the solid state would occur only through $n^{\neq}_{B}$ but not through $n^{\neq}_{A}$.

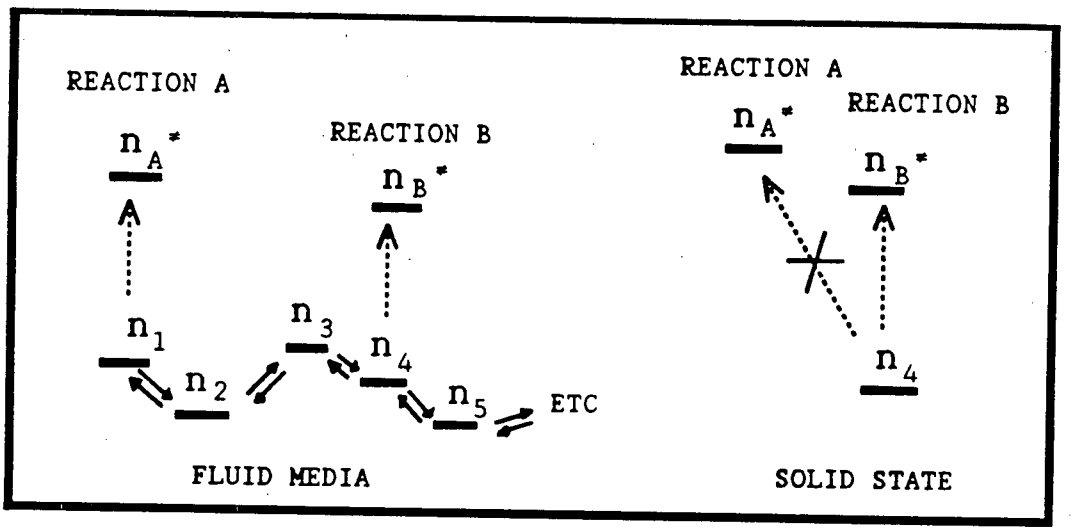

Figure 7. Differences in Number of Available States and Reaction Pathways Between Fluid Media and Solid State.

If the molecules participating in a given solid state reaction are not within the proper distance and orientation as suggested by the topochemical postulate, the energetic expense of bringing the reactants together would have to be paid with the destruction of the crystal

lattice itself. This can be appreciated if we realize that the estimated activation energy for the diffusion of anthracene in the anthracene crystal (42 Kcal/mol) is twice as large as the packing energy of the same compound as estimated from its sublimation energy (~22 Kcal/mol).[34]

Kinetic factors that differentiate liquid and solid state reactivity can operate after the reagents are found in a topochemically favorable orientation. In the liquid state the lifetimes of many intermediates (many reactions occur in more than one elementary step) are much longer than the time taken for reorganization of the solvent.[35] The time averaged environment for most solution reactions is therefore isotropic and essentially identical in all directions. In the solid state, on the other hand, the surroundings keep nearly the same average position throughout the reaction and exert different and specific effects in every direction. The specific anisotropic effect that the crystal lattice may exert on the dynamics of alternative reaction pathways is perhaps one of the most important effects that has been recognized after the topochemical postulate.

M. Cohen described the dynamic effect of the crystal lattice in selecting between alternative reaction pathways with the general intuitive concept of the "Reaction Cavity."[1i] The reaction cavity as defined by Cohen is "the space in the crystal occupied by the molecules which will directly participate in the reaction." Cohen suggested that the atomic movements constituting the reaction will cause pressure on the cavity wall, which will tend to become distorted. Any such a change, however, will be resisted by the closely packed environment of the crystal and only those processes involving a minimum contact will be

allowed (Figure 8).

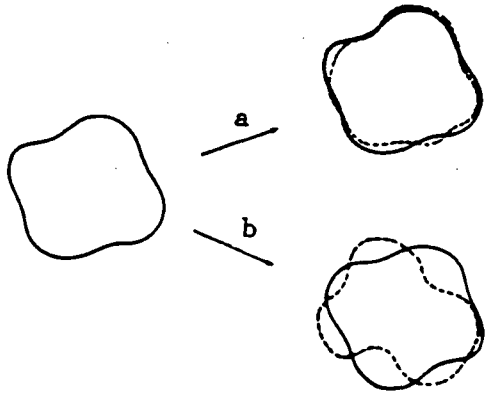

Figure 8. Representation of: (a) Allowed and (b) Disallowed Solid State Reactions in the Reaction Cavity.

Scheffer, Trotter and co-workers[36] have identified and quantitatively studied specific intermolecular effects that modify the solid state reactivity in much the same way of Cohen's reaction cavity concept.[1i] The term "steric compression control" was used to describe this situation and was specifically applied to cases where an unusual reactivity cannot be anticipated from the arrangement of the reactive centers. For instance, the naphthalene derivative shown in Figure 9 was found to be unreactive towards photochemical $2\pi + 2\pi$ solid state dimerization in spite of a topochemically favorable distance and

orientation between the double bonds of neighboring molecules. It was proposed that the lack of reactivity originated from two specific short contacts, between the methyl substituents of the two reacting molecules and those from other molecules in the lattice as shown in Figure 9.

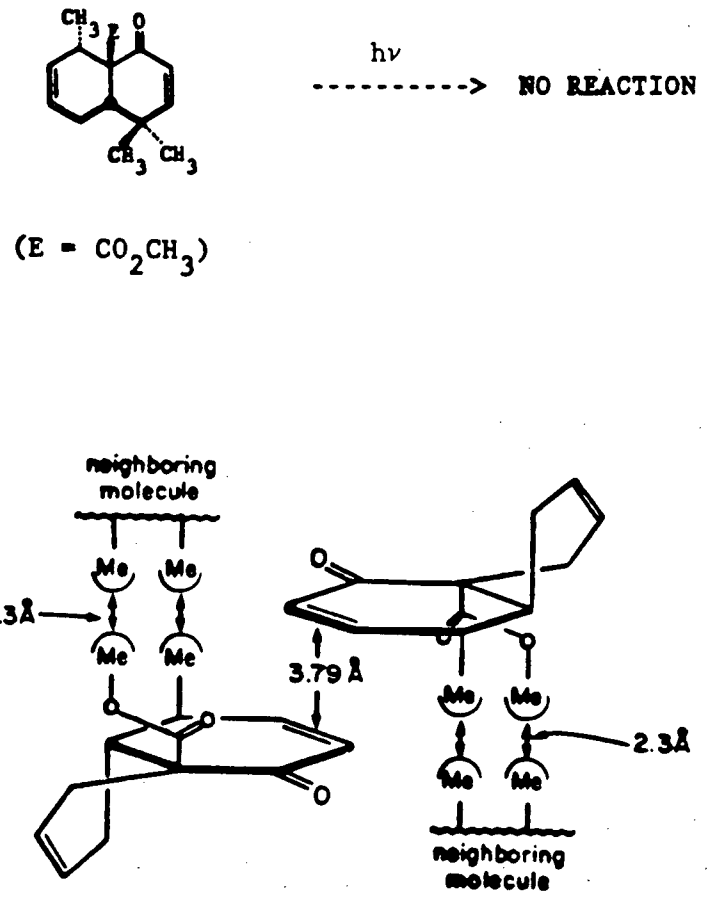

Figure 9. Reaction Inhibition by Steric Compression Control.

The role of kinetic factors in determining the dynamics and selection of reaction pathways in the solid state has also been recognized by Gavezzotti.[37] This author suggests that the free volume around the

reactive centers is what determines the absence, presence and selectivity of a solid state reaction. Although the free volume concept is by no means a departure from Cohen's reaction cavity concept, it possesses the attribute of being a more easily defined and readily measurable quantity.

A different and perhaps complementary approach to the understanding of solid state reactivity has been proposed by McBride and co-workers.[33] After studying a number of solid state reactions known to proceed through the formation of reactive radical intermediates by extrusion of small molecules, McBride et al. proposed that the topochemical factors that one may infer from the reactant structure may not apply to the further behavior of the intermediates. McBride recognized that the formation of the reactive intermediate may occur under very stressful conditions. Its subsequent chemical behavior will therefore be determined by the anisotropic stress generated between the reaction cavity and its new contents. McBride points out that this stress may be sometimes equivalent to pressures from 1 to 10 Kbar, so that a strong influence on chemical reactivity is hardly surprising.

Photochemical Reactions in Molecular Crystals.

Ground state (thermal) reactions are characterized by having their potential energy surfaces, or reaction coordinates, continuous and along the (usually) singlet ground electronic states. In photochemical reactions, on the other hand, at least one of the species involved

exists in an excited electronic state and the reaction coordinate is necessarily discontinuous.

Although the excited state species involved in photochemical reactions are normally generated by absorption of ultraviolet (UV) and visible (VIS) light, other methods can also be used.[38] Alternatives can be found in the use of high energy radiation (gamma rays, X-rays, electron beams, etc.), in thermal excitation by shock waves (as in triboluminescence and sonoluminescence), by chemical methods (as in chemiluminescence and bioluminescence), and finally, by energy transfer.[38]

It is known that the crystalline state has a profound effect on the generation and fate of excited species as compared to their relatively simple solution and gas phase behavior.[38,39] Although the lowest excited states of organic compounds in molecular crystals, especially of polycyclic aromatics, are known to be delocalized, their origin can always be traced to molecular states.[40] It is for this reason that a number of excited state phenomena seem to be satisfactorily explained by considering the crystals as an ordered gas. Many other experimental results, however, seem to require a model that involves a more intricate interaction between the closely packed molecular components.[40]

Electronic spectroscopy in molecular crystals is indeed an extremely fertile area of physical chemistry.[38-41] A superficial review of the literature of this interesting topic seems to indicate a systematic avoidance of chemical reactivity phenomena. This situation is easy to understand when one considers the difficulties involved in carrying out detailed spectroscopic measurements in a system with a changing chemical

composition. The complicated excited state interactions studied by solid state spectroscopists, on the other hand, may often be out of reach and to some extent ignored by the experimental organic chemist. It can be expected that in the years to come a beneficial and symbiotic relationship will arise from the combined study of the photophysical and photochemical behavior of reactive molecular crystals.[42]

Excited State Partitioning.

As a result of their higher energy content, excited state species are not in equilibrium with their surroundings and are, therefore, thermodynamically unstable.[43] After initial excitation by absorption of a UV photon, an electron is transferred to a higher electronic state with the same multiplicity as the ground state (singlet). In the Jablonski[44] diagram shown in Figure 10 this is indicated by the arrow marked with an $h\nu$. Most molecules in the S_2 or higher excited states decay promptly ($\sim 10^{-13}$ sec) into the lowest excited state (S_1) from which all other decay processes take place. Depopulation of S_1 may occur by processes that can be classified as radiative [such as fluorescence (F)], or non-radiative [such as internal conversion (IC), intersystem crossing (ISC) and chemical reactions (R)]. In the internal conversion mode the decay occurs to lower states of the same multiplicity ($S_n \rightarrow S_1$ and $S_1 \rightarrow S_o$), and the excited state energy is lost in the form of heat to its surroundings. Intersystem crossing is the event where the excited states change their multiplicity and the lowest singlet transform into a

triplet excited ($S_1 \rightarrow T_n$) or the lowest triplet decays into the singlet ground state ($T_1 \rightarrow S_o$). Although these processes are formally spin forbidden, they occur by virtue of spin-orbit coupling mechanisms.[43] Finally, a chemical reaction as we know, is the event where an excited state encounters the potential energy hypersurface that leads to a molecular reorganization. It should also be pointed out that similar decay processes are available to the triplet excited state once it becomes populated. The radiative decay of the triplet state, however, is designated as phosphorescence.

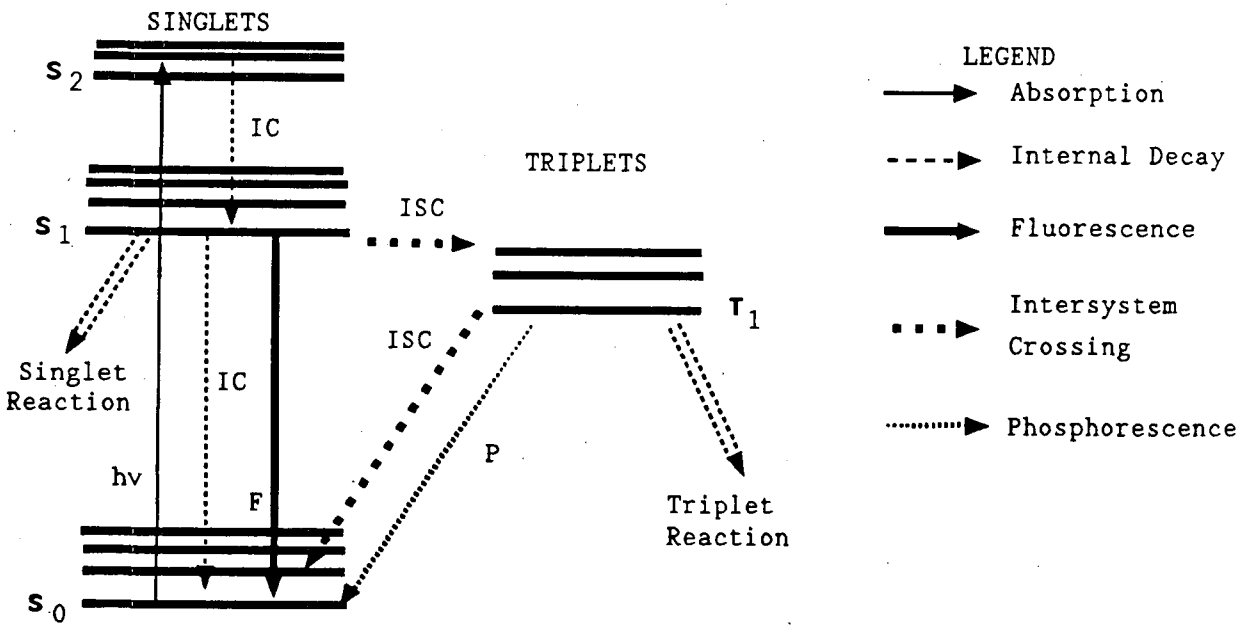

Figure 10. Jablonski Diagram.

Photochemical reactions will occur if they have a rate constant large enough to compete with other excited state decay processes.[43] Associated with each one of the decay pathways (ι) shown in the Jablonski diagram (Figure 10), there is an intrinsic rate constant ($k\iota$). The efficiency of any of these (unimolecular) processes, including unimolecular reactions, depends on the relationship between the rate of this particular process and the rates of all other decay processes available to the excited state. This relationship is called the quantum yield:

$$\Phi = k\iota \ / \ \Sigma k\iota$$

The kinetic feasibility of a photochemical reaction was analyzed by Turro[43] in terms of the rate constant expression, also useful for ground state reactions, which is given by the Arrhenius equation:

$$k_R(sec^{-1}) = A \exp(-E_a/RT)$$

A (unimolecular) chemical reaction with a rate k_R may be observed if the reacting species (the excited state in this case) possesses a lifetime long enough so it can reach the transition state. Obviously, k_R (in sec^{-1}) should be larger than the rate of decay given by the inverse of the excited state lifetime, $1/\tau$ (also in sec^{-1}). Overall, whether an excited molecule will react depends on the activation energy (Ea) of the reaction under consideration, on the probability factor A, and on the lifetime of the excited state (given by the inverse of the sum of all the decay constants, $\tau = 1 \ / \ \Sigma k\iota$). It should be noted that a reaction

having zero activation energy will not occur at all if the reaction possesses a probability factor, A (in sec^{-1}), which is smaller than the inverse of the lifetime, $1 / \tau$, of the excited state.

In the case of a triplet state reaction the quantum yield will depend on the quantum yield for intersystem crossing, Φ_{isc}, which is given by:

$$\Phi isc = k_{isc} / \Sigma k$$

and the quantum yield of triplet product formation, Φ_3, will depend on Φisc and on the fraction of molecules that react from the triplet in accordance with their respective rate constant:

$$\Phi_3 = \underbrace{(k_{isc} / \Sigma k)}_{\text{fraction of molecules reaching the triplet state}} \times \underbrace{(k_3 / \Sigma k_t)}_{\text{fraction of triplet state molecules that react.}}$$

The final product of a photochemical reaction is not always the species originally formed from the corresponding excited state. This intermediate, known as the primary photoproduct, may often be a ground state, high energy species which may possess several thermal decay alternatives.[45] While involvement of the primary photoproduct in a chain reaction gives overall quantum yields higher than one (free radical polymerization), cases in which this species reverts back to the ground state of the starting material are not uncommon.[45] These quantum yield lowering processes are sometimes difficult to differentiate from a low

primary quantum yield. A better expression[45] for the quantum yield of reaction that takes this into account includes a term P (moles of final product / moles of primary photoproduct) indicating the fraction of the primary photoproduct that goes on to the final product.

$$\Phi_{rxn} = (k_{rxn} / \Sigma k) (P)$$

Cases in which a reactive intermediate is formed as the primary photoproduct are of special interest in the context of this thesis. In this respect two general cases can be identified: a) the outcome of the reaction depends directly on the formation of two or more different reactive species or b) a single intermediate can lead to different products. It will be seen that most of the examples studied in this thesis fall into the first category.

The Di-π-Methane Rearrangement.

The reaction model studied in this thesis is the di-π-methane rearrangement, one of the most general and best studied photochemical reactions.[46] Compounds possessing a 1,4-diene unit are converted by absorption of light into products containing a vinylcyclopropane moiety. The two π-bonds involved in the rearrangement can be part of isolated or conjugated systems which are linked to a common saturated, or methane, carbon. Two of the simplest models, 1,4-pentadiene (6) and allyl benzene (7) are shown in Figure 11 along with the commonly accepted mechanism.[46]

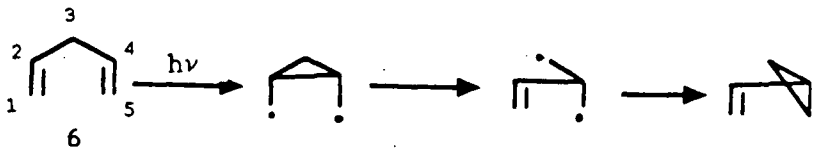

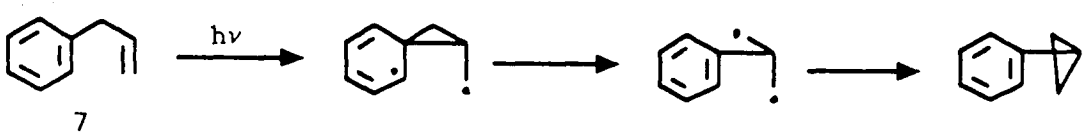

Figure 11. The Di-π-Methane Reaction Mechanism Represented in 1,4-Pentadiene and Allyl Benzene.

The above mechanism, first proposed by Zimmerman in 1967,[47] has been more than adequate for predicting and rationalizing the results of a large number of examples. However, it should be pointed out that controversy remains regarding the nature of the first biradical species formed, as to whether it is a true reaction intermediate or merely a transition state.[48]

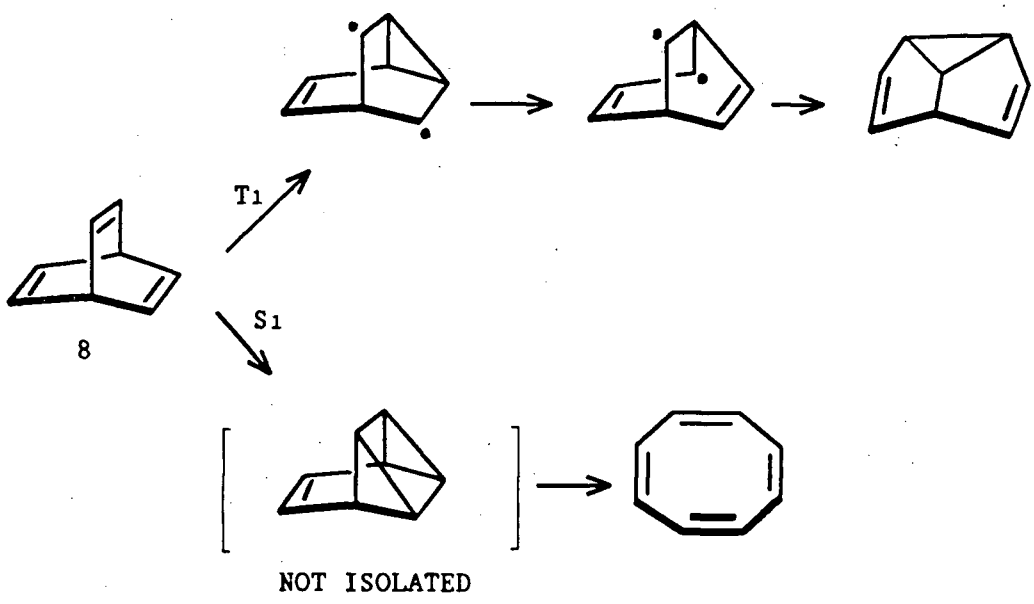

Figure 12. The Multiplicity-Dependent Photochemistry of Barrelene 8.

Like many other olefin photoreactions, the di-π-methane rearrangement is a multiplicity-dependent process.[49] Acyclic dienes such as **6** have been found to react mainly from their singlet excited state, whereas cyclic compounds react from their triplet manifold. Barrelene (**8**) represents an interesting example of the second category (Figure 12).[47] The reason for the multiplicity dependence of the photochemistry of 1,4-dienes is that they may have several reactive pathways. The most important alternatives include electrocyclic reactions[50] and cis-trans isomerizations.[51] The type of reaction to be observed from singlet and triplet states is largely determined by the structure of the diene. This structural dependence can be understood readily when the performance of a given compound is analyzed in terms of how its structure is suited for each of the available reactions. The rate constants for the competing

chemical processes for each excited state can be arranged in decreasing order as in the following relationship:[46a]

Singlet state: ${}^{1}k_{ECR} > {}^{1}k_{DPM} > {}^{1}k_{FR}$

Triplet state: ${}^{3}k_{FR} > {}^{3}k_{DPM} > {}^{3}k_{ECR}$

Where: ECR = electrocyclic reactions.

DPM = di-π-methane rearrangement.

FR = free rotor or cis-trans isomerization.

According to the rate relationship shown above electrocyclic reactions should always be suspected as competitors of the di-π-methane rearrangement in the singlet excited state. This is sometimes the case for dienes with extended conjugation or rigid and parallel double bond arrangements. The reactions in Figure 13 are included in this category.

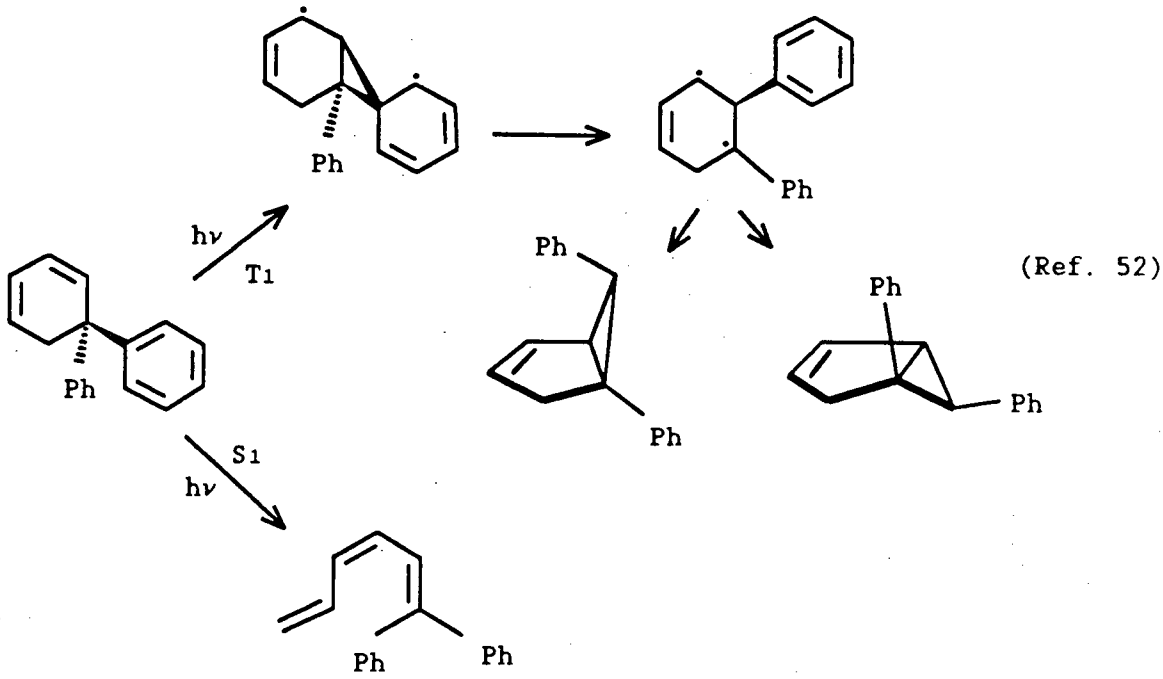

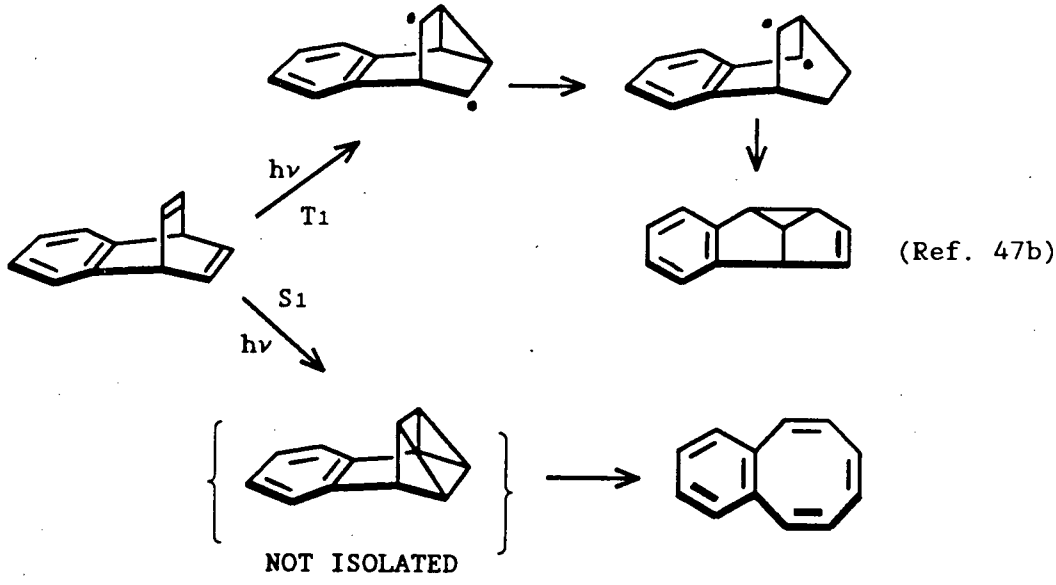

Figure 13. Examples of Substrates that undergo Reactions Other than the Di-π-Methane Rearrangement from the Singlet Excited State.

In the triplet excited state one finds the cis-trans isomerization of an olefinic double bond, or free rotor effect, to be faster than the di-π-methane rearrangement. The free rotor effect, however, is only possible for acyclic olefins such as **6** or in cyclic dienes with an exocyclic double bond. Examples from this category are shown in Figure 14 below.

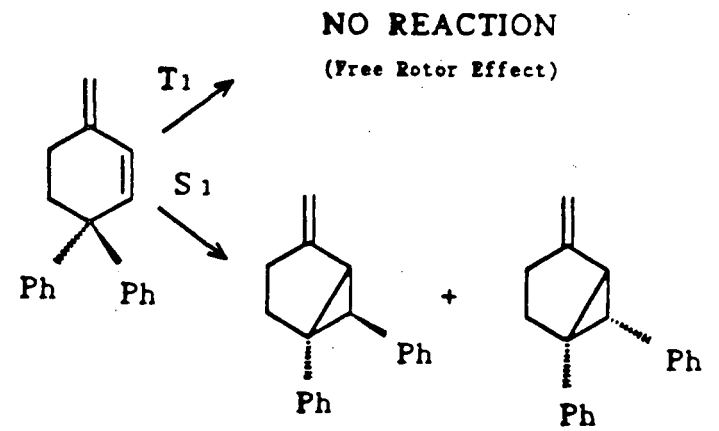

(Ref. 54)

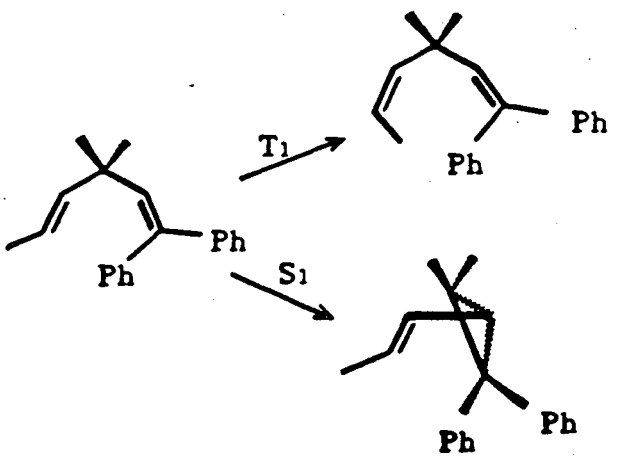

(Ref. 53)

Figure 14. Dienes that Undergo Double Bond Isomerization Instead of the Di-π-Methane Rearrangement from the Triplet Excited State.

The Regioselectivity of the Di-π-Methane Rearrangement.

The first event in the reaction mechanism presented in Figure 11 is the formation of a cyclopropyl dicarbinyl biradical species. Two possible products can be formed when the radical centers at C(1) and C(5) bear different substituents. When compound **9** (Figure 15) was irradiated in solution, it was found to rearrange regioselectively to give **10**. This result was rationalized in terms of the preferential formation of the phenyl stabilized 1,3-biradical **10b'** from the intermediate cyclopropyl dicarbinyl species **10b**. Other examples where the effect of biradical stability can be recognized readily are also shown in Figure 15. In the case of compound **11** the formation of an aryl-vinyl bonded species that gives product **12** is preferred over an aryl-aryl bonded intermediate. Final examples come from compounds **13** and **14** which illustrate the general observation that electron-acceptor groups tend to become part of the cyclopropyl ring in the final product, whereas electron-donating substituents appear on the olefinic double bond.

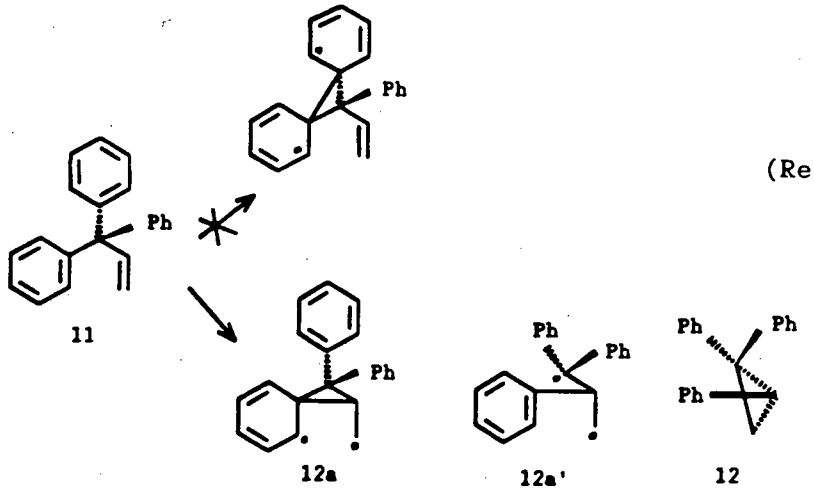

(Ref. 55a)

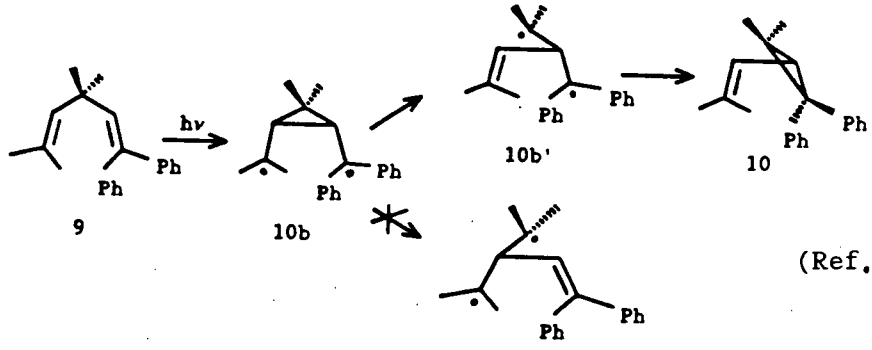

(Ref. 53)

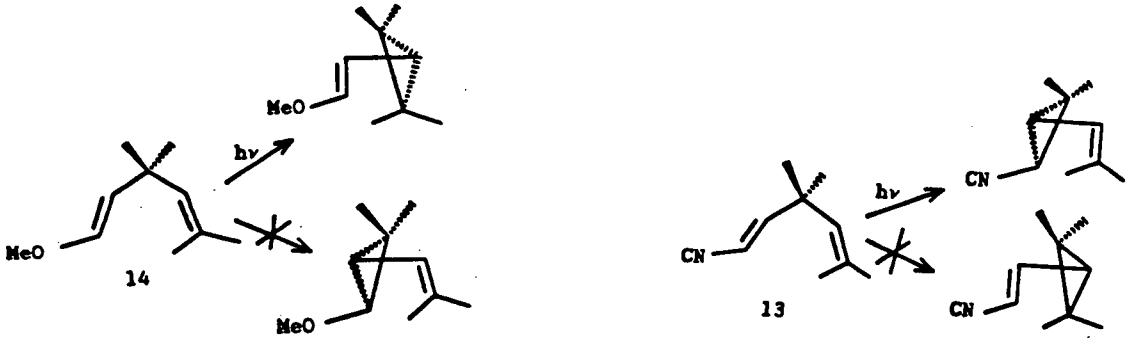

(Ref. 55b)

Figure 15. Examples of Regioselective Di-π-methane Rearrangements.

Objectives of Present Research and Outline of the Thesis.

The first objective of the present research was to establish the viability and generality of the di-π-methane rearrangement in the solid state. With this purpose in mind a model compound was selected according to the following guidelines: (a) the substrates should be crystalline solids in order to have the probability of obtaining their X-ray structures which may in turn facilitate the analysis of the solid state photochemical results, (b) the crystals should have conveniently high melting temperatures in order to avoid crystal melting and reaction in possible liquid phases, (c) the compounds selected for study should be easy to transform into a series of closely related analogs in order to study a number of similar examples from which a data bank can be established, and, (d) the photochemistry of the substrates under study should be relatively well understood in solution media to facilitate the interpretation of the solid state results.

A system presumed to possess all the above attributes was identified in the dibenzobarrelene diester system **15** (Figure 16). The photochemistry of the dimethyl derivative, R = Me (**18**), and a few other derivatives was studied by E. Ciganek in solution 20 years ago.[65] Diels and Alder had shown, much earlier, that compound **18** is a crystalline solid with a relatively high melting point (mp = 160-1°C).[52] Substituted dibenzobarrelenes, as shown by Ciganek, can undergo the di-π-methane rearrangement to give products with the dibenzosemibullvalene skeleton **16**. The formation of these products can be understood by application of Zimmerman's biradical mechanism.[47] The basic reaction steps shown in Figure 16 follow the

photochemical activation and population of the triplet excited state. The rearrangement starts by bond formation between a vinyl and a nearby aromatic carbon to give a biradical **BR-1**. This species reacts in a second step by cleaving the C(9)-C(9a) bond and rearomatizing the previously disturbed benzene ring to give a 1,3-biradical **BR-2**. The rearrangement is completed by bond formation between the two radical centers in **BR-2** to form the cyclopropyl ring in the dibenzosemibullvalene **16**.

Part I of this thesis is related to the solid state photochemistry of the dimethyl diester **18**. This compound was studied in detail in order to verify the feasibility and peculiarities of the solid state photoreaction.

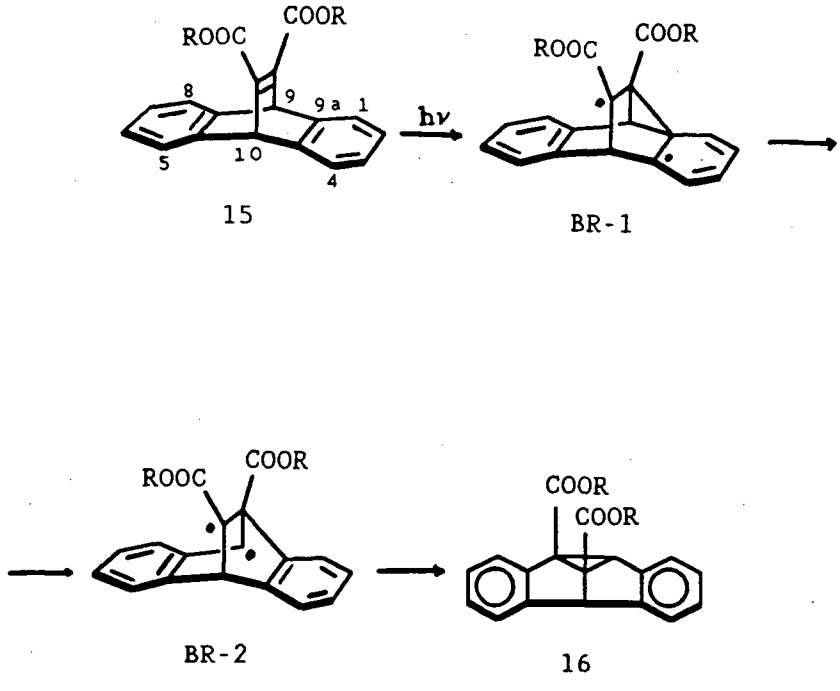

Figure 16. The Di-π-methane Rearrangement of Dibenzobarrelene Diesters.

It should be noted that the dibenzobarrelene skeleton has four distinctively different di-π-methane systems as highlighted in Figure 17. Associated with each of the four 1,4-diene systems there is a formally different reaction pathway which, depending on the substitution on the dibenzobarrelene skeleton, may give different photoproducts. The four different reaction pathways can be recognized depending on which of the two vinyl carbons, C(A) or C(B), engages in the initial benzo-vinyl bridging step, and, depending on which of the aromatic carbons, (I) or (II), participates in the reaction. According to this analysis the four reaction pathways available to the four di-π-methane systems shown in Figure 17 can be labeled as: A-I, A-II, B-I and B-II.

Since the most important conceptual and methodological tool to be used in this thesis is the so-called product analysis approach, the effect of the crystal lattice on the different reaction pathways should be determined and analyzed. The first stereochemical relationship we can identify in the rearrangement of dibenzobarrelene diesters is that symmetrically substituted diesters, such as **15** (Figure 16), are able to give chiral dibenzosemibullvalene photoproducts such as **16**. When the four reaction pathways indicated in Figure 17 are analyzed for this class of compounds, it can be recognized that pathways A-I and B-I give one dibenzosemibullvalene enantiomer, while pathways A-II and B-II give the other. Non-identical amounts of the two enantiomeric products can be expected only under conditions where there is a resolved disymmetric influence operating on the rearrangement. In Part II of the thesis this aspect of the rearrangement will be discussed in more detail in connection with our studies on symmetric dibenzobarrelene derivatives including diesters such

as 15 where R = isopropyl or ethyl.

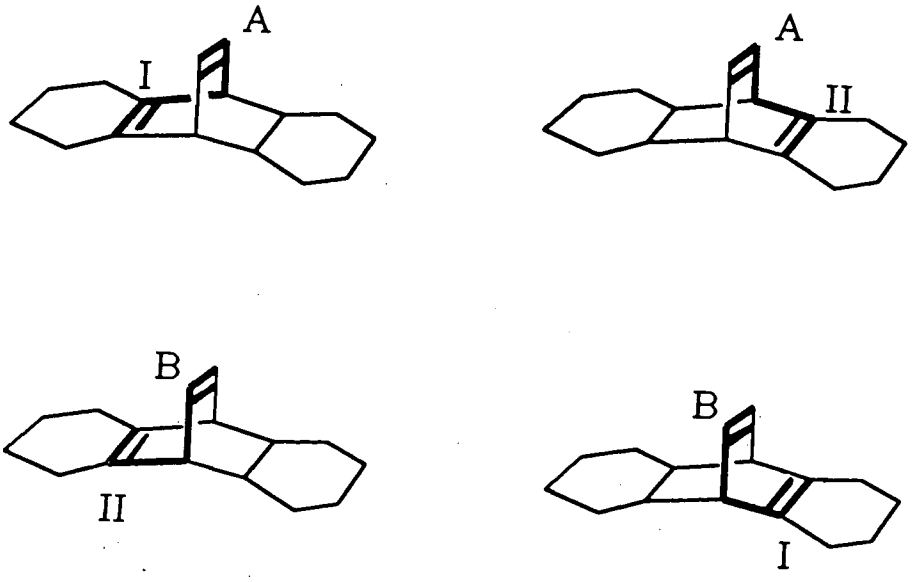

Figure 17. The Four Di-π-methane Systems in the Dibenzobarrelene Skeleton.

In order to distinguish between the reaction pathways A-I and A-II versus B-I and B-II, the two vinyl carbons should bear different substituents. Dibenzobarrelene compounds such as **15** with two different ester groups, $R_1 \neq R_2$, are expected to give two different products whose formation depends on which of the two vinyl carbons engages in the rearrangement. In Figure 18, the reaction via pathways A-I or A-II should give the regioisomer **A** and reaction via pathways B-I and B-II should give

regioisomer B. It should be noticed that the regioselectivity of the rearrangement is determined by the first reaction step, which is also expected to be the rate determining step.[46]

The mixed diesters studied in Part III of this thesis were designed so that a homologous variation on the size and branching of the alkyl substituents would cause a negligible perturbation to the reactive chromophore. These substituents should be remote enough from the reaction centers to exert just a moderate steric effect on the solution regioselectivity but may have profound effects on the crystal packing properties. A very important and interesting by-product of this design is that it should allow us to obtain some information on the steric effects of substituents on the crystallization of the dibenzobarrelene molecules.

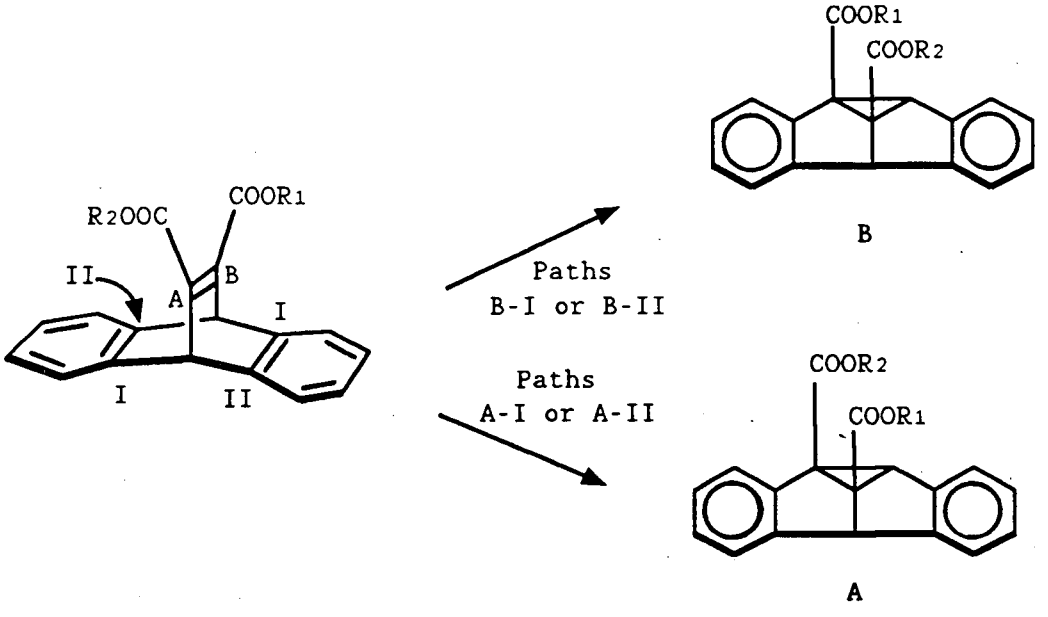

Figure 18. Regioisomeric Products from "Mixed" Dibenzobarrelene Diesters.

Several mixed diesters possessing chiral ester substituents were prepared for the purpose of observing the effects of the crystal lattice on the diastereoselectivity of the reaction. By virtue of the molecular disymmetry given by the chiral substituent, the four reaction pathways, A-I to B-II, are rendered non-equivalent. Four different reaction products can be formed in these circumstances and their relative yields should be related to the partitioning of the excited dibenzobarrelenes into each of the four reaction pathways. The results from compounds included in this category will be analyzed in Part IV of this thesis.

In Part V, the unusual solid state luminescence discovered for most of the diesters studied in the thesis will be analyzed by using the dimethyl diester **18** as a representative example. The possibility of this luminescence being a spectroscopic window that allows direct observation of the postulated reaction intermediates will be discussed.

The final section of the thesis, Part VI, will deal with our studies on 10,11- and 9,11-dibenzobarrelene diesters such as **17A** and **17B** (Figure 19). Although the photochemistry of these compounds has not been studied before, we decided to explore their solution and solid state photochemical reactivity. This class of compounds is very interesting in the context of this thesis because: (a) the di-π-methane rearrangement is expected to occur in solution with quantitative regioselectivity to give products such as dibenzosemibullvalenes **A** and **B** (Figure 19). The biradicals formed by benzo-vinyl bonding at C(12) should be largely favored because of the stabilizing effect of the ester substituents at C(11), (b) the photoproducts expected from diesters **17A** resemble the photoproducts formed from reaction of the 11,12-diesters mentioned above (Figure 18). This should

offer the opportunity of preparing these compounds in a regiospecific manner to confirm our stereochemical assignments, (d) the influence that the ester group on the bridgehead position may have on the reactivity of the dibenzobarrelene skeleton has not been documented. Quantum yields and quenching studies could provide some information on this particular aspect, and, (e) interest in the solid state reaction arises from the fact that while the $-COOR_1$ ester groups in **17A** should suffer large displacements to give the expected major product, the position of the $-COOR_1$ group in **17B** should remain almost unaffected. Different reactivities may be expected for the two types of compounds which may also contrast to the solid state reactivity from the 11,12-diesters.

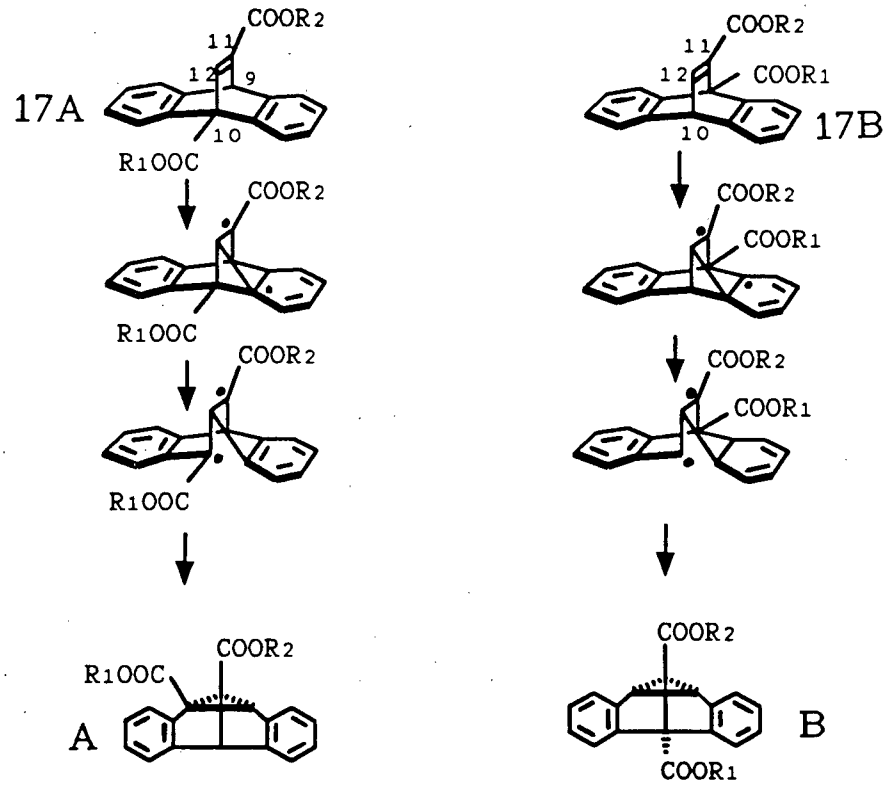

Figure 19. Di-π-Methane Rearrangement of 10,11- and 9,11-Dibenzobarrelene Diesters.

RESULTS AND DISCUSSION.

RESULTS AND DISCUSSION.

Preparation of Substrates.

11,12-Dibenzobarrelene Diesters.

The synthesis of the 11,12-dibenzobarrelene diesters studied in this thesis was based on chemical modifications to the readily accessible dimethyl compound **18** (R = Me) prepared from dimethyl acetylene dicarboxylate and anthracene by the method of Diels and Alder.[56] This procedure was also used in the preparation of the dimenthyl diester **26** (R = (l)-(-)-menthyl) by using di-(l)-(-)-menthyl acetylene dicarboxylate (27). The latter compound was prepared by thermal self-catalyzed esterification of acetylene dicarboxylic acid with (l)-(-)-menthol by employing a modification of the literature[57] procedure consisting of not using a sealed tube, but an open container to heat the two components together.

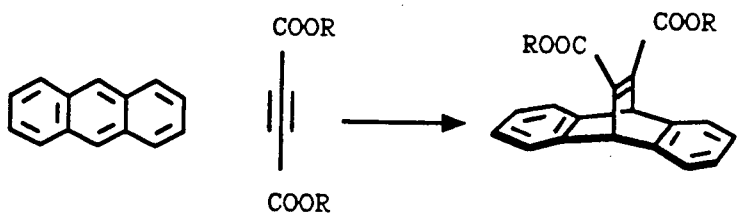

	Dibenzobarrelene
R = Me	18
R = Menthyl	26

Figure 20. Synthesis of Dibenzobarrelene Diesters by Diels-Alder Reaction.

Two transesterification methods were employed in order to exchange the methyl groups of the ester functionalities on **18**. The first method involved a mineral acid catalyzed alcoholysis.[58] Although this method was found to require long reaction times (from a few days to almost two weeks) it was found to be convenient for replacement of both methyl groups (Figure 21). The products of transesterification at a single position could be obtained by stopping the reaction when it had reached an almost statistical distribution of starting material ($R_1 = R_2 = Me$) and the single ($R_1 = Me$, $R_2 = alkyl$) and double ($R_1 = R_2 = alkyl$) transesterification products. Yields of only around 40% and rather difficult purification procedures encouraged us to look for a second and more efficient method for the preparation of mixed esters.

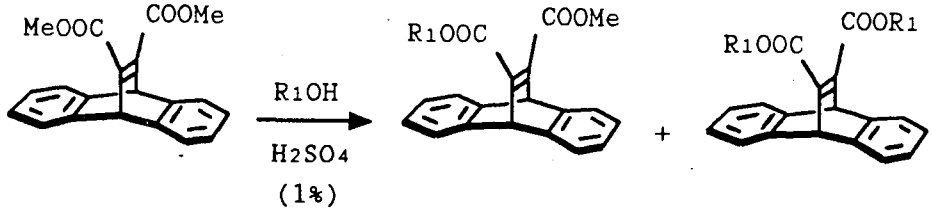

R_1 = Et	**28**	**21**
= nPr	**29**	**22**
= iPr	**30**	**23**
= secBu	**31**	**24**
= iOct	-	**25**

Figure 21. Acid Catalyzed Transesterification of Diester **18**.

The second transesterification method was based on the simple stepwise procedure shown in the figure accompanying Table I. The dimethyl compound **18** was used as a starting point to prepare the diacid **19** by alkaline hydrolysis. The preparation of the anhydride **20** was achieved easily by treatment of **19** with excess oxalyl chloride. This method was found to be cleaner and faster than the cyclodehydration procedure of Diels and Alder which calls for treatment of the diacid **19** in boiling acetic anhydride.[56]

The formation of **20** in oxalyl chloride is an interesting reaction in that it seems to follow an intermediate monoacyl chloride that readily cyclizes with elimination of HCl. Compound **20** was dissolved in the required alcohol in order to generate the corresponding ring opened monoacid. The monoacids formed by addition of alcohols to **20** were not isolated but immediately treated with an excess of oxalyl chloride, either neat or in dry dichloromethane, to give the corresponding acyl chloride-esters. These compounds were normally not isolated but treated <u>in situ</u>, after evaporation of the excess solvent and reagent, with the appropriate dry alcohol to give excellent yields of the final mixed diester products. This one pot reaction sequence was found to be very convenient since the total sequence can be carried out in about two to four hours starting from the diacid **19**, thus representing a great improvement from the acid catalyzed procedure. This method was also found to be ideal for the preparation of optically active compounds. The compounds prepared applying this methodology are included in Table I below.

Table I. Dibenzobarrelene Diesters Prepared by Stepwise Esterification of the Diacid **19**.

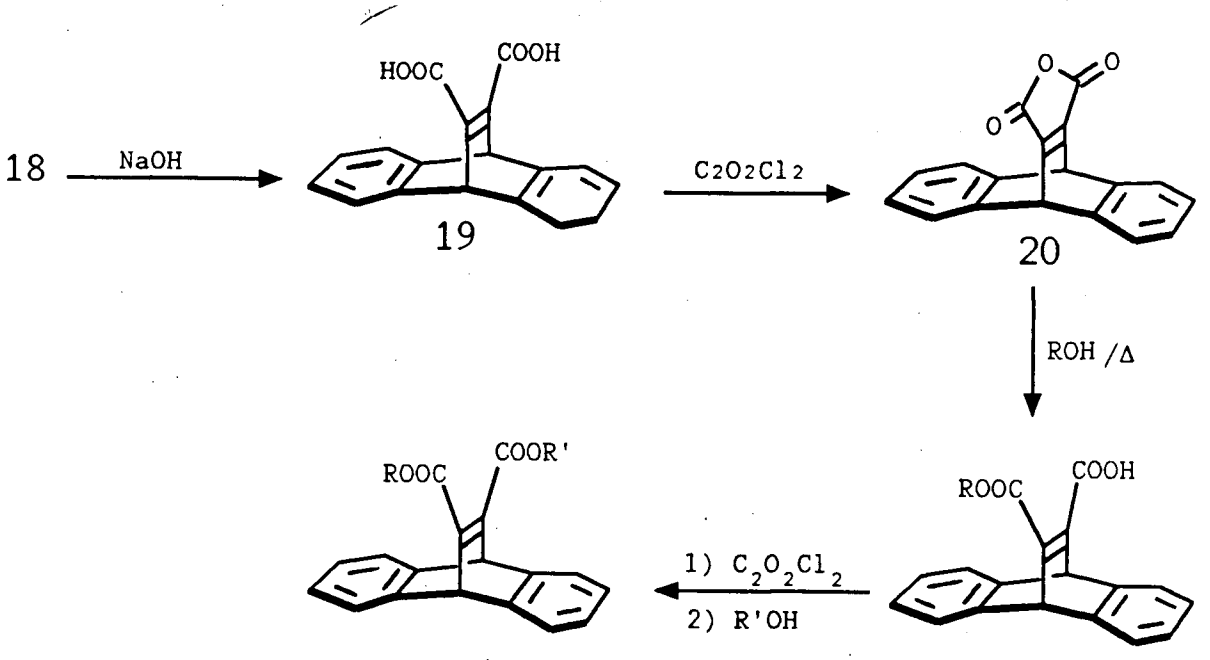

R	R'	Compound	Melting point °C
Me	n-Pr	29	103-4
Me	iso-Pr	30	124-5
Me	(R,S)-sec-Bu	(R,S)-31	94-5
Me	(S)-(+)-sec-Bu	(S)-(+)-31	91-2
Me	tert-Bu	32	128-9
Me	n-Pent	33	liquid
Me	iso-Pent[a]	34	63-5
Me	neo-Pent[b]	35	75-80
Me	(1)-(-)-Menthyl	36	liquid
Me	Phenyl	37	180-1
Et	iso-Pr	38	104-5
Et	(S)-(+)-sec-Bu	39	72-3
iso-Pr	(R,S)-sec-Bu	(R,S)-42	122-4
iso-Pr	(S)-(+)-sec-Bu	(S)-(+)-42	133-5

a) (S)-(-)-2-Methyl-1-butyl; b) 2,2-dimethyl-1-propyl.

Preparation of 10,11- and 9,11-Dibenzobarrelene diesters.

A Diels-Alder reaction between 9-isopropyl-9-anthracenecarboxylate (43)] and methyl propiolate was used as the entry for the title compounds (Figure 23). As shown in Figure 22, the 9-isopropyl-9-anthracenecarboxylate derivative[60] was prepared via the 9-anthracene acyl chloride obtained from the carboxylic acid and oxalyl chloride.

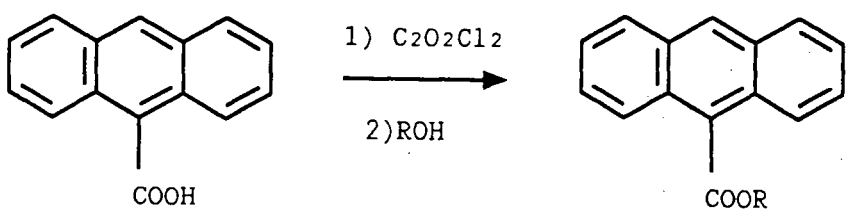

R	Compound.
2-propyl	43

Figure 22. Preparation of 9-Isopropyl-9-anthracene Carboxylate

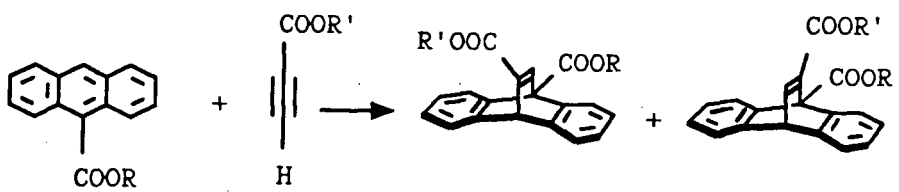

R	R'	Compound (yield)	Compound (yield).
2-Propyl	Me	44 (66%)	45 (23%)

Figure 23. Preparation of 10,11- and 9,11-Dibenzobarrelene Diesters.

The identification of the isomeric diesters was based primarily on the difference in the ^{1}H NMR coupling between the bridgehead and vinylic protons.[62] The diagnostic value of the magnitude of this coupling stems from the significant difference between the allylic [H(9)-H(12) and vicinal [H(10)-H(12)] coupling present in the 10,11- and 9,11-diesters respectively (Figure 24). This assignment was further confirmed by X-ray diffraction analysis on the diester compounds 44 and 45.[63] The regioselectivity observed in the reaction clearly favoured the 10,11-derivative, perhaps on the basis of the steric effects of the substituents.

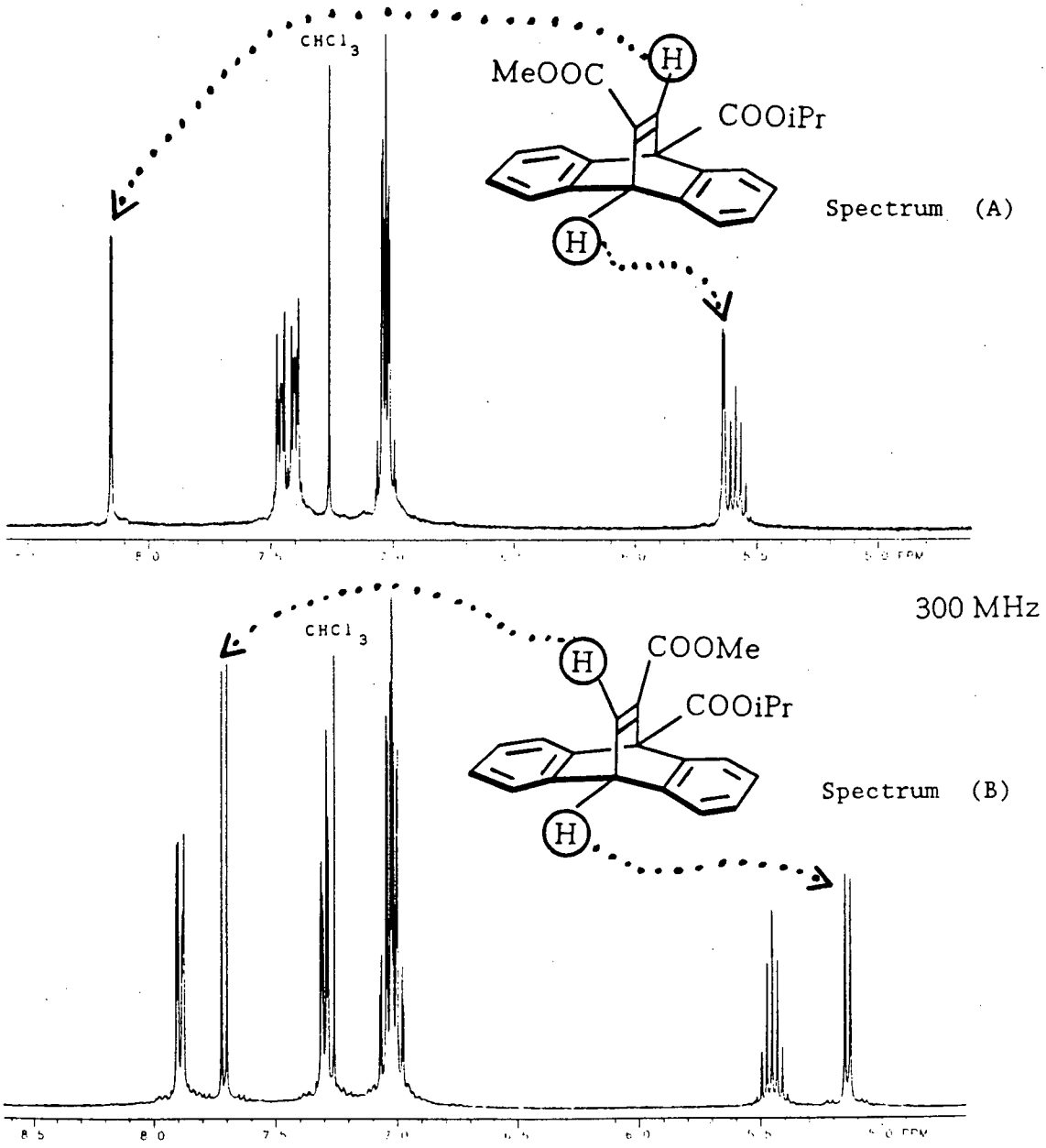

Figure 24. Partial ^{1}H NMR Spectra of (A) 10-Isopropyl-11-methyl- and (B) 9-Isopropyl-11-methyl-dibenzobarrelene Diesters.

PART I. THE DI-π-METHANE REARRANGEMENT IN THE SOLID STATE.

The photochemical behavior of dibenzobarrelene and some of its substituted analogs was first studied in solution by E. Ciganek in 1966.[65] Ciganek reported that direct or sensitized irradiation of a series of dibenzobarrelene compounds gave the corresponding dibenzosemibullvalene derivatives as the only photoproducts (Figure 25). Almost simultaneously, a series of studies on the related photochemical transformation of barrelene to semibullvalene led H.E. Zimmerman to postulate the now classical di-π-methane biradical mechanism.[47] In later studies it was shown that the di-π-methane rearrangement of the dibenzo derivatives is a triplet specific reaction[66a] and that simple alkyl derivatives react from their singlet states upon direct irradiation to give dibenzocyclooctatetraenes.[66]

Although a large number of substrates has been studied in the years following these initial reports and a great deal of understanding has been obtained,[46] no attempt seems to have been made to study the rearrangement in organized media. This lack of interest is surprising in view of the intense research activity developed during the last few years on the study of photochemical reactions in various organized environments.[1] It seems possible that the study of the di-π-methane rearrangement in the solid state, in particular, may not have been attempted because the molecular motions required to reach the products may seem too drastic within the expectations of the topochemical postulate.[1a]

Exploratory Solid State Photochemistry of the Dimethyl Dibenzobarrelene Diester 18.

Compound **18** was photolyzed first in 0.1 M benzene, acetonitrile and acetone solutions and then in the solid state. In agreement with Ciganek's report[65] a single product identified as dibenzosemibullvalene **52** was detected from direct (benzene and acetonitrile) and sensitized (acetone) solution irradiations (Figure 25).

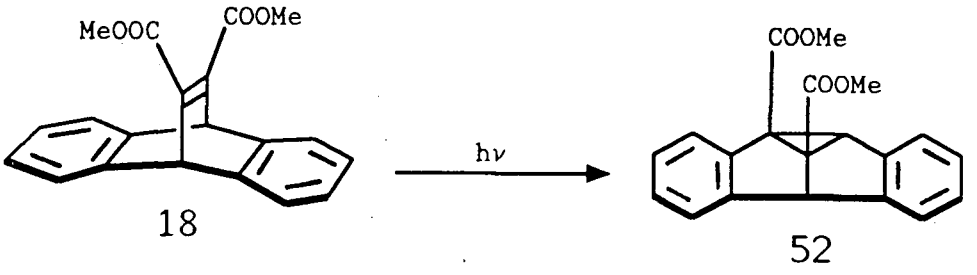

Figure 25. The Di-π-methane Rearrangement of the Dimethyl Diester **18**.

Solid state irradiations resulted in the formation of a product with glc retention time and MS identical to those of the solution photoproduct. The identity of the solution and solid state products was further confirmed by comparison of the spectroscopic and analytical information from the products isolated from preparative photolyses in each media. It should be noted that preparative photolyses in the solid state were

carried out to a limited conversion. The inseparability of the product from the unreacted starting material by normal chromatographic procedures led us to convert the starting material into the separable diazomethane adduct 53[67] (Figure 26).

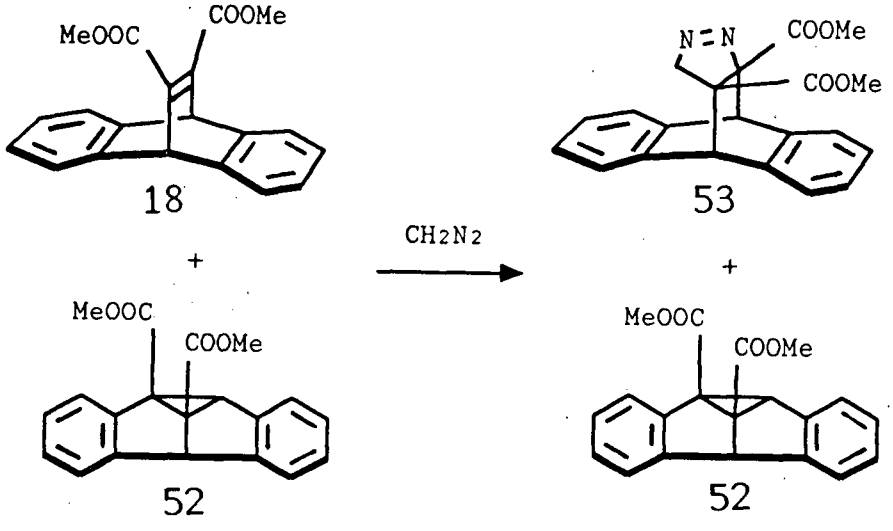

Figure 26. Derivatization of Partially Reacted Diester **18** with Diazomethane to Yield the Chromatographically Separable Adduct **53**.

A striking observation was that side-by-side solution and solid state analytical irradiations indicated larger conversions in the case of the solid state runs. The quantum yield of formation of diester **52** (Φ_{52}) was measured by triplicate in benzene solution and found to be, $\Phi_{52} = 0.2$. Although the absolute solid state quantum yield is not available, the apparently high solid state efficiency is considered to be significant in view of the low efficiency of many solid state photochemical reactions. Some solid state photochemical reactions have been reported to occur over periods as long as few months.[68,20]

On The True Solid State Nature of the Rearrangement.

One of the most important aspects of solid state photochemistry is the determination of the true solid state nature of the reaction. The radiationless dissipation of the excited state energy in the form of internal conversion may constitute a source of heat in light-initiated reactions. In order to apply the techniques of solid state methodology[69] to the study of the di-π-methane rearrangement one should eliminate the possibility of having the reaction occurring by concomitant crystal melting. The generation of microscopic liquid regions in the crystal is expected to be important in reactions of compounds with low melting points, which also display low luminescence (fluorescence and phosphorescence) and low reaction quantum yields. The dimethyl diester **18** has a relatively high melting point of 160-1°C, which should guarantee resistance to melting in the event of having significant amounts of heat evolved during the irradiation. Furthermore, the relatively high efficiency of the reaction and the finding of a relatively intense room temperature fluorescence of diester **18** (see page 62) seem to indicate a low internal conversion quantum yield. Several practical methods can also be implemented in order to detect and diminish melting:

a) Microscopic inspection of photolyzed single crystalline samples.

b) Photolysis to very low conversions.

c) Photolysis at very low temperatures.

d) Derivatization to very high melting point compounds.

e) Derivatization to compounds that may display different solution and solid state reactivity.

Typical results of several experiments covering aspects of the first three categories are shown in Table II. It was satisfying to find that the rearrangement could still occur at temperatures as low as -70°C. The reaction efficiency, however, as judged from the time required to achieve a certain conversion, was found to decrease significantly with decreasing temperature. This observation is in agreement with theoretical models[70] and experimental data[71] that describe the existance of thermal barriers between the various reaction intermediates. The low temperature irradiations were highly satisfactory not only because of their helping to accumulate evidence against the possibility of melting, but also because a fascinating luminescence behavior, to be dealt with in a later section of this thesis, was discovered.

Table II. Analytical Photolysis of **18** in Solution and in the Solid State[a]

Sample	λ,nm	T°C	Irrad. time	% Conversion	Melting
1. 0.1 M CH_3CN	>290	20	75 min	3.8	-
2. 0.1 M Me_2CO	>290	20	75 min	2.5	-
3. Crystalline	>290	20	5-75 min	3-15	No
4. Crystalline	>290	20	1-10 h	20-25	Yes
5. Crystalline	337.1	20	1-10 min	1 - <30	No
6. Crystalline	337.1	-40	10 min	5	No
7. Crystalline	337.1	-70	40 min	2	No
8. Crystalline	>200	20	30 min	15	Yes

a) Irradiations at λ > 290 and λ > 200 were done with the Pyrex or quartz filtered output of a 450 W medium presure Hanovia lamp; Irradiations at 337.1 nm were realized with the nitrogen laser.

The unique solid state stereoselectivity of unsymmetrical compounds, as we will also see below, also contributed to gain more confidence in the true solid state nature of the rearrangement.

The Limiting Conversion on the Solid State Reaction of Diester 18.

When single crystals of **18** were exhaustively irradiated at 337.1 nm it was found that the crystals became unreactive after a limiting conversion of up to approximately 30% had been reached. Solution and solid state irradiations were accompanied by the development of a slight yellow coloration which could not be attributed to any detectable photoproduct. Although there exists the possibility that traces of some colored substance may act as filter at the later stages of the reaction,[72] two other principal factors were analyzed in order to understand the limiting conversion of diester **18**.

The first and simplest possible explanation for the limiting reactivity of **18** could arise from limited UV exposure inside the deepest regions of the crystal. This relates to the fact that in order to have a photochemical reaction occurring in the bulk of the crystal the light must get through. The consequence of irradiating a crystalline sample with light of strongly absorbed wavelengths is that product saturation, with loss of topochemical control and melting may occur near the surface (i.e entry 8, Table II).

In the case of compound **18** an extinction coefficient of approximately 8 liters mol^{-1} cm^{-1} was measured in methanol solution at the resonance wavelength of the nitrogen laser (337.1 nm). By using a crystal density of 1.2 g cm^{-3} we get a crystal concentration of 3.75 M, and combining this value with the above extinction coefficient we can calculate an approximate penetration depth of about 0.5 mm for the unreacted crystal of **18** by naive application of the Beer-Lambert law.

Analysis of concentrated methanol solutions of the di-π-methane product **52** on the other hand revealed a UV-absorption tail starting at a shorter wavelength (approximately 310 nm). Assuming that the absorption spectra of **18** and **52** in the reacted crystals are similar to those obtained in solution, it can be concluded that the photoproduct will be essentially transparent at the laser excitation wavelength (337.1 nm). If this assumption is correct it can be expected that the light should have an increasing penetration depth as the reaction proceeds. Why is it then that the reaction does not go to completion if every molecule in the crystal is in principle able to absorb a photon? Two possible explanations can be anticipated. The first one can originate from perturbations in the excited state decay pathways of the crystalline compound via photoproduct aided channels[38-41] and the second from the possibility of having the final product presenting a limited solubility in the crystalline phase of the starting material.[17,32]

Perturbation of the Excited State Decay Channels of Crystalline 18 by Accumulation of the Photoproduct.

The fate of the excitation energy in organic crystals is known to be strongly dependent on the sample composition.[38-41] Some spectacular situations can be found where the normal excitation decay channels of the molecules of a crystal are completely suppressed by a minor guest or impurity compound. One such example comes from the fluorescence of thin anthracene crystals doped with 1/10,000th parts of tetracene.[73]

Irradiation of these crystals with light of wavelengths mostly absorbed by the anthracene molecules resulted in an almost exclusive detection of tetracene fluorescence. This interesting situation represents an example of excited state perturbation through a very efficient energy transfer mechanism. Phenomena such as this should raise some concern among solid state photochemists, since a reaction of crystals that give products possessing efficient energy trapping mechanisms could be close to being classified as topochemically disallowed.

Molecular crystals in general, whether pure or doped, are extremely prone to energy transfer.[38-43] This property results primarily from the impossibility to localize the excitation energy on one molecule in a system where there are many identical sites. In principle there always exists a finite probability that the energy will "hop" from one molecule to the other giving the excitation a resemblance to a migrating particle. This "particle" has also been called an exciton.[74] If a migrating exciton encounters a foreign molecule with lower energy levels it will find itself in an "energy trap" and will no longer be able to delocalize again. The unimolecular decay channels of the trap are then in conditions to take over.

Other energy transfer mechanisms do not need exciton delocalization but can operate through some favorable features of the prospective donor-acceptor pair. These mechanisms, referred to as the electron exchange and the Förster mechanisms respectively, share some similarities and have some interesting contrasts. One of the main practical differences between the two mechanisms concerns their dependence on the donor-acceptor distance. Whereas the Förster, or dipole-induced, energy

transfer operates over distances as large as 50-100 Å, the rate of transfer by electron exchange drops to negligible values as the donor-acceptor distance increases by more than the order of two or three molecular diameters (~15 Å). Both mechanisms depend on the spectral overlap between the donor emission and the acceptor absorption. The rate of electron exchange, however, does not depend on the intensity of those transitions (and therefore operates in the case of triplet energy transfer where the ground state to triplet absorption probability is almost negligible).

Many intermolecular excited state interactions have been studied in the solid state with the aid of added impurities of variable concentration.[39] In contrast to these photophysical studies where the contents of the samples are constant, in the case of crystalline photoreactive systems the sample composition becomes a dynamic variable. Assuming that there are no other impurities the sample composition is determined by the percent conversion.

In the case of the diester **18**, at the initial stages of the irradiation, the crystal is composed mainly of starting material which will be able to follow its normal decay channels (Eq. 2-7, Figure 27). When the photoproduct (which may be some undetected species other than **52**) starts to accumulate, new heteromolecular decay pathways may start to operate[75] (Eq. 8-9) depending on the nature of the prospective donor-acceptor pairs. If the rate of energy transfer happens to be significant, the excitation energy may be finally dissipated in an unreactive manner from the photoproduct **52** thereby quenching the normal decay pathways of **18**.

1)	$18 \text{ ------>} {}^1 18^*$	Light absorption by 18
2)	${}^1 18^* \text{ ------>} 18 + h\nu_1$ or heat	Fluorescence or internal conversion.
3)	${}^1 18^* + 18 \text{ ------>} 18 + {}^1 18^*$	Homomolecular singlet transfer
4)	${}^1 18^* \text{ ------>} {}^3 18^*$	Intersystem crossing
5)	${}^3 18^* \text{ ------>} 18 + h\nu_2$ or heat	Phosphorescence or intersystem crossing.
6)	${}^3 18^* + 18 \text{ ------>} 18 + {}^3 18^*$	Homomolecular triplet transfer
7)	${}^3 18^* \text{ ------>} \text{-->} \text{-->} 52$	Di-π-methane rearrangement
8)	${}^1 18^* + 52 \text{ ------>} 18 + {}^1 52^*$	Singlet quenching by 52
9)	${}^3 18^* + 52 \text{ ------>} 18 + {}^3 52^*$	Triplet quenching by 52
10)	${}^1 52^* \text{ ------>} 52 + h\nu_3$ or heat	Deactivation of singlet 52
11)	${}^1 52^* \text{ ------>} 52 + h\nu_4$ or heat	Deactivation of triplet 52

Figure 27: Photochemical Activation and Decay Processes Available to Crystals of Reactant 18.

It should be pointed out that the processes shown in equations 2 to 11 account only for a limited number of all the possible excited state decay channels and interactions.[38-43,75] This oversimplified picture however should prove useful within the merely illustrative context of the present discussion.

The rate constants for equations 8 and 9 would be expected to be a function of the intermolecular distance between **18** and **52** as required by the various energy transfer mechanisms (exciton trap, dipole induced and electron exchange).[39,43] The distance between molecules of **18** and **52** will depend on the concentration and distribution of **52** in the parent crystal. We therefore have to be aware of the possibility that a limiting concentration of **52** could be reached after which the rates of energy transfer (i.e. Eq. 8 and 9) become large enough to mask the rate of reaction (Eq. 7).

Two sets of experiments were performed within our instrumental capabilities to study these possibilities. These consisted of measuring the fluorescence and phosphorescence spectra of crystalline **18** before and after irradiation and in the measurement of the relative quantum yield of the reaction expressed as the dependence of the percent conversion as a function of the photolysis time.

a) Luminescence Measurements.

Measurements were realized by front surface illumination and detection at an angle that causes most specular reflection to miss the emission monochromator. Powdered samples were used in order to minimize spectral variations due to scattering problems resulting from variations in sample geometry. The spectra of the solid samples were obtained at 77 K before and after they were irradiated at -20°C with the nitrogen laser.

The uncorrected fluorescence spectrum of polycrystalline **18** consisted of a broad structureless band starting at about 350 nm and reaching a maximum near 400 nm. Qualitatively, the fluorescence spectrum of solid samples (Figure 28) was very similar to that obtained in methyl tetrahydrofurane solution. Irradiation of the solid samples with the nitrogen laser resulted in a series of complicated and temperature dependent spectral changes (these will be discussed in Part V of the thesis). In order to observe the effects due to the stable photoproduct, the fluorescence was recorded when these changes had came to an end after few minutes in the dark at ambient temperature.

Although the shape of the fluorescence envelope of samples photolyzed to less than ~6-8% conversion remained largely unaltered, its intensity was found to be increased. Additional changes were evident, however, when samples were photolyzed to 15% conversion (Figure 28). Besides the previously detected increase in intensity, the presence of a new fluorescence band with a maximum around 470 nm was clearly evident. We have assigned the new band to the fluorescence of the di-π-methane rearrangement product, the dibenzosemibullvalene **52**. The latter assignment is based on the fact that the new band could be reproduced when the fluorescence of **52** was measured in methyl tetrahydrofurane. Changes in the phosphorescence spectrum, on the other hand, were mainly related to the spectral intensity. A relatively strong phosphorescence at 550 nm (only detected at 77 K) was found to be considerably quenched after the sample had been irradiated (Figure 28).

Although perturbations into the normal decay channels of diester **18** were clearly evident, no definite conclusion of these effects in

reactivity can be reached without studying the spectral changes that follow immediately after irradiation (Part V). It seems that the effect of the stable photoproduct is rather moderate in view of the rather large percent conversion accompanying these spectral changes. The decrease in the phosphorescence intensity, an aspect directly associated with the triplet state reaction, is somewhat intriguing. Phosphorescence quenching through energy transfer seems at first unlikely because of the relatively far location of this band (550 nm). It is reasonable to expect that there should be no triplet energy absorption levels of the photoproduct in that spectral region. It is possible that the decrease in phosphorescence may result from environmental effects caused by the accumulation of the product.

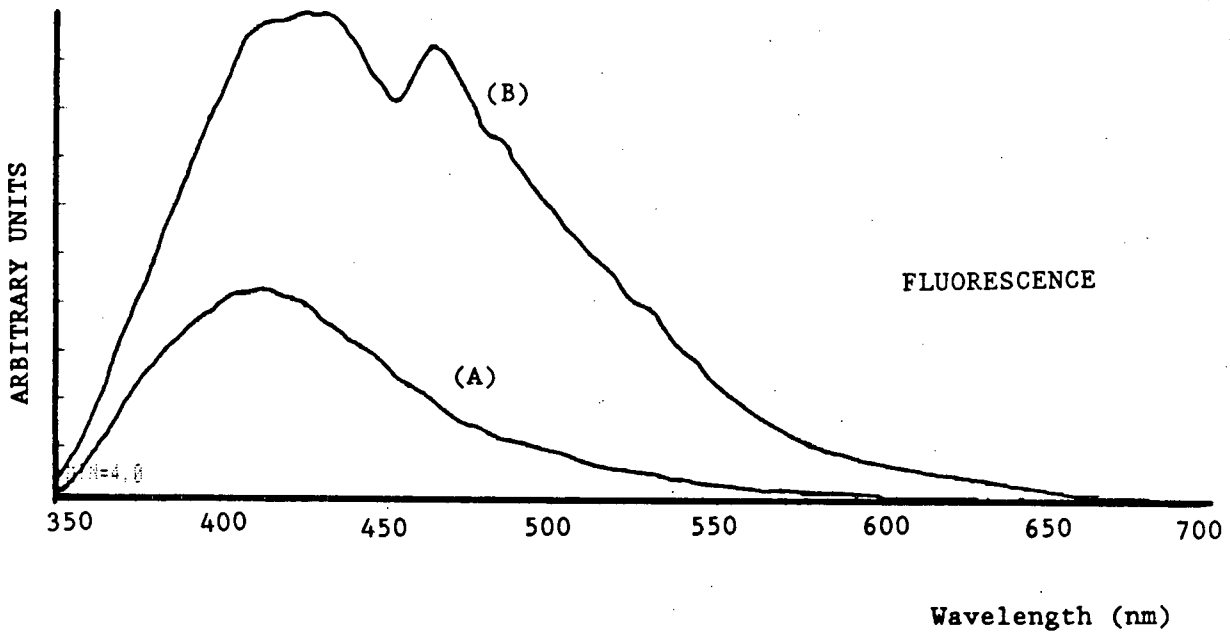

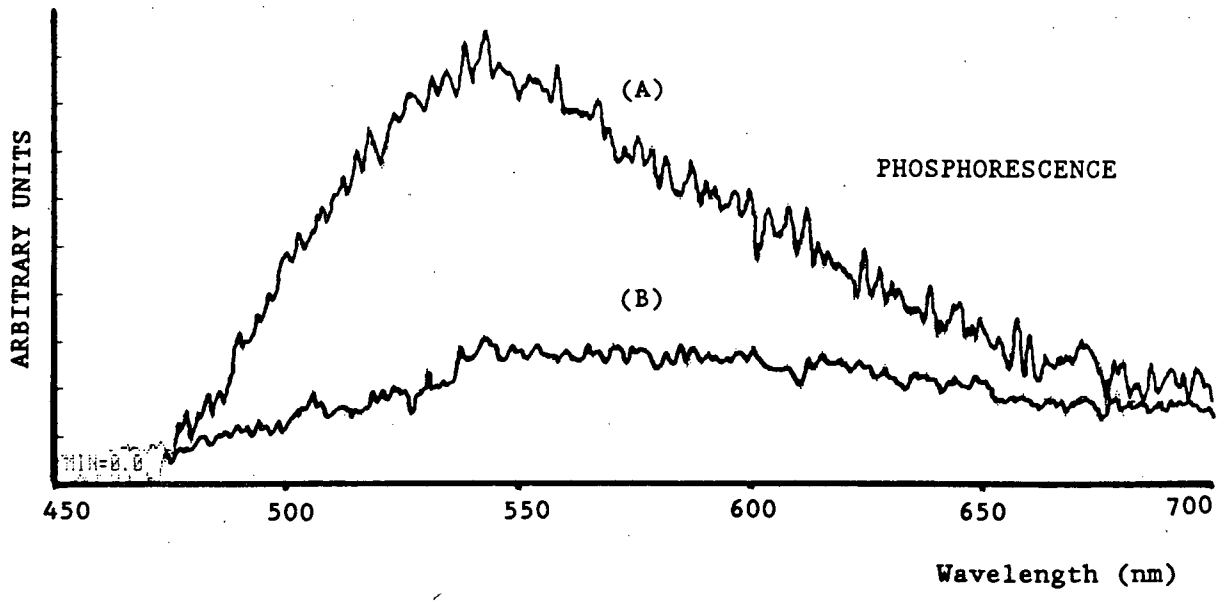

Figure 28. Uncorrected Fluorescence and Phosphorescence Spectra of Polycrystalline 18 at 77 K (a) Before and (b) After Irradiation with the Nitrogen Laser.

b) Conversion Dependence of the Relative Quantum Yield of Reaction of Diester 18.

Although measurable under steady state conditions, the quantum yields of photochemical reactions are true excited state kinetic parameters since they reflect the balance between the rate constants for all the excited state activation-decativation processes. As pointed out by Wagner,[45] the quantum yield for a particular photochemical reaction is the product of several probabilities: 1) the probability that absorption of light will produce the required excited state, 2) the probability that the excited state will undergo the primary photoreaction necessary for the process in question, and, 3) the probability that any reaction intermediate will make it to the final product instead of reverting back to the starting material. If no excited state starting material-photoproduct bimolecular interactions alter the product of the above (unimolecular) probabilities, the quantum yield is expected to remain constant as the photoproduct accumulates.

If one measures the change in concentration, d[**18**], of the reacting species produced by an irradiation of duration dt, then d[**18**]/dt is the amount of diester **18** converted per unit time. The quantum yield for the disappearance of the reacting species **18** is given by:[75]

$$-d[18]/dt = \Phi\ I_a \qquad \text{Eq. 12}$$

where Φ is the ideally constant quantum yield and I_a is the average absorbed intensity.[75] However, if one uses a light source with constant

intensity and we assume that I_a is directly proportional to [**18**] we have that:

$$d[\mathbf{18}]/dt = -k_{ap}\,[\mathbf{18}] \qquad \text{Eq. 13}$$

where k_{ap} will be a complex first order rate constant that includes terms that account for the intensity of the laser photon flux, the absorption coefficient of **18** at 337.1 nm and the reaction quantum yield. Clearly, a plot of log[**18**] vs time should give a straight line unless the decay channels of the excited state are altered in such a manner that those changes reflect in the reaction quantum yield.

In order to minimize scattering problems and maximize the reproducibility of these measurements the diester **18** was photolyzed in homogeneous KBr matrices.[76] This methodology offered the additional advantage of allowing the determination of starting material consumption by monitoring the decay of the IR vinyl absorption of the starting material at 1640 cm^{-1}. The samples were initially photolyzed for periods of 30 sec that were extended to up to 3 min to give a total irradiation time of 10 min. The results shown in Figure 29 indicate a clean first order decay of **18**, to be interpreted as a constant quantum yield, up to approximately 20% conversion. After this conversion value a decrease in the slope value indicates a decrease in the reaction quantum yield (or, although it is less likely, a decrease in the absorption coefficient). When the same experiments were repeated in benzene solution it was observed that no bending occurred over a similar conversion range in the corresponding log[**18**] vs t plot.

The large conversion range of constant solid state quantum yield, as well as the fluorescence and the phosphorescence results, seem to indicate the unlikelihood of energy transfer mechanisms being responsible (at least uniquely) for the limiting conversion of crystalline diester **18**.

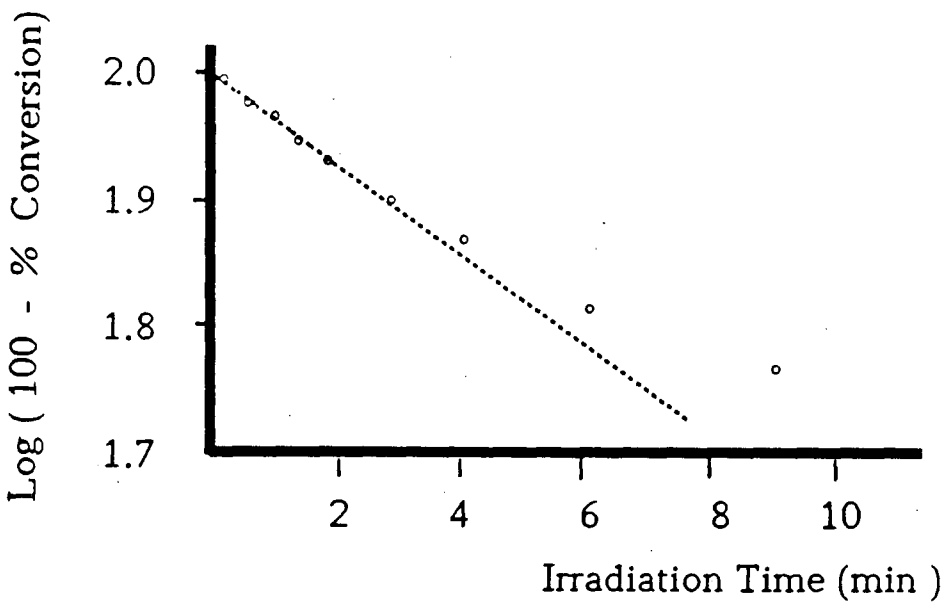

Figure 29. Consumption of Diester **18** as a function of Photolysis Time Plotted as a First Order Decay (Variations in the Quantum Yield as a Function of Conversion).

Mechanical Effects and Limiting Conversion.

The presence of a limiting conversion value may also come from a mechanical effect that results from an increase in the internal stress of the crystal lattice as a consequence of more product accumulating.[32,33] This factor is directly associated with a limited product solubility and the steric interactions resulting from the structural mismatch between the product and its environment. McBride has shown these factors in operation during the conversion dependent kinetics of the reactions of the radicals generated upon oxygen and carbon dioxide extrussion from single crystalline peroxides and peresters.[33]

Experiments aimed to test for the involvement of internal stress on product saturation included a visual inspection of the mechanical relaxation manifested as a change in texture[17] of single crystals of 18 photolyzed to saturation. Single crystalline samples with an approximate size of 0.2 x 0.5 x 0.2 mm^3 were mounted on a glass fiber and photolyzed with the nitrogen laser for 15-20 min. The crystal size was a critical parameter that in principle guaranteed that the light was getting through in the entire crystal (see page 55). Microscopic examination of the crystals after photolysis showed a remarkable change in texture including a significant loss of transparency. It was noticed that some photolyzed crystals displayed a large number of cracks distributed randomly along their entire volume. No signs of melting could be detected but the crystals turned out to be extremely fragile as they could be fractured with extreme ease. The same observations were made when much larger crystals (8 x 4 x 2 mm^3) were photolyzed. Figure

30 presents an example of one such experiment carried out on crystals of the di-isopropyl compound **23** (Pbca modification, see PART II).

From these results we tentatively conclude that the phenomenon of a limiting conversion of crystalline **18** is largely (if not uniquely) due to the mechanical effects of the increasing internal stress caused by a limited solubility of the photoproduct. We propose that the di-π-methane rearrangement of crystalline **18** is a largely non-topotactic[18] transformation.

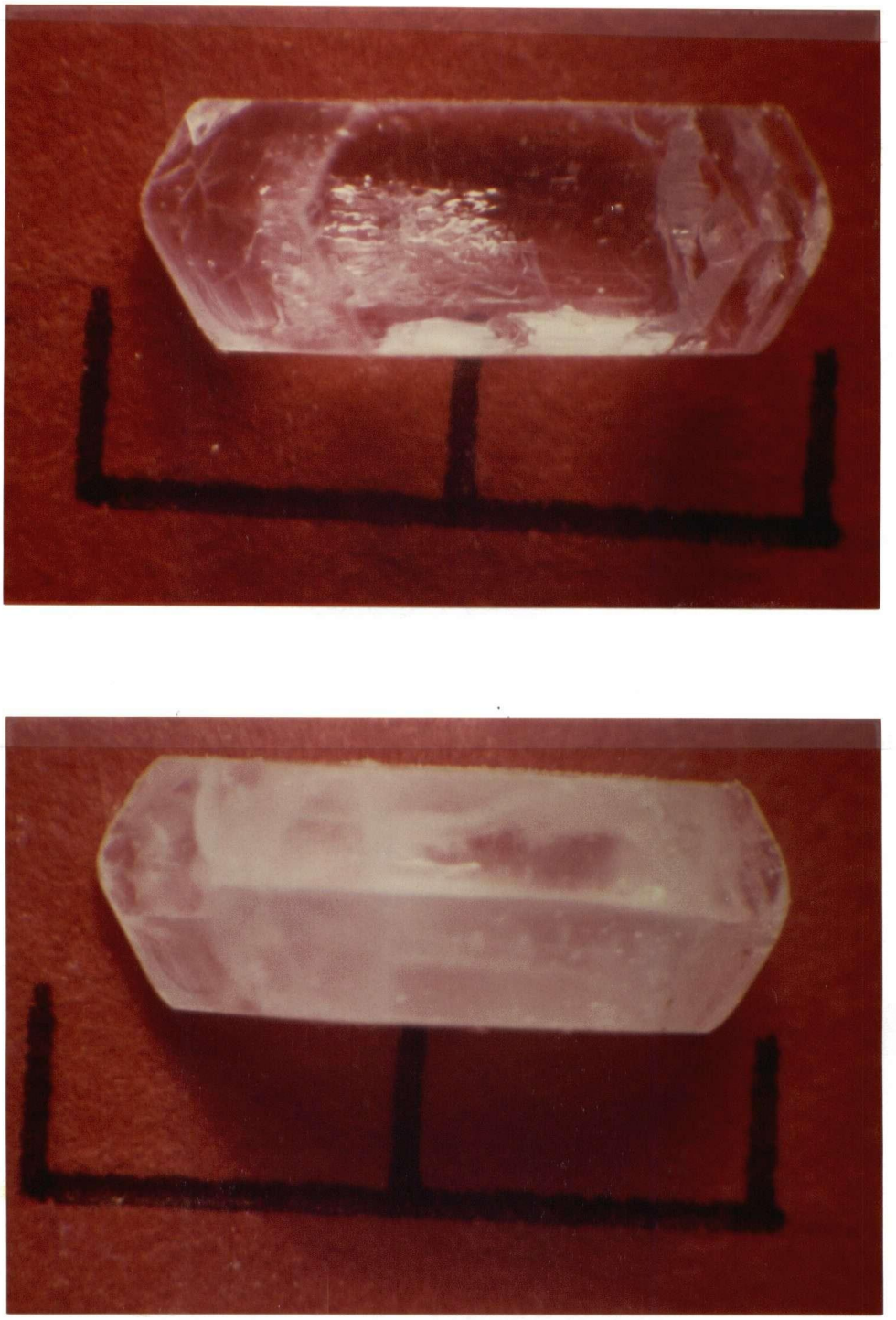

Figure 30. Photographs of a Single Crystal of Diisopropyl Diester 23 (Pbca Modification) Before (top) and After Photolysis (bottom). A 1 cm scale is shown in both pictures.

The Crystal and Molecular Structures of Diester 18.

Many reactions studied in the solid state have been designed so that the principal variable to study from a chemical and structural point of view is a critical distance between two reaction centers.[9,10,19,69] Examples come to mind from the repeatedly mentioned $2\pi + 2\pi$ olefin cyclodimerization[1,9,19] and from studies on the photochemical hydrogen abstraction of excited carbonyl compounds.[1j,n,o,69] The presence or absence of solid state reactivity in these cases is primarily (but not exclusively) associated with some critical geometry for the reaction to occur. The di-π-methane rearrangement of the rigid dibenzobarrelene system is, however, a complete departure from this approach (see reaction mechanism on page 35). The bonding distance required for the first reaction step, the benzo-vinyl bonding step (C12-C4a, C12-C10a, C11-C8a or C11-C9a), is held essentially constant by the design of the rigid dibenzobarrelene framework (Figure 31). The occurrence of the di-π-methane rearrangement in the solid state is therefore expected to be dependent on the dynamic behavior of the excited state of the starting material and of the postulated biradical intermediates.[33,69]

The X-ray molecular structure* of **18** shown in Figure 31 clearly indicates that the average C_{2v} symmetry inferred in solution from the ^{13}C NMR spectrum (7 lines) no longer exists in the solid state. As

---

*All the X-ray crystal structure elucidation work was carried out by Fred Wireko, Department of Chemistry, U.B.C.

suspected, the X-ray derived benzo-vinyl distances of the first reaction step were all found to be nearly the same (2.43 Å). A C_1 solid state molecular symmetry results from the fact that the two carbonyl ester groups conjugate to a different extent with the central vinyl double bond. The disymmetry and the degree of conjugation are determined by the dihedral angles between the mean planes of the two carbonyl groups and the vinyl double bonds [torsion angles O(2)-C(13)-C(11)-C(12) and O(4)-C(15)-C(12)-C(11)].

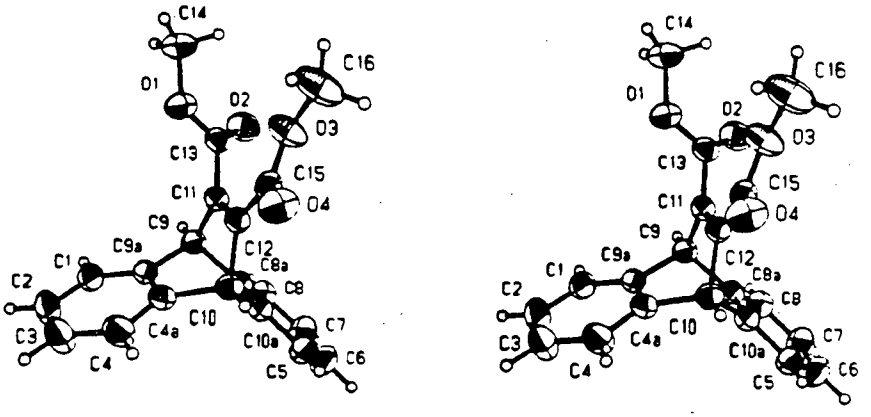

Figure 31: Stereoview of the Molecular Structure of the Dimethyl Diester **18**

PART II. STUDIES ON SYMMETRIC DIBENZOBARRELENE DIESTERS.

It was recognized that in order to explore the generality of the di-π-methane rearrangement in the solid state the study of a large number of compounds was required. At the same time, the detailed description of the rearrangement requires identification of the factors that may be controlling the solid state reactivity. Since crystal lattice and molecular factors may be involved to different extents, variations of their structures are necessary in order to analyze their respective contributions.

In order to gain some information regarding the structural alternatives available to the dibenzobarrelene diester skeleton in the solid state, several symmetric diesters were prepared, their photochemistry studied and their X-ray crystal structures obtained when possible. The compounds studied in this series were the diester derivatives: diethyl (21), di-n-propyl (22), diisopropyl (23), di-sec-butyl (24), diisooctyl (25) and dimenthyl (26).

With the exception of the isooctyl derivative 25, all the diesters in this series turned out to be crystalline solids at ambient temperatures and their crystallization was achieved with relative ease. While crystals of the diesters 21, 22 and 23 turned out to be of excellent quality for diffraction studies, diesters 24 and 26, crystallized from ethanol, proved to be opaque prisms and flakes respectively which were unsuitable for X-ray diffraction analysis. Compounds 21 and 23 were found to occur in two different crystal forms (dimorphs[77]) depending on the crystallization experiment. The X-ray crystal structures of the two dimorphs of the

diethyl and diisopropyl diesters **21** and **23** were obtained along with the structure of the di-n-propyl compound **22**. A summary of this information including the melting points and space groups of each compound (where appropriate), is presented in Table III.

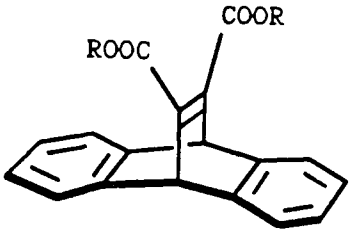

Table III. Symmetrically Substituted Dibenzobarrelene Diesters.

Compound	Substituent (R)	mp(°C)	Space group.
18[a]	Me	160-1	$P\bar{1}$
21(I)	Et	93-4	$P2_1/c$
21(II)	Et	97-8	$P2_12_12_1$
22	nPr	72-3	$P\bar{1}$
23(I)	iPr	145-6	Pbca
23(II)	iPr	145-6	$P2_12_12_1$
24	sBu	95-6	b
25	iOct	liquid	-
26	Menthyl	147-9	b

a) Diester **1** was studied in the previous section. b) Not determined.

Photochemistry in Solution.

All the symmetric diesters of this series were photolyzed in solution by direct and sensitized irradiations. The corresponding dibenzosemibullvalene derivatives expected from the di-π-methane rearrangement were found to form as the only detectable products. Their identification was supported by ^{1}H NMR, FTIR, mass spectrometry and elemental analysis or exact mass measurements which were consistent with the expected structures and with the data previously obtained for diester **18**.

The di-sec-butyl compound **24** deserves additional comment since this material was prepared with racemic sec-butanol and the sample, although giving rise to only one glc signal, was presumably composed of a mixture of the racemic (R,R- and S,S-di-sec-butyl-**23**) and the meso (R,S- and S,R-di-sec-butyl-**24**) forms. The photolysis products possess five chiral centers (three of them in the dibenzosemibullvalene skeleton), but only three independent disymmetric or chiral elements, two in the sec-butyl groups and one in the dibenzosemibullvalene structure. These compounds can be expected to be formed in up to $2^3 = 8$ different stereoisomers[78] which can be differentiated in four enantiomeric pairs. Although tlc chromatographic separation could not be achieved in several solvent systems, evidence for the different products was found in the glc trace and in the ^{1}H NMR spectrum of the photolysis mixtures. While the glc of the mixtures consisted of two poorly separated peaks in a 55:45 ratio, the ^{1}H NMR spectrum presented noticeable resolution in the signal assigned to the cyclopropyl hydrogen at C(8d), which was split into three peaks of approximate ratio 1:2:1. No further attempt was made to separate this

mixture or to quantify the relative amounts of the various photoproducts.

Photochemistry in the Solid State.

The generality of the solid state di-π-methane rearrangement was confirmed when we observed that all the crystalline diesters reacted in a manner similar to that of crystalline **18**. Solid state reactions were carried to conversions of less than about 30%, since further conversion seemed either difficult or accompanied by crystal melting. The products observed were identified by comparison of the glc, glc-MS and ^{1}H NMR spectral data of the solid state reaction mixtures with the data from the solution isolated products. Before discussing the solid state photochemical results in more detail, the structural features of the compounds that had their X-ray crystal structures solved and some other relevant details will be analyzed.

The Solid State Molecular Structures of the Diethyl Diester 21.

Diester 21 was crystallized by slow evaporation from ethanol solution. Crystals with plate-like morphology (mp = 93-4°C) and a tendency to form laminar aggregates were easily grown over a period of 24-48 hours. Repeated crystallizations under the same conditions were sometimes found to give crystal batches that showed remarkably different morphology. The new solid state material was obtained as large prisms with remarkably well developed faces and edges and a different melting point (97-8°C). These materials were found to be dimorphic[77] and their

structural differences were clearly manifested in their crystallographic, spectroscopic and chemical properties. Selective crystallization of either material was possible by seeding of concentrated ethanol solutions of 21.

The plate-like material, or form I, crystallized in the monoclinic space group $P2_1/c$ with two molecules per asymmetric unit (molecules A and A'). The two independent molecules were found to posses the same absolute configuration and to be related by an approximate two fold screw axis. The crystal, however, is racemic since both enantiomers of each molecule are present in equal amounts. Only minor conformational changes at the ester substituents differentiated the structures of the two molecules in the asymmetric unit (Figure 32a). The carbonyl-vinyl double bond torsion angles O(2)-C(13)-C(11)-C(12) and O(4')-C(16')-C(12')-C(11') of molecules A and A', for instance, vary from 249.34° to 248.62°. The torsion angles O(4)-C(16)-C(12)-C(11) and O(2')-C(13')-C(11')-C(12') that define the dihedral angle between the other carbonyl-vinyl double bond mean planes also varied slightly, from 6.56° to 4.42° for molecules A and A' respectively. The ene-dioate chromophore in this crystalline modification can be described as possessing one carbonyl very close to a perfectly conjugated s-cis conformation (torsion angle 0°) while the other is in a conformation that is nearly out of conjugation (torsion angle 270° or 90°)[79] with the C(11)=C(12) double bond. The conformation of the ethyl substituents, which is similar in molecules A and A', can be described by the C(16)-O(3)-C(17)-C(18) and C(13)-O(1)-C(14)-C(15) torsion angles (molecule A) which maintain an anti-periplanar relationship. This conformation can also be described as having the carboxyl group and the two ethyl carbons all in approximately the same plane (Figure 32a).

The prisms of form II were found to contain the diester **21** packed in the chiral space group $P2_12_12_1$ with only one molecule per asymmetric unit. The molecular conformation of the diester **21** in this dimorph was significantly different from that observed in the $P2_1/c$ modification (Figure 32b). The most salient features of this structure were also represented by the carbonyl-vinyl double bond torsion angles and by the conformation of the carboethoxy groups. Similar to the structure of form I, the structure of form II was grossly characterized by having one carbonyl group almost perfectly conjugated and the other almost perfectly out of conjugation with the central double bond.[79] Interestingly, the conjugated carbonyl group, C(16)-O(4), and the central double bond, C(12)-C(11), exist in the more stable s-trans conformation.[80] The values of the dihedral angles O(2)-C(13)-C(11)-C(12) and O(4)-C(16)-C(12)-C(11) were 96.2 and 176.5° respectively. The conformation of the carboethoxy groups differed significantly from the conformations present in form I. Instead of having all the heavy atoms of the ester substituent lying in approximately the same plane, the C(13)-O(2)-C(14)-C(15) and C(16)-O(4)-C(16)-C(17) torsion angles were rotated +80° and -80° to give the two possible synclinal (gauche) forms.

(a)

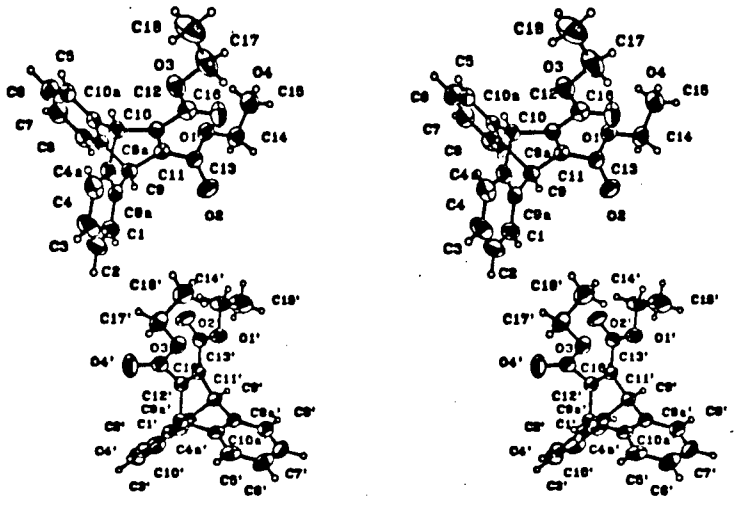

(b)

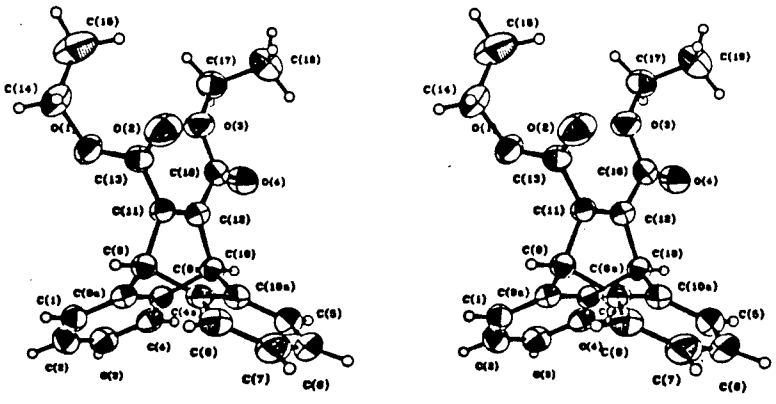

Figure 32. Stereoviews of the Molecular Structures of the Diethyl Dibenzobarrelene Diester 21 in (a) the $P2_1/c$ and (b) the $P2_12_12_1$ Modifications.

The Solid State Molecular Structure of the Di-n-Propyl Diester 22.

Diester 22 was crystallized by slow evaporation of a solution prepared by dissolving this compound in a small amount of diethyl ether to which ethanol was added. Large prisms were obtained and found to contain diester 22 packed in the space group $P\bar{1}$. The most important feature of the molecular structure of 22 was a disymmetric conformation defined by the carbonyl-vinyl double bond torsion angles, O(2)-C(13)-C(11)-C(12) and O(4)-C(17)-C(12)-C(11) with values of 161.41° and 6.51° respectively (Figure 33). The two alkyl groups also display significant conformational differences along their three carbon chains. Although the molecular structures are chiral, the crystals are racemic since they contain both enantiomers in equal amounts.

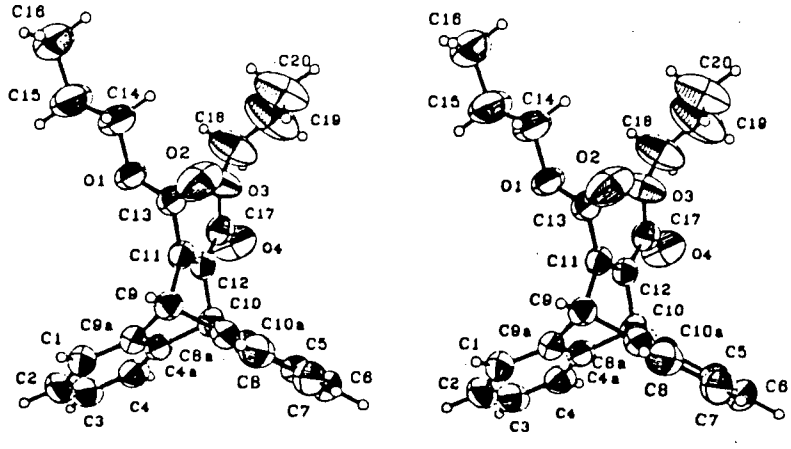

Figure 33. Stereoview of the Molecular Structure of the Di-n-propyl Diester 22 (Space Group P1).

The Solid State Molecular Structure of the Diisopropyl Diester 23.

The diester 23 was first crystallized from concentrated chloroform solutions to which ethanol was added as the precipitating solvent. Large prisms with mp = 145-6 °C were observed to form in an apparently homogeneous batch. The crystals obtained by this method were similar to those obtained from neat ethanol by slow evaporation. The space group of this material was identified as $P2_12_12_1$ and the molecular conformation was determined as being disymmetric with carbonyl-double bond torsion angles O(2)-C(13)-C(12)-C(11) and O(4)-C(15)-C(11)-C(12) of 196.2° and 63.7° respectively (Figure 34a). The conformation of the isopropyl group conformed to the expected synperiplanar relationship between the isopropyl methine hydrogen and the carbonyl oxygen observed in other isopropyl containing ester compounds.[81] As required by the symmetry of this space group the molecules in any given single crystal are present in only one chirality.

A larger specimen with identical morphology was selected from the same batch in order to explore its solid state chemistry. When a space group confirmation was attempted it was discovered that we were not dealing with the same material but with a dimorph in the space group Pbca and then a full structure analysis was performed. Even though the melting points of the two dimorphs were identical, their crystallographic and solid state spectroscopic and chemical properties were significantly different. Having learned how to identify the two materials (solid state FTIR and luminescence, see below), specific crystallization from solution was analyzed and found successful only in the case of the Pbca material, which was obtained

pure from cyclohexane solution. Crystallization from other solvents gave mixtures of the two dimorphs. Crystallization from the melt was gratifying since crystals of the $P2_12_12_1$ material were obtained in an exclusive manner.

The molecular structure of the Pbca dimorph was quite similar to that of the chiral modification (Figure 34b). The torsion angles O(2)-C(13)-C(11)-C(12) and O(4)-C(17)-C(12)-C(11) were 228.5° and 36.1° respectively. The isopropyl groups of both modifications were found to have similar conformations. Since the Pbca modification is part of the group of non-chiral space groups both enantiomers of 23 are present in equal amounts.

(a)

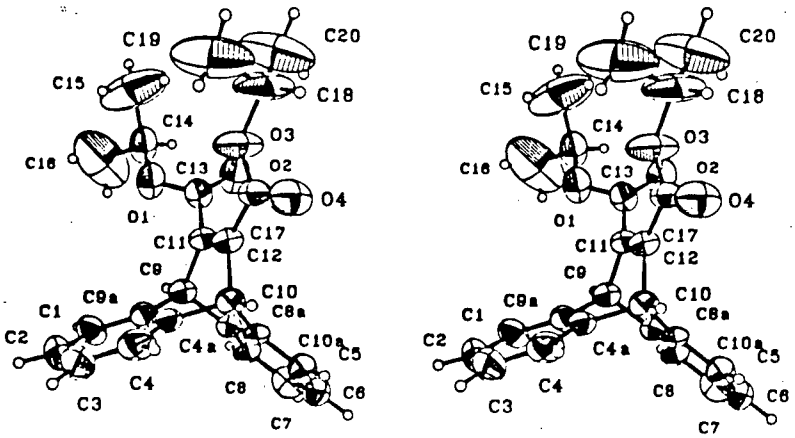

(b)

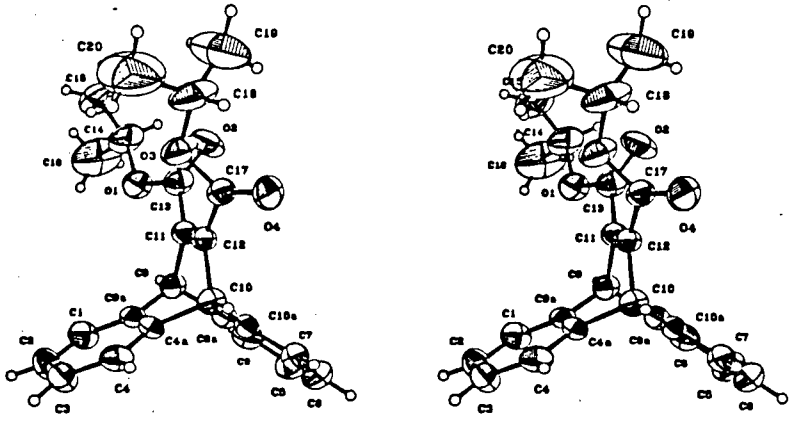

Figure 34. Stereoviews of the Molecular Structures of the Diisopropyl Diester 23 in its (a) $P2_12_12_1$ and (b) Pbca Modifications.

Conformational Polymorphism.[82]

Conformational polymorphism was defined by Corradini as the existence of different conformers of the same molecule in different solid state modifications.[83] The conformation of an organic compound is determined by its shape and is defined by three molecular parameters: bond lengths, bond angles, torsion angles.[82] Very often these structural descriptors can be significantly different for the same compound if it crystallizes in alternative solid state modifications. It has been pointed out by Bernstein[82] that even compounds that appear to have very rigid structures, such as lepidopterane (Figure 35), may present significant geometrical differences.[84] Since measurable structural differences can be expected for all organic compounds presenting polymorphic modifications, it can be argued that all organic polymorphism can be strictly defined as conformational polymorphism.

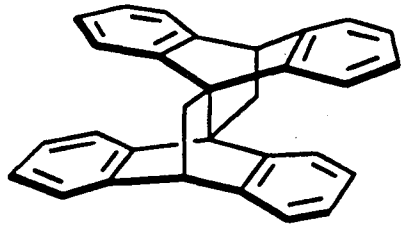

Figure 35. The Molecular Structure of Lepidopterane.

Conformational polymorphism is clearly evident in the crystal structures of the two dimorphs of diesters **21** and **23**. Interestingly, two slightly different conformers of Et/Et-**21** occur in crystals of the $P2_1/c$ modification. This phenomenon is known as conformational isomorphism.[82]

The existence of different conformations, or molecular structures, in different solid state modifications can be justified by considering that crystallization phenomena occur from a balance of intra- and intermolecular forces.[30,85] First there is a tendency to maximize the occupied space, which according to the close packing principle, results from the weak attractive forces between the non-bonded atoms.[85] While the interatomic non-bonded forces search for the lowest energy structural arrangement, the molecular structure may not be uniquely defined and may have several closely related conformational structures. The energetic balance between the intermolecular forces and the intramolecular energy may lead to more than one structurally different free energy minima. Variations in crystal forms may represent alternative structures where an increased intermolecular potential may be accompanied by a decrease in conformational energy or vice versa. For instance, it is interesting to notice that the antiperiplanar conformation that the carboethoxy group presents in the molecular structure of the $P2_1/c$ dimorph of **21** has been shown to be the preferred conformation of primary alkoxy ester substituents.[81] Suggested from the X-ray structural analysis of a large number of compounds, there are also a significant number of exceptions to this conformation. This information indicates that the preference of the antiperiplanar form can be outweighed by other energetic factors. In the case of the dimorph II these factors can probably be attributed to the

additional stabilization gained from the s-trans conformation of the α,β-unsaturated system of the C(16)=O(4) carbonyl group.[80] The trans ester group attached to C(12) in dimorph II should clearly disfavor the antiperiplanar conformation since this would project the ethyl group against the neighboring vinyl substituent. The crystallization behavior of the diethyl diester **21** nicely illustrates how some rather drastic structural differences can be explained from very subtle alternatives in a delicate intra-intermolecular energetic balance.

Spectral Differences Between the Dimorphs of Diesters Et/Et-21 and iPr/iPr-23.

Diethyl Diester 21.

1) Solid state FTIR spectra.

The solid state infrared spectra of the two dimorphs of compound **21** were obtained in KBr matrices (Figure 36), while a solution spectrum was run in chloroform for comparison purposes. The number of bands, the relative intensities and the absorption frequencies were found to be strongly dependent on the media. No apparent correlation could be found between the number of bands of the assignable frequencies and the number of molecules per asymmetric unit.[86] A qualitative study of the conjugated ene-dioate spectral portion was attempted since structure-spectral data correlations have been proposed for the similar enoate and enone systems.[62,87] The proposed effects of molecular structure on the absorption

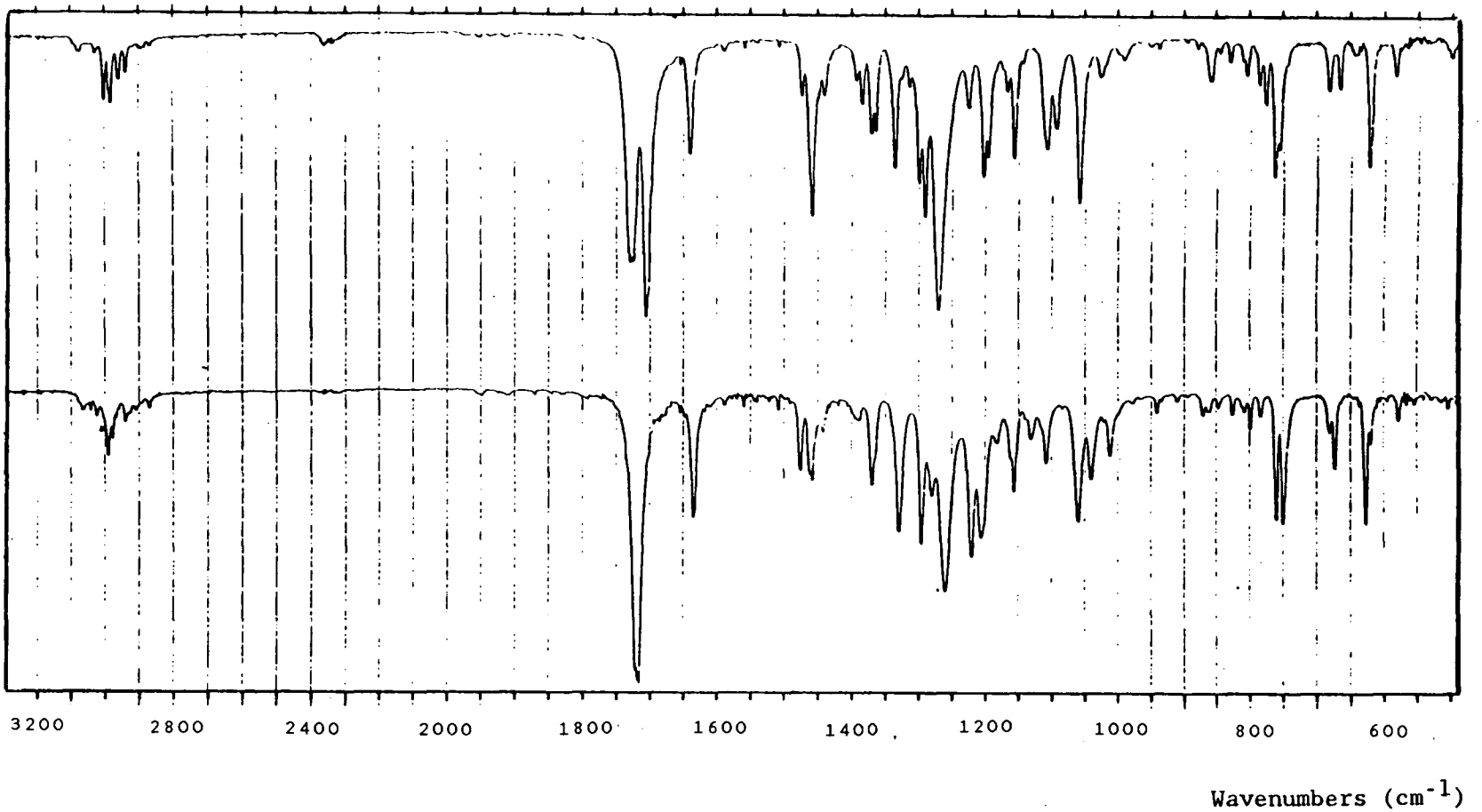

Figure 36. Solid State FTIR Spectra of Diester Et/Et-21 in its $P2_12_12_1$ (top) and $P2_1/c$ Modifications.

frequency of conjugated carbonyl systems are included in the following list.

a) Conjugation with a C=C bond causes the carbonyl stretching absorption to appear at lower frequencies.

b) Steric effects that reduce the coplanarity of the conjugated system reduce the effect of conjugation.

c) Conjugated systems with s-trans conformations will absorb at lower frequencies than the s-cis conformers.

d) The absorption of the olefinic bond in conjugation with the carbonyl group occurs at lower frequency than an isolated C=C bond.

e) The difference in absorption frequency between the conjugated C=O and C=C bonds is smaller for the s-trans ($\Delta\bar{\nu} \leq 60$ cm^{-1}) than for the s-cis forms ($\Delta\bar{\nu} \geq 70$ cm^{-1}).

f) The ratio between the C=O and C=C absorption intensities is greater than 5.2 in the s-trans, and between 0.6 and 3.5 in the s-cis conformers.

The ene-dioate system of dimorph I, as shown in the bottom spectrum of Figure 36, was characterized by a very sharp carbonyl band at 1716 cm^{-1} and a relatively strong vinyl absorption at 1633 cm^{-1}. Dimorph II on the other hand presented two strong carbonyl absorptions at frequencies of 1727 and 1704 cm^{-1} and a relatively weaker vinyl absorption at 1639 cm^{-1}. In solution the ene-dioate system is characterized by a strong carbonyl absorption at 1705, a shoulder at 1710, and a very weak vinyl absorption at 1630 cm^{-1}.

The spectrum of dimorph I was rather surprising in view of the different degrees of conjugation of the two carbonyl groups which were expected to be manifested in the form of two absorption frequencies. The spectrum of dimorph II, on the other hand, seemed to agree well with all the above spectral expectations. The different absorption frequencies of the two carbonyl bands, the position of the vinyl absorption (closer to the presumably more conjugated carbonyl, $\Delta\bar{\nu} = 65\ cm^{-1}$), and the apparent increase in the carbonyl/vinyl intensity ratio all seem to agree well with the presence of an s-trans conjugated and a non-conjugated carbonyl groups in the molecular structure. In the solution spectrum (not shown) the most striking observation relates to the low absorption intensity of the vinyl band which would indicate a preferential s-trans conformation for both carbonyl groups.

The unexpected appearance of the spectrum of form I calls into question the validity of the structure-spectral data correlations as applied to these systems and suggests the operation of specific factors dependent on the crystal structure. The spectral differences between the two dimorphs can almost be observed peak by peak and the value of solid state infrared spectral measurements can be proposed as a valuable aid to differentiate polymorphic materials.[86] Our results should also be considered as a serious warning to the normal procedure of assigning the conjugational properties of carbonyl compounds uniquely from infrared spectroscopic measurements.

2) Solid State CPMAS ^{13}C NMR Spectra.[a]

The solid state CPMAS ^{13}C NMR spectra of dimorphs I and II of diester **21** were recorded at 45 MHz (Figure 37). The molecular disymmetry of both solid state molecular structures was evident from the number of peaks in the spectra. In solution, the spectrum of diester **21** shows only 8 bands indicating an average C_{2v} symmetry. In contrast, the spectrum of dimorph II contains up to 16 resolved bands corresponding to 22 non-equivalent carbons. The assignment of the various peaks, however, seems possible only within groups of structurally similar carbons (methyl, methylene, bridgehead, protonated and tetrasubstituted aromatic and carbonyl carbons). The case of modification I is even more complicated since there are two independent molecules per asymmetric unit.[88] From 44 formally non-equivalent carbon resonances expected, the spectrum was composed of 22 well resolved signals. In contrast to the infrared spectrum where only one carbonyl absorption band was found, the CPMAS ^{13}C NMR spectrum can resolve the four non-equivalent carbonyl carbons into three peaks spread over a range of 11 ppm. There is unfortunately not enough certainty as to the nature of the chemical shift differences in the solid state and this information cannot be directly correlated with the structural properties of the substituent[89] (sometimes, however, assignments can be proposed based on the shifts from the better understood solution spectra).[86,90]

---

a) The CPMAS ^{13}C NMR spectra were kindly recorded by Prof. J. Ripmeester at the Chemistry Division of the National Research Council in Ottawa.

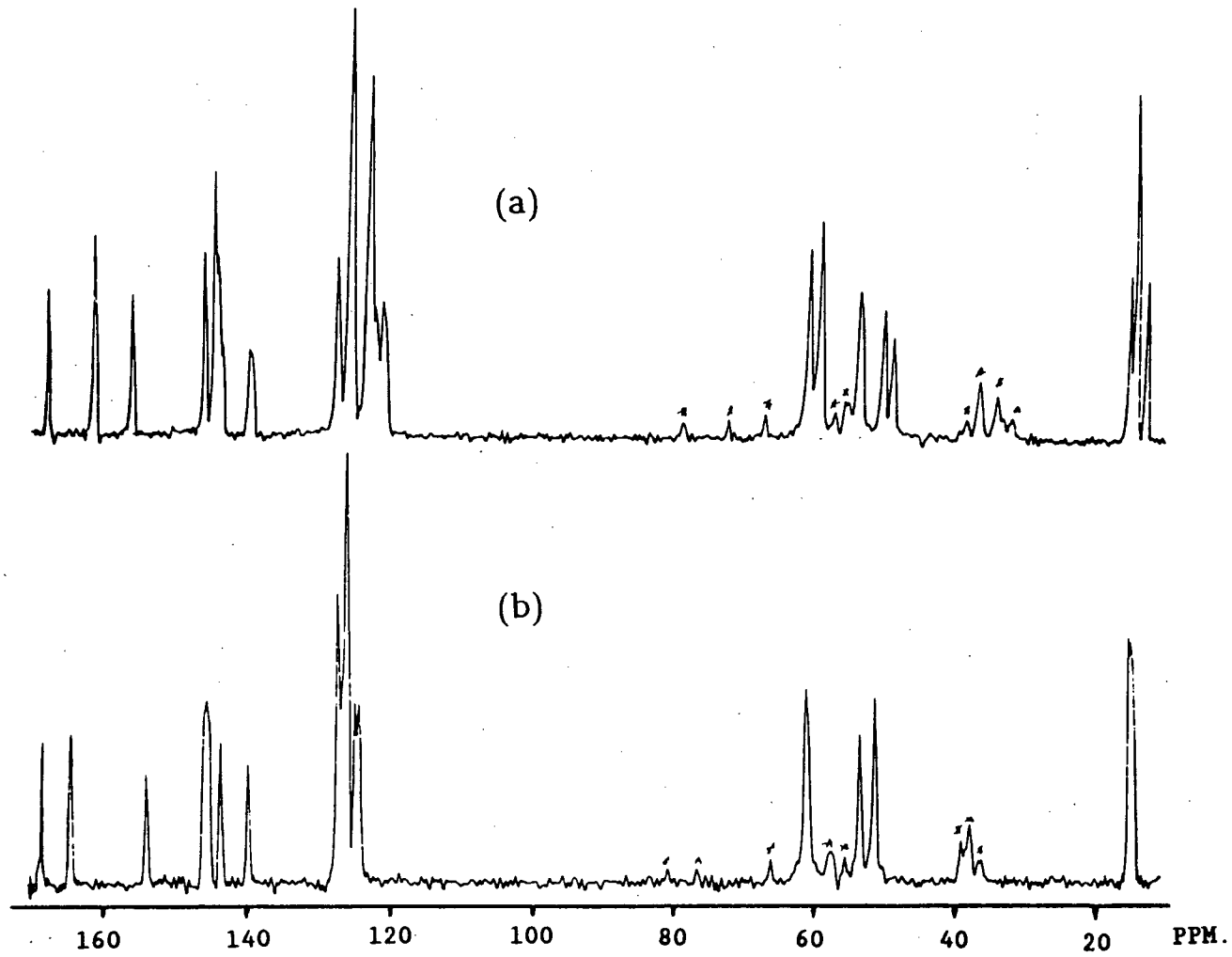

Figure 37. CPMAS ^{13}C NMR Spectra of Et/Et-21 in its (a) $P2_1/c$ and (b) $P2_12_12_1$ Modifications (* = Spinning Side Bands).

Diisopropyl Diester 23.

1) Solid State FTIR spectra.

Even though the molecular structures of the two dimorphs of diester 23 present relatively smaller differences, the two infrared spectra were just as different as those from the dimorphs of the diethyl compound. The ene-dioate band system in the case of the $P2_12_12_1$ modification was similar to the one observed in the equivalent dimorph of the diethyl compound (Figure 38). Two strong carbonyl stretching bands at 1724 and 1704 cm^{-1} were accompanied by the vinyl absorption at 1636 cm^{-1}. The spectrum of the Pbca modification, on the other hand, was composed of only one carbonyl absorption at 1713 cm^{-1} and a relatively weak vinyl absorption at 1635 cm^{-1}. Interestingly, however, some other absorption bands were very similar in both dimorphs. Such was the case in the carbon-hydrogen stretching and bending frequency regions,[62,87] which had been found to be completely different for the two dimorphs of 21. The symmetric and asymmetric C-H bending[11c] of the isopropyl groups, for instance, occurred at 1458 and 1387, 1374 cm^{-1} in the Pbca form, and at 1459 and 1387, 1374 cm^{-1} in the $P2_12_12_1$ modification respectively (doublets in the asymmetric bands are typically observed for isopropyl groups).[62]

There is again no obvious correlation between the expected and observed spectral features of the ene-dioate chromophore.

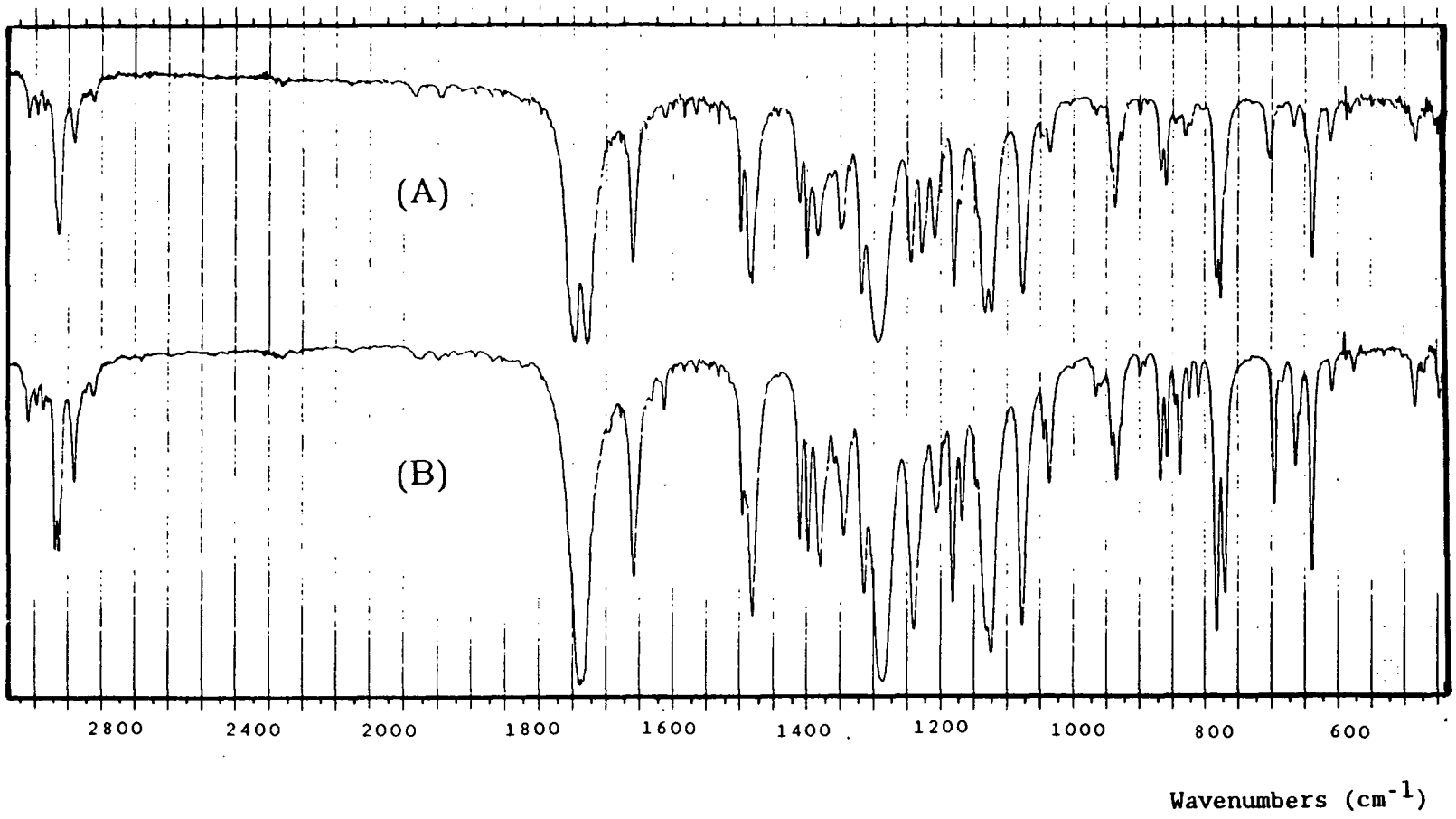

Figure 38. Solid State FTIR spectra of Diester 23 in its (A) $P2_12_12_1$ and (B) Pbca Modifications.

2) Solid state CPMAS ^{13}C NMR spectra.

The solid state spectra of the two dimorphs of the diisopropyl compound (Figure 39) were obtained in the same manner as the spectra of compound **21**. The spectrum of the chiral modification was found to resolve in up to 17 bands from the 24 non-equivalent carbons expected. Excellent resolution was observed in the signals belonging to the carbonyl (δ 165.8 and 163.6), vinyl (152.7 and 144.9), isopropyl methine (69.5 and 68.7), bridgehead (54.3 and 51.7) and all methyl carbons (23.1, 21.9, 20.8 and 19.1), probably indicating substantial molecular dissymmetry. The signals in the spectrum of the Pbca modification did not have much coincidence with the signals of the other dimorph. The spectrum consisted of 19 well resolved bands for the same number of non-equivalent carbons (24). An increased resolution was observed in the tetrasubstituted sp^2 region where all six carbons were well resolved (two vinylic and four aromatic), and in the isopropyl methine carbons that resolved from a $\Delta\delta$=34 Hz in the $P2_12_12_1$ modification to $\Delta\delta$=64 Hz in the Pbca dimorph. The methyl region of this dimorph presented only three signals for the four methyl groups. No obvious correlation can be made between the observed chemical shifts and the previously determined X-ray structures.

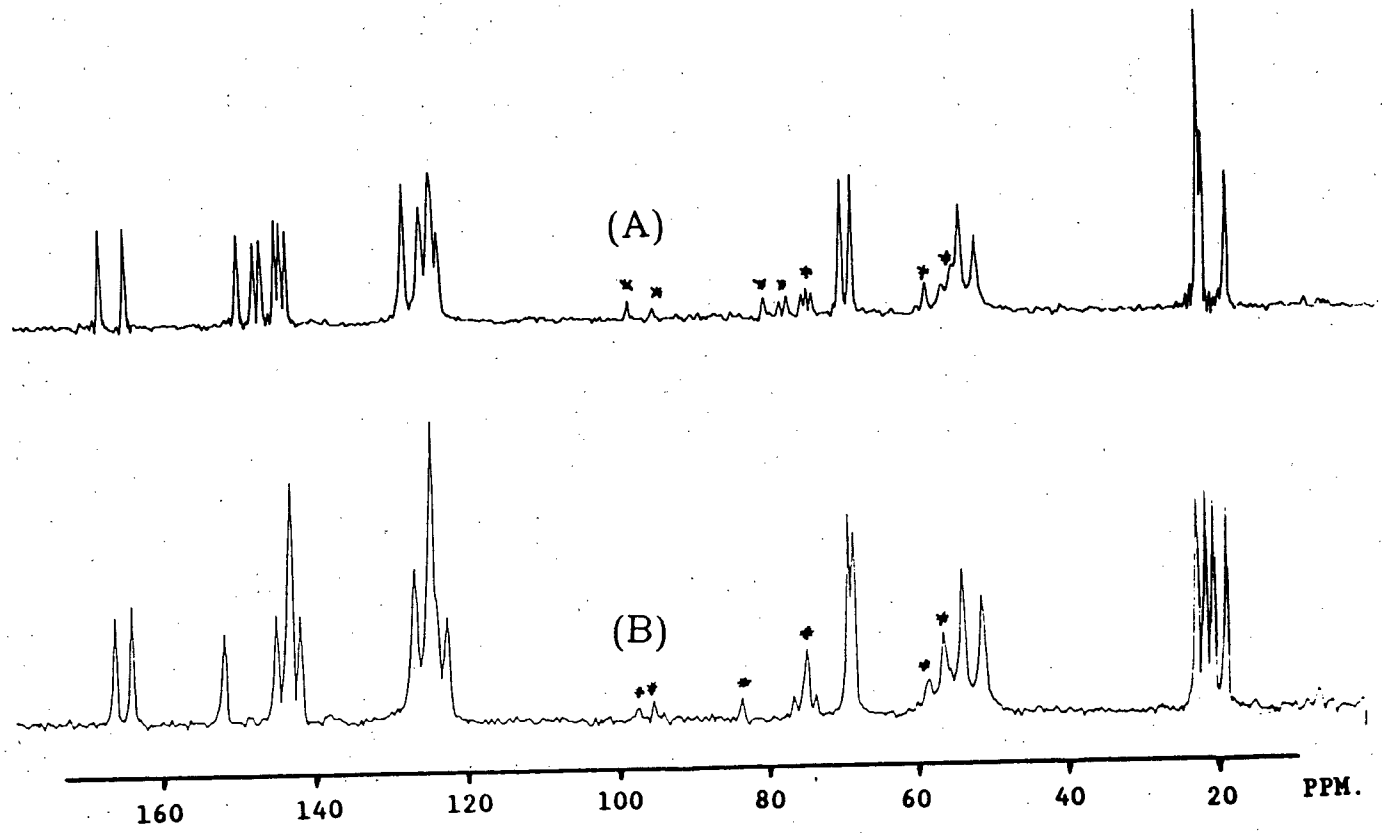

Figure 39. CPMAS ^{13}C NMR Spectra of iPr/iPr-23 in its (A) Pbca, and (B) $P2_12_12_1$ Modifications (* = Spinning Side Bands).

Differences in Reactivity Between Dimorphs.

Differences in the relative reaction efficiency of the solid state rearrangement were noticed between some of the crystalline materials. A particularly interesting case was that of crystals of the diethyl compound **21** in its $P2_12_12_1$ modification which reacted the most sluggishly of all. Single crystals photolyzed for up to 20 min with the nitrogen laser resulted in 2-4% conversion under conditions where the crystals of other compounds had reacted to an extent of 15-25%. Longer irradiations of the unreactive crystals resulted in increased conversions only at the expense of crystal melting.

Specific solid state effects of this nature have sometimes been very valuable in establishing the principles that control a solid state reaction.[1a,90] The opportunity of having a reactive compound crystallizing in different packing and molecular arrangements can sometimes give important clues as to the influence of molecular or environmental solid state effects. In order to have a quantitative measurement relating the reaction efficiency for the different dimorphs of diesters **21** and **23**, their relative quantum yields were measured in a manner similar to that described for diester Me/Me-**18**. The samples were dispersed in KBr matrices and photolyzed with the nitrogen laser using the conditions described before. The percent conversions were determined by observing the consumption of the infrared vinyl absorption of the ene-dioate system of the starting materials after photolysis periods of 30, 60 or 120 seconds. Assuming a constant laser intensity for all samples, differences in conversion after a given photolysis time are due only to differences in

their extinction coefficients and absolute quantum yields.[75] The higher the extinction coefficient or the quantum yield of a crystalline sample, the larger the reaction efficiency will appear. At low conversion values the relative reaction efficiency of two samples is given by the ratio of the amount of products formed after a common irradiation time. The results obtained were normalized with respect to the more reactive diisopropyl compound **23** in its Pbca modification and are presented in Table IV. These results confirmed the initial observation that indicated a distinctively low reactivity for the $P2_12_12_1$ modification of the diethyl compound. Interestingly, the larger differences in the reaction efficiency observed for the dimorphs of compound **21** perhaps reveal the larger differences found in their X-ray crystal and molecular structures. The results presented are also important since they demonstrate the fact that solid state reactions that appear similar from the product analysis point of view may have substantially different kinetic requirements.

Table IV. Relative Reaction Efficiencies of Crystalline Dibenzobarrelene Diesters.

Compound	Space group	Relative Efficiency[a]
18	$P\bar{1}$	1.0
21	$P2_1/c$	0.8
21	$P2_12_12_1$	0.1
23	Pbca	1.0
23	$P2_12_12_1$	0.6

a) Relative conversion values constant within conversions of 3--20%.

Several other examples of polymorphic-dependent reactivity have been recorded in the literature. The effect of polymorphism on the photochemical results from the cinnamic acids was in fact one of the main factors which helped Schmidt and Cohen in establishing the foundations of modern topochemistry.[1a]

The effect of polymorphism on unimolecular photochemical phenomena, which is highly relevant to the cases presented here, has also been the subject of rare but interesting investigations.[90a,91] The effects encountered have been measured mainly from the product analysis point of view, but the kinetics of the reactions, at least in a relative manner, must have been affected as well. Topochemical reactions in polymorphic crystals have been shown to be controlled by their crystal and molecular arrangements.[1a,90] The difference in the chemical behavior between polymorphs depends on the influence of their structures on the reaction mechanism. Cases where two crystal modifications present the same solid state reactivity, which may be totally different from the one observed in solution, may occur if the solid state determining factors are similar. This is precisely the case of the thermally or photochemically generated radical pairs from the dimorphs of azobisisobutyronitrile (77) studied by McBride and co-workers.[91]

The solution reaction of 77 was shown to give four products, 95% of which originate from coupling of the radical fragments A and B (Figure 40). In contrast, in the two crystal forms an indistinguishable reactivity was observed and the preferred products were shown to form from radical disproportionation. It was proposed that in the solid state the formation of products would be impeded by the extruded nitrogen molecule and by

disturbance of the balanced dipolar interactions between the nitrile groups and their neighboring molecules.[91] These disturbances, however, were postulated to be more serious in the case of the motions required for the recombination compared to those required for the alternative hydrogen abstraction that would lead to the disproportionation products. The similarity between the reaction controlling factors was also shown from a 100% cage effect found to operate in both crystal modifications.[91]

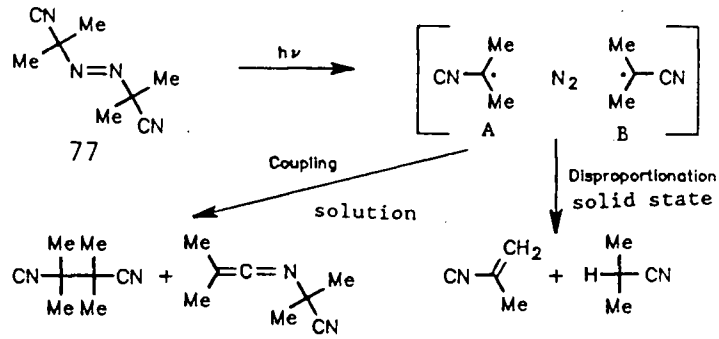

Figure 40. Solution and Solid State Photochemistry of Azabisisobutyronitrile.

Another example of solid state photochemical phenomena, this time with substantial reactivity differences between two dimorphs, comes from the study of the Norrish type II reaction of α-adamantyl-p-chloro-acetophenone (78) studied in this laboratory.[90a] Cis and trans cyclobutanol products were found to form in amounts that depended on the reaction medium (Figure 41). In solution and in one of the crystal forms ($P2_1/n$) large amounts of cis (~30%) and trans (~70%) cyclobutanols were formed. In the other

modification (C2/c) the more stable trans isomer was found to form in quantitative amounts. The remarkable difference between the two dimorphs was found to correlate with the molecular geometry in the two crystal lattices. The geometries of the 1,4-biradicals generated from the initial γ-hydrogen abstraction were found to be very similar, however, the motions required to form the cis cyclobutanol product would be prohibitive in the C2/c modification. Substantial steric hindrance would develop in this case between the edge-on aryl group and the bulky adamantyl moiety. The latter interaction was not present in the $P2_1/n$ modification and was obviously unexpected in the solution media.[90a]

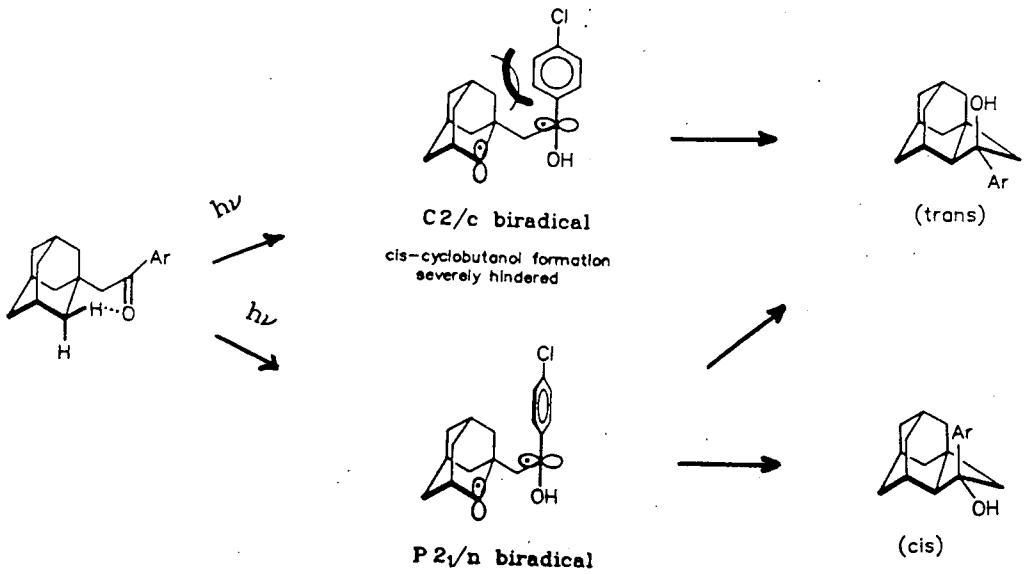

Figure 41. Solid State Photochemistry of α-Adamantyl-p-chloro-acetophenone.

The effects of polymorphism presented above relate to measurable influences of the crystal lattices on the constitution or relative configuration of the products formed. In the case of the symmetric diesters studied in this thesis the reaction model and substrate are not amenable to this type of selectivity. The dibenzosemibullvalene products presented here, however, can be formed by four theoretically different reaction pathways (Figure 42). Two of these pathways (i.e. paths 1 and 2) will give one product enantiomer while the other two (paths 3 and 4) will give the opposite antipode. These alternatives are expected to be all degenerate in isotropic solution media since there is no influence that may favor the preferential formation of any of them. In the solid state, on the other hand, the molecular structures and crystal environments have been found to be disymmetric therefore making the four reaction pathways no longer equivalent. Under these conditions the solid state reaction is expected to be stereoselective and give preferentially products arising from one of the four alternative reaction pathways shown in Figure 42. Since this stereoselectivity refers to the unequal formation of enantiomeric products, as we will see, it will be amenable to experimental determination in the case of the crystal with a chiral space group.

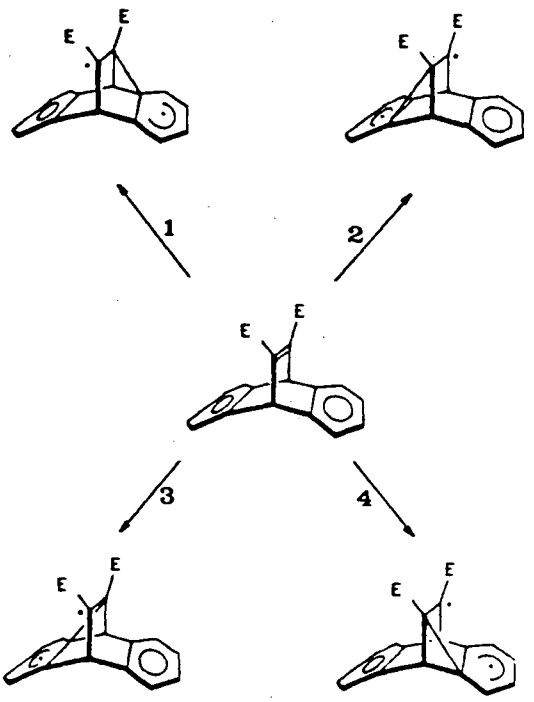

Figure 42. The Four Reaction Pathways of Symmetrically Substituted Dibenzobarrelene Diesters.

Molecular and Crystal Chirality.

An interesting feature, common to all the diesters studied up to this point, is the disymmetry of their solid state molecular structure. The consequences of structural disymmetry on chemical reactivity are very profound and require additional comment.[92]

Chirality is the non-identity of two objects that are related by a mirror symmetry relationship and is a property that can be common to molecules and crystals.[92] A crystal is said to be chiral if it lacks

symmetry operations such as inversion centers, mirror and glide planes that convert an object into its antipode. Crystal chirality does not require permanent molecular chirality since a chiral periodic ensemble can be constructed by organizing any repeating object in a disymmetric, three dimensional arrangement. While homochiral molecules must always form chiral crystals, achiral and racemic compounds can also sometimes crystallize in chiral space groups.[93]

Crystal chirality without molecular chirality is relatively rare. From the 230 possible ways (space groups) of building a crystal, it has been demonstrated that 65 can be categorized as chiral.[94] It has been noticed that two space groups are the most commonly found, $P2_12_12_1$ and $P2_1$, and account for approximately 18% of all the crystal structures determined up to 1983.[95] This percentage, however, is probably dominated by chiral molecules from natural sources with only a small amount corresponding to compounds that are achiral in solution. Crystal chirality without molecular chirality can be found in compounds that can be classified in two general categories according to their liquid phase conformational characteristics:[92a,93] (1) flexible molecules that adopt chiral conformations in the solid state, while in solution maintain an average molecular symmetry through fast conformational motions, and, (2) rigid molecules that, except for minor deformations, cannot form significant chiral conformations in solution or in the solid state. This distinction is sometimes useful when one considers the separate contributions of molecular and crystal lattice chirality in a solid state chemical reaction.[92]

The diesters **21** and **23** clearly fall in the first category and can be

considered to undergo a process analogous to the classic "spontaneous resolution" of binaphthyl studied by Pincock.[96] Nucleation here can occur in the racemic ($P2_1/c$ and Pbca) and the chiral ($P2_12_12_1$) modifications of **21** and **23** respectively. If nucleation occurs in one of the racemic crystals, the two enantiomers will be present in equal amounts in conformations that may be similar to (compound **23**), or very different (compound **21**), than the one observed in the chiral modifications. If nucleation occurs first in a chiral modification the entire sample, which is in dynamic enantiomeric equilibrium in solution, may crystallize with only one chirality.[96,97,98]

Since two crystal forms usually differ in energy[92] there exists the possibility that preferential crystallization of one of them will be favored under a given set of experimental conditions. Diester **23** was found to be such a case since crystallization from the melt or cyclohexane was found to give specifically crystals of the $P2_12_12_1$ and Pbca modifications, respectively. Sometimes, however, the conditions for nucleation are so similar that either form can appear under repeatedly similar conditions as was the case with diester **21**. Fortunately in the case of this compound the rate of crystal growth seemed to be so large with respect to the nucleation rate that pure crystals of the presumably first seed formed precipitated the entire sample.

Absolute Asymmetric Synthesis.[92]

Asymmetric synthesis was defined by Markwald[99] in 1904 as "a reaction which produces optically active substances from symmetrically constituted

compounds with the intermediate use of optically active materials but with the exclusion of all analytical processes." Later, this definition was modified by Morrison and Mosher[100] in order to include other stereochemical aspects such as diastereoselectivity: "Asymmetric synthesis is a reaction in which an achiral unit in an ensemble of substrate molecules is converted by a reactant into a chiral unit in such a manner that the stereoisomeric products are produced in unequal amounts."

At the present time, the main goals of asymmetric syntheses are more in line with Markwald's definition since enantioselective asymmetric synthesis has become without doubt one of the most important challenges of synthetic chemistry.[101] The asymmetric synthesis process occurs because the transition states of the normally degenerate enantiomeric reaction pathways are rendered energetically different, or diastereomeric in nature, by the disymmetric chiral influence.[102,107] Research in this area has brought an increasing number of literature reports where optically active products have been generated through the influence of resolved reagents,[100,101] catalysts,[100,103] solvents,[104] host molecules[105] and also, with very modest success, with physical agents such as circularly polarized light.[106]

A very special circumstance may arise when the disymmetry originates from the chiral environment or molecular structure that many compounds display in the solid state.[92] If these compounds are symmetric in solution and their chirality can only exist in the solid state the scenario is set for the intriguing possibility of an absolute asymmetric synthesis if a solid state reaction converts the crystal chirality into permanent molecular chirality. It should be noted that the term absolute asymmetric

synthesis refers more to the fact that these processes can generate optically active products without imposition by man of any external chiral influence than to the formation of products in quantitative enantiomeric yield.[92a]

The formation of optically active substances from achiral starting materials has been one of the most dramatic demonstrations of the capabilities of solid state chemistry. Although the possibility of exploiting crystal chirality for the purpose of asymmetric synthesis was recognized over 80 years ago by Ostromisslensky,[108] it was not until the 1960s that this became an experimental fact. Following a pioneering report by Farina and Natta[109] on the use of crystalline chiral inclusion compounds to induce enantiospecific polymerization, Schmidt and Penzien[110] demonstrated the feasibility of asymmetric induction by chiral crystals of achiral compounds in the solid state by bromination of p,p-dimethyl-chalcone. Subsequent work carried out by workers at the Weizmann Institute of Science brought about remarkable developments in the field by making use of the well known [2+2] photocycloaddition reaction of crystalline olefins.[111] The results described by these workers over a period of about ten years constituted the rational development of feasible reaction models through some of the first and most elegant examples of crystal engineering.[112a-d] The problems to overcome came from the requirements for cycloaddition which include a parallel face-to-face orientation between the two double bonds with a center-to-center distance of less than approximately 4.2 Å.[1a,9,10] Monoolefinic compounds can have this arrangement in the solid state when the two molecules undergoing dimerization are related by a translation axis, inversion center or a

mirror plane. As mentioned before, only the first symmetry element is allowed in a chiral crystal, and simple olefinic compounds would give products necessarily having a mirror plane perpendicular to the translational axis.[112a] This situation was found to be the case in chiral crystals of the achiral diarylbutadienes **79** and **80** (Figure 43) which were found to crystallize in the chiral space group $P2_12_12_1$. While photolysis of these compounds gave the expected mirror-symmetric cyclobutanes **81** and **82** respectively, the possibility of generating optically active products was made effective by preparing dilute solid solutions of compound **80** in crystals of compound **79** and photolyzing the former in a selective manner. The mixed dimer **83** was satisfyingly found to be formed with an enantiomeric excess of 70%.[112a]

Further work in this area was focussed on a reaction model that included the use of chiral crystals of disubstituted diolefinic compounds with the general structure **84**, in Figure 44. The strategy employed was based on the initial use of the optically active material **84-sBu** [R= (R)-or (S)-sec-butyl] in order to ensure crystals with a chiral space group. This compound was subsequently used as a crystal template from which crystals of other achiral compounds could be designed and photolyzed to give optically active products. The approach was quite successful and has been the topic of detailed analysis in several review articles to which the reader is referred in order to obtain additional information.[92,112b,c]

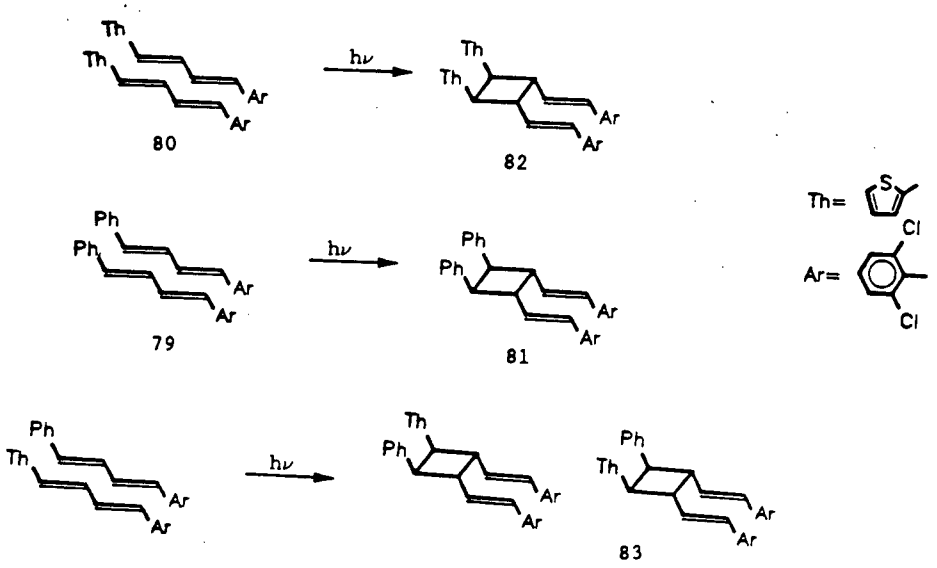

Figure 43. Solid State Photochemistry of Chiral Crystals of Pure and Mixed Aryl Butadienes.

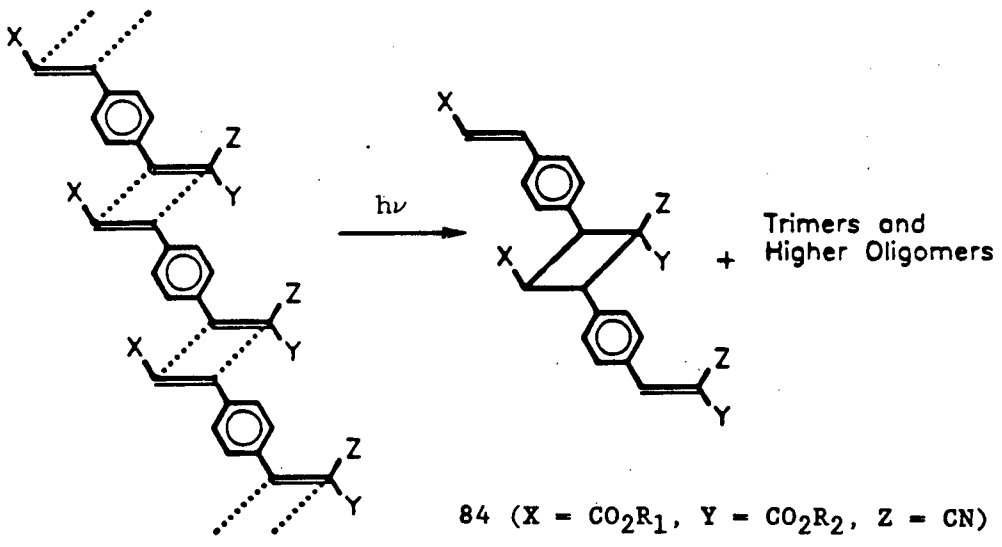

Figure 44. Asymmetric Synthesis by Reaction of Unsymmetrically Substituted Vinyl Diacrylates.

Asymmetric Synthesis by Reaction of Diethyl Diester 21.

Four chiral single crystals of **21** selected at random, one crystal of the racemic modification and 1 ml of a 0.1 M benzene solution were photolyzed with the nitrogen laser for 20 min at ambient temperature (20°C). Although the same photolysis product was detected in all the samples by glc analysis, polarimetric analysis revealed optical activity only in the case of the chiral crystal irradiations (Table V). The optical rotation of the samples containing chiral products varied by as much as a factor of two. However, when the specific rotations were calculated, the specific rotation of all four samples was found to be constant within approximately 5%. The specific rotation of the photoproduct **55** from each sample was calculated from the weight of the crystal and the percent conversion determined by glc. The substantial amounts of unreacted **21** contribute nothing to the rotation since this compound is achiral in solution.

The low conversions obtained in these experiments confirmed the previous observation of the relatively low reaction efficiency of **21**. It was also observed that longer photolysis periods did not increase the amount of product without resulting in significant crystal melting.

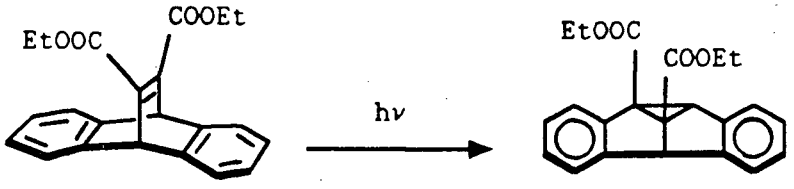

21 55

TABLE V. Solid State Induced Optical Activity in Crystals of 21

w (g)	space group	α_D[a]	% conversion	[α]D	melting
0.1303	$P2_12_12_1$	0.050	2.8	13.6	no
0.9650	"	0.040	2.9	14.3	no
0.0824	"	0.036	3.2	13.7	no
0.2024	"	0.056	2.0	13.8	no
0.0236	$P2_1/c$	0.000	12.3	0.0	no
Solution	-	0.000	96.0	0.0	-

a) Reading uncertainty ± 0.002°

The enantiomeric excess of the dibenzosemibullvalene **55** was determined by ^1H NMR chiral shift reagent studies.[113] A sample of racemic dibenzosemibullvalene **55** was first analyzed with the chiral shift reagent $Eu(hfc)_3$ [3-(heptafluoropropyl hydroxymethylene)-d-camphorato)europium (III)] in order to analyze the possibilities of suitable enantiomeric resolution. The non-equivalent protons Ha, Hb, Hc and Hd (two diaste-

reotopic pairs in Figure 45) of the methylene groups of the ester substituents presented significant resolution after addition of 1 eq of $Eu(hfc)_3$. Two overlapping multiplets initially at 4.32 (Hc and Hd) and at 4.15 ppm (Ha and Hb) shifted and resolved into six out of the eight possible signals, four non-equivalent protons each as an enantiomeric pair: (+)-Ha, (-)-Ha, (+)-Hb, (-)-Hb, etc., at 5.20 (1H), 5.05 (1H), 4.70 (1H), 4.5-4.3 (4H) and 4.10 (1H).

Although assignment of the resolved signals, as arising from the chemical non-equivalence or from the enantiomeric resolution is not possible with this information, it was presumed that analysis of the optically active material should shed some light on this question.

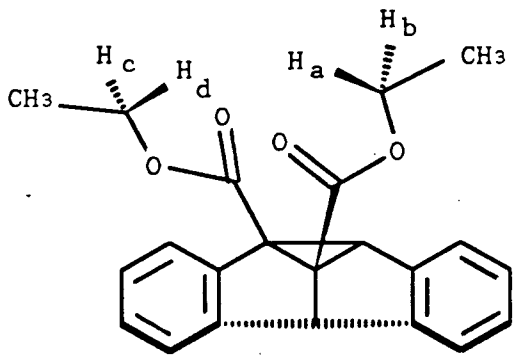

Figure 45. The Four Non-Equivalent Protons in the Methylene Groups of the Diethyl Dibenzosemibullvalene Diester **55**.

A single crystal of **21** weighing 65.4 mg was photolyzed with the nitrogen laser for approximately three hours at -10 °C in order to get the largest possible conversion. After photolysis the crystal presented evidence of melting and the conversion and specific rotations were

determined to be 13.2% and 10.8° respectively. When analyzed with 1 eq of the chiral shift reagent this sample presented resolution similar to the pure racemate but with a significant interference from the signals of the starting material (86.8%) around 4.5 ppm. However, the two signals at the lower end of the methylene section were found (similar to the previous experiment) at 5.50 and 5.30 ppm. Since the relative intensity of these two signals was found to be in a ratio of 4 to 1 (± 10%) we concluded that they must be assigned as belonging to the two different enantiomers. Integration from two chemically non-equivalent protons of the same enantiomer would be expected to be identical.

The relative intensity of these two signals corresponds to an enantiomeric excess (e.e.) of 60%. This enantiomeric excess suggests that the samples photolyzed to low conversions present an optical purity of 80% and a maximum optical[114] rotation of ca. $[\alpha]_D max=18°$.

Asymmetric Synthesis by Reaction of Diester 23.

The asymmetric induction in the chiral crystals of compound 23 was studied in a manner similar to that described for compound 21. As before, the specific optical rotation from a relatively large number of samples was found to be consistent and fairly high. The percent conversion, however, could be varied from 2 to 22% with no apparent prejudice to the specific optical rotation obtained. The first two entries in Table VI correspond to crystals from the first, spontaneously obtained material, and the samples that follow correspond to a second batch where crystallization was deliberately induced by seeding of a solution of diester 23.

TABLE VI. Solid State Induced Optical Activity in Single Crystals of 23

w (g)	space group	α_D	% conversion	$[\alpha]_D$	batch*
0.0515	$P2_12_12_1$	+0.102	15.5	+25.6	1
0.0325	"	-0.016	1.8	27.7	1
0.0212	"	-0.072	13.4	-25.3	2
0.0229	"	-0.120	22.1	-23.7	2
0.0273	"	-0.107	17.6	-22.3	2
0.0842	"	-0.222	9.4	-28.2	2
0.0195	"	-0.066	18.2	-18.6	2
0.0318	"	-0.163	20.9	-24.5	2
0.0451	"	-0.212	22.2	-21.2	2
0.050	Pbca	0.000	20.0	0.0	-
Solution	-	0.000	95.0	0.0	-

*Batch 1 obtained by spontaneous crystallization. Batch 2 obtained by deliberate seeding.

The optical yields of the chiral diisopropyl dibenzosemibullvalene photoproduct **57** were investigated in a similar manner as for the diethyl diester **55** by chiral shift reagent analysis. The enantiomeric resolution ($\Delta\Delta\delta$) of the two non-equivalent isopropyl methine protons, $-C\underline{H}(CH_3)_2$, was obtained after addition of 1 eq of $Eu(hfc)_3$. From original chemical shifts at δ 5.20 and 5.00 (the latter signal overlapping with a singlet of H(C4b), the isopropyl methine multiplets shifted and split into four signals at δ 5.73, 5.63, 5.20 and 5.08 (Figure 46).

In order to estimate the enantiomeric purity of the chiral photopro-

ducts the chiral shift reagent analysis was performed on two different samples. The first sample came from a single crystal photolyzed to 15% conversion ($[\alpha]_D$ = -25°) from which the product was not separated in order to avoid alteration to the enantiomeric content during purification (recrystallization). The second sample was obtained by partially recrystallizing the products from a number of single crystals until a purity of 66% could be reached ($[\alpha]_D$ = - 24.6°).

The spectra obtained in both experiments were consistent with each other. Two signals (δ 5.95 and 5.25) were clearly observed under conditions where the racemate had presented four. The spectrum shown in Figure 46 clearly indicates a quantitative enantiomeric excess within the limitations of the method (e.e.≥97%). The results presented here are the first of their type in that (1) they represent the first example of a solid state asymmetric synthesis through a unimolecular photochemical reaction and (2) for the first time consistently high enantiomeric yields are obtained over a relatively large number of experiments.[115]

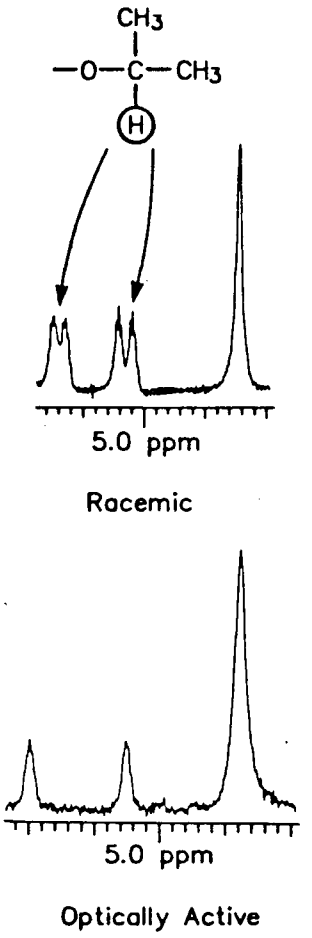

Figure 46. Partial ^{1}H NMR Spectra (300 MHz) of Racemic (top) and Optically Active (bottom) Diester 57 after Addition of 1 eq of $Eu(hfc)_3$.

The optical yields reported for all previous examples of solid state asymmetric syntheses, all in bimolecular reactions, have been capricious and sometimes found to vary from zero to 100%.[112] Our results suggest that unimolecular reactions may have some advantages over their bimolecular counterparts. First, unimolecular reactions do not in principle require specific <u>intermolecular</u> arrangements which may decrease the chances of finding a suitable chiral crystal structure. Second, each chemical event in a bimolecular reaction involves disturbance of two lattice sites rather

than one, and this may lead to a faster loss of topochemical control which translates into a decrease in asymmetric induction.[115]

Mechanistic Implications of the Solid State Asymmetric Synthesis.

The results obtained with both sets of dimorphs, from diesters **21** and **23**, clearly indicate that the di-π-methane rearrangement of crystalline dibenzobarrelene compounds is a highly stereoselective and stereospecific reaction. If we assume the biradical mechanism proposed by Zimmerman,[46] the first, product-determining step necessarily involves bond formation between one of the carbon atoms of the vinyl group and a nearby aromatic carbon atom. Since there are two reaction sites, C(11) and C(12), and two faces of the vinyl π-system, there are four possible benzo-vinyl bridging modes, paths 1-4 (Figure 42), all of which are isoenergetic in isotropic solution as discussed before. In the solid state, starting from one dibenzobarrelene enantiomer, paths 1 and 2 lead to one dibenzosemibullvalene enantiomer, and paths 3 and 4 give the other.[116] The fact that the reaction proceeds with 100% enantioselectivity in the case of diester **23** indicates that there is total discrimination between paths (1 + 2) versus paths (3 + 4). These results, however, do not tell us whether (1 + 2) is favored over (3 + 4), or vice versa, nor do they give any information regarding the relative importance of path 1 versus path 2, or of path 3 versus path 4.

It is possible however to differentiate between paths (1 + 2) and (3 + 4) by determining the absolute configuration of the starting material and correlating it with the absolute configuration of the photoproduct.

Studies of this type were carried out.

Correlation of the Absolute Stereochemistry of the Crystalline Diisopropyl Diester pro-(-)-23 ($P2_12_12_1$ form) and its Optically Pure Photoproduct (-)-Dibenzosemibullvalene 57.

A large single crystal (55 mg) of pro-(-)-**23** was grown by slow evaporation from a seeded (batch 2) ethanol solution. A small fragment was cut and X-ray anomalous dispersion analysis was performed[143] to obtain the absolute configuration of diester pro-(-)-**23** by using oxygen as the heavy atom. At the same time the remaining fragment was photolyzed and confirmed to give levorotatory photoproduct ($[\alpha]_D$ = -25.4, $CHCl_3$). The X-ray results indicated that pro-(-)-**23** corresponds to the absolute configuration designated as 11P, 12M by the conformational chirality formalism.[117] The designation 11P, 12M focuses on the conformational disymmetry conferred to the molecule by the ester groups at C(11) and C(12) (Figure 48a). In this approach one determines the smallest torsion angle between the groups of highest priority, or fiduciary groups, attached to each end of the single bond about which the conformation is to be specified: torsion angles O(2)-C(13)-C(11)-C(12) and O(4)-C(17)-C(12)-C(11). A positive torsion angle (clockwise rotation) is designated P (plus) and a negative torsion angle (counter-clockwise rotation) is designated M (minus).

In order to obtain the absolute configuration of the levorotatory product (-)-**57**, a sample of this material was isolated by fractional crystallization, up to 56% pure, and then further purified by derivatizing

the remaining starting material with diazomethane and following by chromatographic separation. Crystallization of pure (-)-57 was easily achieved from ethanol to give perfectly square crystals (space group $P4_32_12$) suitable for X-ray anomalous dispersion crystallographic analysis.[118] The absolute configuration of the four chiral centers, as shown in Figure 47, was found to be (S)-4b, (S)-8b, (S)-8c, and (S)-8d (due to the different numbering used in the crystallographic analysis the absolute configuration in Figure 48c can be described as: (S)-9, (S)-10, (S)-11 and (S)-12).

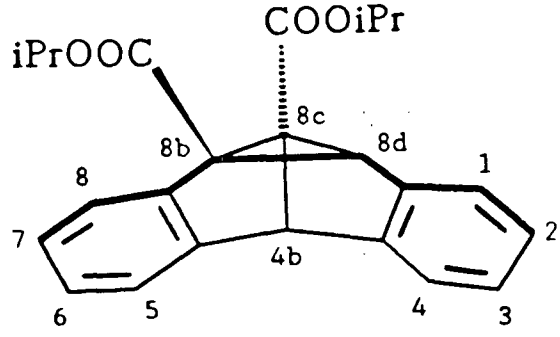

Figure 47. Absolute Configuration of Diester (-)-57.

As indicated in Figure 49, where drawings of the reactant and photoproduct absolute configuration are given, the di-π-methane rearrangement of pro-(-)-23 proceeds either via path 1, path 2 or a combination of the two. It is interesting to notice that path 2, with a small amount of atomic and molecular motions, would lead to a photoproduct structure that resembles the X-ray derived structure 57-I. Path 2 on the other hand, also assuming the least amount of molecular motion, which involves no change in the relative orientation of the ester groups during the reaction, would lead to structure 57-II.

(A)

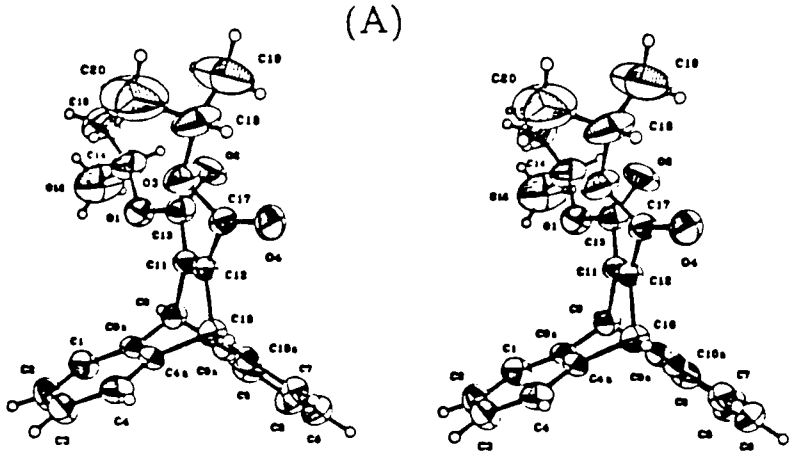

(B)

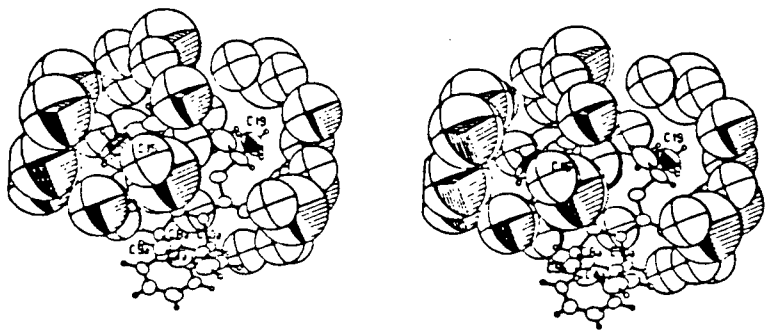

(C)

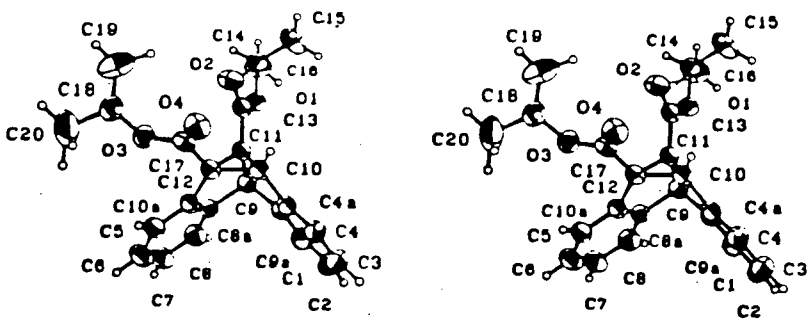

Figure 48. Stereodiagrams with Absolute Configuration of: (a) Diester 23 in the Pro-(-) Enantiomorphic Phase , (b) Local Lattice Environment of Diester 23, and (c) Diisopropyl Dibenzosemibullvalene (-)-57.

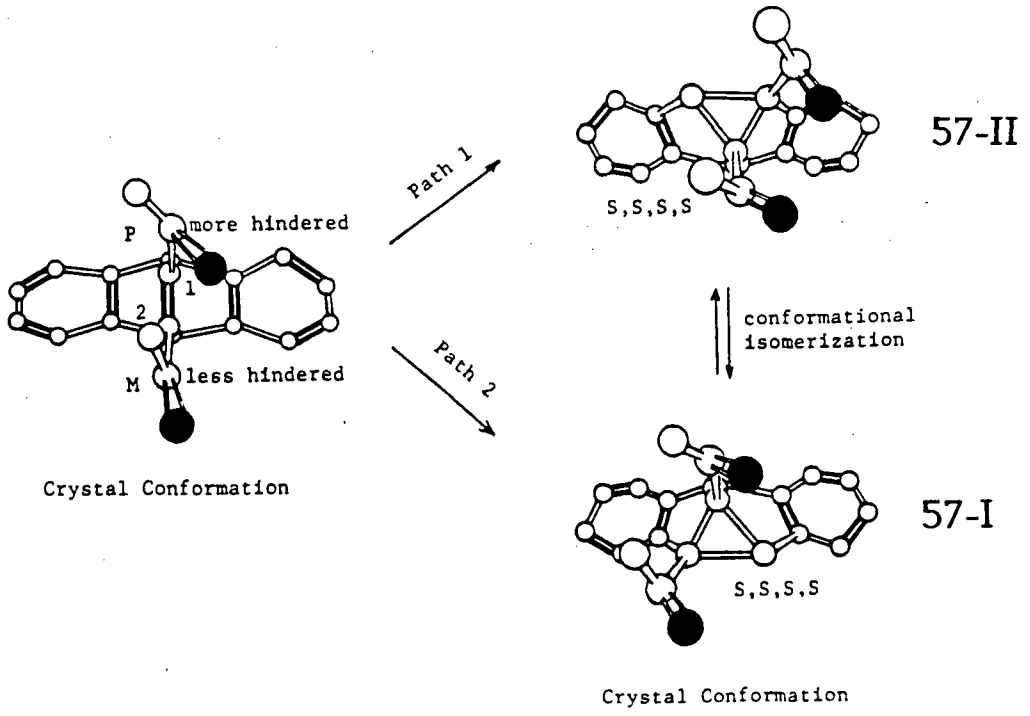

Figure 49. Possible Reaction Pathways of Diester 23 that Account for the Observed Absolute Configurations.

It is known that the preferred conformation of carbonyl groups attached to cyclopropane rings is a cis-bisected conformation.[119] This feature, present only in the X-ray molecular structure 57-I, supports the involvement of pathway 2. It seems possible, however, that this pathway may be the preferred one not only from the point of view of conformational arguments. Paths 1 and 2 involve aryl-vinyl bridging between C(11)-C(9a) and C(12)-C(10a) respectively. Inspection of the local lattice environment indicates that the free space surrounding the ester group at C(12) is larger than the free space surrounding the ester at C(11). This aspect can be appreciated in Figure 48b where diester 23 is shown with the van der Waals contact atoms at d ≤ 3.3 Å.

It should be considered that other factors, such as differences in the stereoelectronic influence of the two carbonyl groups, may also play

important roles in the reaction. The work to be described in Part III of this thesis is aimed at exploring the effects of the solid state on products that differ because the reaction takes place at the two alternative vinyl carbons. As we shall see, the results reported there will further support the involvement of path 2 on the basis of crystal lattice steric effects.

Studies on The Spontaneous Resolution of Diester 23.

The crystals from batch 2, whose photolysis was reported in Table VI, were deliberately seeded because this experiment was planned and realized before we found a convenient way to prepare selectively and identify the crystals of the chiral diisopropyl modification. Once a method was established it was desirable to analyze the spontaneity of the resolution of diester 23 into the crystals of the two possible enantiomorphous modifications.[96-98] The two enantiomorphous phases were labeled as the pro-(-)-, or pro-(+)-enantiomorphs depending on the sign of the optical activity that the crystal confers to the products. In principle it is expected that the two enantiomorphous phases will occur with statistical probabilities unless a foreign chiral influence induces preferential crystallization of one of the two enantiomorphs.[108,97] Identification of any such chiral influence is extremely significant since a mechanism that provides the means for an absolute asymmetric synthesis with preferential formation of only one of the two possible enantiomeric products is highly relevant to the question of how optical activity could have originated under prebiotic conditions.[92,112,120] Before describing in detail the

studies performed to detect the probable nature of this chiral influence, the methods used to identify each crystal modification should be mentioned briefly.

Differentiation between the $P2_12_12_1$ and Pbca dimorphs of 23 was attempted by several methods. Visual and microscopic identification of the two dimorphs was ambiguous and serious attempts to find even subtle differences in their morphology were unsuccessful (microscopic analysis with polarized light was, however, not attempted). Solid state infrared spectroscopy was found to be a useful tool (see page 91). This method, however, was too time consuming and therefore inappropriate for analyzing a large number of crystals obtained from several crystallization batches. The best analytical method was discovered from the unique luminescence behavior that the crystals of the $P2_12_12_1$ modification display when illuminated with the nitrogen laser. Chiral crystals of diester 23 were found to present a very intense red luminescence that develops over a period of few seconds of laser irradiation (see PART V of the thesis). Since the accumulation of photoproduct would be undesirable under identification procedures, the irradiation can be quickly performed at very low temperatures, by immersing the crystals contained in a proper vessel into a liquid nitrogen bath. Since this luminescence is totally absent in the crystals of the Pbca modification and the procedure takes only about twenty seconds per crystal, this was the identification method of choice.

1) Enantiomorphism of Chiral Crystals of Diester 23 from Ethanol Solution.

A sample consisting of 800 mg of diester 23 was dissolved and kept in boiling ethanol for few minutes before it was allowed to crystallize by slow evaporation. The largest crystals were collected and classified as belonging to the racemic or chiral modifications. The chiral crystals were then photolyzed and the optical and specific rotation of the photoproducts were measured and calculated. The results presented in Table VII indicated a striking and absolute preference for material crystallizing in the pro-(-)-enantiomorph of diester 23. Further experiments were primarily directed to test the involvement of a chiral impurity or seed in determining such enantioselective crystallization.[97]

Table VII. Photolysis of Single Crystals of 23 from Batch 3.

w (g)	space group	α_D	% conversion	$[\alpha]_D$	batch*
0.0319	$P2_12_12_1$	-0.038	4.1	-29.0	3
0.0265	"	-0.050	7.4	-25.5	3
0.0230	"	-0.038	6.7	-24.7	3
0.0327	"	-0.052	5.1	-31.2	3
0.0267	"	-0.027	3.1	-32.6	3
0.0292	"	-0.028	3.4	-28.2	3
0.0453	"	-0.095	8.3	-25.3	3
0.1255	"	-0.093	2.6	-28.5	3
0.0292	"	-0.066	10.4	-21.7	3
0.0230	"	-0.047	8.1	-25.2	3

*Batch 3 was obtained from ethanol solution without deliberately seeding.

2) Enantiomorphism of Chiral Crystals of Diester 23 Grown from the Melt in Open Containers.

Six samples of diester **23** of approximately 100 mg were placed in long necked, 1 ml vials, introduced in a Kugelrohr oven, melted, and kept 20°C above their melting point for 20 min in an attempt to destroy the suspected seeds. The viscous liquid was allowed to crystallize by lowering the temperature to 10°C below the melting point of 145°C. Crystallization of the whole sample was complete after no more than 10 min and in all cases the material obtained turned out to be of polycrystalline appearance. The samples were photolyzed, 1 ml of $CHCl_3$ was added, and their optical rotations and percent conversions were measured. The results in Table VIII indicate still an absolute preference for the pro-(-)-enantiomorph. Surprisingly, the magnitude of the rotations encountered in these experiments clearly indicated optical purities comparable to those obtained from the single crystalline specimens.

Table VIII. Photolysis of Chiral Crystals of 23 from Batch Melt I

w (g)	space group	α_D	% conversion	$[\alpha]_D$	batch
0.1228	$P2_12_12_1$	-0.245	8.5	-23.5	melt I
0.1093	"	-0.221	9.6	-21.1	melt I
0.0973	"	-0.160	7.0	-23.5	melt I
0.1148	"	-0.171	6.3	-24.5	melt I
0.1249	"	-0.196	6.5	-24.1	melt I

3) Enantiomorphism in Crystals of Diester 23 Grown from the Melt in a Sealed Container (A).

The experiment described in (2) was repeated by sealing the sample vials before melting. The analysis of the enantiomorphous phase of the starting material was performed in the usual way, by observing the rotation of the products, and to our surprise, the results obtained were much in the same line as those presented in the previous experiment. Seven out of nine samples were still pro-(-) and the optical purity of the samples, as deduced from that of the photoproduct, was still very high.

Table IX. Photolysis of Chiral Crystals of 23 from Batch Melt II.

w (g)	space group	α_D	% conversion	$[\alpha]_D$	batch
0.0540	$P2_12_12_1$	-0.147	11.4	-23.9	melt II
0.0614	"	+0.153	11.1	+22.5	melt II
0.0515	"	+0.171	14.6	+22.7	melt II
0.0636	"	-0.159	11.0	-22.8	melt II
0.0678	"	-0.215	14.4	-22.0	melt II
0.1016	"	-0.210	9.6	-21.5	melt II
0.0952	"	-0.236	12.7	-19.5	melt II
0.1026	"	-0.176	8.6	-20.0	melt II
0.0996	"	-0.189	9.6	-19.8	melt II

4) Enantiomorphism in Crystals of Diester 23 Grown from the Melt in a Sealed Container (B).

The experiments performed up to this point were very intriguing since all attempts to destroy the presumed seed were unsuccessful even under the careful conditions employed. The involvement of an adventitious chiral impurity seemed rather remote since the glc purity of the samples employed was 100% under conditions where impurities of the order of 1/2000th (integrated glc area = 0.05) would have been detected easily (provided they had similar detector response and did not have identical retention time as 23). In order to exclude completely the possibility of having a "resistant" seed accompanying all the samples analyzed so far, we designed the following experiment: a sample consisting of 1.5 g of diester 23 was dissolved in cyclohexane in order to obtain crystals of the racemic, Pbca, modification. The largest single crystals were collected and their dimorphic identity confirmed. The crystals were deposited again in individual vials, sealed, melted and then allowed to crystallize.

The first significant observation was a clearly distinctive tendency for the samples to form supercooled glassy material instead of the previous tendency for fast crystallization. Attempts to induce crystallization by touching the vials with a piece of dry ice were unsuccessful. Crystallization could be induced however when the vials were opened and pricked with a rigorously flame-cleaned stainless steel needle. The samples were then photolyzed and analyzed as before and the results are shown in Table X.

Table X. Photolysis of Chiral Crystals of 23 from Batch Melt III.

w (g)	space group	α_D	% conversion	$[\alpha]_D$	batch*
0.0636	$P2_12_12_1$	+0.084	6.0	+22.0	melt III
0.0781	"	+0.066	4.5	+18.8	melt III
0.1704	"	+0.052	4.9	+18.2	melt III
0.1004	"	-0.112	5.5	-20.3	melt III
0.1242	"	-0.173	6.0	-10.6	melt III
0.1047	"	-0.119	4.7	-24.2	melt III
0.1027	"	+0.124	6.8	+17.8	melt III
0.0996	"	-0.105	4.1	-24.2	melt III

Inspection of the results in Table X gives evidence of a random distribution of both enantiomorphous phases of crystals of the $P2_12_12_1$ modification. The magnitude of the specific rotation of the photoproducts still suggests a very high enantiomeric purity for most of the crystalline samples. The reluctance to crystallize and the high enantiomeric purity are interpreted as indicative of nucleation being the rate determining step in the crystallization process. While the methodology employed in the initial crystallization experiments was planned and executed by using the normal procedures to reduce the possibilities of self-seeding,[121] our final results indicate that this phenomenon may be responsible for the persistence of the pro-(-)-enantiomorph. Self-seeding is a concept that

implies residual seeds as the determining factor for a preponderance of a given solid phase. This phenomenon was observed and documented by Havinga[97] while experimenting on the spontaneous resolution of ethyl-allyl-anilinium iodide (**85**).

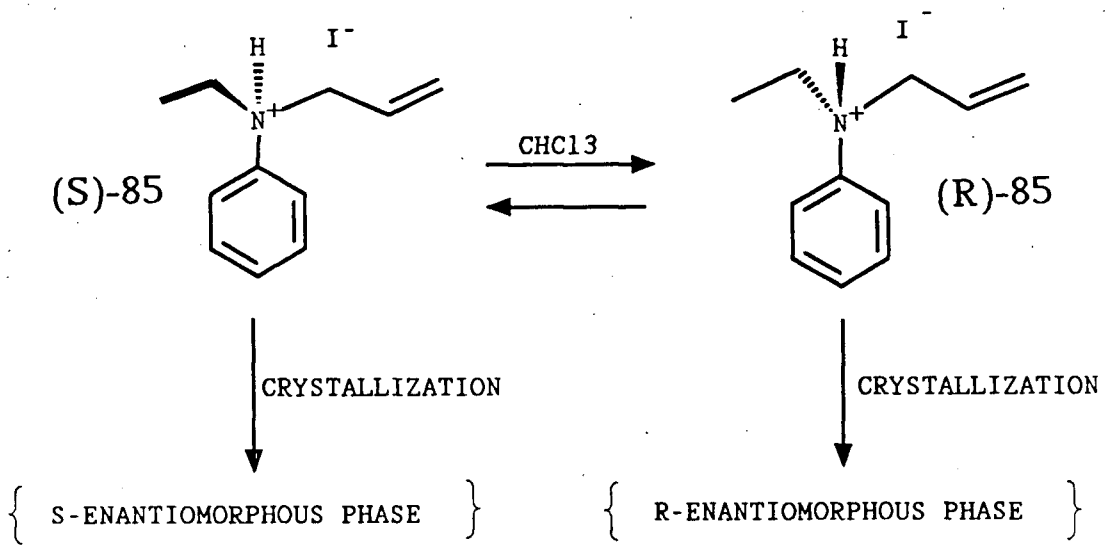

Figure 50. Spontaneous Resolution of Ethyl-allyl-anilinium Iodide.

Crystals of the quaternary salt grown from chloroform (containing one equivalent of solvent of crystallization) had been shown to present hemihedral faces because the sample crystallizes in a chiral space group.[122] The relation between hemihedral phases and optical activity had been established many years before by Pasteur in his classical studies on the sodium ammonium tartrate salt.[123] It was also shown that **85** slowly racemizes in the same solvent but remains stabilized in ethanol.

The quaternary salt **85** resembles diesters Et/Et-**21** and iPr/iPr-**23** in that they all exist in solution as an equilibrium of two interconverting enantiomers and in that all can also crystallize in optically active

modifications. Havinga observed that in twelve out of fourteen crystallization experiments where chloroform solutions of **85** had been paper-filtered, sealed and heated to destroy adventitious seeds, the crystalline material obtained gave dextrorotatory ethanol solutions.[97] Also similar to our results, when **85** was more carefully treated, this time by additional glass-filtering, the material was highly reluctant to undergo crystallization. From seven experiments the materials obtained were: three racemic, one ambiguous (probably dextrorotatory), one certainly dextrorotatory and two levorotatory. Havinga interpreted his results as an indication of true spontaneous resolution, that is, an event where the enantiomorphous phases can appear without any chiral influence, either a seed or a strange impurity. Other observations of self-seeding have appeared from time to time in the scarce literature of this topic.[121]

PART III. THE REGIOSELECTIVITY OF THE DI-π-METHANE REARRANGEMENT IN THE SOLID STATE.

Compounds Studied and Identification of Photoproduct Stereochemistry.

The compounds studied in this section are the mixed diesters 28 to 39 shown in Figure 51 below.

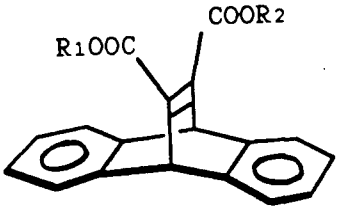

Compound	R_1	R_2
28	Methyl (Me)	Ethyl (Et)
29	Methyl	1-Propyl (nPr)
30	Methyl	2-Propyl (iPr)
31	Methyl	2-Butyl (sBu)
32	Methyl	1,1-Dimethyl-1-ethyl (tBu)
33	Methyl	1-Pentyl (nPen)
34	Methyl	2-Methyl-1-Butyl (iPen)
35	Methyl	2,2-Dimethyl-1-propyl (neoPen)
36	Methyl	Menthyl (Menth)
37	Methyl	Phenyl (Ph)
38	Ethyl (Et)	2-Propyl (iPr)
39	Ethyl	2-Butyl (sBu)

Figure 51. Mixed Diesters Used in the Study of the Regioselectivity of the Di-π-Methane Rearrangement.

Compounds **28** to **37** comprise a series of derivatives of diester **18** where one of the methyl groups was exchanged by an alkyl substituent of increasing size and/or branching or a phenyl group. In compounds **38** and **39** the two methyl ester groups were exchanged, one by an ethyl and the other for an isopropyl or a sec-butyl ester groups respectively.

Compounds **28** to **39** were photolyzed initially in benzene, acetonitrile and acetone solutions. As it was expected, the photolysis mixture from each compound gave spectral and glc evidence of two photoproducts in quantities that varied according to the substituents but not with the solvent used. Mass spectral analysis (glc-mass spectra) indicated that the products were isomeric with the starting materials as required in the case of a molecular rearrangement. The two products were clearly found to have the ^{1}H NMR spectral properties of the dibenzosemibullvalene regioisomers, structures **A** and **B**, expected from the triplet state di-π-methane reaction (Figure 18).

Common to the NMR spectra of all the reaction mixtures studied in this series was a complicated peak pattern at δ ~7.5-7.0 and two sharp singlets at ~4.5 and ~5.0 ppm.[64,124] The first group of signals was attributed to the overlapping non-equivalent aromatic protons, eight from each regioisomer. The other two peaks, sometimes resolved in pairs, were assigned to the corresponding tertiary cyclopropylic and bisbenzilic hydrogens attached to C(8d) and C(4b) respectively (Figure 52). Other signals in the spectra were attributed to the alkyl (or aryl in the case of **37**) portion of the ester substituents which were present in duplicate (a set of signals from each regioisomer) and with variable relative intensity and resolution.

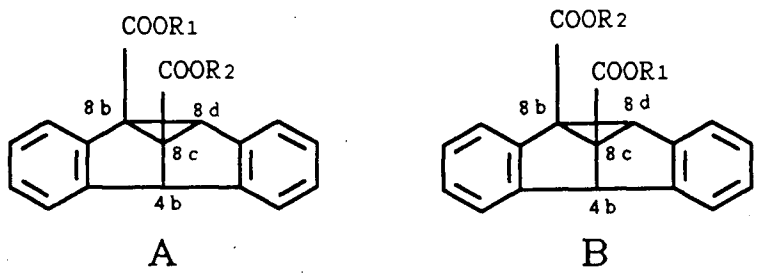

Figure 52. Products from the Di-π-Methane Rearrangement of Mixed Dibenzobarrelene Diesters

It has been shown in several literature reports that the stereoisomeric products from related di-π-methane reactions may sometimes be inseparable by conventional chromatographic procedures.[48,124,125] The determination of the stereochemistry of the products and their relative yields, however, can normally be inferred from analysis of the ^{1}H NMR spectra of the reaction mixtures.[48,124,125] The methyl ester resonances in the spectra of the products from compounds **28** to **37** have been found to be ideally suited for easy quantification and identification purposes. The methylene from the ethyl substituents of the products from diesters **38** and **39** have also been found to be useful in this context.

The spectrum of each product mixture clearly showed two sharp and well resolved singlets at δ 3.70 and 3.85 (methylene quartets at 4.15 and 4.32) that were assigned respectively to the methyl (ethyl) esters groups attached respectively to C(8c) and C(8b)[64,124] (Table XI). This assignment is consistent with having the more deshielded alkyl group (i.e. 3.85 ppm) at the ester attached to C(8b), the benzylic position.

The integrated intensities of the two methyl (ethyl) signals were found to correlate well with the integrated areas from the glc analysis of the same mixtures (the results from solution photolyses are shown in Table XI and in Figure 56).

Table XI. Glc and ^{1}H NMR Results From Solution of Photolysis Mixtures of "Mixed" Dibenzobarrelene Diesters.

Compound		Major Product				Minor Product			
		^{1}H NMR (CO_2CH_3)		glc		^{1}H NMR (CO_2CH_3)		glc	
	Glc†	δ	Area%	r.t.	Area%	δ	Area %	r.t.	Area%
28	a	3.70	52	15.30	‡‡	3.86	48	15.15	‡‡
29	b	3.70	55	16.21	57	3.86	45	16.00	43
30	b	3.70	55	10.80	55	3.86	45	10.27	45
31	c	3.70	64	22.8/23.2*	60	3.85	36	21.25	40
32	a'	3.70	61	16.23	60	3.86	39	15.58	40
33	d	3.70	50	9.10	51	3.86	50	8.85	49
34	a'	3.70	50	19.64	49	3.84	51	19.26	51
35	d	3.70	61	6.65	57	3.85	39	6.06	43
36	e	3.71	55	10.14	54	3.86	45	8.80	46
37	a	3.80	30	13.85	‡‡	3.91	70	13.85	‡‡
38	a'	4.20‡	53	12.47	52	4.35	47	12.10	48
39	g	4.20‡	50	20.7/21.1*	49	4.35	50	19.88	51

† Glc Conditions [Oven temperature (°C), column head pressure (psi)]: a) 195, 10; a') 195, 15; b) 200, 15; c) 195, 10; d) 220, 15; e) 245, 15; g) 270, 10.
* Two diastereomers formed, see PART IV.
‡ The signals of the ethyl ester methylenes were used for integration.
‡‡ Not enough resolution obtained on glc.

That the spectral assignment of the photoproducts was correct could be demonstrated in the case of compounds **63A** and **63B**, the products from the diester Me/iPr-**30**. The ^1H NMR spectrum and the X-ray crystal structure of each of these two regioisomeric dibenzosemibullvalenes were obtained after they had been separated by a lengthy and low yield fractional recrystallization procedure. The diester **63A** was also synthesized independently in a stereospecific manner from the 10-isopropyl-11-methyl-dibenzobarrelene diester **44** which is discussed in Part VI of the thesis (Figure 53). The ^1H NMR spectra of compounds **63A** and **63B** are shown in Figure 54.

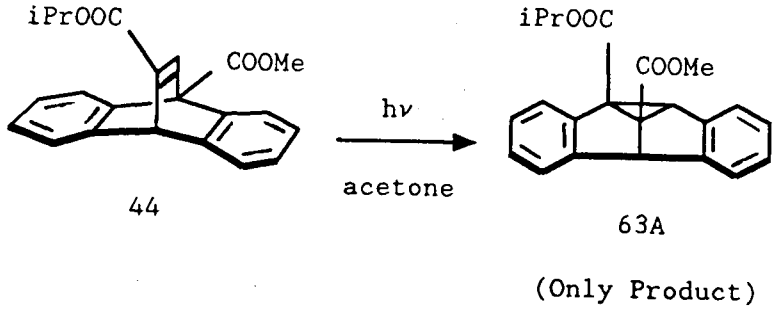

Figure 53. Independent Synthesis of Photoproduct **63A**.

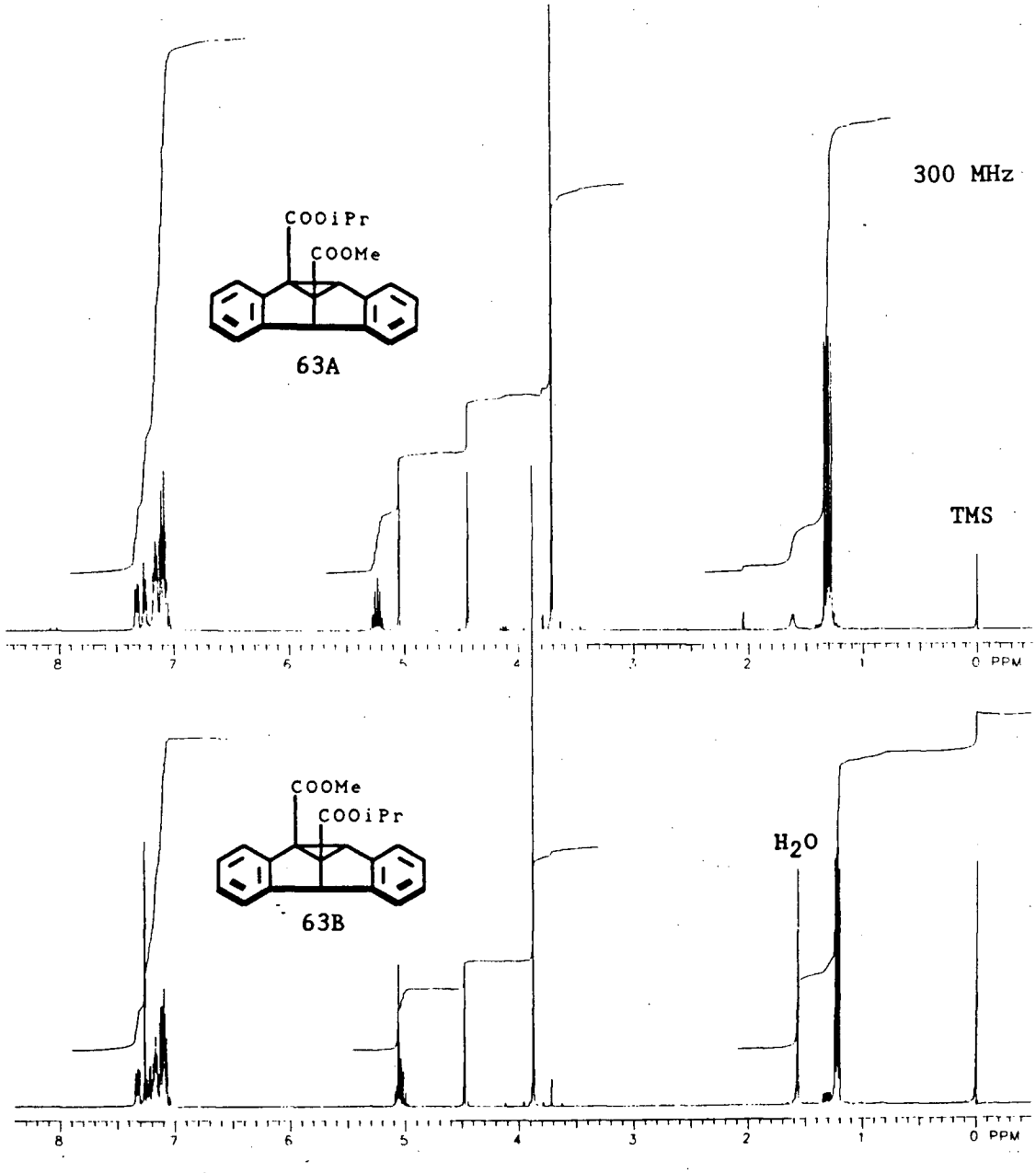

Figure 54. ^{1}H NMR Spectra of Dibenzosemibullvalenes **63A** (top) and **63B** (bottom).

Another consistent and probably structure-diagnostic feature throughout the mixed diester series was found on the glc retention times measured on a DB-1 capillary column. The trend was characterized by

shorter retention times for the starting materials compared to the photoproducts and by the fact that the isomers **A** had longer retention times than the isomers **B**. The retention times of each solution product and the integrated area of their glc peaks are also presented in Table XI.

Once the structural identity of the glc peaks had been determined it was found that the fragmentation patterns obtained from the glc-mass spectrometric measurements obtained by 70eV electron impact ionization could be correlated successfully with the dibenzosemibullvalene regiochemistry. The fragmentation pattern in the high mass range was characterized by the loss of the two ester substituents, either as molecular or as radical fragments. The key to the mass spectral behavior is that the nature of these fragments depends on the location of the ester group on the two non-equivalent cyclopropyl positions and consists of the following (compare with Table XII and Figure 55):

(1) Ester substituents at C(8b) can be lost partially to give $[M - R\text{-}OH]^+$, or in a more consistent manner to give $[M - (ROH + CO)]^+$.

(2) Ester substituents at C(8c) are lost mainly as $[M - R\text{-}O\cdot]^+$ or as $[M - (R\text{-}O\cdot + CO)]^+$.

(3) Ester substituents at C(8b) bearing abstractable γ-hydrogens can undergo the normal McLafferty rearrangement besides the fragmentation indicated in (1) above. This fragmentation pathway is not shared by substituents at C(8c) even if hydrogens suitable for abstraction are available.

It has been proposed on the basis of stereochemical evidence, often with the aid of deuterated compounds,[127] that the loss of methanol or any other alcohol from carboxylic esters arises from a double hydrogen atom transfer.[126] A requirement for the loss of an alcohol molecule is the presence of a second functional group able to make the first hydrogen abstraction (alcohols, ethers, amines, carbonyls, etc.). The loss of an alcohol molecule from an ester compound with the aid of a second functional group has been referred to as "intramolecular catalysis."[126] Evidence for the double transfer mechanism is based on: 1) the required stereochemistry between the first proton abstractor and the ester group losing the alcohol fragment, 2) in esters, hydrogen abstraction by the alkoxy oxygen is unimportant, and, 3) esters protonated on the carbonyl oxygen do not undergo (uncatalyzed) 1,3-hydrogen shifts.[126] The geometry required for the double transfer, or catalysis, should permit a close proximity between the two functional groups involved in the double rearrangement. A mechanism of this type in the case of the regioisomeric dibenzosemibullvalene photoproducts would require that: 1) a hydrogen atom be first abstracted by the carbonyl oxygen of the ester group at C(8c), 2) the same hydrogen should be transferred as a proton to the alkoxy oxygen of the ester group at C(8b), and, 3) the protonated alkoxy group should be lost as a molecular fragment (Figure 55). As suggested in Figure 55, it seems that the hydrogen most likely to be involved in this process is the bisbenzylic hydrogen attached at C(4b). The involvement of this, presumably more reactive hydrogen, may also explain why there is no significant hydrogen transfer in the other direction [from ester at C(8b) to ester at C(8c)].

The loss of the [R-OH + CO] fragments that account for peaks of consistently large intensity, may occur via two consecutive steps. It is possible that the second step may, in some cases, be sufficiently fast not to allow for the observation of the M^+ - R-OH ion. It seems reasonable that this type of fragmentation at the C(8b) ester group is realized by initial charge localization at C(8c) but that the competing McLafferty rearrangement is probably the fragmentation occurring by initial charge localization at that position.

Competing with the first hydrogen abstraction and subsequent transfer, the ester group at C(8c) fragments in a normal α-cleavage fashion to yield abundant M^+ - RO· and M^+ - (RO· + CO) ions. The lack of McLafferty rearrangement at the ester group at C(8c) is somewhat intriguing and probably results from being a relatively slower process compared to the other (hydrogen abstraction [H(4b)] and α-cleavage) alternatives. Although a detailed machanism should necessitate studies with isotopically labeled compounds, the structure-diagnostic value of the mass spectra of these compounds seems almost undeniable.

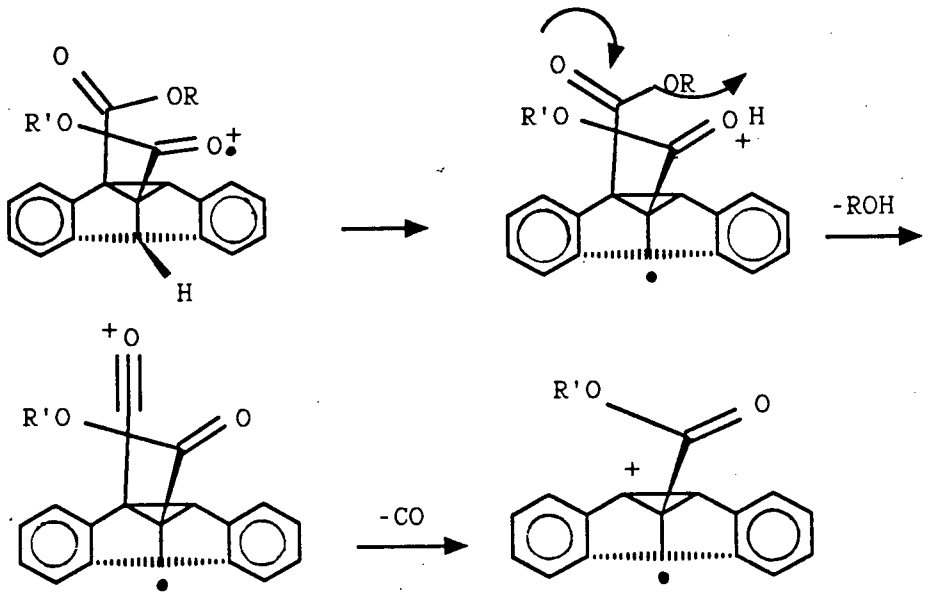

Figure 55. Stereospecific Electron Impact Induced Fragmentation of Dibenzosemibullvalene Diesters.

Table XII. High Mass Fragmentation of the Dibenzosemibullvalene Diesters.

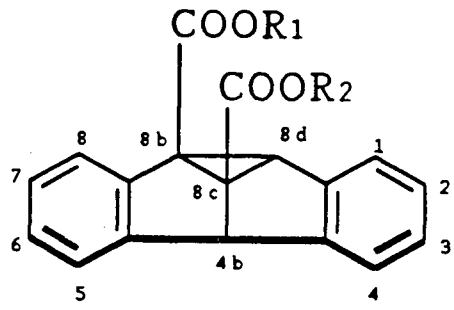

Compound			Alkyl group lost as (rel. intensity):				
	R_1	R_2	R-OH	R-O·	ROH + CO	RO· + CO	McLafferty
63A	iPr	Me	iPr(5)	-	iPr(65)	Me(10)	iPr(30)
64A	sBu	Me	-	-	sBu(94)	-	sBu(58)
65A	tBu	Me	tBu(5)	-	tBu(96)	-	tBu(100)
66A	nPen	Me	-	-	Pen(30)	Me(3)	-
67A	iPen	Me	iPen(3)	-	iPen(60)	Me(5)	iPen(20)
68A	neoPen	Me	-	-	neoPen(10)	-	neoPen(10)
72A	Sbu	Et	sBu(15)	-	sBu(100)	-	sBu(11)
63B	Me	iPr	Me(15)	iPr(10)	Me(20)	iPr(100)	-
64B	Me	sBu	Me(9)	sBu(11)	Me(8)	sBu(100)	-
65B	Me	tBu	-	tBu(11)	-	tBu(100)	tBu(6)
66B	Me	nPen	-	nPen(25	Me(20)	nPen(100)	-
67B	Me	iPen	-	-	iPen(25)	iPen(5)	-
68B	Me	neoPen	-	-	neoPen(25)	neoPen(5)	-
72B	Et	sBu	Et(11)	sBu(8)	Et(80)	sBu(100)	-

Photolysis of Mixed Diesters in Solution and in the Solid State.

With only two exceptions, presented by compounds Me/nPent-33 and Me/Menth-36, we found that the mixed diesters prepared for the studies described in this section were solids at ambient temperatures. These compounds were therefore photolyzed in the solid state and the product ratios determined in the same manner as in the solution photolyses. The regioselectivity observed in the solids was found to be reproducible from sample to sample and not affected by powdering the crystals or by reducing the temperature to as low as -50°C. Detailed studies carried out on crystals of compound Me/iPr-30 indicated that the product ratio was independent of the percent conversion in irradiations that led to up to ~25% of starting material consumption (after which the crystals became unreactive). A summary of the results on the regioselectivity obtained in the solid state is shown in Figure 56, where the solution results are also included for comparative purposes.

The first observation one can draw from the graph in Figure 56 is that the product selectivity can be more profoundly affected in the solid state than in solution when small variations are introduced to the dibenzobarrelene diester structure. The solution results indicate that the regioselectivity in these media tends to be moderate and to follow what seems to be a general trend. The regioselectivity in the solid state, in contrast, ranges from moderate to large and seems to vary in a discontinuous and unpredictable manner.

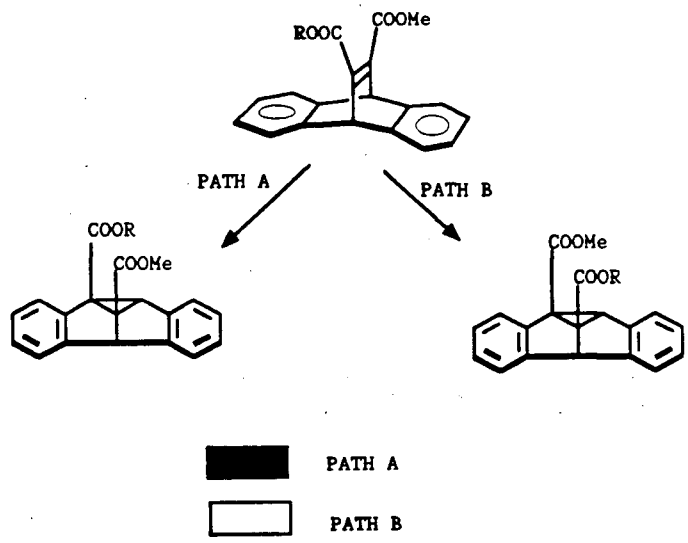

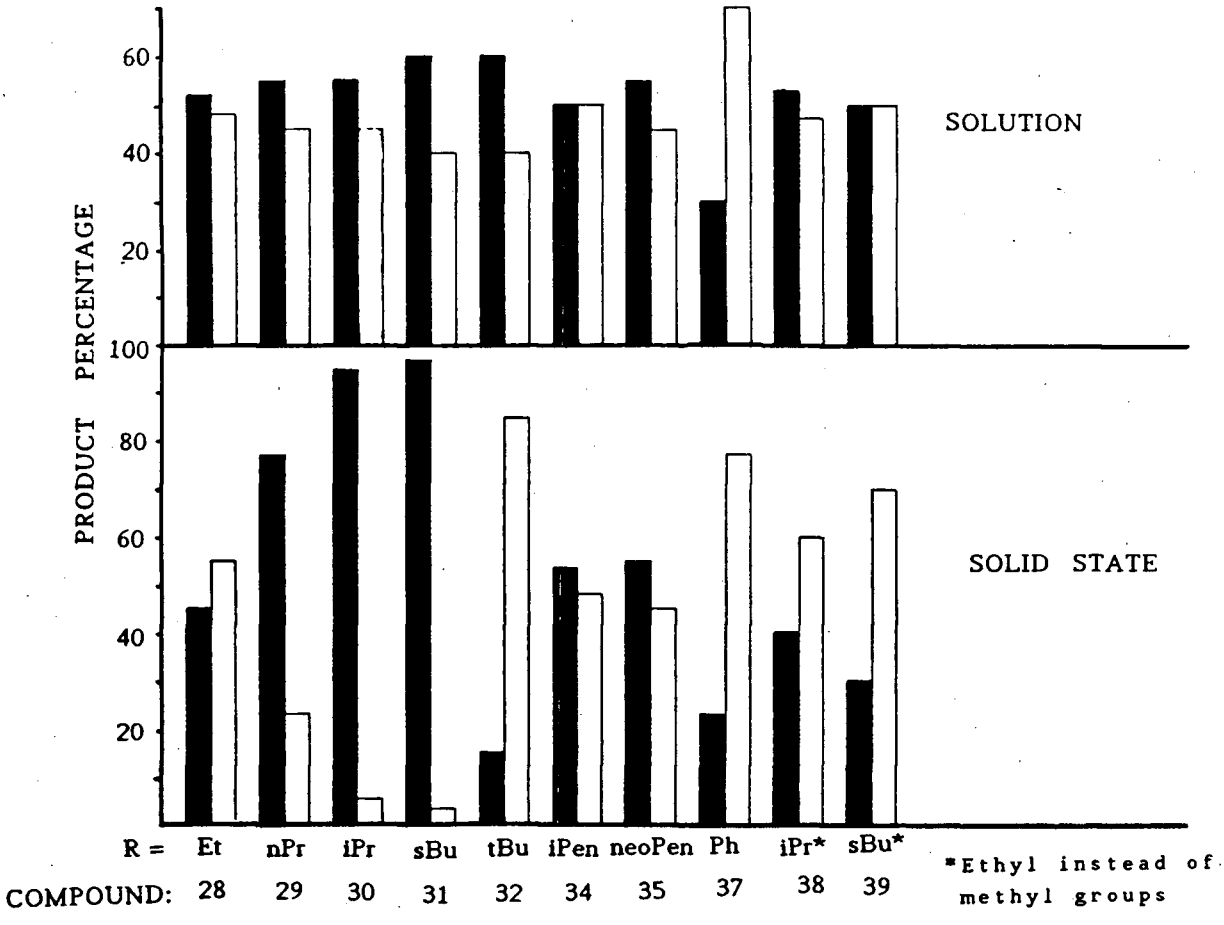

Figure 56. Comparison Between the Solution and Solid State Regioselectivity of Compounds 28 to 39.

Analysis of the Solution Regioselectivity.

Given the similar nature of the electronic properties of the substituents used in the present work it seems reasonable to postulate that the trend found in the solution regioselectivity originates mainly from steric factors.[128] These factors can operate either by inducing a steric inhibition of one of the reaction pathways, that is by a primary steric effect, or by influencing the resonance properties of the attached carbonyl groups[129] consistent with a secondary steric effect.

A Primary Steric Effect?

It was indicated in Figure 18 that the regiochemistry of the final product will depend on the successful continuation of the first reaction step.[48,124,130] Provided there is no significant reversibility to the excited state of the starting material once the cyclopropyl dicarbinyl species BR-1 is formed (or BR-2 if a 1,2-aryl shift occurs[48]), it must proceed to the final product in a stereospecific manner.[130] The steric effect of the substituents can therefore originate from differences in crowding during the formation of the alternative cyclopropyl dicarbinyl biradical intermediates.

The possibility of having the photoproducts being formed under conditions which could facilitate thermodynamic equilibration was investigated and ruled out. After long photolysis periods of samples of the pure photoproduct **63A**, under typical laser and lamp irradiation procedures, the starting material was recovered unreacted.

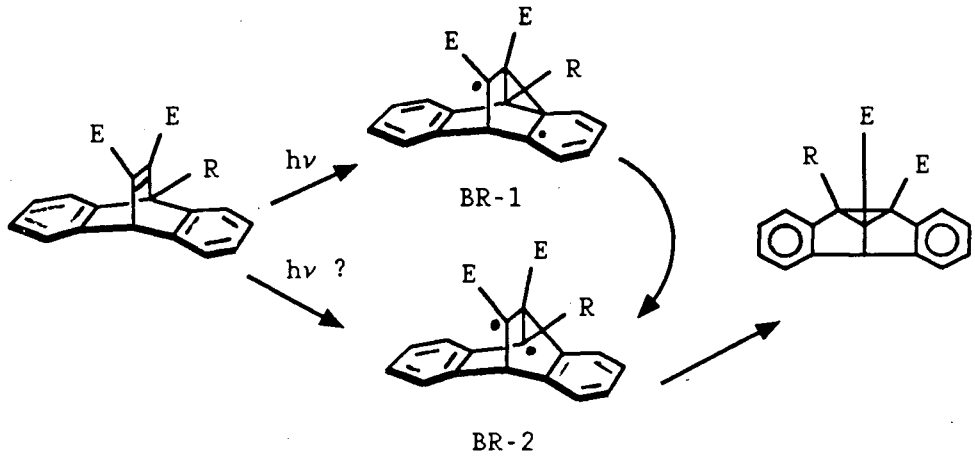

Figure 57. Radical Center Stabilization by Bridgehead (R) Substituents in **BR-2**

A primary steric effect has been put forward previously to explain the regioselectivity of the di-π-methane rearrangement of the 9-alkyl substituted dibenzobarrelene compounds shown in Figure 58.[124] The steric effects of substituents in this case, however, were found to be obscured by participation of electronic effects that can be discerned from the observed results.[124] It has been postulated that substituents at the 9-position favour a mechanism in which a direct 1,2-aryl shift to give **BR-2** may be involved[48,70b] (Figure 57). In this case an inductive effect of the substituents would offer the advantage of further stabilizing the benzylic radical center in **BR-2** without having to

disturb the aromaticity of the benzene ring, as is the case in **BR-1**. The vinyl-benzo bridging is therefore favored to occur at the side of the radical stabilizing substituent, which can even be manifested as an isotope effect, as was found in the case of the 9-deuterated analog[48a] (Figure 58). The primary steric effect on the other hand should disfavor the formation of the same intermediate when the size of the substituent becomes sufficiently bulky. The importance of this steric effect arises from the involvement of a cyclopropyl species "**BR-1**-like", even if it represents the transition state to the "true intermediate"[48a] **BR-2**. Even under this circumstance such a mechanism would make **BR-1** the transition state which determines the regioselectivity.

The nature of the steric effect of the ester substituents, however, cannot be so readily identified. Our results reveal that up to a certain point an increase in the size difference between the two alkyl groups brings about a modest increase in the reaction regioselectivity. Such is the case in the mixed diesters Me/Et-**28** to Me/tBu-**32**, in which a regular increase in the size of one of the alkyl groups from ethyl to tert-butyl results in an increase in the **A**:**B** product ratio from 52:48 to 60:40.

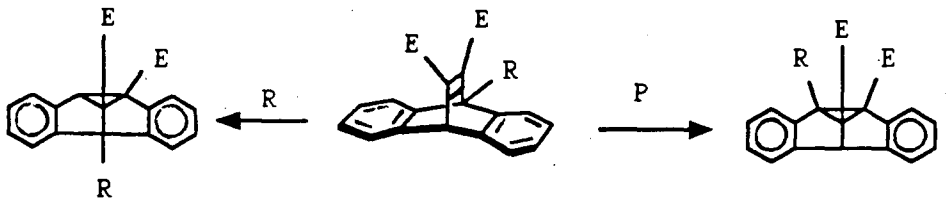

P=Proximal Bonding

R=Remote Bonding

	Bonding Regioselectivity*	
Substituent	Proximal	Remote
D	53	47
CH_3	29	71
$(CH_3)_2CH$	23	77
$(CH_3)_3C$	0	100

*References 48 and 124.

Figure 58. The Involvement of a Primary Steric Effect on the Regioselectivity of the Di-π-Methane Rearrangement of 9-Substituted Dibenzobarrelenes.

Whether the above change in product ratio can be taken as a small but measurable primary steric effect is difficult to determine. The normal procedure would be to analyze the effect of the substituents on the photoproduct ratio in terms of Taft's E_S steric parameters in order to search for a linear correlation.[131] These parameters, however, would only apply in cases where the substituents are directly attached to the reaction center and not separated by a CO_2 spacer as in the present case.

It is interesting to note that a primary steric effect would indicate that the bulkier substituent rests in a sterically less demanding position at the transition state. This may be a reasonable possibility considering that the most demanding steric interaction for the substituents arises among themselves. These interactions may be relieved to some extent in the transition state (which will probably look like **BR-1**)[70b] after the carbon supporting the bulkier group rehybridizes, the attached substituent separate away from each other, and the short vinyl double bond lengthens by acquiring single bond character (Figure 59).

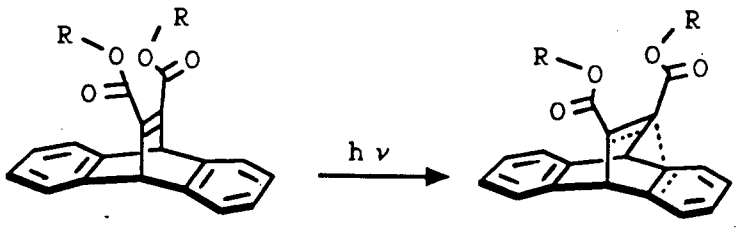

Figure 59. Possible Relief of the Steric Interactions by Bond Formation at the Carbon Attached to the Bulkier Substituent.

Besides the low regioselectivity, other observations seem to indicate that a primary steric effect would be largely diminished by the remote location of the substituent.[128] These include the insensitivity of the product ratio to further branching of the substituents (Me/nPr-29 to Me/iPr-30 and from Me/sBu-31 to Me/tBu-32), and to the surprising

lack of an effect of the larger substituents of compounds Me/nPen-33 and Me/iPen-34. Furthermore, the highly branched and bulky neo-pentyl and menthyl derivatives exert an effect equivalent to that observed in the compounds of the butyl series.

In compounds 38 and 39 the small size difference between the ethyl, and isopropyl or sec-butyl ester groups is consistent with the poor discrimination between the two regioisomers. The Me/Phe diester 37 results are more difficult to analyze within this context as a result of the possible electronic effects arising from the phenyl substituent. This may be indicated by the relatively large and reversed regioselectivity observed (70A:70B = 30:70)

A Secondary Steric Effect?

An alternative explanation for the regioselectivity observed in solution rests on the possibility that the repulsive interactions between the two alkyl groups may drive and keep one of the adjacent carbonyl group out of conjugation with respect to the vinylic double bond.[129,132] Theoretical models suggest that the resonance stabilization of an α,β-unsaturated system should depend on the torsion angle, θ, defined by the mean planes of the two double bonds.[79] The angular dependence of the resonance energy has been proposed to vary in relative terms as a function of a $\cos^2\theta$ and, as represented in Figure 60, will be a maximum at 180° and 0°C and a minimum at 90°.

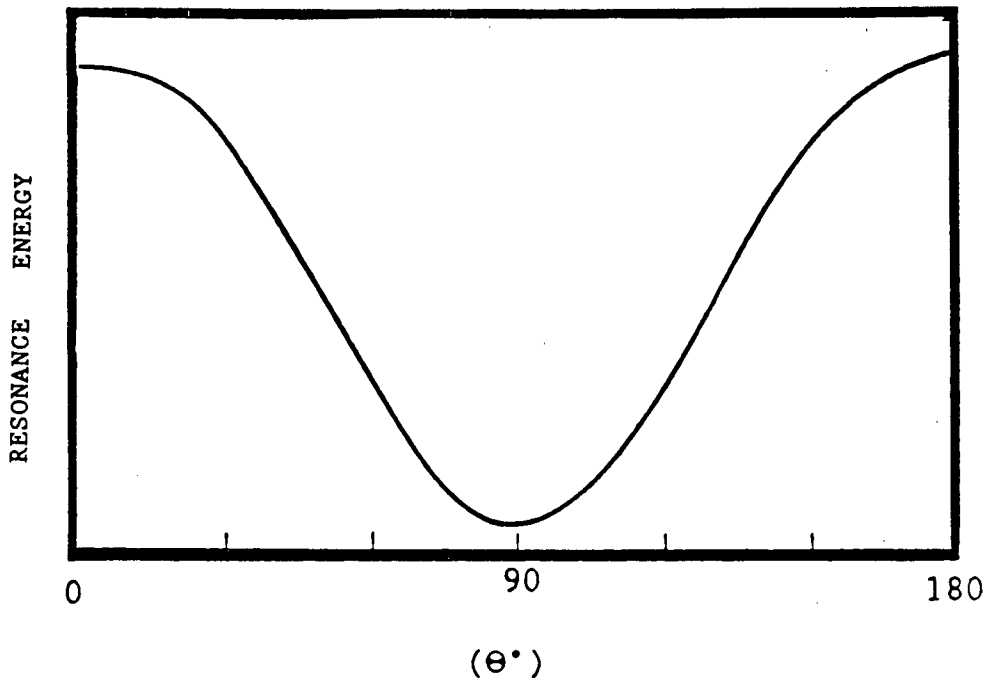

Figure 60. Resonance Energy of Two Conjugated π-Systems as a Function of the Torsion Angle (θ).

The consequences of having a carbonyl group out of conjugation can in principle affect the outcome of the reaction from two different reactivity levels. The first concerns the excited state of the dibenzobarrelene diester that can be regarded as a resonance stabilized 1,2-triplet biradical (Figure 61). The radical center next to the least conjugated carbonyl (carbon 1) is expected to have a larger odd electron

density which can conceivably make it more reactive towards aromatic ring attack. This point of view is consistent with a model that compares the di-π-methane reactivity with the well known free radical rearrangement of dibenzobarrelenes [133] (Figure 62).

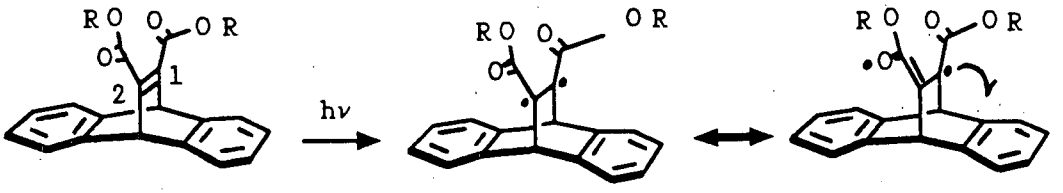

Figure 61. The Triplet Excited State of Dibenzobarrelene Diesters as a 1,2-Biradical.

At the level of the reaction intermediates, attack by the same carbon (carbon 1) is expected to occur since it would generate the most stable, resonance delocalized, 1,4-biradical. The relative radical stability factor is known to play a decisive role in determining the reaction regioselectivity of vinyl substituted compounds.[65,66,130]

It seems therefore quite possible that different degrees of conjugation between the two carbonyl groups and the central vinyl bond may determine the observed results. Having one carbonyl group out of conjugation can be regarded as approaching the situation found in the methyl and ethyl dibenzobarrelene monoesters studied by Ciganek and

Cristol[65,134] (Figure 63). The stereochemistry of the product in these cases was found to be completely determined by the formation of the product that proceeds through the more stable intermediate.

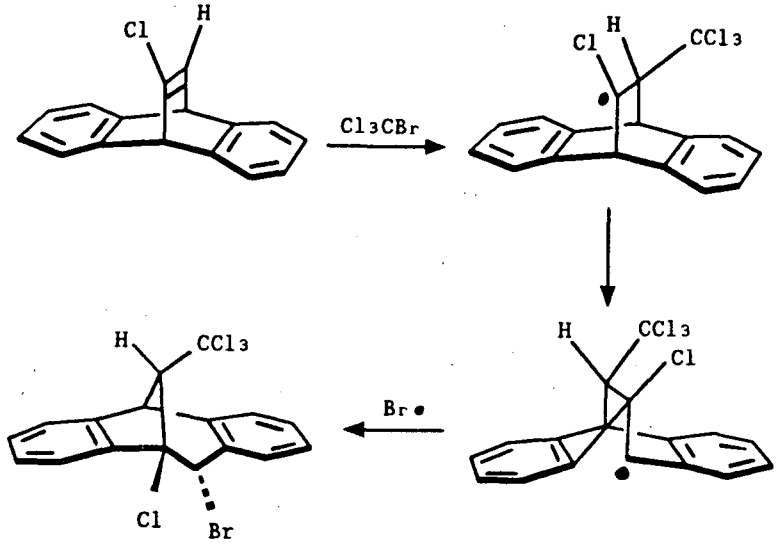

Figure 62. Free Radical Rearrangement of Dibenzobarrelenes.

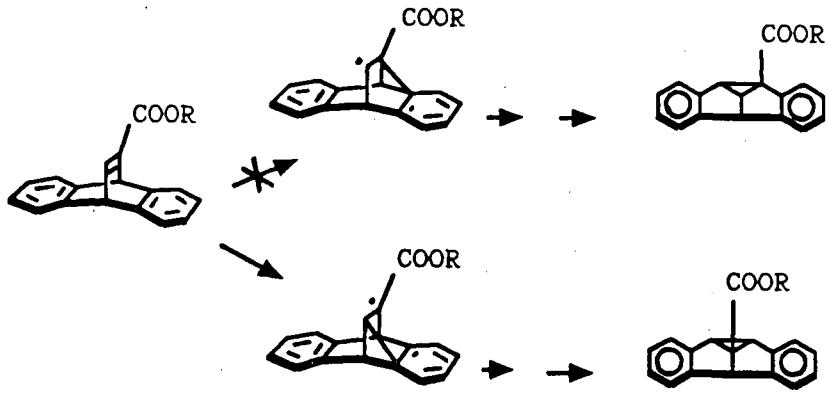

R = Me, Et

Figure 63. Regioselectivity in Dibenzobarrelene Monoesters.

Spectroscopic evidence for different degrees of conjugation between the two carbonyl groups can sometimes be obtained in solution from infrared measurements. Empirical criteria for assigning conjugation takes advantage of the normally lower frequency at which a conjugated carbonyl band occurs (see page 87). It has been postulated that differences between s-cis and s-trans conformers can also be identified from measurements that include the carbonyl-double bond intensity (I) ratio[62,87a] (I s-trans / I double bond > 5.2; I s-cis / I-double bond = 0.6-3.5).

The ene-dioate structure of the dibenzobarrelene compounds studied here is partially characterized by an infrared band system in the range between 1750-1600 cm-1. In the case of diester Me/iPr-30, two intense and partially overlapping carbonyl bands (in $CHCl_3$ solvent) can be discerned at 1720 and 1705 cm^{-1}. The vinylic fragment can be located with about half the intensity of the carbonyls at 1630 cm^{-1}. The difference in the carbonyl band frequency unfortunately cannot be unambiguously assigned to differences in conjugation. It is known that an isopropyl substituent is capable of decreasing the stretching frequency of the carbonyl ester group by as much as 20 cm^{-1} relative to a methyl substituent. Such substituent effect is normally attributed to the inductive stabilization of the polar resonance form of the carboxylate group. This effect can be nicely illustrated in operation in the series of alkyl benzoates shown in Figure 64 below. The uncertainty in the assignment of the carbonyl bands was found to carry over to the entire mixed diester series.

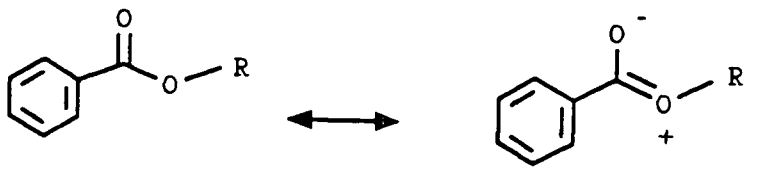

R	C=O(cm^{-1})
Me	1727
Et	1720
iPr	1708

Figure 64. Inductive Effect of the Alkyl Substituents on the Carbonyl Frequency of Alkyl Benzoates.

Alternatively, the use of NMR spectroscopy has also been proposed not only to determine whether a carbonyl group is conjugated or not, but also to determine carbonyl-double bond torsion[135,136] angles of relatively rigid compounds. Both ^{13}C NMR[135] and more recently ^{17}O NMR[136] techniques have been applied and, in the case of the latter, it was claimed to provide values that compare well with gas phase geometries estimated from force field methods.

An analysis of the carbonyl carbon resonances in the ^{13}C NMR spectrum of diester Me/iPr-30 was carried out for exploratory purposes. Two distinct bands were actually found at 165.9 and 164.6 ppm respectively.

In the case of ^{13}C NMR spectroscopy the more conjugated carbonyl carbon is normally expected to resonate at higher field strength.[135] The relative shielding originates with the expected electronic delocalization contributed by the resonance structure II:

$$\underset{\text{I}}{-C{=}C{-}C{=}O} \;\; \langle\text{-----}\rangle \;\; \underset{\text{II}}{-C^{+}{-}C{=}C{-}O^{-}}$$

In order to determine whether the difference in chemical shift between the two carbonyl carbons of diester Me/iPr-30 was due to such differences in electronic delocalization, the spectra of the symmetric diesters Me/Me-18 and iPr/iPr-23 were also obtained in the same solvent ($CDCl_3$). The spectra of the symmetric diesters were found to contain a single carbonyl carbon resonance and had overall spectra that indicated a time-averaged C_{2v} symmetry in each case. The chemical shift of the carbonyl carbons of each spectrum (Me/Me-18: 165.8 and iPr/iPr-23: 164.7 ppm) was found to correlate with each of the two chemical shifts observed in the unsymmetric compound Me/iPr-30. This result clearly indicates that the difference in the chemical shifts of the carbonyl resonances in 30 is due to the inductive effect of the two different substituents. We can also conclude that, within the time scale of the NMR experiment, the two carbonyl groups in 30 have indistinguishable delocalization geometry.

The gas phase molecular conformation of several diesters was also obtained from molecular mechanics (program MMP2).[137] In order to obtain the global energy minimum as a function of the carbonyl system conforma-

tion, the energy of a large number of conformations was calculated by variation of the two carbonyl-double bond dihedral angles (Figure 65, $\theta 1$ = O(2)-C(13)-C(11)-C(12) and $\theta 2$ = O(4)-C(15)-C(12)-C(11). The structure of 49 different conformers (carbonyl rotamers) was obtained by use of the dihedral angle driver facility of the computer program.[137c] One dihedral angle was kept constant (e.g., $\theta 1$) while the other ($\theta 2$) was rotated 360° in 30° increments in order to obtain a different rotamer at every step. Within all the possible conformations covered with this resolution, an energy minimum defined by the carbonyl conformation shown in Figure 24 was found for the compound Me/Me-**18**.

It was very interesting that the same carbonyl conformation ($\theta 1$ = 30°, $\theta 2$ = 210°) was reached as minimum in diesters with significantly different alkyl substituents (Me/Me-**18**, Et/Et-**21** and iPr/iPr-**23**). This observation suggested that the alkyl group may not play a very important role in determining the conjugation of the ene-dioate system. The factors that tend to place the carbonyl groups out of planarity may be already contained in the two carboxylate ester groups regardless of the alkyl substituent.

An interesting observation comes from the fact that resonance structures, where both carbonyl groups of the cross-conjugated ene-dioate system are involved in resonance with the central double bond, cannot be drawn at the same time. It is possible that the cost of deconjugating one of the two carbonyl groups, in terms of resonance energy, may not be so high given the possibility of partially delocalizing the two carbonyl systems at the same time.

The suggestion that the same non-conjugated conformational minimum may exist independently of the nature of the alkyl group may explain the NMR data obtained. This requires a rapid equilibrium where both the methyl and the isopropyl ester groups take turns adopting the two carbonyl conformations that define the energy minimum. Any such conformer, however, should have a lifetime shorter than the time required for discrete detection in the NMR experiment.

In order to eliminate the possibility of differential carbonyl conjugation as the stereochemical controlling factor, another requirement must be fulfilled: the lifetime of a diester conformer should be shorter then the lifetime of the excited state or reaction intermediates whose behavior it may be influencing.[138] Although the lifetimes of the di-π-methane diradical intermediates in the case of the dibenzobarrelene diesters are not presently available, the lifetime of the triplet excited state of diester 30 was measured during the course of the present work. The lifetime of the triplet $^{3}30^{*}$ was measured by Stern-Volmer kinetics in 0.1 M benzene using 1,3-cyclohexadiene as the triplet quencher. From a $kq\tau = 4.86\ M^{-1}$ and $kq = 5 \times 10^{9}\ M^{-1}\ sec^{-1}$, a lifetime of <u>ca</u>. 1.0×10^{-9} sec was obtained.[139]

From the standpoint of the triplet state, in order to observe a secondary steric effect such as the one indicated in Figure 61, the conformer lifetime (determined by the rates of rotation around the C=C-C=O single bonds) would be required to be longer than in the nanosecond range. This lifetime range may also apply to the triplet biradical intermediates in the di-π-methane rearrangement since those observed so far are known to be extremely short lived. In the case of

the naphthobarrelene 73 studied by Shaffner et al. (Figure 67, page 162), a lifetime of 20 X 10^{-9} sec was measured by flash photolytic experiments[18].

Without the rates of rotation around the C-C-C-O single bonds, which determine the lifetime of the ene-dioate conformers, no certain conclusion can be drawn about the involvement of a secondary steric effect. However, the extremely short lifetime of the triplet state, and probably of the triplet biradicals, seem to make this a viable hypothesis.

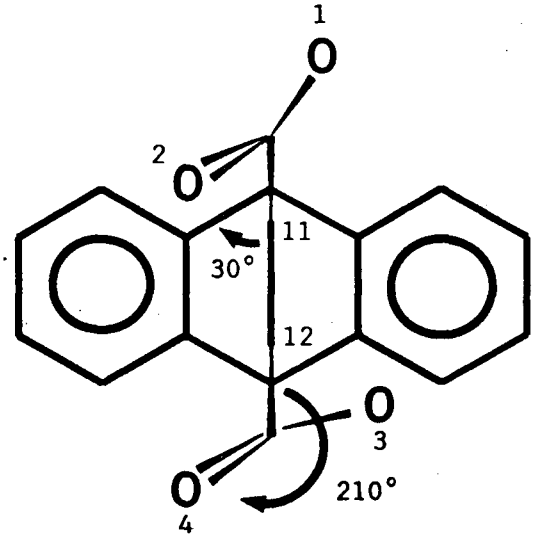

Figure 65. Gas Phase Conformation of the Ene-Dioate System in Dibenzobarrelene Diesters as Obtained from Molecular Mechanics (MMP2).

The Regioselectivity in the Solid State.

The Materials.

It is clear from the results summarized in Figure 56 that different factors determine solution and solid state regioselectivity. In order to look for the possible factors controlling solid state reactivity we turned our efforts to trying to obtain the X-ray crystal and molecular structures of the substrates employed.

Attempts to obtain crystalline materials suitable for structure elucidation led us to crystallization procedures that involved the use of several solvents and of molten materials. Initially promising materials were obtained for compounds Me/Et-28, Me/nPr-29, Me/iPr-30, Me/sBu-31, Me/Ph-37 and Et/iPr-38. Compounds Me/Pen-33 and Me/Menthyl-36, as mentioned before, were liquids at ambient temperatures, and diesters Me/iPen-34 and Me/neoPen-35 spontaneously solidified on storing in the absence of solvent over periods of 12 and 20 months.

The diesters Me/tBu-32 and Et/sBu-39 turned out to exist as extremely thin plates unsuitable for diffraction analysis. The diester Me/iPen-34 was recrystallized and also found to give similar material. Compound Me/neoPen-35, a material devoid of crystalline transparency, presented properties that were in agreement with a glassy structure with a long range softening instead of a sharp melting point. Some crystals of Me/Et-28 and Me/nPr-29 were analyzed and found not to diffract X-rays as required for the structural determination. A sample of Et/iPr-38 was found to have a disordered structure which could not be fully resolved. Finally, suitable crystals (both with a needle like morphology) were

found for compounds Me/iPr-30 and Me/Ph-37, for which full crystal structures were determined. The solid state photochemical results for these two compounds will now be analyzed in detail to see if we can extrapolate the structural information obtained into the other crystalline compounds.

Stereoelectronic Factors in the Solid State.

In analogy with the structure of compound Me/Me-18, Et/Et-21 (dimorphs I and II) and iPr/iPr-23 (dimorphs I and II), the structures of the diesters Me/iPr-30 and Me/Ph-37 are characterized by possessing a disymmetric conformation that "freezes" the two carbonyl groups at different extents of conjugation with the central double bond. The idea of having the regioselectivity determined by the relative radical-delocalizing abilities of the carbonyl groups seems to be amenable to experimental verification in the solid state. The extent of conjugation,[79,140] defined by the dihedral angle between the mean planes of the carbonyl and the vinyl double bonds, can be estimated from the X-ray crystal structures.

If conjugation, a secondary steric effect, were the product determining factor in the solid state, one would predict that the reaction would proceed by bond formation at the vinyl carbon attached to the least conjugated carbonyl group (see above). This reaction pathway would guarantee attack to the aromatic ring by the expectedly more reactive vinyl carbon center (Figure 61) as well as the formation of the more stable, carbonyl delocalized, 1,4-biradical. The predicted reaction

pathway and photoproduct of diesters **30** and **37** along with the experimental observations on the rearrangement are presented in Figure 66. Three more examples, **23** (dimorph I), (R,S)-**42** and (S)-(+)-**42**, borrowed from other sections of the thesis are included in the same Figure (66).

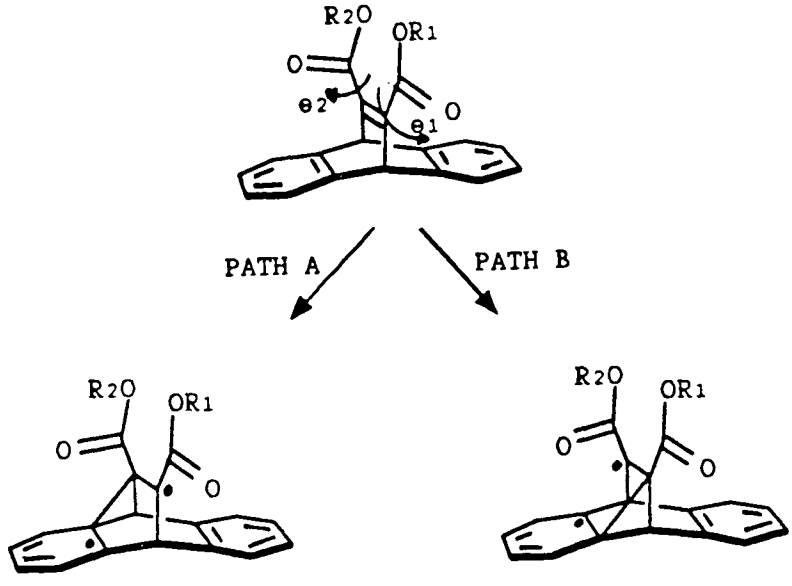

Compound						Pathway	
R1	R2	$\theta 1$	$\theta 2$	$\cos^2\theta 1$	$\cos^2\theta 2$	predicted	observed
iPr	Me	315.5	143.4	0.51	0.64	A	B
Me	Phe	225.1	214.7	0.50	0.68	A	A
iPr	iPr*	164.3	63.7	0.92	0.20	A	B
iPr	(S)-sBu	166.2	68.4	0.94	0.14	A	B
iPr	(R,S)-sBu	167.4	70.1	0.95	0.12	A	B

* Regioselectivity obtained from absolute configuration studies (Part II) and by analogy with isomorphic crystals of iPr/sBu-42 (see Part IV).

Figure 66. Stereoelectronic Effects of the Carbonyl Groups on the Predicted and Observed Regioselectivities from the Di-π-Methane of Some Dibenzobarrelene Diesters.

The angles $\theta 1$ and $\theta 2$ tabulated in Figure 66 are defined as the dihedral or "twist" angles between the mean planes of the p-orbital lobes of each of the two carbonyl groups and of those from the central double bond. The resonance energy of the system varies with the $\cos^2$ function of the angles given and reaches a maximum value when all the atoms lie in the same plane[140] (Figure 60). Although the difference in $\cos^2\theta$ between the two adjacent carbonyl groups of the compounds in Figure 66 ranges from very small (i.e. Me/iPr-30) to large (i.e. iPr/iPr-23 and iPr/sBu-42), the regioselectivity only agrees in one case (Me/Ph-37) with our mechanistic expectations.

A very interesting observation from the $\cos^2\theta$ values in Figure 66 is that the sum of the two contributions adds up to a value of 1.1, which is slightly more than the value of one fully conjugated carbonyl group (1.0). As mentioned before, the ene-dioate system clearly prefers to have partial delocalization at the two carbonyl groups rather than having one carbonyl perfectly conjugated and the other perfectly orthogonal.

It is interesting to notice that the lack of resonance stabilization has been proposed to be sometimes sufficiently important as to determine the presence or absence of di-π-methane reactivity. The photochemistry of the unsaturated carbonyl compound **73**, studied by Shaffner et al[18] was precisely studied in this context (Figure 67).

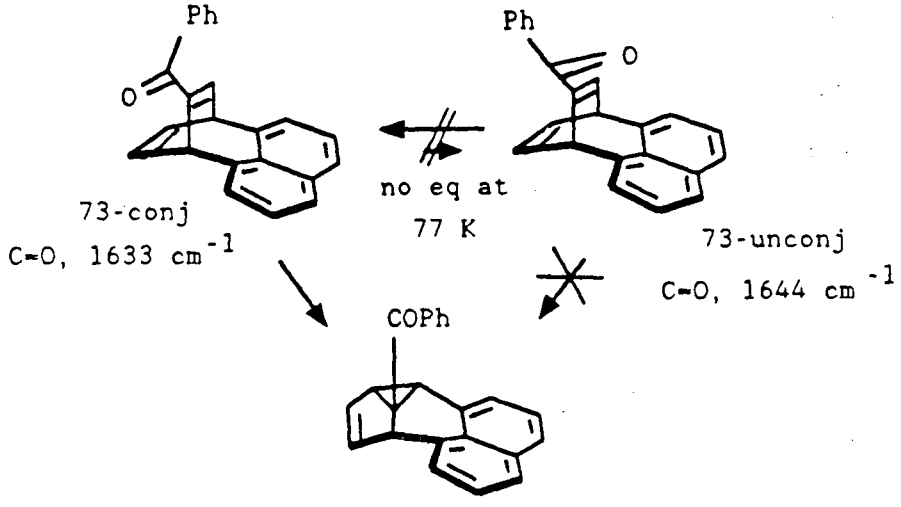

Figure 67. Differential Photochemistry from the Conjugated and Non-Conjugated Rotamers of Benzoyl Naphthobarrelene **73**.

The infrared spectrum of compound **73** in a methyl tetrahydrofuran matrix at 77K was found to show two distinctively well defined carbonyl stretching bands at **1633** and **1644** cm^{-1}. These bands were attributed to the two carbonyl conformers **73-conj** and **73-unconj** respectively, from which the former was found to be the most abundant component.[71] A series of changes was observed in the spectrum when the matrix was photolyzed

at low temperature and then slowly warmed in the dark. The most important aspect of those observations in connection with the present discussion is that only the species responsible for the lower frequency band was affected during the photochemical and subsequent processes. This result was interpreted as an indication of the exclusive reactivity of the carbonyl-conjugated conformer **78-Conj**. The authors observed that even after exhaustive photolysis the non-conjugated naphthobarrelene species remained inert and clearly accounted for the recovery of the starting material the end of the experiments.[71]

Although a definitive assignment of the carbonyl bands to differently conjugated species has to remain speculative in the case of **78**, this is not the case in the diesters included in Figure 66. In contrast to **78**, in the case of the diester compounds the degree of conjugation seems not to affect the dibenzobarrelene reactivity. It should be pointed out that our results arise from internal (intramolecular) comparison and require the involvement of radical stabilization factors. Those of Schaffner et al., on the other hand, may arise from differences in the absorption of light (extinction coefficients) or in the quantum yields or reaction of the two carbonyl conformers.

Clearly, having one carbonyl group almost perfectly out of conjugation in the solid state does not parallel the reactivity shown in the case of having only one carbonyl group as in the monoesters of Figure 63. A fundamental difference arises primarily from the fact that a substantial degree of radical stabilization can be expected by the inductive effects of the unconjugated carbonyl group[141] relative to the hydrogen substituent in the monoesters of Figure 63.

Solid State Primary Steric Effects. Steric Compression.

Most solution steric effects are necessarily defined by factors related to molecular structure. Steric effects in solution were adequately defined by Shorter[142] as "the intense repulsive forces operating when two non-bonded atoms approach each other so closely that such approach originates non-bonded compression energy". This approach can occur either intermolecularly or, as in the case of the di-π-methane rearrangement, it can be intramolecular. The most fundamental difference between solution and solid state steric effects is that in the latter, larger non-bonded repulsive interactions may arise between the reacting molecule and its relatively fixed and anisotropic surroundings.[1i] In solution, as suggested by Lazar,[35] the lifetimes of the intermediates are longer than the time required for the organization of the solvent and the molecular environment will be essentially identical in all directions. Solid state steric effects are specifically determined by the crystal and molecular structures and by the motions required by the operating reaction mechanism(s). Scheffer et al have shown how specific solid state steric effects can be identified when both the reaction mechanism and the crystal structure are reasonably well determined.[36]

Analysis of the di-π-methane reaction mechanism based on molecular models indicates that the most dramatic changes in the dibenzobarrelene structure occur during the two cyclopropyl ring-forming steps. Since the success of the reaction depends primarily on the first aryl-vinyl bonding step, we decided to analyze this process in detail.

From an original distance of about 2.43 Å,[143] the reacting vinyl and

aromatic carbons must come together to a C-C single bond distance of approximately 1.54 Å. Notably, when this process takes place the substituent attached to the moving vinyl carbon undergoes a large displacement in the direction of bonding (Figure 68). This motion may cause the substituent to push the relatively fixed atoms of the neighboring molecules in the crystal. Since the non-equivalent ester groups should be surrounded by different lattice environments, the amount of non-bonded repulsive energy accompanying each process may also have different magnitudes. The reaction regioselectivity may originate when one reaction mechanism increases the energy of the transition state more than an alternative one.

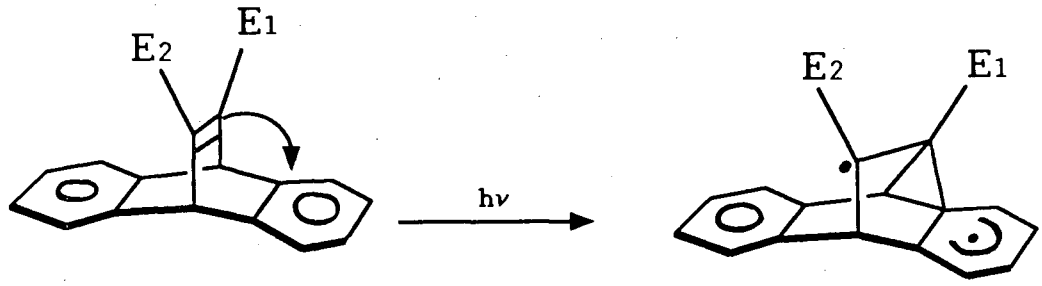

Figure 68. Displacement of the Vinyl-Attached Substituent During the Benzo-Vinyl Bridging Step on Vinyl Disubstituted Dibenzobarrelenes.

The packing differences around each of the ester groups of the diesters Me/iPr-30 and Me/Ph-37 can be visualized in Figure 69. The large spheres represent atoms from neighboring molecules at contact distances of less than 3.0 Å (the hydrogen atoms are not shaded). Qualitatively, the methyl and phenyl ester groups are more tightly surrounded than the isopropyl and methyl groups in **30** and **37** respectively. The regioselectivity observed is in agreement with the larger motions from part of the less tightly surrounded isopropyl and methyl groups of **30** and **37** respectively (Figure 63).

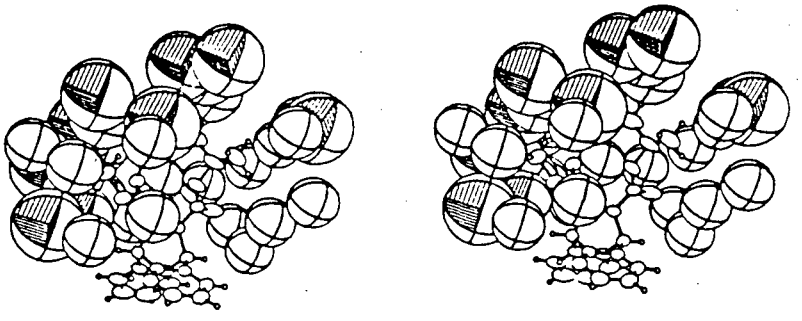

Me/iPr

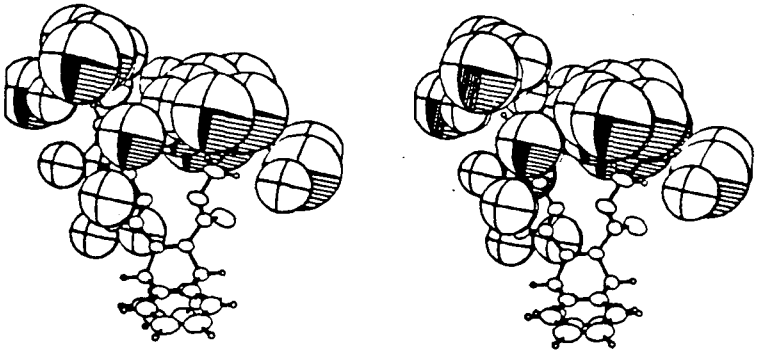

Me/Ph

Figure 69. Lattice Environment Around the Vinyl Substituents of the diesters Me/iPr-30 and Me/Ph-37.

Although the free lattice space concept can be useful as a first qualitative approximation,[144] a more quantitative approach to the mechanistic problems of solid state reactivity is highly desirable. Quantitative approaches, as pointed out by Gavezzotti,[144] can be conveniently based on calculations involving semi-empirical non-bonded intermolecular potentials instead of on rigorous quantum mechanical methods.[30,144] The most useful parameter in this context is the packing potential energy (PPE, Eq 14)) that formally describes the difference in potential energy between an isolated molecule in the gas phase and the same molecule in the environment of its crystal lattice.[30,144b]

$$V_{6,12} = \epsilon[(r^*/r)^{12} - 2(r^*/r)^6]. \qquad \text{Eq 14.}$$

r^* = equilibrium distance in A

ϵ = depth of potential well (Kcal/mol).

The choice of the PPE as the parameter to analyze the solid state reactivity comes from the fact that it results from exactly the same phenomena that controls steric effects in chemically reacting systems.[30,145] These phenomena are also the same that give meaning to concepts such as molecular shape and size: the Van der Waals interactions.[145]

When it is extrapolated to problems of chemical reactivity, it is meaningful to consider the PPE as a potential energy field defined by the surroundings of the reacting molecule. In equation 14 the potential energy is calculated between every atomic pair of two interacting molecules with respect to their relative positional parameters, the

interatomic distances (r).[146] The dispersion attractions of the London type [given by the term: $2(r^*/r)^6$] and the repulsion forces caused by the overlap of electron clouds [given by: $(r^*/r)^{12}$] define the magnitude of the field for every atom in the reacting molecule, for every molecule in the crystal, and after complete summation, for the crystal as whole.[30,146]

Before reaction, the molecules are found at their equilibrium positions in the parent crystal and the magnitude of the attractive forces perfectly balances the magnitude of the repulsive ones. When a molecule absorbs a photon it can undergo atomic displacements in search of a more stable excited state geometry. While the electronically excited compound reaches the transition state of a chemical reaction it will undergo atomic displacements with even larger amplitudes. The event in which an excited compound reaches the potential energy surface of a reaction while in the solid state and by changing into a favorable structural geometry has been called dynamic preformation.[147]

Although any such displacement will be energetically costly, motions that steer the atoms of the reacting molecule against its neighbors will be comparatively forbidden. This results from the sharper increase in repulsive energy due to the r^{12} dependence of the potential energy function[146] and explains the reason for the need of the often invoked "empty space" for chemical reactivity.[144]

Several potential energy functions have been used to describe the PPE in terms of the positional atomic parameters.[146] The function presented in equation 14 is commonly referred to as the "6-12" Lennard Jones potential function and was the one used in the present work.[147]

The approach used in this work consisted in calculating the PPE as a function of the atomic displacements required in following the motions of the assumed di-π-methane rearrangement mechanism.[46,47] The details of these calculations, performed by Mr. Fred Wireko of this department, can be found elsewhere.[143]

The plots shown in Figure 71 indicate that there is a rise in the potential energy as each vinyl carbon is displaced in the direction of the neighboring aromatic carbons. The mechanics of these motions have been simplified for computational purposes by considering a flexible vinyl fragment and a perfectly rigid aromatic framework and lattice environment. The motion of each vinyl carbon was simulated by rotation of an operational vector joining the bridgehead carbon, next to the moving fragment of the molecule, to the vinyl carbon at the other end of the double bond (Figure 70).

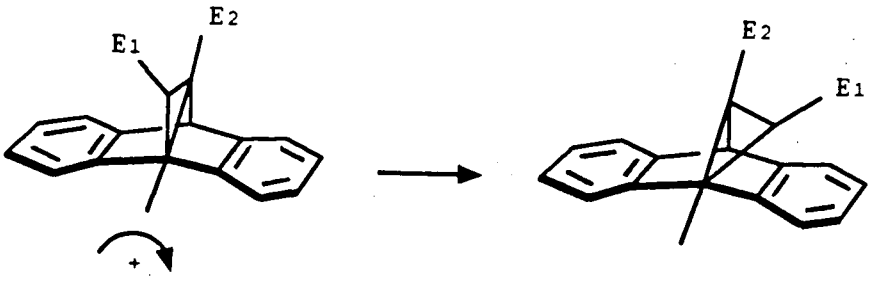

Figure 70. Simulation of the Aryl-Vinyl Bridging Step in the Di-π-Methane Rearrangement of Dibenzobarrelene Diesters.

Displacements are labelled in degrees as positive (clockwise) or negative (counterclockwise) according to the sense of rotation. The PPE was calculated at 2° intervals with equation 14 by using the r* parameters described by Hagler, Huler and Lifson.[147] It should be noticed that four distinct operations can be made and that each of them accounts for a different solid state reaction pathway. In Figure 71, each curve represents the energy profile accompanying the movement of each ester group. Positive and negative values on the horizontal axis represents movement of the ester group in question to either side of the vinyl group. In the case of the diesters Me/iPr-30 and Me/Ph-37, however, we only have experimental results that account for motions taking place at either vinyl carbon, or reaction regioselectivity. The results shown in Figure 71 are in agreement with the experimental results and indicate that the rise in packing potential energy with respect to the displacement of the ester groups is larger for the methyl group in compound 30 and for the phenyl group in 37.

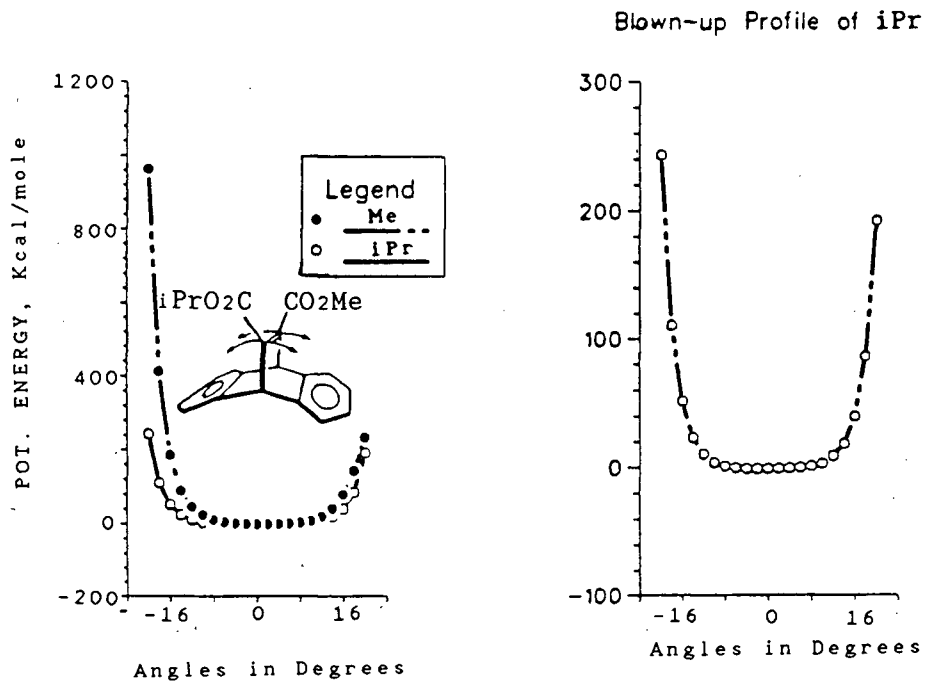

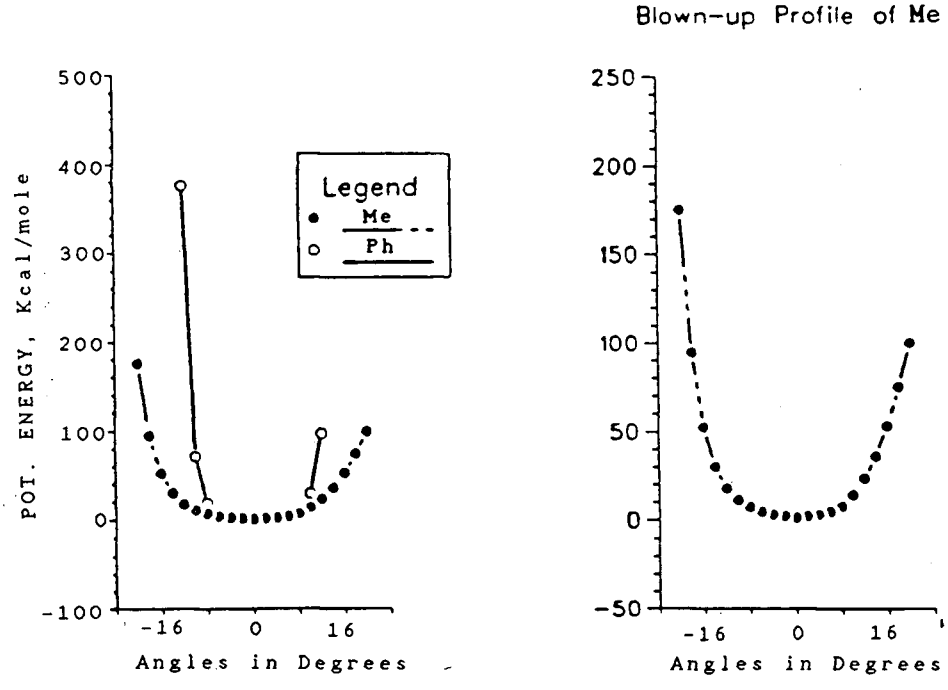

Figure 71. Plots of Change in Packing Potential Energy Resulting During the First Step of the Di-π-Methane Rearrangement of Dibenzobarrelenes Me/iPr-30 and Me/Ph-37.

Regioselectivity in Chiral Crystals of Diester iPr/iPr-23.

With the aid of absolute configuration studies on the chiral dimorph iPr/iPr-23 and its optically active photoproduct, we found that two pathways can explain the solid state photochemical results (page 119, Part II). The question we could not answer in page 119 regarding the reactant-product correlation shown in Figure 49 could be posed in the following manner: which of the two isopropyl ester groups moves during the first step of the reaction to give the observed photoproduct? We are now in the condition to test apply our solid state steric compression hypothesis in an attempt to answer this question.

The PPE plots corresponding to the chiral dimorph of compound iPr/iPr-23, included in Figure 72, indicate that motions at the isopropyl ester group attached to C(11) (absolute configuration 11P) cause a substantially steeper increase in energy. These results suggest that pathways 2 in Figure 49, which involves motions of the ester attached to C(12), is the preferred solid state pathway. This result supports our initial suggestion, based on the observation of having a larger free space around the C(12) isopropyl ester group, and agrees with the conclusions drawn from studies on isomorphic crystals of diester iPr/sBu-42 (see page 201).

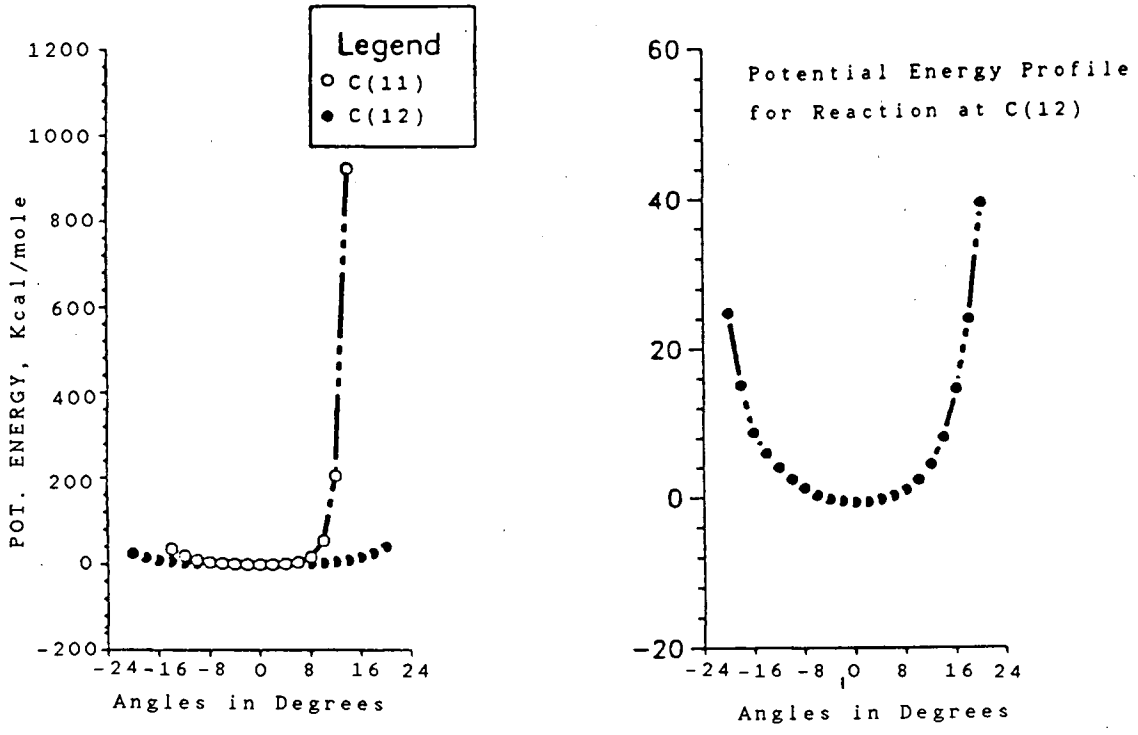

Figure 72. Changes in PPE During the First Step of the Di-π-Methane Rearrangement of Diester iPr/iPr-23.

The Solid State Results at Large.

When the solid state results are analyzed in the context of the solid materials studied, several groups of compounds can be recognized according to the regioselectivity observed. The most interesting and largest group is made up of the diesters Me/nPr-29, Me/iPr-30, Me/sBu-31

(racemic), Me/sBu-31 (optically pure), Me/iPen-34 and Et/sBu-39. The crystals of these materials are characterized by enhancing the solution regioselectivity and, with the exception of 34, by the relatively similar size of their alkyl substituents.

The compounds that reverse the solution selectivity when irradiated in the solid state can be classified in a second group where fewer structural features are probably shared. The mixed diesters Me/Et-28, Me/tBu-32 and Et/iPr-38 can be included in this category. The neo-pentyl derivative 18 should probably be classified alone, since as it was mentioned before, it seems to form a glassy rather than a crystalline material. Photolysis of this material does not affect the regioselectivity with respect to that observed in the solution media. Finally, it seems that the structure of the phenyl substituted derivative 20 should share very little in common with the rest of the compounds and should also be considered separately.

That this classification may not be totally artificial can be appreciated by taking a closer look at the members of the first group. The substituents in this group vary from methyl to ethyl and from n-propyl, isopropyl and sec-butyl to isopentyl. With exception of the pentyl residue, the size (volume) of the alkyl groups under comparison is very similar[144]. It can be expected that these substituents should alter almost insignificantly the size and shape of the entire dibenzobarrelene molecule. Furthermore, it is known that the weak intermolecular forces that determine the crystallization behavior of organic compounds are determined by factors related to the molecular structure, size and shape[30]. It seems therefore possible that the mentioned compounds, having so much structural resemblance, may crystallize with

some common structural features as variations around an optimum crystal structure. Some support for this highly speculative hypothesis may be found in the very interesting observation that the solid state infrared spectra of these compounds (excluding 34 and probably 39) share a large number of common features. The lack of more materials suitable for X-ray structure determination is perhaps not a misfortune but an indication of the stringent requirements for ideal crystallization.

It is interesting to continue speculating by supposing that crystals of compound Me/iPr-30 (for which a full X-ray structure was obtained) may represent the ideal structural model within the compounds of the first group. The relatively high crystal quality obtained is an indication of structural homogeneity throughout the entire crystalline phase. The result of modifying the structure of 30 into that of 29 by a hypothetical 1,2-methyl shift (or other similar compound by a similar operation) may not result in the formation of a totally different crystal structure. Perhaps most of the intermolecular interactions, such as those present in crystals of 30, may still be energetically favorable to crystals of 29. It seems possible that given the relatively small size of the molecular change the new structure will tend to be isomorphic even if somewhat disordered. Kitaigorodski and others have shown that some solid state phenomena such as isomorphism and disorder may result from a delicate energetic compromise.

The speculation presented here may gain the rank of hypothesis when we analyze another set of closely related and isomorphic structures composed of compounds iPr/iPr-23, optically active iPr/sBu-42 and racemic iPr/sBu-42.

PART IV. STUDIES ON CHIRAL MIXED DIESTERS.

It was shown in Part II of this thesis that the solid state may have a pronounced effect on the enantioselectivity of the di-π-methane rearrangement of dibenzobarrelene diesters.[115] The formation of optically active products with exceptionally high enantiomeric yields was interpreted as an indication of a substantial degree of selectivity between reaction pathways at the alternative sides of the vinyl double bond. In Part III, from the study of a series of crystalline mixed diesters, we concluded that the reaction at the two alternative vinyl carbons can also be subject to significant discrimination.[116,149] A combination of the above results suggested that the solid state may influence the selectivity of the rearrangement so that the reaction occurs preferentially by following one of the four alternative reaction pathways presented in Figure 73.

We decided to analyze an experimental model that would allow us, at least in principle, to determine the relative amounts of products arising from each of the four reaction pathways. Such a model could be constituted by dibenzobarrelene diesters possessing two different alkyl substituents, one of which should be chiral. In Figure 73, the products arising from paths A-I and A-II would be differentiated from the products from paths B-I and B-II as being regioisomeric since they originate from benzo-vinyl bridging at different vinyl carbons [C(11) or C(12)]. At the same time, products from pathways A-I and A-II, and from B-I and B-II, would be recognized as diastereomers of each other.

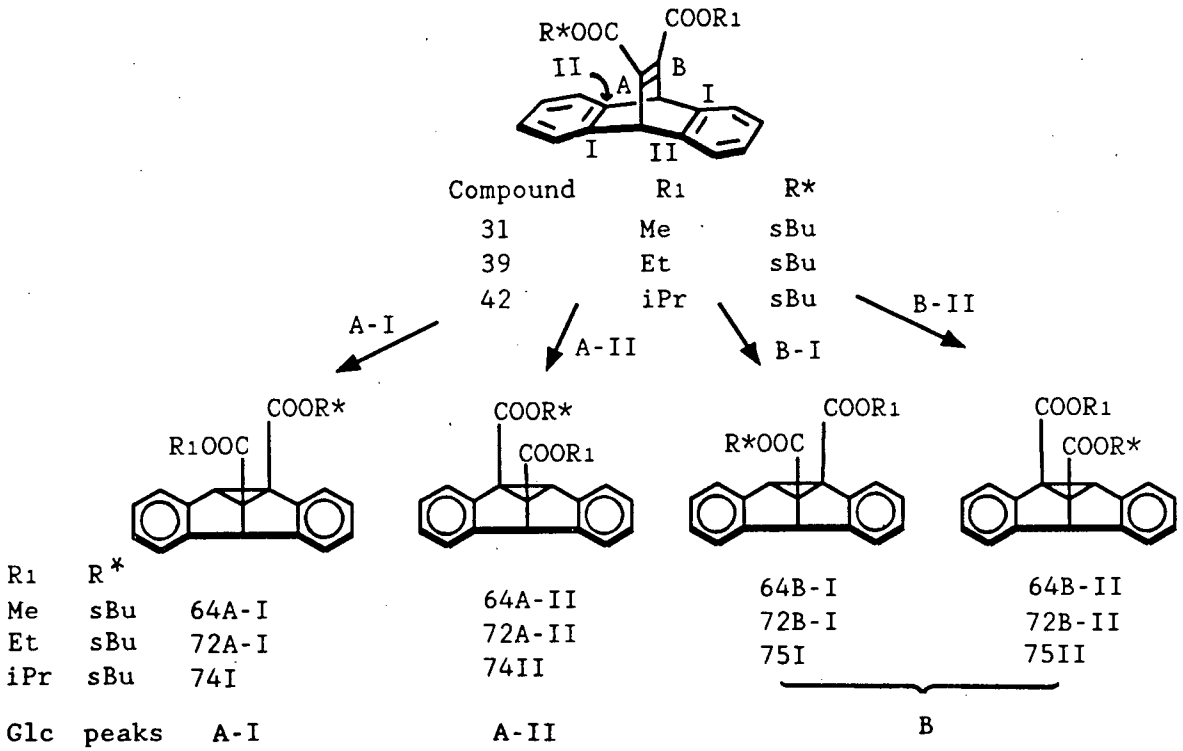

Figure 73. The Di-π-Methane Rearrangement of Chiral Mixed Diesters.

Several compounds were initially synthesized for this purpose. These included the mixed diesters Me/sBu-31, Me/iPen-34, Me/Menth-36, Et/sBu-39 and iPr/sBu-42. However, due to experimental difficulties in the determination of the diastereomeric products from compounds Me/iPen-34 and Me/Menth-36, these compounds were not analyzed in the context of this section. The solution regioselectivity of these two compounds was discussed in the previous section. The solid state regioselectivity of Me/iPen-34 was also included there, along with some aspects of the photochemistry of diesters Me/sBu-31 and Et/sBu-39.

The sec-butyl derivatives studied in this thesis were prepared with commercial (S)-(+)-, and (R,S)-sec-butanol. Crystals of diesters 31 and 42 were prepared with racemic and optically pure materials with the purpose of comparing possible differences in their solid state photochemistry.

Photochemistry in Solution.

The diesters Me/sBu-31, Et/sBu-39 and iPr/sBu-42 were photolyzed by direct irradiation in benzene and acetonitrile solutions and by sensitization in acetone. Glc analysis of the sec-butyl containing compounds resulted in three peaks (B, A-I and A-II) with retention times slightly longer than those of the starting materials. The integrated areas of these peaks, presented in Table XIII, were independent of the two enantiomeric compositions used in the cases of compounds Me/sBu-31 and iPr/sBu-42. Compound Et/sBu-39 was only studied in its optically pure form.

Table XIII. Glc Analysis of the Photoproducts of Diesters Me/sBu-31, Et/sBu-39 and iPr/sBu-42.

	glc[a] Area % (RT)[b]		
Compound	peak B	peak A-I	peak A-II
(S)-(+)-(31)[c]	40(21.3)	27(22.7)	33(23.2)
(R,S)-(31)[c]	40(21.3)	27(22.7)	33(23.2)
(S)-(+)-(39)[d]	50(19.9)	23(20.7)	27(23.2)
(S)-(+)-(42)[e]	56(16.3)	21(16.6)	23(16.9)
(R,S)-(42)[e]	56(16.3)	21(16.6)	23(16.9)

(a) Column: DB-1 15M; (b) Retention time (min); (c) Oven temperature (°C): 195, column head pressure (psi): 10; (d) 200, 10; (e) 200, 12.5.

The regioisomeric identity of the products giving rise to the three glc signals could be established by glc-MS and ^{1}H NMR analysis of the photolysis mixtures and, in the case of diester iPr/sBu-42, by comparing their spectroscopic data with the data from the authentic products obtained by independent regioselective synthesis. The glc-MS identification was based on the structural correlation described in Part III. This information was presented in Table XII (page 139) for the photoproducts from compounds Me/sBu-31 and Et/sBu-39, and is shown in Table XIV (below) for the photoproducts from compound iPr/sBu-42.

The mass spectra of the products from compounds 31, 39 and 42 corresponding to peak B were consistent with the structures expected from

products via pathways B-I and B-II (bonding, in Figure 73, at the vinyl carbon next to the ester groups R_1 = Me, Et and iPr respectively). The spectra were characterized, in part, by fragments indicative of the loss of MeOH and MeOH + CO, EtOH and EtOH + CO, and iPrOH and iPrOH + CO respectively (Figure 74). The fragment ions from products giving rise to peaks A-I and A-II, which were essentially identical to each other, were indicative of the photoproducts arising from pathways A-I and A-II and were characterized by loss of sBuOH, sBuOH + CO and 2-butene, among other specific fragments (Figure 74). It should be noted that the present analysis does not distinguish between diastereomeric products from pathways I and II.

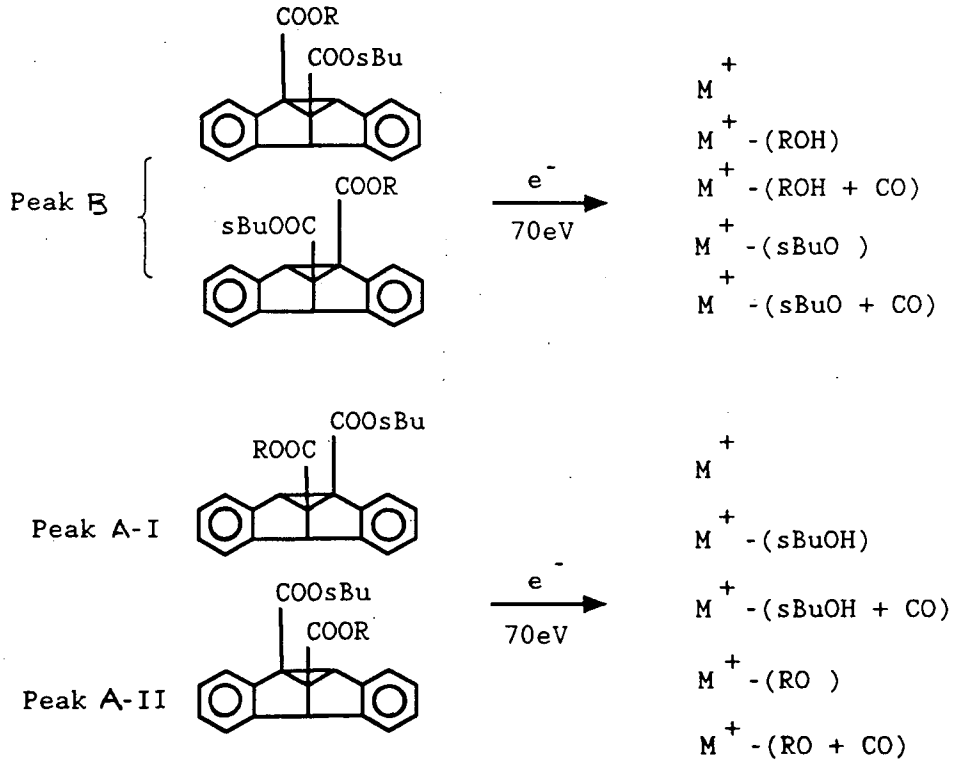

Figure 74. Mass Spectrometric Fragmentation of the Photoproducts from Photolysis of Sec-butyl containing Dibenzobarrelene Diesters.

Table XIV. Selected Fragment-ions from Photoproducts of Diester 42.

	Relative Intensity			
m/e	peak B	peak A-I	peak B-II	Fragment lost
390(M^+)	15	10	9	-
334	0	7	10	C_4H_8
330	9	0	0	iPrOH
316	0	11	12	sBuOH
303	4	5	4	iPrOH + CO
302	14	2	1	iPrO· + CO
289	23	4	5	sBuOH + CO
288	6	19	22	sBuO· + CO
247	100	100	100	$C_8H_{16}O_2$
202	80	73	70	$C_{12}H_{16}O_4$

The regioisomeric glc-MS peak assignments were further supported in the case of the photolysis products from diester iPr/sBu-**42** when authentic samples of compounds **75I/75II** and compounds **74I/74II** were analyzed by the same method. These compounds were synthesized[152] in two steps (90% regioisomeric purity by glc) from the isopropyl monoacid **40** and the sec-butyl monoacid **41** respectively (Figure 75). The regioselectivity from these preparations could be established by using a similar procedure where the isopropyl monoacid **41** is converted into the previously isolated and X-ray characterized dibenzosemibullvalene **63A** by treatment with methanol.

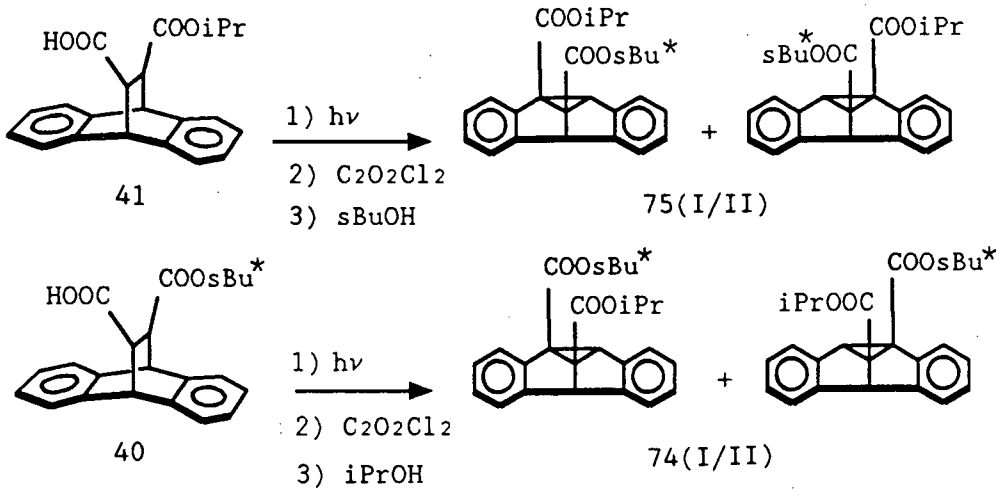

Figure 75. Regioselective Preparation of Dibenzosemibullvalenes **75I/75II** and **74I/74II**.

The relative diastereoselectivity arising from pathways A-I and A-II, as we saw above, can be determined by glc analysis (peaks A-I versus peaks A-II). Contrastingly, products arising from pathways B-I and B-II give a single peak (peak B), and their relative amounts cannot be determined by the same methodology. With authentic samples of the regioisomeric pair **75I/75II** in hand, it became desirable to develop an analytical method able to resolve and quantify their relative amounts in the total photolysis mixture of the starting material iPr/sBu-**42**. With this purpose in mind, a series of ^{1}H NMR spectra of the total photolysis mixture from compound **42** and of the samples containing **74I/74II** and **75I/75II** were explored in several solvents. The goal of this study was to find an ideally well

resolved signal from each photoproduct for the purpose of assigning the relative diastereomeric ratios by ^{1}H NMR integration. It was found that the best resolution came from the signals of H(8d) (see formula in Table XV for numbering), since these were sharp singlets isolated from the rest of the dibenzosemibullvalene diester signals. The chemical shifts of the signals corresponding to these hydrogens and of those at C(4b) are included in Table XV.

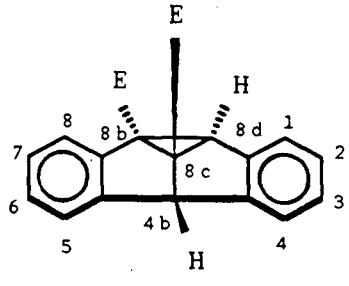

Table XV. The ^{1}H NMR Resonances of H(8d) and H(4b) from Products of Diester iPr/sBu-42 as a Function of Four Different Solvents.

Solvent-d	δH8d(No. of H)	H4b(No. of H)
Acetone	4.35(1), 4.37(2), 4.39(1)	5.06(2), 5.08(2)
Acetonitrile	4.38(1), 4.39(2), 4.41(1)	5.06(4)
Chloroform	4.41(1), 4.42(3)	5.03-5.01(4)
Benzene	4.76(1), 4.77(3)	5.10(2), 5.12(1), 5.14(1)

The best resolution of H(8d) was obtained in acetone-d_6 where the signals of **75I/75II** appeared at δ 4.35 and 4.37 and the signals of **74I/74II** at δ 4.37 and 4.39 respectively. Even though only the signal from one of the two diastereomers of **75** was resolved (either **75I** or **75II**), the relative diastereoselectivity between pathways B-I and B-II can be calculated (normalized with respect to a total of 100% of the four products) by subtracting the integration from the signal at 4.35 ppm (as percent) from the glc-determined regioselectivity (also as percent).

A summary of this information in the case of the products from solution photolysis of diester iPr/sBu-**42** is presented in Table XVI. It should be pointed out that the absolute stereochemistry of the diastereomeric products [given by the four chiral dibenzosemibullvalene carbons C(4b), C(8b), C(8c) and C(8d)], cannot be deduced from the present information and the structural assignments between diastereomeric pairs, up to now, remains only illustrative.

Table XVI. Relative Yields of Photoproducts from Diester iPr/sBu-**42**.

	Photoproduct Integration (%)							
Analysis:	**75I**		**75II**		**74I**		**74II**	
glc[a]	---	56[c]	---		21		23	
^{1}H NMR[b]	27		---	49	---		24	
Combined	27		29[d]		21		23	

a) Estimated error ± 5 %; b) Estimated error ± 10 %;

c) Signals not resolved; d) Calculated value.

The results shown in Tables XII and XVI indicate that compound iPr/sBu-**42** follows a reaction pathway that involves reaction by benzo-vinyl bridging at the vinyl carbon to which the isopropyl substituent is attached. The regioselectivity observed for compounds Me/sBu-**31** and Et/sBu-**39**, on the other hand, favors the normally observed (see Part III) bond formation at the vinyl carbon attached to the bulkier sec-butyl substituent. The different regioselectivity of the isopropyl containing compound is unexpected and may be due to a systematic error in our analytical methodology. It should be noted that the glc regioisomeric resolution, upon which our results are heavily based, is poorer in the case of iPr/sBu-**42**. The statistical error in all our determinations is of the order of ≤5%, systematic errors, however, may be slightly larger depending on the analytical resolution between the photoproducts observed from a given compound.

A small diastereoselectivity between pathways A-I and A-II was observed from the glc determination of compounds **31**, **39** and **42** (peak A-I:peak A-II ≈ 45:55, Table XIII above). In the case of the isopropyl containing compound (**42**), the selectivity between products **74I** and **74II** from pathways B-I and B-II was also found to be in a similar range. These results indicate that the sec-butyl group does not impose a significant stereo-differentiating[102] influence on the vinyl-face selectivity of the reaction. This conclusion was further supported when the photolysis mixture of (S)-(+)-**42** (four diastereomers, see Figure 73 in page 177) was submitted to hydrolysis and reaction with diazomethane (see page 203) to give a sample of dibenzosemibullvalene Me/Me-**52** (two enantiomers). The sample obtained in this manner presented a small optical rotation ($[\alpha]_D$ =

0.24°), which reflects the disymmetric induction of the sec-butyl handle on the face selectivity of the rearrangement (one enantiomer of **52** from **74I** and **75I**, and the other from **74II** and **75II**). The enantiomeric excess of **52** calculated of from this treatment (e.e. = 1.5±0.5%) correlates well with the diastereomeric excess[102] of **74** and **75** calculated by glc and ^{1}H NMR:

$$\text{d.e.} = \frac{[(74II + 75II) - (74I + 75I)]}{[(74II + 75II) + (75I + 75I)]} \times 100 = 2\%$$

Studies in the Solid State.

The solid state reactivity, as we have seen, depends substantially on the packing arrangement present in the crystal lattice. The crystallization behavior of compounds having permanent molecular chirality presents some particular features which will be reviewed briefly in order to facilitate the discussion of the solid state photochemical results.

Crystallization of Chiral Compounds.[93]

The crystallization of chiral compounds depends primarily on whether they are present as the pure enantiomers or as the racemate. When a crystal lattice is built up with molecules of a pure enantiomer it will necessarily pack in one of the 65 enantiomorphous space groups.[94] Samples of the racemate, which is an equimolar mixture of the two enantiomers in an unspecified physical state,[78] have been found to present three

different crystallization alternatives:[93]

1) A racemic modification or racemic compound, which consists of a single crystalline phase composed of equimolar amounts of the two enantiomers, obviously with a racemic space group.

2) Crystallization by spontaneous resolution results when the racemate crystallizes as a heterogeneous mixture of chiral crystals of the two enantiomorphous phases. The samples resulting from such crystallizations are also referred to as racemic mixtures or conglomerates.

3) Crystallization in a solid solution, which is a phase that can be composed of variable amounts of the two enantiomers, usually in a disordered manner and with space groups and crystal properties that can be either those of the chiral or of the racemic modifications.

The identification of the different types of crystalline racemates can be realized by considering a binary system (ternary if solvent is needed in crystallization) whose properties may be described by the phase rule.[149] Three fundamental types of enantiomeric mixtures have been proposed according to their melting point diagrams as shown in Figure 76. Additional complications to the phase diagram can be expected when more than one crystallization behavior occurs at the same time; these will not be discused here.

In the phase diagrams in Figure 76 the vertical axes represent the equilibrium temperature of the sample and the horizontal axes represent the sample composition from 100% one enantiomer, (+) to the left, to 100% the opposite enantiomer, (-) to the right. There are three regions in the phase diagrams depending on the phases present. At temperatures below the dotted lines, or <u>solidus</u> lines, only solid phases can coexist under

equilibrium conditions. Above the filled, or liquidus lines, only a single homogeneous liquid phase can exist. The space between the two previous regions is the region of the phase diagram where solid and liquid can coexist in equilibrium.

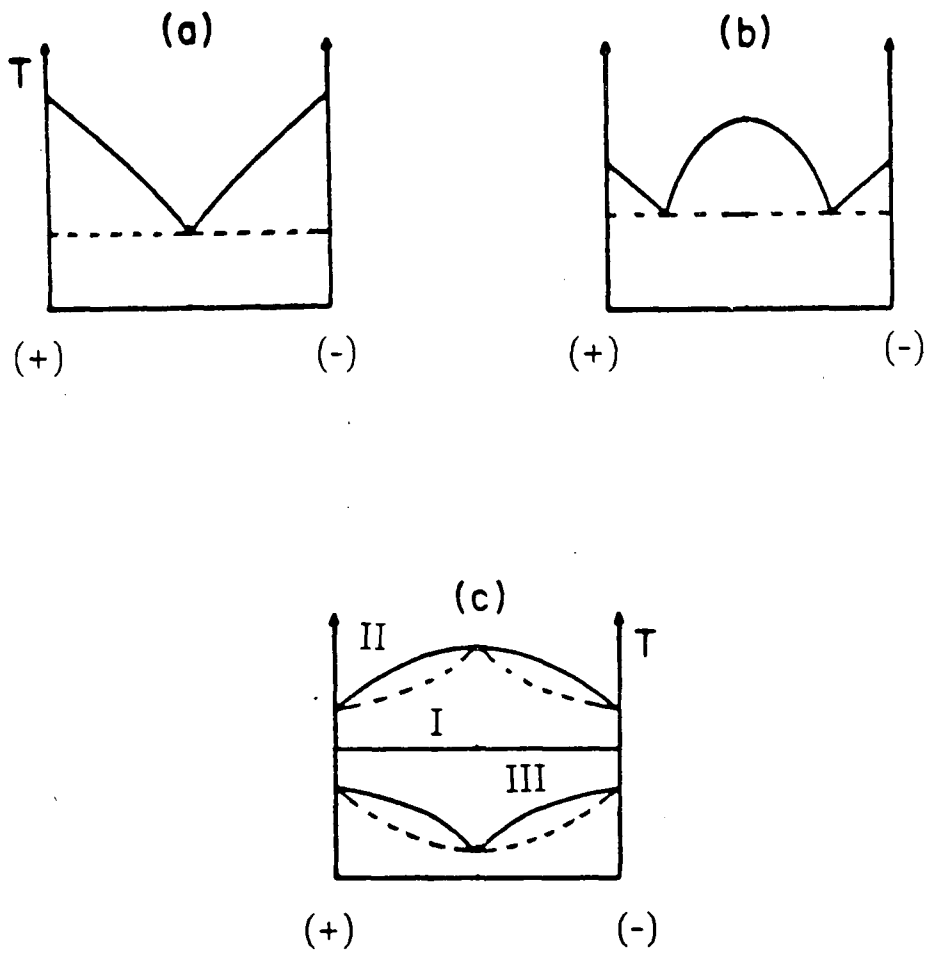

Figure 76. Binary Phase Diagram of (a) the Racemic Mixture, (b) the Racemic Compound and, (c) Solid Solutions (Mixed Crystal) of the Enantiomers: (I) Ideal or Roozeboom Type I, (II) Non-Ideal with a Maximum or Roozeboom Type II and (III) Non-Ideal with a Minimum or Roozeboom Type III. (Adapted from Reference 93)

The binary phase diagram of the racemic mixture, diagram (a), is characterized by the maximum melting points of the two pure enantiomorphous phases and a lower melting point of the eutectic. The solid region of the diagram is composed of two different and enantiomorphous solid phases along the entire composition range. Any single crystal is necessarily composed of only one enantiomer and the composition of the entire solid phase is given by the amount of crystals of each enantiomer. At the eutectic point, equal amounts of crystals of the two enantiomorphous phases are present in equilibrium with a racemic liquid phase and should not be mistaken with the solid phase corresponding to the racemic compound.

The typical phase diagram of the racemic compound is represented in Figure 76(b) and may vary in shape depending on whether the racemic modification possesses a higher or a lower melting point with respect to the pure enantiomers. These diagrams are characterized by two eutectic points at which the sample is composed of a mixture of crystals of the racemic modification and of enantiomorphous crystals of the pure enantiomers which are in equilibrium with the liquid phase.

In the case of a solid solution of the enantiomers three limiting cases (assuming unlimited solubility) have been found depending on the variation of the melting point with the composition given by the optical purity of the sample (Figure 76(c)). The first case, an ideal solid solution (Roozeboom type I), is one in which the melting point is maintained constant along the entire enantiomeric composition. The classification of the other two types of non-ideal solid solutions depends on whether the melting points, that vary with the sample composition, have

either a maximum (Roozeboom type II) or a minimum (Roozeboom type III). The solid region of the phase diagrams of solid solutions is determined by a single homogeneous solid phase along the entire composition range.

The melting points (of single crystals), solid state infrared and ^{13}C NMR spectra of the racemic mixture are always identical to those from the pure enantiomers and different, at least in principle, from those from the racemic compound and the solid solution.[93] In the case of non-ideal solid solutions the melting points of two single crystals should normally be different if they have different enantiomeric composition. Single crystals of the racemic mixture (enantiomorphous) and of the racemic compound will always have fixed composition and melting points.

It has been observed that the racemic modification is by far the most common crystallization alternative adopted by samples containing the same amounts of the two enantiomers.[93] However, the occurrence of spontaneous resolutions and of solid solutions of the enantiomers, or mixed crystals, have also been documented since the time of Pasteur. It has been suggested[93] that the racemic mixture (spontaneous resolution) is thermodynamically unstable with respect to the racemic modifications by 0.2 to 2 Kcal/mol according to the following thermodynamic relationship:

(L)-Crystal + (D)-Crystal ---> Racemic compound

It has been proposed that the reason for this difference results from the closer intermolecular packing possible in the crystals of the racemic compound.[150] It has also been suggested that the crystal structures of the pure enantiomers and of the racemic compound may exhibit significant one

or two dimensional similarities and that the crystal structure of one may frequently be deduced from that of the other.[150] Pedone and Benedetti have proposed that the packing of chiral compounds occurs such that homochiral molecules arrange first in compact layers or columns which may then repeat by translation in the enantiomorphous modification and by mirror planes and inversion centers in the case of the racemic compound.[150c].

Solid solutions or mixed crystals of the enantiomers are the least common of all the crystallization alternatives for optically active compounds.[93] This situation has been found to occur when the structures of the two enantiomers are so similar that they can occupy the lattice space of each other in the solid state.[13] Large molecules with a small chiral handle can be good candidates for formation of solid solutions of the enantiomers. In some cases the two enantiomers fit the same crystal lattice site at the expense of some minor molecular adjustment such as a small conformational change (conformational isomorphism).[83]

Optically pure samples can sometimes pack in crystals typical of the racemic compound and samples of the racemate can sometimes pack in crystals of the optically pure enantiomers. The former situation can be mentally constructed by hypothetically taking out of a racemic crystal the molecules of one enantiomer and replacing them by molecules of the other enantiomer until the crystal becomes optically pure. The symmetry elements present in the original crystal are transformed so that inversion centers and mirror and glide planes can no longer operate and the crystal becomes chiral with two independent (quasienantiomeric) molecules per asymmetric unit. Crystals of the chiral modification can be built with the racemate by following a similar procedure where 50% of the molecules

of the chiral crystal are exchanged by molecules of the other enantiomer. Solid solutions of the enantiomers can be considered to result from a poor chiral recognition between the chiral molecular space in the crystal lattice and the chiral molecular structure that will occupy it.[92]

Solid solutions of the enantiomers can occur in three general types according to the manner in which the enantiomeric exchanges take place:[93]

1) Crystallization in a disordered solution results when one of the enantiomers is replaced by the other in a totally random way (Figure 77). Statistical distributions of the enantiomers occur independently of the occupancy of the neighboring sites.

```
R R R R R R R R R                          R S R S R R S R S
 R R R R R R R R R          (S)             R R R R S R R R S
R R R R R R R R R     --------------->     S R R S R R R R R
 R R R R R R R R R                          R R S R R S R S R
R R R R R R R R R                          R S R R S R R S R
```

Figure 77. Solid Solution with Statistical Disorder.

2) Crystallization in solid solutions with short-range order occurs when substitution of one enantiomer by the other takes place in a macroscopically random way but the occupancy of the neighboring sites is largely influenced by each enantiomeric molecule (Figure 78).

```
R R R R R R R R                          R R S S S R R R R
 R R R R R R R R          (S)              R S S S S R R R R
R R R R R R R R     --------------->      R R S S S R R R S
 R R R R R R R R                          R S R R R R S S S
R R R R R R R R                          R S S S R R S S S
```

Figure 78. Solid Solution with Short Range Order.

3) Crystallization in solid solutions with non-statistical inverse symmetry order occurs when molecules in the enantiomorphous crystal occupy two non-equivalent sites R and R′ in their crystal lattice. The occupancy of these two sites in the mixed crystal then occurs in a non-statistical manner where one enantiomer always occupies R-sites and the other enantiomer always occupies R′-sites. Under these circumstances a real inversion center may appear leading to the crystal structure of the racemate (Figure 79).

```
R R′R R′R R′R R′R                        R S R S R S R S R
 R R′R R′R R′R R′R          (S)            R S R S R S R S R
R R′R R′R R′R R′R     --------------->    R S R S R S R S R
 R R′R R′R R′R R′R                        R S R S R S R S R
R R′R R′R R′R R′R                        R S R S R S R S R
```

Figure 79. Solid Solution with Non-Statistical Inverse Symmetry Order.

It has been pointed out that the most important requirement for the formation of a solid solution refers to the size and shape similarity between the compounds forming a mixed crystal.[13] Interestingly, this requirement is also determining in the formation of isomorphic crystal structures and it has been observed that isomorphic crystals of different

compounds can often form continuous solid solutions. Kitaigorodsky has proposed an empirical and semiquantitative estimate of the likelihood of two compounds forming a solid solution or isomorphic crystal structures.[13] This estimate can be obtained from the coefficient of geometrical similarity ϵ that results from the ratio between the non-overlapping and overlapping volumes of the compounds under comparison after the best molecular fit has been obtained. The coefficient ϵ is defined mathematically according to the following formula:

$$\epsilon = 1 - (\text{non-overlapping volume}) / (\text{overlapping volume})$$

The closer the value of ϵ to unity the more the two molecules will look alike and the larger the probability of solid solubility and isomorphism. Although a proper estimate of the molecular volume usually requires the knowledge of the conformation of the two molecules under comparison, approximate measurements can sometimes be useful. A simple and useful method was devised by Kitaigorodsky[13,30] and Bondi[151] which is based on a group increment approach. In this approximation the molecules are considered to be formed by smaller radicals or groups which are defined by overlapping atomic spheres with volumes defined by their X-ray derived van der Waals radii. Gavezzotti[144] has recently updated and tabulated a number of useful group increments deduced from an improved methodology to calculate atomic and molecular volumes from X-ray measured structural parameters.

The Solid State Properties and Photochemistry of Diester 42.

The solid state properties and photochemical results for diester iPr/sBu-42 will be discussed first since partial X-ray structural data could be obtained for the two crystalline materials.[152] The results and information obtained form these compounds will be useful in interpreting the solid state photochemistry of compounds Me/sBu-31 and Et/sBu-39.

Crystals of diester iPr/sBu-42 were grown from the melt, from ethanol and from many other solvents (diethyl ether, acetonitrile, hexane, etc.) by using optically pure and racemic materials. No indication of polymorphism was obtained from materials analyzed by solid state FTIR spectroscopy. The melting point of single crystals of the optically pure material was 11° higher (133-5°) than the melting point of the racemate (122-4°C). The difference in melting points, indicative of two different crystal phases, and the lack of optical rotation from solutions of several single crystalline samples of the racemate, excluded the possibility of a spontaneous resolution into crystals of the pure enantiomers. A few single crystals grown from the racemate indicated a small enantiomeric enrichment of 10% or less without any preference for either of the two antipodes. The solid state infrared spectrum of the optically pure material was almost identical to the spectrum from crystals of the racemate suggesting the similar solid phase of a solid solution of the enantiomers (Figure 80). The FTIR spectra and the crystal morphology of the two materials were almost identical to those of crystals of the chiral $P2_12_12_1$ modification of the diisopropyl diester 23 (Figure 38, Part II) suggesting an isomorphic crystal structure relationship.

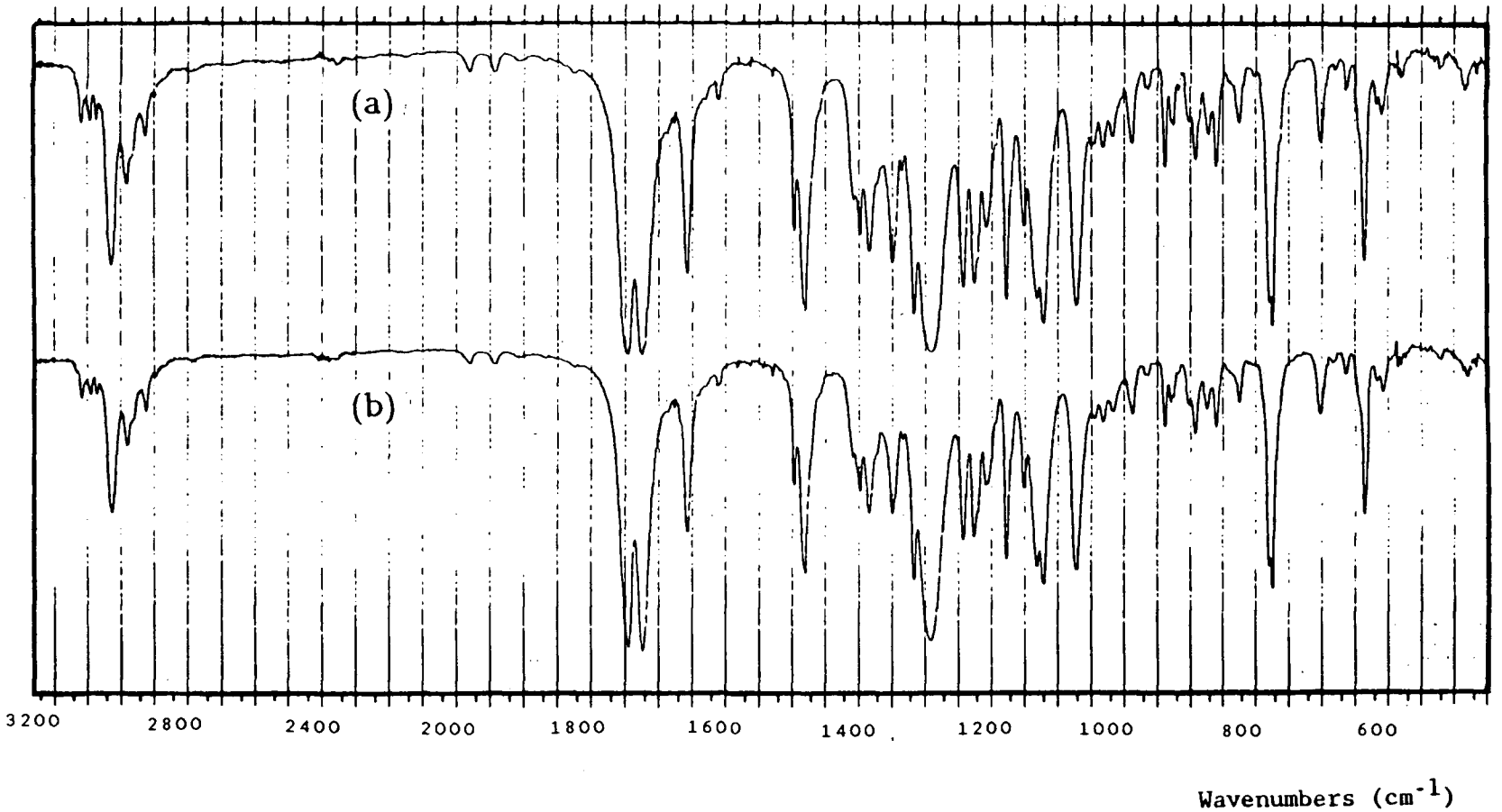

Figure 80. Solid State FT-IR Spectra of Chiral $P2_12_12_1$ Crystals of Diester iPr/sBu-42: (a) Racemic and (b) Optically Active.

Our empirical conclusions were supported by the photochemical generation of optically active products not only from the optically pure material but also from the racemate. The isomorphism was definitely confirmed when single crystal X-ray diffraction analyses were performed on crystalline samples of the optically pure and racemic materials. Convincing evidence was found not only in the expectedly identical space groups, $P2_12_12_1$, but also on the lattice parameters of the crystals of the three samples (Table XVII).

Further resemblance between the above crystalline materials was found in their X-ray molecular structures. This can be documented from the most characteristic structural parameters used to describe the molecular structure of the dibenzobarrelene compounds studied in this thesis, the carbonyl-vinyl torsion angles presented in Table XVIII. The molecular disymmetry conferred by the conformation of the ene-dioate system was essentially identical for all three compounds.

Table XVII. Lattice Parameters of $P2_12_12_1$ Crystals of Compounds **23**, (S)-(+)-**42** and (R,S)-**42**.

	iPr/iPr-**23**	iPr/(S)-(+)-sBu-**42**	iPr/(R,S)-sBu-**42**
a(Å)	8.3304	8.4936	8.4624
b(Å)	11.6893	11.9210	11.8705
c(Å)	21.7937	21.6691	21.6788
$\alpha=\beta=\eta$ (degrees)	90	90	90
Space group	$P2_12_12_1$	$P2_12_12_1$	$P2_12_12_1$
Z	4	4	4
Volume ($Å^3$)	2122.20	2194.14	2177.70
Density[a] (g/cm^3)	1.1767	1.1381	1.1467

(a) Calculated density.

Table XVIII. Conformation of the Ene-dioate System in Diesters 23, (S)-(+)-42 and (R,S)-42.

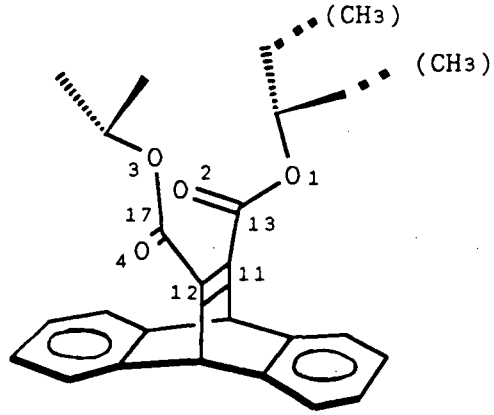

Torsion Angle	Diiso-23	(S)-(+)-42	(R,S)-42
O(2)-C(13)-C(11)-C(12)	63.7	68.4	70.1
O(4)-C(17)-C(12)-C(11)	164.3	166.2	167.4

The conformation of the ene-dioate chromophore gives the dibenzobarrelene structure a molecular disymmetry that is independent of the chirality of the sec-butyl group substituent. A single lattice site can be occupied in a non-selective manner by molecules of (S)-(+)-42 or (R)-(−)-42 in the case of the racemate. The X-ray molecular structure, although not fully elucidated as a result of substantial crystallographic disorder, revealed that the location of the sec-butyl group in the structures of the two forms of diester 42 resulted from replacement of the isopropyl group attached to the alkoxy oxygen O(1) in the diisopropyl diester 23. This disorder was present in both the optically active and racemic materials, thus suggesting that both structures may correspond to a non-ideal statistically disordered solid solution of the enantiomers.

Further evidence for the mutual solid state solubility of the enantiomers of compound 42 was obtained by observing different melting points from single crystals grown from solutions prepared by mixing different amounts of the optically pure and racemic materials (Table XIX). Although the exact composition in the solid phase was not determined, our measurements are strongly indicative of a non-ideal solid solution (Roozeboom type III) with a minimum melting point.

Table XIX. Melting Points of Mixed Crystals of Diester 42.

mole % (S)-(+)-42 in solution	melting point (°C)
50	122-4
60	126-8
70	129-31
80	131-2
90	132-4
100	133-5

The relative yields of all four possible diastereomeric products were determined by the ^{1}H NMR and glc methodology developed in the case of the solution photolysis (Table XV, page 183). The product distribution was found to be substantially different when photolyses were carried out in the optically pure and racemic crystalline materials.

Table XX. Solid State Stereoselectivity from Compound 42[a].

Compound	75I	/	75II(%)	74I	/	74II(%)
iPr/(+)-sBu-42[b]	85		5	5		5
iPr/(±)-sBu-42[b]	31		31	8		31

a) Structures shown in Figure 83, page 206; b) Values determined by ^1H NMR and glc.

Photochemistry of the Optically Pure Crystalline Material.

Photolysis of crystals of the optically pure sample resulted in a significant regio- and diastereoselectivity indicative of a preference for one of the four available solid state reaction pathways. The regioselectivity observed indicates that the more favored (90%, Table XX) benzo-vinyl bonding step occurs at the vinyl carbon, C(11), which is next to the isopropyl substituent attached to the O(1)-C(13)-O(2) carboxylate group (bonding 12-I and 12-II, Figure 82). This result is consistent with our steric compression hypothesis that predicted bonding at the same vinyl carbon in the isomorphic diisopropyl derivative (page 172).

Distinction between pathways 12-I and 12-II and the assignment of the absolute stereochemistry of the respective photoproduct structures requires knowledge of the absolute stereochemistry of the asymmetric centers, C(4b), C(8b), C(8c) and C(8d), in the dibenzosemibullvalene skeleton (see Table XV for numbering). Pathways 12-I and 12-II, as shown in Figure 82, generate the {(S)-C(4a), (S)-C(8b), (S)-C(8c), (S)-C(8d)} and the {(R)-C(4a), (R)-C(8b), (R)-C(8c), (R)-C(8d)}-dibenzosemibullvalene

stereochemistry respectively. This assignment is possible in the case of the solid state mixture since we know the absolute stereochemistry and specific rotation of the analogous diisopropyl dibenzosemibullvalene diester all-(S)-(−)-57, and we can perform a stereochemical correlation[78] between this compound and the major photoproduct ((+)-75I) from diester (S)-(+)-42.

A direct polarimetric comparison would not be valid because the rotation of the photoproducts from (S)-(+)-42 could have a significant and perhaps obscuring contribution arising from the chiral sec-butyl ester. Ideally, in order to obtain its absolute configuration from the sign of its optical rotation, the major photoproduct from diester (S)-(+)-42 and the optically pure dibenzosemibullvalene iPr/iPr-57 should be converted into the same compound without modifying their absolute stereochemistry during the homologation process. For practical reasons we have converted the total solid state photoproduct mixture into the dibenzosemibullvalene Me/Me-52. The absolute configuration deduced in this manner should be that of the major photoproduct 75I(+) since it comprises 85% of the total reaction mixture and its absolute configuration should clearly dominate the optical activity of the entire photoproduct mixture.

The pure solid state photoproduct mixture from 0.110g of (S)-(+)-42 ($[\alpha]_D$ = 20.6°, (c=0.3, $CHCl_3$)) was obtained by partial photolysis and subsequent derivatization (diazomethane) and separation of the unreacted starting material. The products were transesterified by alkaline hydrolysis and treatment with diazomethane (Figure 81) to give the optically active dimethyl dibenzosemibullvalene (+)-52. The sign of the optical rotation so obtained ($[\alpha]_D$ = 14.5, (c = 0.12, $CHCl_3$)) was opposite to that

from the diisopropyl dibenzosemibullvalene all-(S)-(−)-57. This result indicates that the absolute stereochemistry of the major product from solid (S)-(+)-42 (compound 75I(+)) possesses the {(R)-4b, (R)-8b, (R)-8c, (R)-8d} absolute stereochemistry, and establishes the preference for pathway 12-I and the absolute stereochemistry of diester (+)-75I shown in Figure 82.

Since the dibenzosemibullvalene absolute stereochemistry of products arising from pathways "I" are the same, it should be noted that our hydrolysis treatment and esterification should give a mixture of 90% (+)-52 and 10% (−)-52 arising from (75I + 74I) and (75II + 74II) respectively (i.e. Figure 73). This was confirmed by chiral shift reagent ^1H NMR studies on the obtained sample of 52 with 1 equivalent of $Eu(hfc)_3$ performed as in the case of the diethyl and diisopropyl dibenzosemibullvalene compounds described earlier.

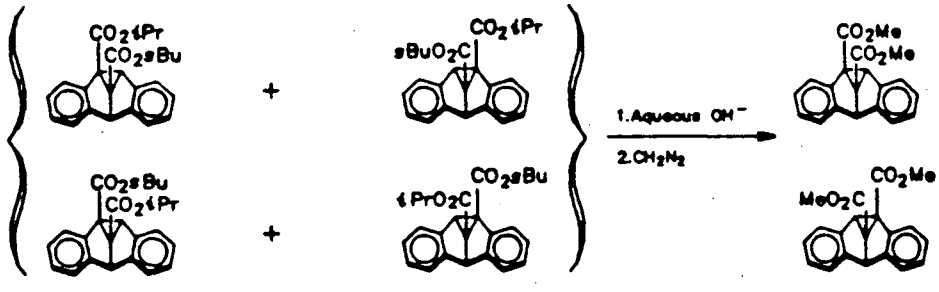

Figure 81. Conversion of the Photoproducts from (S)-(+)-42 into the Dimethyl Dibenzosemibullvalene (+)-52.

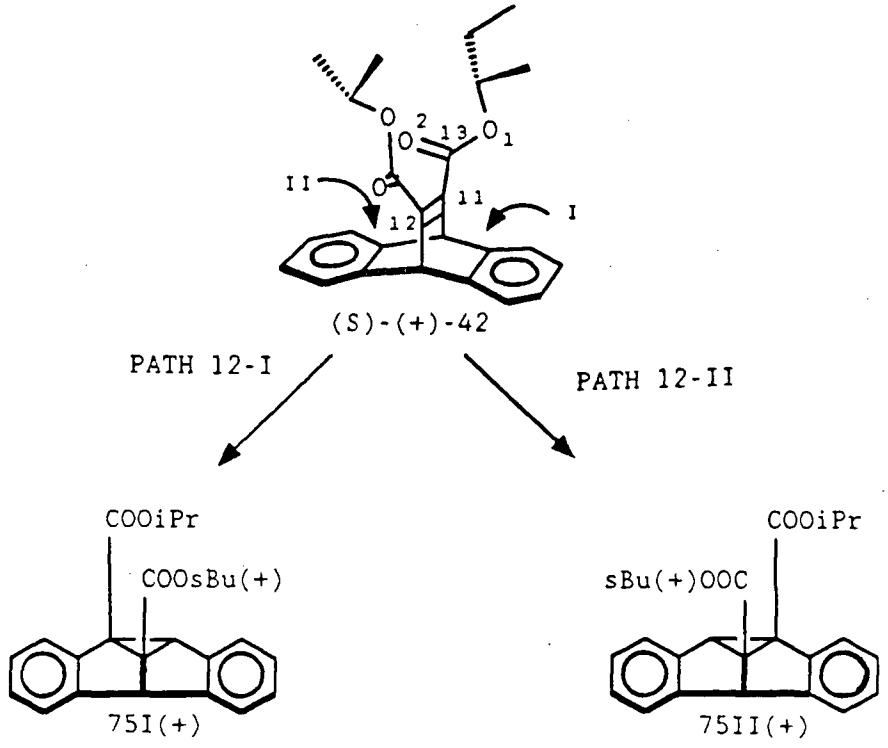

Figure 82. Formation of Dibenzosemibullvalenes 75I and 75II from (S)-(+)-42.

A final point concerning the formation of (+)-75II in the solid state involves the solid state conformation of the ene-dioate system of the starting material (S)-(+)-42. The absolute configuration of the dibenzobarrelene structure as 11M,12P or 11P,12M requires the knowledge of the absolute configuration of the enantiomorphous crystal phase (i.e. right or left 2_1-screw axes). With a chiral handle in the molecular structure this procedure should normally be trivial and require only a well resolved X-ray structure. Unfortunately, the disorder present in the sec-butyl group prevents us from an experimental determination of this

information since the sec-butyl conformation and structure could not be unambiguously established. However, based on our results with the isomorphic chiral diisopropyl diester 23, we can propose that the 11M,12P conformation shown in Figure 82 should be the reacting molecular structure in the chiral crystals of (S)-(+)-42.

Photochemistry of the Racemate of Compound 42.

The photochemical results from crystals of the racemic diester 42 differed significantly from the results of the optically pure compound (Table XX). A redistribution of the photoproducts was detected and the regioselectivity, still favoring bonding at the vinyl carbon next to the isopropyl ester group, diminished to a ratio (75I+77II):(74I+74II) = (31+31):(7+31). Three out of the four diastereomerically different products were detected in relative large amounts (31% each).

It should be noticed that the two enantiomers of the crystals of the starting materials can give up to eight possible photoproducts (Figure 83). Each product has three stereochemically independent elements and all should be described in order to establish their relative structures. Compounds labeled 74 differ from compounds 75 in that they are regioisomers, compounds labeled "I" differ from compounds "II" in the absolute stereochemistry of the dibenzosemibullvalene asymmetric carbons, either all R or all S, and finally compounds labeled (+) differ from compounds labeled (-) depending on their respective enantiomeric sec-butyl handle.

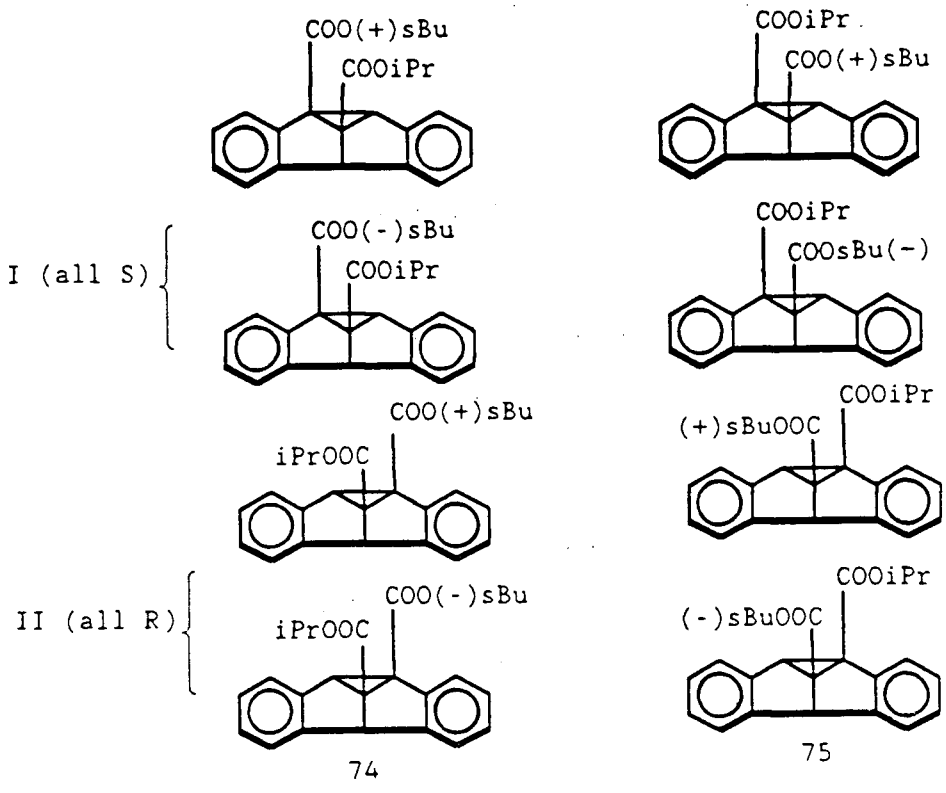

Figure 83. Structural Possibilities for the Photoproducts From Diester (±)-sec-butyl/isopropyl-42.

The first question we address here relates to the effect of the chiral crystal lattice on the stereochemistry of the dibenzosemibullvalene skeleton, that is, the relative ratio of products "I" versus products "II."

Asymmetric Synthesis by Solid State Reaction of the Racemate of 42.

If the reaction of the racemic diester 42 occurs through the control of the crystal lattice symmetry, it may generate optically active products even though both enantiomers are present in equal amounts. The generation of optically active products from racemic starting materials, without imposition of any external chiral influence, is a most uncommon phenomenon with only one literature precedent.[112] The first step in the present study was to determine the feasibility of this type of absolute asymmetric synthesis, carried out for the first time in a unimolecular reaction.

The procedure used to study the asymmetric induction in chiral crystals of the diisopropyl diester 23 was applied to six large single crystals of racemic 42 selected at random from several crystal batches. The results shown in Table XXI indicate high specific rotations, either positive or negative, for all the samples studied. Slightly larger variations in the specific rotation values as compared with the symmetric diesters 21 and 23, cannot be taken as evidence of inconsistency in the enantiomeric induction, as the optical rotation in the case of these photolysis mixtures may result from up to ten possible optically active compounds, eight products (Figure 83) and two starting materials.

Table XXI. Solid State Induced Optical Activity by Photolysis of Crystals of the Racemate of Diester **42**.

Sample	Weight (g)	% Conversion	α (degrees)	$[\alpha]_D$(degrees)
1	0.0258	11.8	0.065	21.4
2	0.0217	14.9	0.071	21.9
3	0.0138	18.9	0.046	18.0
4	0.1029	12.1	-0.218	-17.2
5	0.1385	11.4	-0.303	-19.2
6	0.1005	11.5	-0.193	-16.7

Since the disymmetric influence of the crystal lattice, in analogy with the chiral crystals of compounds iPr/iPr-**23** and (S)-(+)-**42**, should be on the configuration of the dibenzosemibullvalene skeleton [all-(R) or all-(S)] we may start by disregarding the nature of the ester substituents and their final disposition in the final photoproducts. Our strategy should therefore include conversion of the total photoproduct mixture into a single compound, conveniently and based on our experience with the resolved material, the dimethyl dibenzosemibullvalene derivative **52**.

Extent of Asymmetric Induction in Crystals of the Racemate.

In order to have a consistent account of the solid state reaction an extremely careful experimental procedure was devised. A large single crystal (0.1676 g) of **42** was grown from the racemate, finely divided by crushing, and separated into two portions of 0.1232 and 0.0434 g. The smaller portion was used to determine the exact enantiomeric composition of the entire sample ($[\alpha]_D$ = -0.9°, (c=0.043, $CHCl_3$), e.e. = 8%). The remaining compound was photolyzed at 0°C with the nitrogen laser to 15 % conversion and the products (0.0154 g) were separated by chromatographic procedures (after derivatization of the remaining starting material with CH_2N_2). The pure photoproducts, {$[\alpha]_D$ = -14.4°, (c=0.15, $CHCl_3$)}, were hydrolyzed, esterified with diazomethane to give diester **52** and analyzed by ^1H NMR with 0.2 equivalents of $Eu(hfc)_3$. The spectrum of this sample and that of an authentic racemate of **52**, shown in Figure 84, indicate an identical result as in the case of the optically pure starting material with an enantiomeric ratio of 90:10 or a e.e. = 80%.

Interestingly, by keeping track of the starting material mass balance we could notice that the amount of (S)-(+)-**42** reacted was 1.5 times as much as the amount of (R)-(−)-**42** (11.1 versus 7.4 mg). This conclusion was reached by measuring the enantiomeric compositions of the starting material before and after the photochemical reaction.

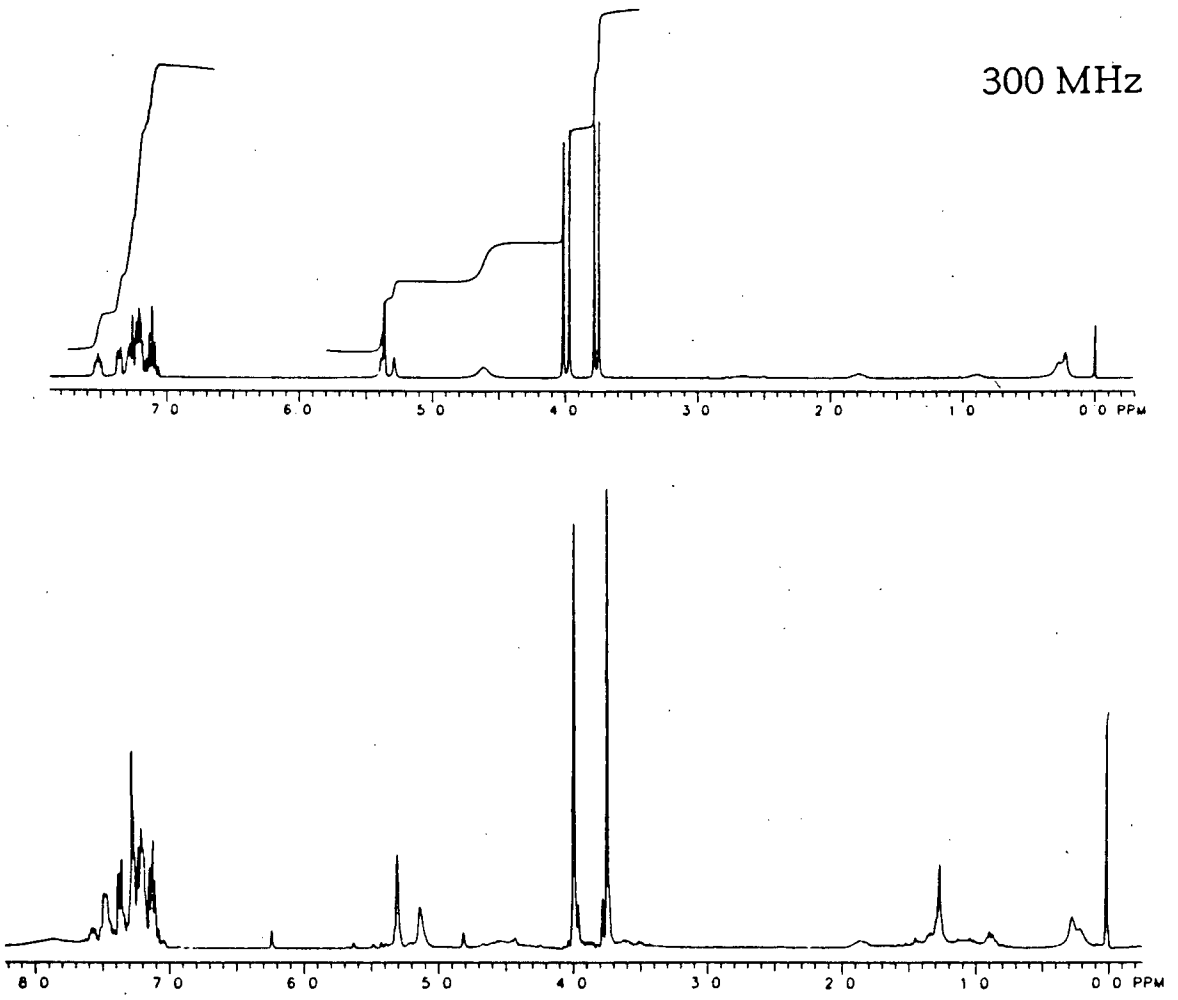

Figure 84. ^1H NMR Spectra of Racemic (top) and Optically Active (bottom) Dibenzosemibullvalene **52** After Addition of 0.2 eq. of $Eu(hfc)_3$.

An intriguing question that evolved from the above result was whether the crystal phase that makes the (+)-enantiomer 1.5 times more reactive is the crystal lattice preferred by the pure (+)- or of the pure (-)-enantiomer. It seems the latter alternative is the correct one since the absolute configuration of the derivatized products obtained here was opposite to that obtained from the products of the pure (+)-enantiomer crystal phase. It seems therefore that the more reactive [(+)-42] component is the solid solute in pro-(-)-enantiomorphous phase.

On the Reaction Diastereoselectivity.

The enantiospecific generation of the dibenzosemibullvalene skeleton in the crystals of the racemate is a remarkable manifestation of the face selectivity of the solid state rearrangement. The formation of three different diastereomers with the same dibenzosemibullvalene absolute stereochemistry can illustrate one of the most interesting concepts of solid state reactivity, namely the reaction cavity. As we shall see, we interpret the results as arising from a "cavity"[1i] controlled reaction of three different solid state molecular structures of diester 42. In other words, the reaction regio- and diastereoselectivity in the racemate (75I:75II:74I:74II = 31:31:8:31) is less with respect to that in the pure enantiomer (75I:75II:74I:74II = 85:5:5:5), not because of a loss of topochemical control, but because of a loss of steric control during the crystallization process.

For illustration purposes we can consider a crystal lattice of the diisopropyl diester **23** which is converted into a crystal of the racemate of **42** by isomorphic replacement of molecules of **23** by molecules of **42**. It should be noticed that every lattice site, or reaction cavity, initially occupied by iPr/iPr-**23** can be filled up with molecules of **42** in four different manners. In Figure 85 we represent such lattice space, (D), initially filled with a molecule of diester **23** surrounded by the four structures of **42** that define the different occupancies, **DU(+)**, **DU(-)**, **DC(+)** and **DC(-)**.

Every crystal lattice occupancy in the **D** or **L** lattices (the enantiomorphous phases that give Dextro- or Levorotatory photoproducts) is defined by the enantiomer [(+) or (-)-sec-butyl] of **42** filling the space and by the location of the sec-butyl group, **C** or **U**. As we have seen, there are two non-equivalent ester sites in the chiral $P2_12_12_1$ structure. The two esters can be differentiated as "C" and "U" depending on whether the carbonyl group is close to Conjugation (~160°) or Unconjugated (~65°) with the vinyl C(11)-C(12) double bond.

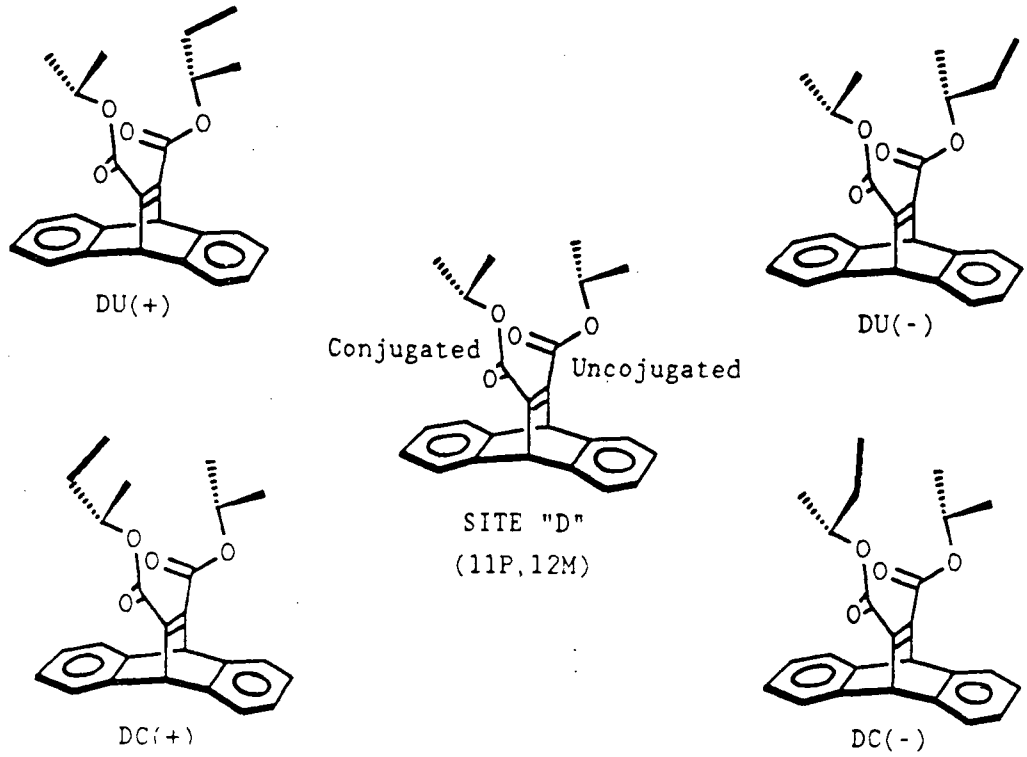

Figure 85. The Four Modes of Isomorphic Replacement of Diester 23 by Diester 42.

Crystals built up with the pure enantiomers [(S)-(+)] of iPr/sBu-42 present a single occupancy, DU(+), where the isopropyl substituent, without apparent crystallographic disorder, is situated in a position corresponding to the C ester group (Figure 85). Here the reaction occurs by lattice-controlled bonding at the vinyl carbon next to the isopropyl group (path 12-I, Figure 82), and since the reaction cavities are filled up with a single component, the reaction is highly regio- and diastereoselective (85%).

In the case of the racemate, every reaction cavity can be filled up with either (+)- or (−)-**42**. If the ester occupancies were similar to those in the crystals of the resolved compound, with the isopropyl groups always at the **C** site, there would be only two occupancies **DU(+)** and **DU(-)** in Figure 86. Reaction at the two lattice sites would give rise to the two diastereomeric products **75I(+)** and **75I(-)** (Figure 86). The formation of the third diastereomer, either **74I(+)** or **74I(-)**, can be interpreted as a partial occupancy of the corresponding (+) or (-) enantiomer of **42** with the sec-butyl group in the **C** ester position, **DC(+)** or **DC(-)** (Figure 87).

Although a reaction cavity controlled process accompanied by crystallographic disorder can explain the results observed in the case of the racemate, it should be noted that we cannot strictly differentiate an alternative model where pathways other than 12-I take place in the solid state.

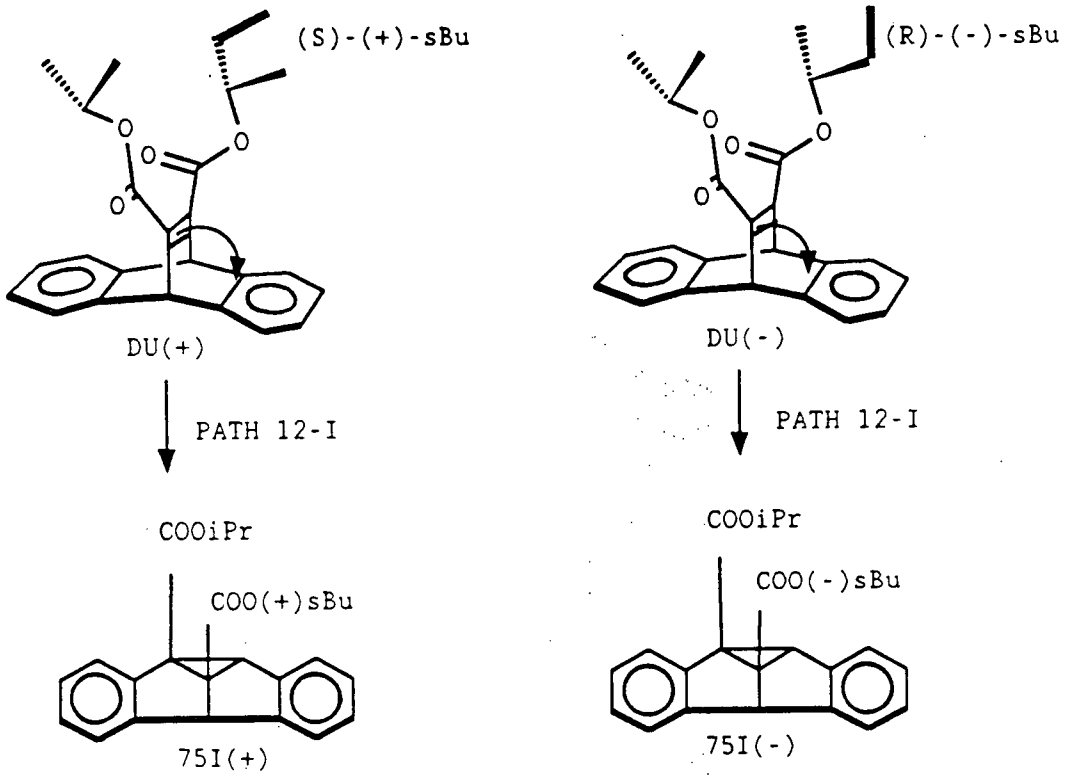

Figure 86. Loss of Diastereomeric Control in the Product Stereochemistry by Means of Occupancy of the Same Chiral Lattice Site by two Different Enantiomers.

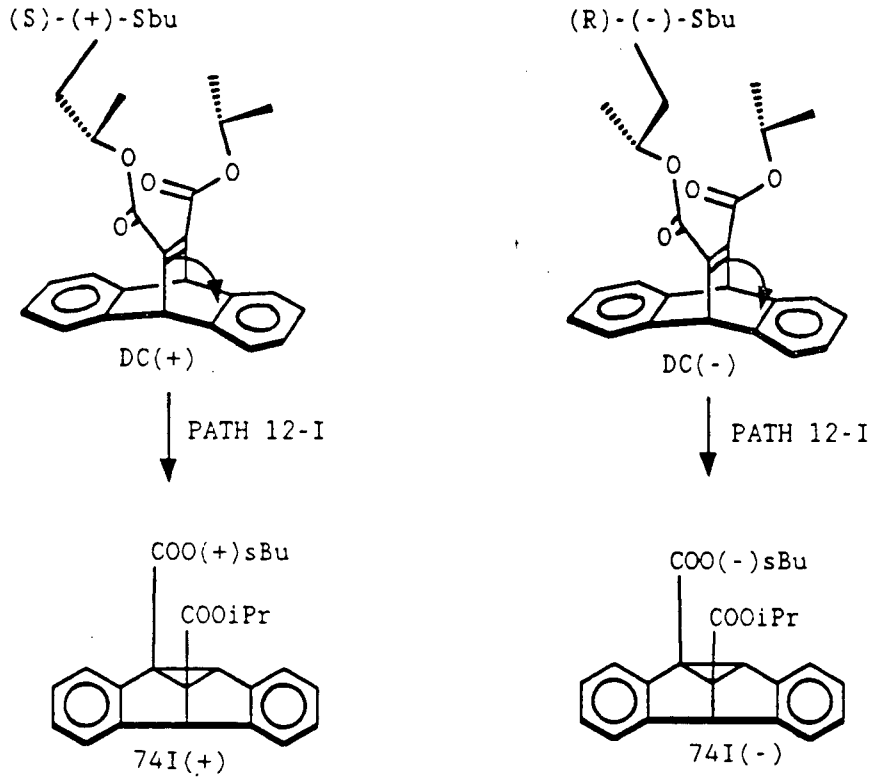

Figure 87. Loss of Regioisomeric Control by Means of Positional Disorder in the Crystal Lattice of (R,S)-42.

The Solid State Properties and Photochemistry of Diester Me/sBu-31.

While some of the solid state characteristics of compound 31 were briefly discussed in Part III, some additional comments seem timely with respect to the two samples employed. Crystals grown with optically pure and racemic materials were both found to be unsuitable for X-ray diffraction studies. The melting points of single crystals of the two samples varied by four degrees (Table I, page 45) indicating that the racemic material had not undergone a spontaneous resolution. This indication was confirmed by the lack of optical activity of solutions of single crystal specimens. An additional observation was that the melting point of the optically pure form was lower (91-2°C) than that of crystals of the racemate (94-5°C). Solid state FTIR spectra of crystals of both materials were obtained in KBr in an attempt to find possible spectral evidence for two different solid state modifications. Instead of finding any evidence that could substantiate the possibility of having racemic and enantiomorphous crystals, the two spectra were essentially identical. This information very strongly suggests the possibility of a non-ideal solid solution of the enantiomers with a maximum melting point, or Roozeboom type II. Interestingly, the solid state FTIR spectra of the two samples of Me/sBu-31 (Figure 87A) very closely resembled the spectra obtained for the diesters Me/nPr-29 and Me/iPr-30. It was suggested in the previous section that these compounds may form isomorphous crystals with the racemic space group of diester 30, and as we will see this hypothesis serves well to explain the diastereoselectivity observed from the racemate and the optically active crystalline materials of compound 31.

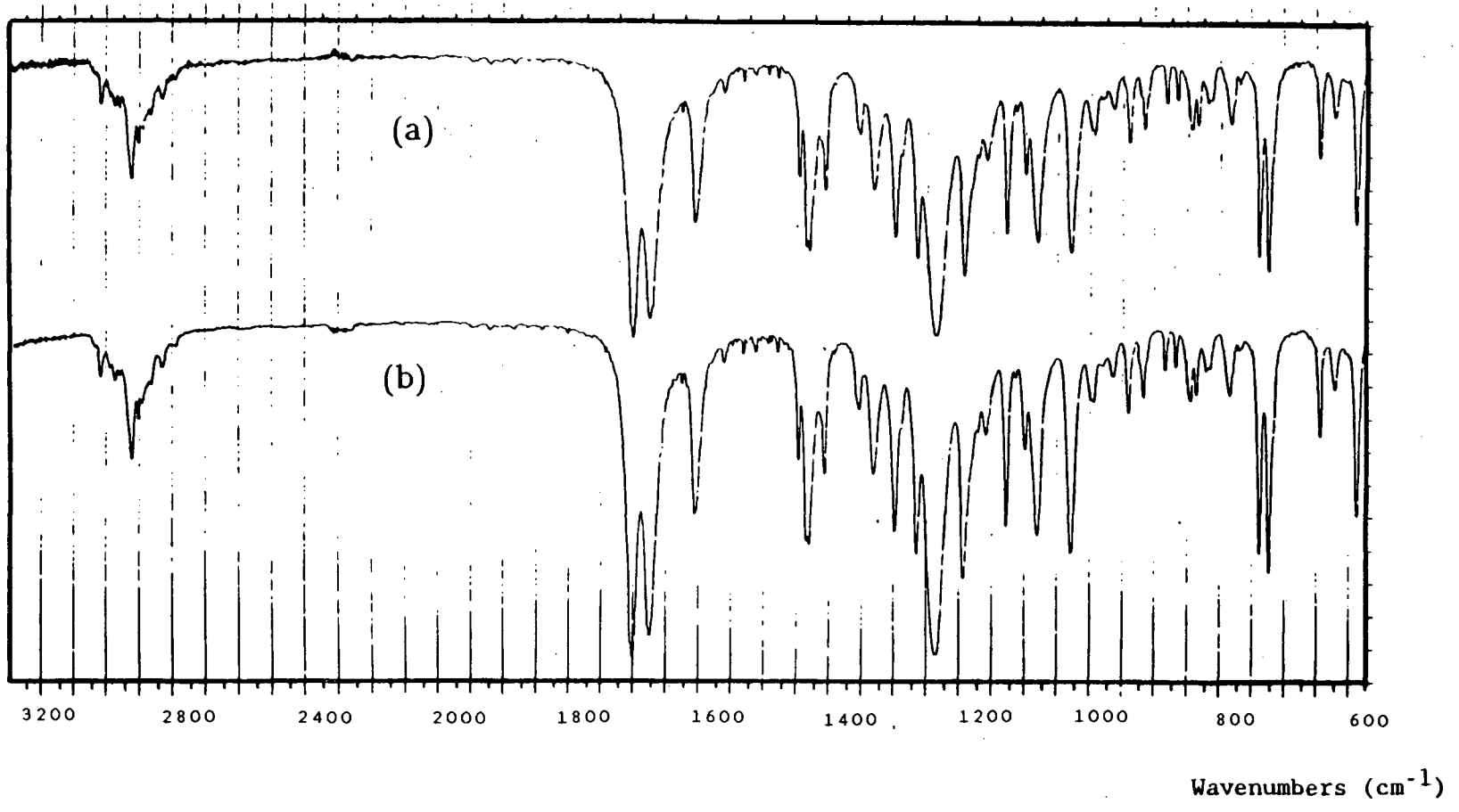

Figure 87A. Solid State FTIR Spectra of (a) Racemic and (b) Optically Pure Diester Me/iPr-31.

The glc determined solid state selectivity of crystals of (S)-(+)-31 and (R,S)-31, in contrast to compound 42, was surprisingly identical (Table XXII). The solid state regioselectivity, as indicated in Part III, overwhelmingly favors the benzo-vinyl bridging step at the carbon next to the sec-butyl group. This preference compares well with the results observed in the crystals of the diesters Me/nPr-29 and Me/iPr-30 in agreement with our hypothesis of an isomorphous crystal structure.

Table XXII. Relative Solid State Stereoselectivity[a] from Crystals of Compounds Me/sBu-31.

Compound	Path A-I / Path A-II (%)		Path B-I / Path B-II (%)		
Me/(+)-sBu-31	42	55	---	~3	---
Me/(±)-sBu-31	42	55	---	~3	---

a) Absolute stereochemistry of the products not known.

The insensitivity of the solid state reaction to the formation of the two diastereomers from paths A-I and path A-II, and to the different enantiomeric composition of the two crystalline materials is surprising and requires further analysis. Previous literature reports on the study of the racemic compound and the resolved modification of chiral substrates are very scarce. These studies suggest that a different solid state reactivity should be expected between the two phases as a result of their different crystal packings.[153] The apparently identical photochemical behavior from the racemate and of the optically pure materials would

normally suggest a spontaneous resolution from the former. Such an event, however, is not operative in the case of the racemate of compound 31.

The simplest explanation of the results shown in the first two columns in Table XXII would be that there is little preference between the two alternative pathways and that both can occur with almost equal probability in the two solid state materials (Figure 88). Although we cannot rule out this possibility, it is interesting to notice that exactly the same results can be obtained under conditions where the reaction proceeds in the solid state with an absolute control on the reaction face-selectivity. This possibility can come about as a result of the disorder present in the solid solution of the enantiomers, which in contrast to that of compound 42, crystallizes in a racemic space group.

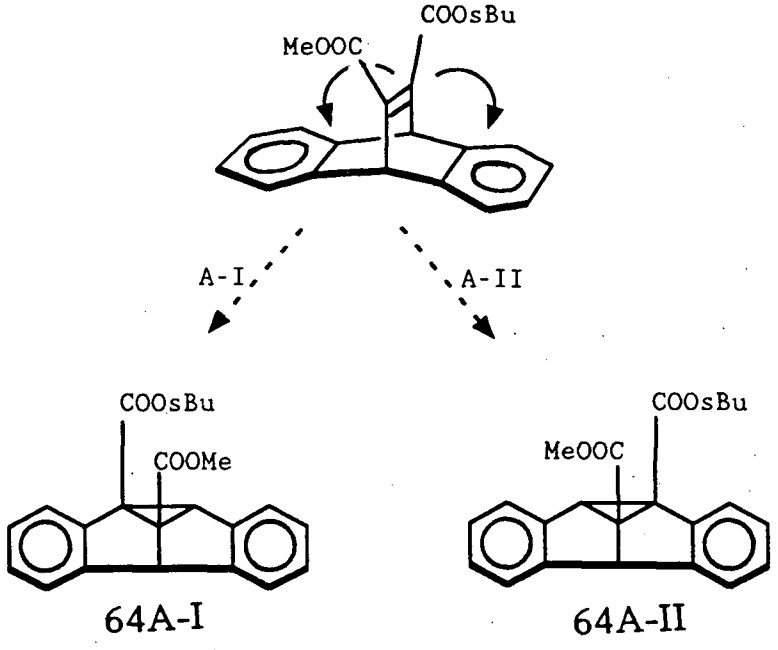

Figure 88. Hypothetical Reaction of Diester 31 to Give the Two Diastereomers **64A** as a Result of a Lack of Lattice Control on the Face-Selectivity of the Rearrangement.

We start by considering that (S)-(+)-31 and (R,S)-31 are the two extremes of a solid solution of the enantiomers that pack in a racemic space group. Crystals of this solid solution, as mentioned before, seem to be isomorphous with crystals of diesters Me/iPr-30 which crystallizes in the racemic space group $P\bar{1}$. Crystallization in a racemic space group would imply the existence of two equivalent and enantiomeric crystal sites, D and L, related by inversion centers (or mirror and glide planes). The conformation of the molecules filling these spaces, similar to the structure of Me/iPr-30, should be disymmetric and with chiralities defined by the carbonyl-double bond torsion angles O(2)-C(13)-C(11)-C(12) and O(4)-C(15)-C(12)-C(11) (Figure 89). The two conformations adopted by the ene-dioate system would be defined as 11M,12P and 11P,12M respectively (Figure 89). In the case of the resolved material the two enantiomeric lattice sites would be occupied by the same enantiomer of the (S)-(+)-sec-butyl derivative 31, rendering a "quasiracemic" crystal lattice. In Figure 89, a lattice controlled reaction at the site D through pathway A-I would be similar to a lattice controlled reaction via pathway A-I' in the crystal lattice site L. The products formed at the two reaction centers, 64A-I(+) and 64A-I'(+) would possess opposite absolute configurations in the dibenzosemibullvalene asymmetric carbons (all S or all R) but would posses the same (S)-(+)-sec-butyl chiral handle and would give rise to two glc signals as observed for diastereomers.

In the case of the solid solution with the composition of the racemate an interesting alternative could take place. If there were substantial chiral recognition between the disymmetry of the crystal lattice sites, D and L, and the molecular chirality of the two dibenzobarrelene enantiomers

(S)-(+)-31 and (R)-(-)-31, the solid solution would be ordered and more properly called a racemic compound. Molecules of (S)-(+)-31 occupying crystal lattice sites D would react through pathway A-I to give product 64A-I(+), and molecules of (R)-(-)-31 would occupy the crystal lattice site L and would react through pathway A-I' to give product 64A-I'(-). It should be noticed that the products generated during such events would be enantiomers and would give rise to a single glc signal (Figure 90). Obviously, our experimental results do not agree with this since we observe signals corresponding to the two diastereomers.

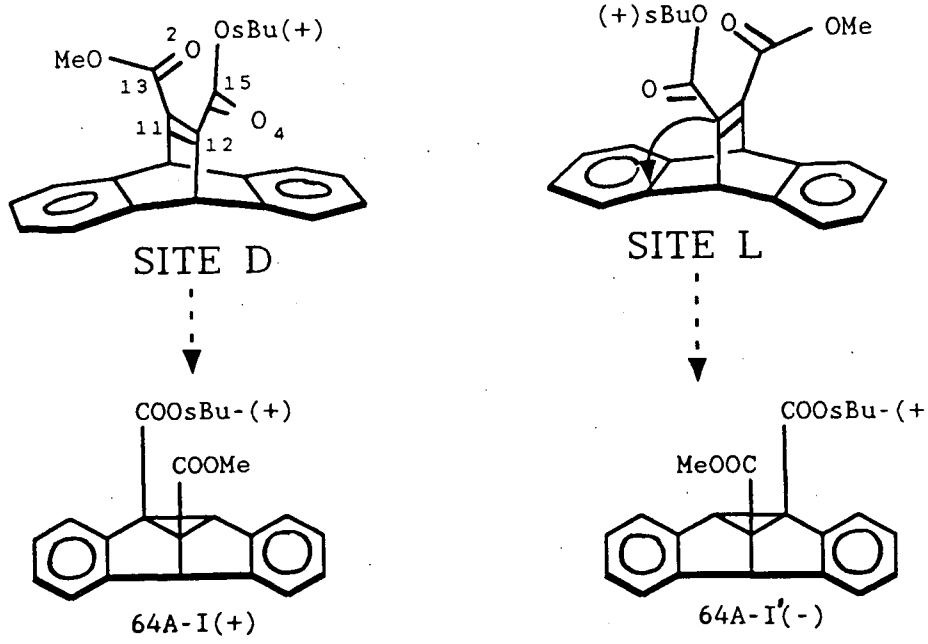

Figure 89. Hypothetical Reaction of One Enantiomer of 31 at Two Enantiomeric Crystal Lattice Sites.

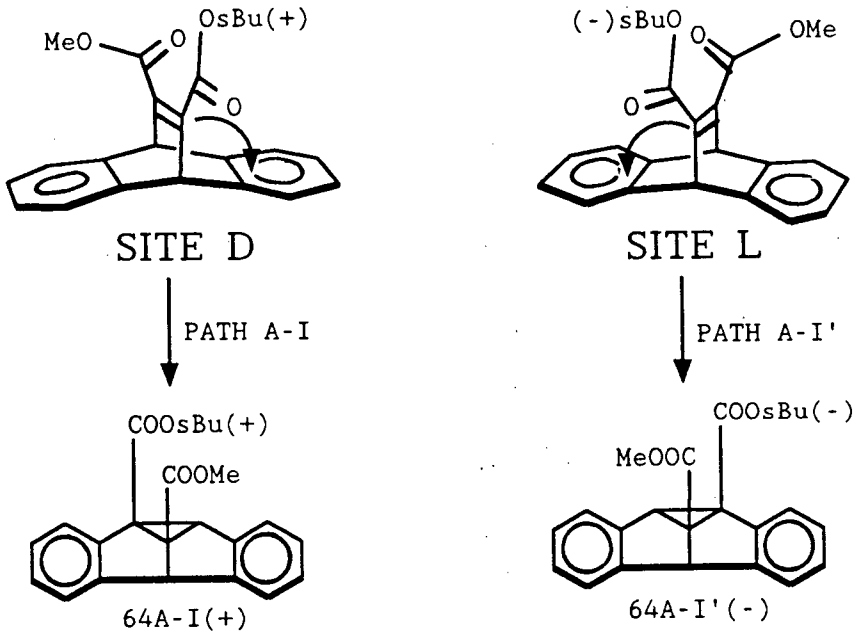

Figure 90. Hypothetical Reaction of Two Enantiomers at Two Enantiomeric Crystal Sites.

Suppose that there is no chiral recognition between the two enantiomers of diester **31** and the two chiral lattice sites, D and L. The two lattice sites would be occupied indiscriminately by the two molecules (S)-(+)-**31** and (R)-(-)-**31**. In Figure 91 it can be seen that reaction of both enantiomers of **31** at the same lattice site would give diastereomeric products, as we saw for compound **42**. This is illustrated by reaction of

(S)-(+)-**31** and (R)-(-)-**31** through pathway A-I to give diastereomers **64A-I(+)** and **64A-I(-)**.

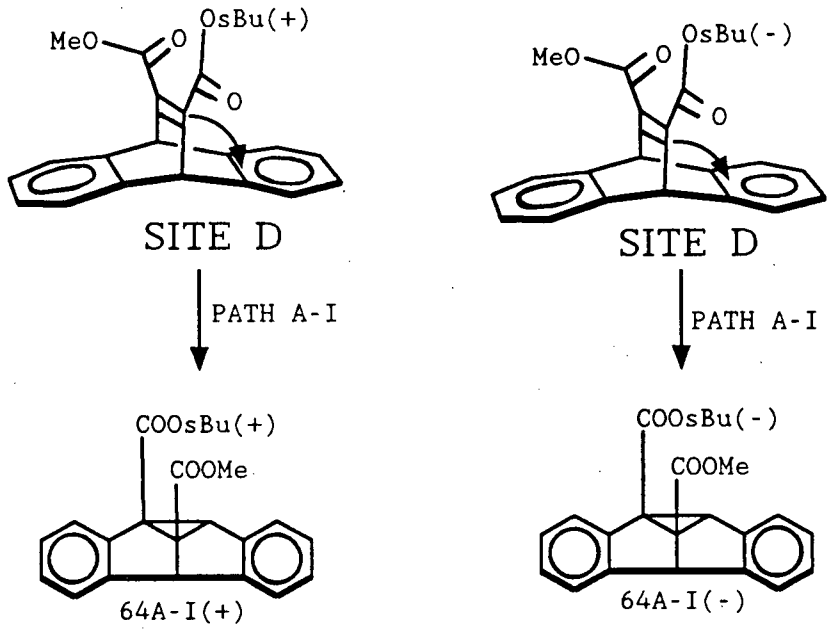

Figure 91. Reaction of Two Enantiomers at the Equivalent Reaction Site Through Equivalent Reaction Pathways.

Even though X-ray structural data is lacking, the above ideas are supported by the likely isomorphous relationship between Me/iPr-**30** and racemic and resolved **31**. This is reasonable considering that there are only minor structural differences between diesters Me/iPr-**30** and Me/sBu-**31**. Substitution of the isopropyl for the sec-butyl compounds in

the P1 crystal lattice of 30 seems reasonable in light of the similar molecular volumes and shapes of the two diesters.

The molecular volumes of compounds Me/iPr-30 and Me/sBu-31 can be calculated in an approximate manner by the group increment approach of Kitaigorodsky[13,30] and Bondi[151] mentioned earlier. Using the increment values recently updated by Gavezzotti[144] we arrive at the following:

Compound	Calculated Volume($Å^3$)
30	327.3
31	344.1

The coefficient of geometric similarity, ϵ, in the case of compounds 30 and 31, calculated with the above volume values, turns out to be 0.95, a much better value than the lower limit of 0.85 proposed by Kitaigorodsky.

It could have been expected that some chiral recognition may have occurred between the chiral crystal sites, D and L, and the chiral molecular structures of the sec-butyl enantiomers, (R) and (S) of 31. Chiral recognition, to form an ordered racemate of 31 isomorphous to 30, would require substantial volume differences between the molecules of (R)-and (S)-31 on one hand and the D and L lattice spaces on the other. However, if the coefficient of structural similarity between the two enantiomers of 31 were also very close to unity, the two enantiomers would be not only structurally similar to each other, but also to the lattice spaces D and L in the isomorphous crystal structure. That is to say that both (R)-and (S)-31 would occupy two enantiomeric crystal sites with no

(or little) discrimination.

Although it has been shown that the conformational freedom of the sec-butyl substituent can facilitate polymorphism and solid solubility, it is interesting to calculate an approximate value for ϵ in the case of the two enantiomers of **31**. The coefficient would give us some insight into the probability of forming a disordered solid solution of the enantiomers according to the criteria given by Kitaigorodsky ($\epsilon > 0.85$)

We can assume that a complete molecular overlap between the enantiomers will occur with the exception of the two sec-butyl groups. The non-overlapping volumes between the two enantiomers result from the two methyl groups represented by the dots in Figure 92. It is apparent that the non-overlapping volume between the two enantiomers should be close to twice the volume of a methyl group (44.6Å^3). This results in a coefficient $\epsilon = 0.86$ between (R)- and (S)-**31** which should, according to Kitaigorodsky, still allow for occupancy of the (R)-enantiomer in the space of the (S)-compound.

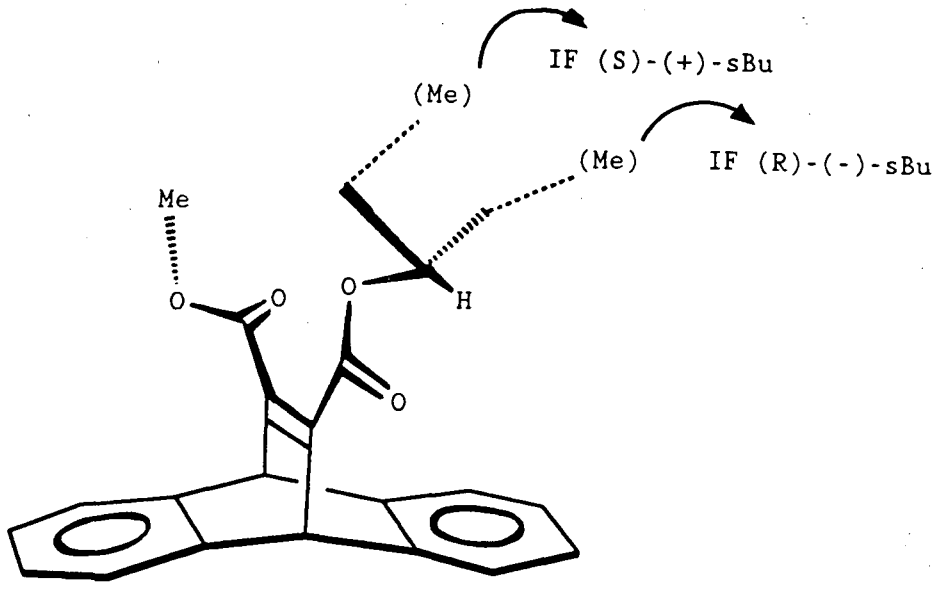

Figure 92. Comparison of (R)- and (S)-31 in Order to Determine their Coefficient of Geometrical Similarity (ϵ).

It seems that the above criteria and our photochemical results justify the reaction models we have proposed. Furthermore, the crystallographic behavior of sec-butyl containing compounds has been documented and often found to present disorder as a result of a non-statistical conformational isomorphism. In this manner, as we have proposed, the two sec-butyl enantiomers indiscriminately fill each other's spaces without any chiral recognition.

Our model should therefore conform to a crystal structure very similar to the one observed for diester 30, where the two enantiomeric lattice spaces are filled with only one enantiomer of 31 in the optically active modification, and with two enantiomers of 31 in the racemate. If the occupancies are statistical, we can represent the three crystal structures according to the data shown in Table XXIII:

Table XXIII. Proposed Occupancies in the Isomorphic Crystal Structures of Diesters 30 and 31 (optically pure and racemic).

	Crystal Lattice Site	
	D	L
30	50%	50%
(S)-(+)-31	50% (S)-(+)	50% (S)-(+)
(R,S)-31	25% (S), 25% (R)	25% (S), 25%(R)

It should be recalled that the D and L sites are enantiomeric and that the conformations of the dibenzobarrelene-dioate structures (even ignoring the alkyl groups) are chiral. Molecules of one of the enantiomers of 31 in the two different lattice sites will therefore be diastereomeric in the solid state since they contain two disymmetric elements.

The Solid State Properties and Photochemistry of Diester Et/sBu-39.

The solid state photochemistry of diester Et/sBu-39 was explored only in its resolved modification. The regioselectivity observed turned out to be slightly in favor of bonding at the vinyl carbon next to the ethyl substituent (69%). The diastereoselectivity between the pathways A-I and A-II (refer to Figure 73) was similar to that observed in the optically active samples of Me/sBu-31. It seems that this result is indicative again of a disordered solid solution of the enantiomers in a racemic space group. No further attempts were made to analyze this compound due to the lack of more structural information, and of an isomorphous compound from which to deduce information.

Table XXIV. Relative Solid State Stereoselectivity from Crystals of Compound Et/sBu-39

Compound	Path 1 / Path 2 (%)			Path 3 / Path 4 (%)	
Et/(+)-sBu-39	---	69	---	14	17

Concluding Remarks.

All the possible alternatives available to optically active compounds are very interesting from the point of view of solid state reactivity. The stereochemistry of the products in the solid state, as we have seen in the

case of the di-π-methane rearrangement, can be profoundly influenced by the local microenvironment of the reacting molecule and the reaction cavity. Even if the one or two dimensional structural similarities between the racemic compound and the enantiomorphous modification proposed by Pedone and Benedetti[150] were to operate, the three dimensional molecular environment can be expected to be at least slightly different when chiral molecules crystallize in any of those alternatives or in a solid solution of the enantiomers.

The stereospecificity of a lattice-controlled solid state reaction has been shown to depend drastically on the crystal symmetry. While chiral crystals can be viewed as having only one enantiomeric reaction cavity, either D or L, racemic crystals will have both enantiomeric reaction cavities, D and L, in equal amounts. Dramatic effects on the product constitution can occur when the absolute configuration of a newly generated chiral center, R or S, is controlled by the chirality of the reaction cavity, D or L, which can be filled by different enantiomers and in different orientations. Enantiomorphous crystals of the pure enantiomers and racemic crystals of the racemate will give products according to the regioselectivity induced at each reaction site.

There are few literature reports dealing with the unique solid state chemical properties encountered in solid solutions of enantiomers. One such, is also concerned with sec-butyl containing compounds such as the vinyl diacrylate **76** (Figure 93). The optically active and racemic forms of compound **76** were found to crystallize in the chiral space group of the resolved modification (space group P1) as a result of solid solubility of the enantiomers. The solid state intermolecular arrangement between the

molecules of the diacrylate **76** was suitable for $2\pi + 2\pi$ dimerization according to the molecular packing motif present in Figure 93. As indicated in the figure, the absolute configuration of the cyclobutane carbons is determined by the intermolecular arrangement which can occur in the two enantiomeric motifs D and L depending on the enantiomorphous phase. The chiral sec-butyl groups were shown to be distributed in a disordered manner so that a mixture of four diastereomeric products was formed. That the extent of the asymmetric induction was quantitative was shown by removing the sec-butyl groups and replacing them by methyl esters to give a single chiral photoproduct.

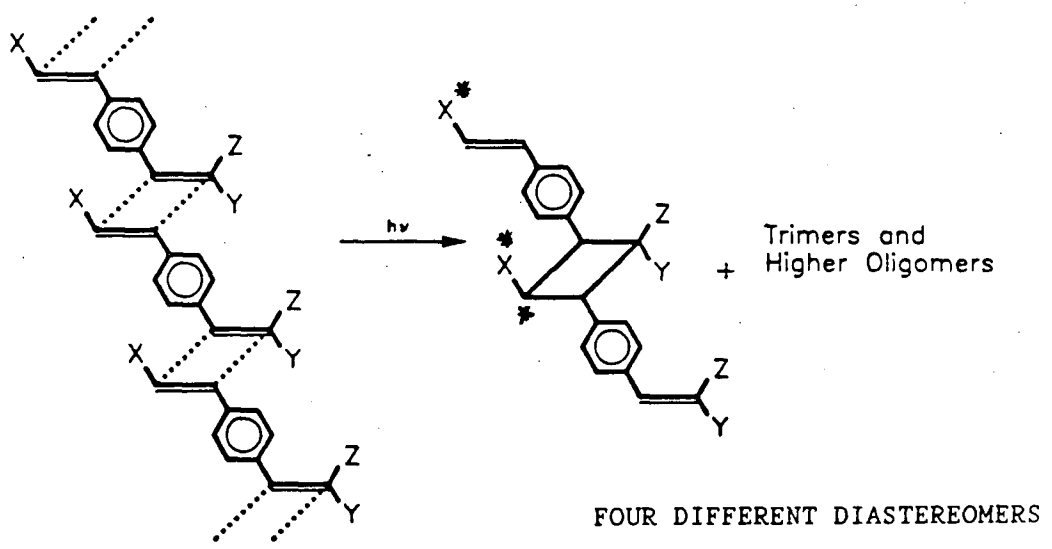

Compound 76

X = (+)- or (-)-sBu

Y = COOET

Z = CN

Figure 93. Asymmetric Synthesis in Crystals of Vinyl Diacrylate 76.

PART V. LUMINESCENCE STUDIES ON THE DIMETHYL DIESTER 18.

The phenomenon whereby a substance changes color upon absorption of light is called photochromism.[154] Studies on photochromic systems have shown that the change in color is due to the formation of a photoproduct with an absorption spectrum that differs from that of the original species or starting material. Photochromism may be reversible or irreversible depending on the process from which it originates. Reversible photochromism is often associated with light-induced tautomeric phenomena and cis-to-trans isomerizations where the absorption properties of conjugated unsaturated systems are changed. Irreversible photochromism results from an irreversible chemical process where a colored photoproduct may be formed as the end-product or as an intermediate.[154]

The detection of a photochromic system is usually carried out by absorption or reflectance spectrophotometry.[154] The photochromic species is irradiated at an absorbing wavelength so it can react and generate the colored species which is in turn analyzed with absorbing or reflected light of different wavelengths. The technique of flash spectroscopy,[155] widely used for the study of reactive intermediates, can be considered a sophisticated example of detecting transient photochromism. The direct detection of the reactive intermediate by these techniques is possible only if it absorbs at different wavelengths compared to those of the precursor compound (indirect detection, however, is often also possible).[156]

The detection of a photochromic system by making use of luminescence spectroscopy is also possible in favorable circumstances.[157] Here the

colored species is generated in the same manner as before but its detection is performed by measuring its fluorescence (or phosphorescence) instead of its absorption spectrum. Luminescence spectroscopy is particularly well suited for the study of crystalline solids.[38] The problems related to the high concentration and opaqueness of the species under study are minimized by performing measurements by front-surface excitation and detection.[158] The onset of the luminescence band gives valuable information regarding the difference between the two energy levels responsible for the observed transitions, and the shape of the emission envelope can sometimes be used to extract information as to the possible nature of the emitting species.[154,159] By measuring the luminescence excitation spectrum one can also obtain the absorption properties of the new "colored" species. An important requirement and common limitation for the use of luminescence spectroscopy for the study of photochromic systems, however, is that the species under study should have a sufficiently large fluorescence or phosphorescence quantum yield.

A large number of the 11,12-diesters studied in this thesis were found to present interesting photochromic behavior that could be detected easily from their solid state luminescence properties (the only exceptions were the diesters Me/Ph-37, Et/Et-21 and iPr/iPr-23, the latter in their $P2_12_12_1$ and Pbca dimorphs respectively). The dimethyl diester Me/Me-18 was selected as a representative example to perform most of the studies reported in this section. This selection was based on the fact that diester **18** is the most ready available and easy to purify among all the compounds observed to present the phenomenon discussed here. As we shall see, compound iPr/iPr-23 was also used in special circumstances.

General Observations.

When irradiated with the nitrogen laser, single crystals and powdered samples of compound **18** presented a strong blue emission later characterized as the fluorescence of the corresponding dibenzobarrelene compound (Figure 94a). After about five seconds of irradiation (vide infra) at ambient temperature, the fluorescence intensity was found to decrease until it was replaced by a new strong red emission (RE) that was maintained for about one additional minute (Figure 94b). Following this, the RE decreased in intensity until it was replaced by a slightly different blue luminescence (Figure 94c). The latter emission was found to possess a significant contribution from the fluorescence of the corresponding dibenzosemibullvalene compound Me/Me-**52**, the photoproduct from the concurrent di-π-methane reaction (see pages 60-63). Additional experiments indicated that, by the time the RE disappears from single crystalline specimens (irradiated on all crystal faces until there is no trace of RE), there has already occurred about 15% reaction. The RE appeared without any delay within the time resolution of our instrument (40 μsec), and seems to be due to an allowed transition (fluorescence).[43] The spectrum was independent of the excitation wavelength (see below) and could be reproduced without difficulty from sample to sample either as single or powdered crystals.

For most experiments, powdered samples of Me/Me-**18** were irradiated with a nitrogen laser (337.1 nm, 330 mW average power, 20 Hz repetition rate) and rapidly transferred to the low temperature device of the Perkin-Elmer LS-5 spectrofluorimeter. The experimental observations

presented here could also be repeated by irradiation with intense continuous sources such as a 400 W high pressure mercury lamp (337 nm wavelength selected through a Bausch and Lomb monochromator). Irradiation with the weak pulsed xenon lamp of the Perkin-Elmer LS-5 spectrofluorimeter did not produce observable intensities of the **RE** photochromic behavior. This indicated that the room temperature photochromism of crystalline dibenzobarrelene diesters is not a laser specific phenomenon but requires a relative large photon intensity in order to accumulate the red-emitting species. It should be mentioned that in solution we could only detect the dibenzobarrelene fluorescence which does not differ qualitatively from that observed in the solid state. At 77K in glassy matrix (methyl cyclohexane) a strong phosphorescence could also be detected.

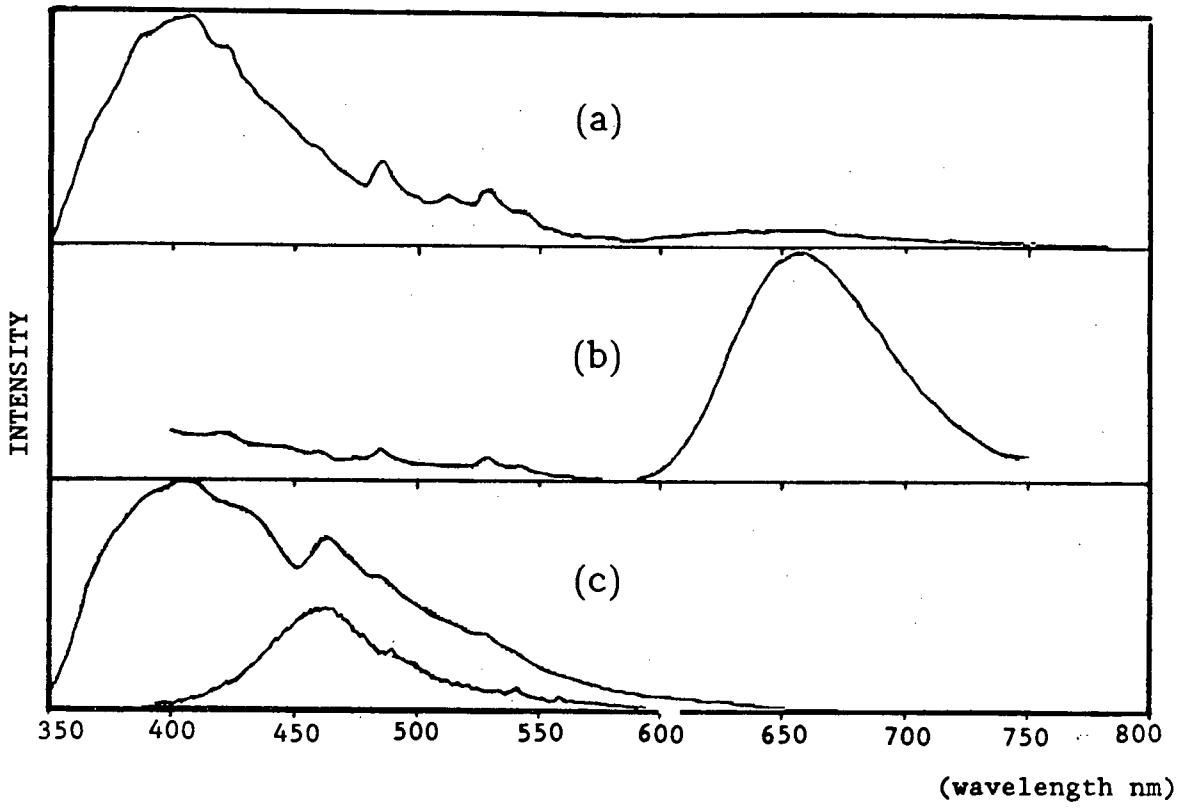

Figure 94. Uncorrected Emission of Crystals of Diester Me/Me-**18** Irradiated at 337 nm: (a) As it Appears During the First 5 Seconds, (b) During the Following 60 sec (spectrum taken at maximum intensity) , and, (c) After the Luminescence in (b) had Disappeared (The Solution Spectrum of Dibenzosemibullvalene **52** is Included in the Same Figure).

That the **RE** originated from a species not present initially in the crystalline samples, species "**X**", could be determined not only by the induction time required to detect it, but also from its temperature dependent thermal decay and from its fluorescence excitation spectrum.

Observations at Different Temperatures.

Red-emitting samples that had been removed from the irradiation source, kept in the dark for as long as ~3 min (ambient temperature), and then analyzed in the spectrophotometer, were still found to present the **RE**. When the red-emitting samples were kept in dark for longer periods and then re-irradiated, it was noticed that the **RE** had completely vanished. Interestingly, the **RE** could be regenerated by another five seconds photolysis time with the laser. This result has been interpreted in terms of a relatively long lifetime and eventual thermal decay of the red-emitting species.

Laser irradiation of crystalline samples performed at four different temperatures (77, 155, 200, and 230 K), resulted in substantially different photophysical and photochemical behavior. Prolonged irradiation (1 h) with the nitrogen laser at 77 K resulted in no change in the original fluorescence emission of the diester compound. A relatively strong long lived emission was readily observed and assigned as the phosphorescence of the dibenzobarrelene derivative (see Figure 28b, page 63). No trace of reaction could be detected by glc analysis of these crystals. Photolysis at 155 K, on the other hand, resulted in the appearance of the **RE** after about five seconds, but no reaction could be observed when the irradiation was continued for as long as two hours. The red emission persisted for the entire irradiation time and no apparent decay could be observed from the species from which it originates. Instrumental limitations prevented us from measuring the thermal decay of the red emitting species **X** at temperatures other than 77 and 293 K.

Attempts, however, were made to measure the thermal decay of **X** at 77 K. Samples irradiated at 155 K and put in the low temperature accessory of the LS-5 spectrofluorimeter (77 K) were shown not to present any observable decay in the **RE** intensity after a 20 min period. The luminescence intensity was monitored at 660 nm by excitation at 337 nm. The emission intensity was sampled every 30 sec with the aid of the "kinet" program available from the PECLS-I software provided by Perkin-Elmer. It was the extremely long lifetime of the red-emitting species at 77 K that allowed us to perform accurate luminescence emission and excitation spectral measurements at this temperature.

The irradiations at 200 and 230 K were characterized by the appearance and increase of the photochemical reactivity. Photolysis for more than one hour (70 min) at 200 K resulted in no apparent (visual detection) change in the red emission intensity but in the accumulation of 2% of photoproduct. In contrast, at 230 K the reaction occurred to a larger conversion (5%) in shorter photolysis time (10 min). The 293 K irradiation was dominated by enhanced chemical reactivity and by the brief duration of the **RE** phenomenon as described above.

Excitation Spectrum of the Red-Emitting Species.

The luminescence excitation spectrum is the most convincing evidence indicating that the **RE** is due to a photochemically induced phenomenon in the crystalline dibenzobarrelene diesters. Provided that one species (**X**)

is responsible for a given emission, that quenchers are absent, that the quantum yield is independent of wavelength, and that a properly calibrated light source and detector are used, the excitation spectrum should correspond to the absorption spectrum of the emitting species.[160] The fact that the emission envelope shown in Figure 94b is independent of the excitation wavelength suggests that there is only one species involved in the observed luminescence. In the present case, the possibility of having quenchers seems unlikely in view of the low energy of the transition giving rise to the RE. Quenching should normally be an exothermic process and the quencher should have a lower lying excited state than the donnor.[161] The excitation spectrum, shown in Figure 95, is also corrected by the instrument for variations in the lamp intensity and should closely resemble the solid state absorption spectrum of the red-emitting species. The fact that the excitation spectrum of the RE is completely different from that of the absorption spectrum of diester **18** indicates that the red-emitting species, **X**, has a different nature.

The excitation spectrum presented in Figure 95 was obtained by setting the emission monochromator at the maximum of the emission band of the RE (660 nm). The spectrum is composed by two band systems. An intense absorption band apparently starts at ~325 nm and has a maximum intensity centered at 366 nm. At wavelengths longer than 410 nm, where the intensity of the previous band becomes very low, there is a band system characterized by three relatively weak maxima at 430, 455 and 525 nm. It can be seen that this band system extends to up to 570-580 nm where the onset of the red emission begins. It should be pointed out that the left end of the excitation spectrum probably does not reflect the absorption

spectrum of the red-emitting species. At wavelengths shorter than 325 nm the absorption of the crystal matrix (the dibenzobarrelene compound **18**) should become very intense, so that it probably can act as a filter to the shorter wavelength absorption bands of **X**.

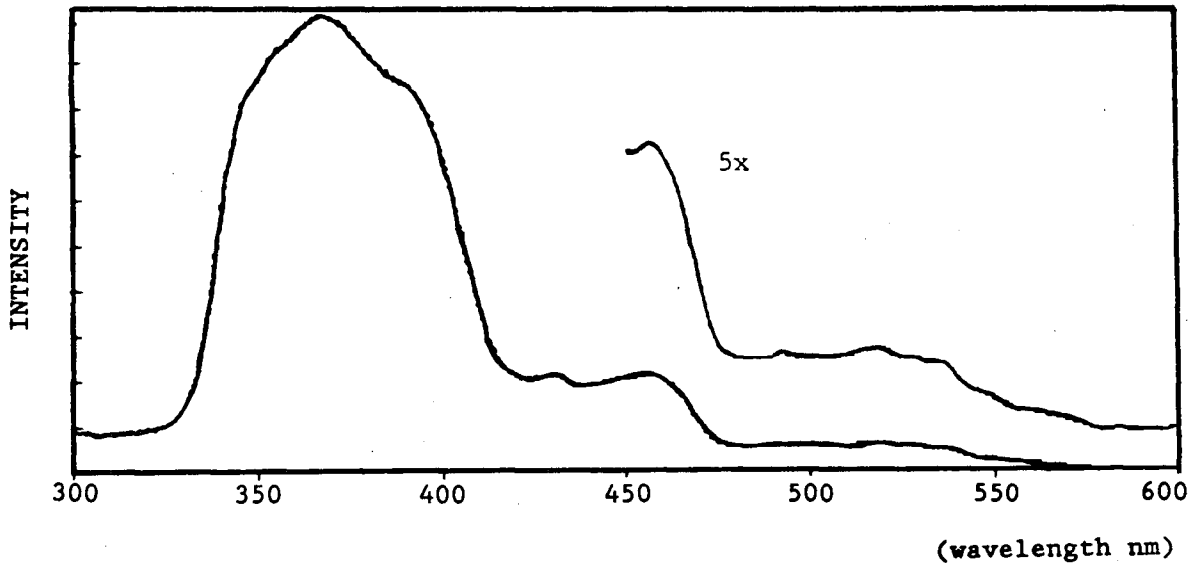

Figure 95. Corrected Excitation Spectrum of the Red-Emitting Species (**X**) in Crystalline Samples of Diester **18**.

Observations at Different Wavelengths.

Our analytical irradiations with the nitrogen laser at 337 nm have been a fortunate circumstance in view of the substantial absorption from the compound that originates the red-emitting species **X** (which we have not assigned yet), and from the red-emitting species itself. It was observed that samples irradiated at 313 nm at ambient temperature did not produce any **RE** in spite of being photochemically reactive. Samples irradiated at 366 nm, near the maximum absorbance of the red emitting species, presented no photochemical reactivity and at the same time no **RE** could be observed. On the other hand, samples first irradiated at 313 nm and then at 366 nm clearly displayed the **RE** band suggesting a direct correlation between the chemical reactivity of Me/Me-**18** and the **RE** phenomenon.

The 313 nm light is absorbed by the most abundant compound in the crystal, the dibenzobarrelene diester **18**, which may monopolize all the incident irradiation. The lack of **RE** upon excitation of dibenzobarrelene **18** is a very significant observation that indicates the absence of energy transfer from excited **18** (either singlet or triplet) to the red-emitting species. This seems quite a remarkable fact in view of the outstanding overlap existing between the fluorescence and phosphorescence of **18** and the absorption of the **RE**-species. It is interesting that the lack of energy transfer from part of the singlet state may originate from a spin barrier if the red-emitting species is a triplet state compound. The lack of energy transfer, however, may originate from the possibility that it may be a relatively inefficient process with respect to other faster decay alternatives available to the excited **18**.

What is the Precursor of the Red-Emitting Species?

Several models can be proposed to account for the red luminescence (RE) in crystalline samples of dibenzobarrelene diesters such as **18**. These models can be subdivided into two groups depending on whether the red-emitting species (**X**) originates from the dibenzobarrelene molecules (**18**), as our previous experiments seem to indicate, or if it comes from an impurity (**IMP**). In Figure 96, four alternative pathways can be proposed in order to generate **X**, all of which should account for the thermal barrier observed during its formation (the **RE** does not form at 77K). In the pathways given by equations 1 and 2 the red-emitting species **X** originates from singlet or triplet diester **18**. The pathways given by equations 3 and 4 are characterized by the involvement of an impurity, **IMP**. The latter two pathways differ in that pathway 4 requires the involvement of molecules of both, **18** and **IMP** while pathway 3 would not necessitate the participation of diester **18**. Before engaging in a systematic study of the first three, and most interesting possibilities, we should eliminate the more trivial alternatives given by equations 3 and 4.

1) 18 $\xrightarrow{h\nu'}$ ^{1}18* --------> [X] ------> Singlet Product.

2) 18 $\xrightarrow{h\nu'}$ ^{1}18* -------> ^{3}18* ------> [X] ------> 52

3) IMP $\xrightarrow{h\nu'}$ [X] -------> Product

4) 18 + IMP $\xrightarrow{h\nu'}$ [18-IMP] =(X) -----> Product

5) X $\xrightarrow{h\nu''}$ X*

6) X* ---------> X + $h\nu'''$ (Red Luminescence)

Figure 96. Possible Formation Pathways for the Red-emitting Species X and Biphotonic Mechanism for the Appearance of the Red-Emission.

Is the RE Produced by an Impurity?

The involvement of a trace impurity as being responsible for the RE was analyzed by two principal methods. The first method involved exhaustive purification of compound Me/Me-18. Most studies were performed on samples of Me/Me-18 that had been shown to be 100% pure when analyzed by glc under conditions where impurities of the order of 0.05% (1/2000th) could have been detected easily (assuming similar detector response as for 18). The purity of 18 also seemed to be evident from UV-absorption and fluorescence measurements in solution. A crystal batch, however, was found that actually contained a trace, blue luminescent impurity. This impurity was readily identified as anthracene by its fluorescence emission and excitation spectra. The luminescence spectrum of anthracene, however,

could only be detected by direct excitation into its lowest singlet excited state in the wavelength range between 345 and 410 nm (Figure 97). Samples containing anthracene presented no difference in their luminescence behavior aside from the accompanying anthracene fluorescence. This, and all other samples, were exhaustively re-purified by up to four chromatographic passes through silica gel using spectro-grade hexane solvent and by a number of recrystallizations. When the re-chromatographed samples were irradiated, they presented no evidence of containing any anthracene fluorescence within the detection limits of the instrument, and displayed no apparent decrease in the **RE** intensity.

Given the concern raised by the possible involvement of anthracene, which had been used as a starting material to prepare **18**, a second method was devised in order to eliminate the possibility of the **RE** originating from this or another impurity. We took advantage of the differential luminescent behavior of the two dimorphs of compound iPr/iPr-**23**. As mentioned in Part II of this thesis, crystals of the two modifications grown from the same batch only displayed the **RE** if they belonged to the $P2_12_12_1$ modification. It could be expected that both modifications should contain the same impurity (if any) unless the impurity were only soluble in the $P2_12_12_1$ but not in the Pbca crystals. In order to test this possibility crystals of the red-luminescent modification ($P2_12_12_1$) were obtained from the non-red-luminescent modification (Pbca) by crystallizations from the melt and from seeded solutions (see Part II). Material that had not been previously luminescent was in this manner converted into luminescent material.

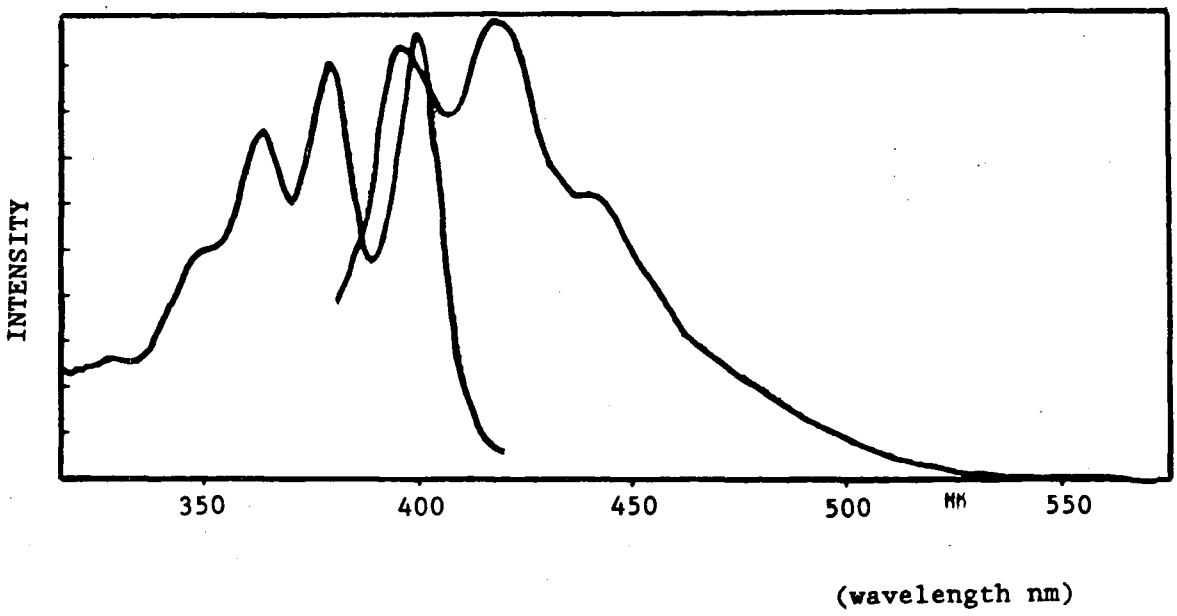

Figure 97. Fluorescence Excitation (a) and Emission (b) of Anthracene Impurity in Crystals of Diester Me/Me-18.

In the remainder of this section we review the possible involvement of impurity suspect number one, anthracene, in the RE phenomenon. The assignment of the RE to any of the primary unimolecular photophysical events known for anthracene can be discarded immediately. Not only do the anthracene fluorescence and phosphorescence occur at very different wavelengths (~400 and 700 nm respectively), but the RE, as indicated from the required accumulation time, and from our experiments at different wavelengths, clearly seems to be a multiphotonic process. The involvement of an excimer emission,[162] on the other hand, could possibly account for part of our observations. Single-photon excimer emission has been observed in anthracene and a number of its derivatives in crystals,[163] in hydrocarbon glasses,[164] and in solution.[165] Although the spectral region of this emission (λmax 550-570 nm) is substantially different from that of

the RE observed here, it is known that under special conditions that include biphotonic processes, a red anthracene excimer emission can be observed.[166] These occur when anthracene monomers are formed in a fixed sandwich intermolecular configuration as schematized and explained below:

1. **A-A** $\xrightarrow{h\nu(254\ nm)}$ **A A** Formation of Anthracene from its Dimer

2. **A A** $\xrightarrow{h\nu(365\ nm)}$ **(A A)*** Formation of Anthracene Sandwich Excimer

3. **(A A)*** ------> **A-A** Re-dimerization

4. **(A A)*** ------> **A A** + $h\nu$ Red Excimer emission (λmax 570 nm)

Figure 98. Formation of Anthracene Sandwich Pairs and their Red Excimer Emission.

In the first step (eq. 1, Figure 98), two anthracene molecules in a sandwich configuration (**A A**) are generated photochemically from the anthracene dimer (**A-A**) in crystals of the latter (first photon, 254 nm). When the ground state sandwich dimer is irradiated (second photon, 365 nm), it can react photochemically at high temperatures (200 K) to give back the anthracene dimer (eq. 3) or, at lower temperatures, it can emit a characteristic red luminescence (eq. 4, λmax 570 nm) that extends broadly into the red. Both the chemical reaction and the red emission were demonstrated to arise from the same intermediate which was postulated to be the excimeric species **(A A)***.[166] This excimer emission, however, is

different from the RE observed here, and, although it could be argued that spectral differences could be accounted for by the different crystalline environments, other arguments can also be found against this possibility occurring in crystals of diester **18** (vide infra).

The mechanism by which an anthracene excimer emission could explain our results would require the anthracene molecules to be in close proximity in crystals of diester **18** but not in microcrystallites (the anthracene red excimer emission has not been observed in crystals of pure anthracene). The original intermolecular configuration should not be appropriate for immediate red excimer emission, but suitable for dimerization to occur (eq. 1', Figure 99). Once the anthracene dimers are formed, they should photochemically revert back to two monomers, but this time, with a "perfect" sandwich configuration (eq. 2'). The newly formed monomers would the be in a disposition favorable for red excimer emission (eqs. 3' and 4,' Figure 99).

```
     A          hν
1')   A   --------->   A-A        Dimer Formation

              hν
2') A-A   ---------->   A A        Sandwich Pair Formation

              hν
3') A A   ---------->   (A A)*     Excimer Formation

4') (A A)* ---------->  A A + hν   Red Excimer Emission
```

Figure 99. Hypothetical Formation of Anthracene Red Excimer Emission in Crystals of Diester **18**.

Although the above model could explain: (1) the lack of red luminescence at 70 K (there is likely to be thermal barrier to dimerization), (2) the induction period (accumulation of the sandwich pair would occur after some irradiation time), and (3) the decay of the red emitting species (sandwich pair would probably tend to diffuse apart), a very important argument against this model comes from the excitation spectrum of the red-emitting species **X**. The excitation spectrum of the anthracene excimer mentioned above is almost indistinguishable from the anthracene monomer absorption,[166] and is very different from that of **X**.

Although other processes, such as the one discussed above that involve the participation of impurity molecules, could explain the origin of the **RE**, the subsequent thermal behavior of the species **X** seems to indicate strongly that its origin may be directly traced to the dibenzobarrelene diesters.

What is the RE Species?

In order to answer the above question we tried to obtain more information on this phenomenon by asking ourselves a closely related question. What is the fate of the **RE** species?

As indicated in Figure 96, the red-emitting species, **X**, could ultimately decay into a stable photoproduct, or alternatively, it could revert back to its precursor or starting material. We decided to investigate the possibility that **X** might transform into a different, hopefully luminescent product **Y**. Such was indeed found to be the case.

The emission spectra of "pure" samples in which the **X** species had been

previously accumulated were analyzed at 77K before and after they were taken out of the low temperature accessory for periods of approximately 30 sec. The emission was recorded upon excitation at 313, 337 and 360 nm after each warming period in order to increase the probability of detecting any new luminescence band accompanying the decay of **X**. Excitation at 360 nm was revealing when it was observed that the thermal decay of **X** was accompanied by the appearance and increase of a new, somewhat structured luminescence band with λmax at 510 and a shoulders at ~475 and 540 nm (Figure 100).

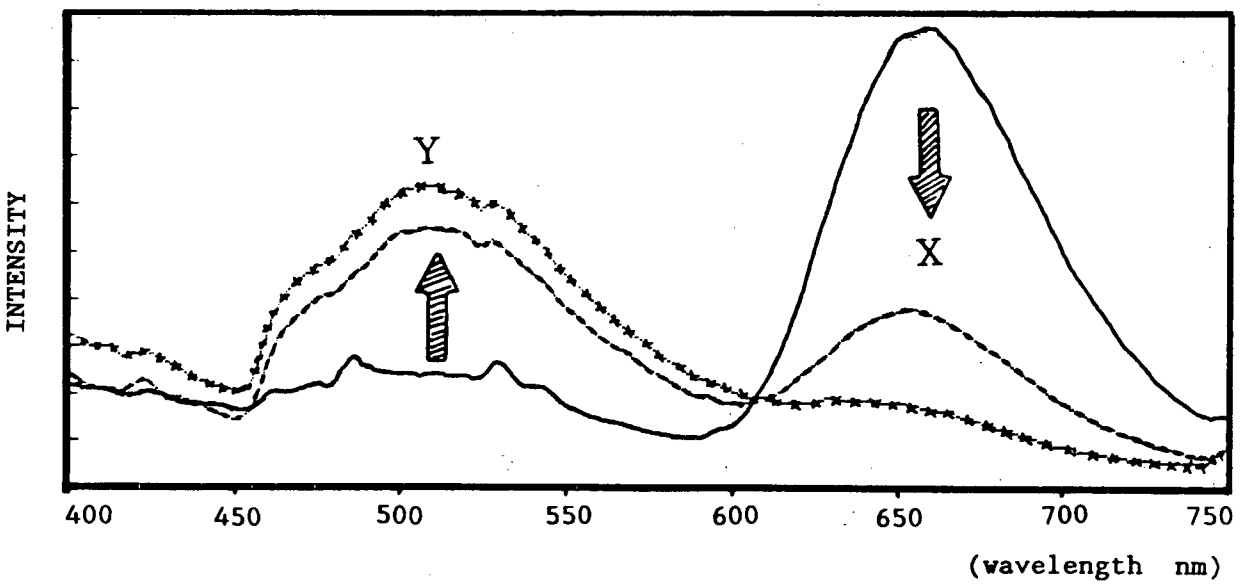

Figure 100. Thermal Decay of the Red-Emitting Species **X** and Appearance of New Species **Y**.

The new band, of a species now called Y, also had the characteristics of an allowed transition since it could only be detected in the fluorescence mode of the instrument. The excitation spectrum of this band, shown in Figure 101 along with the corresponding emission, was found to possess two maxima at 430 and 455 nm although it extends from near 380 to 480 nm. The lack of absorption of Y at 337 nm had prevented the detection of its luminescence, as most of our analytical irradiations had been performed at this wavelength. Interestingly, the species giving rise to this band also turned out to have a limited lifetime and was found to decay thermally until there was no trace of its existence after the sample had been left at ambient temperature for a few minutes. The decay of the latter band was not followed by any other detectable luminescence, and the final appearance of the samples has already been discussed in section I of this thesis.

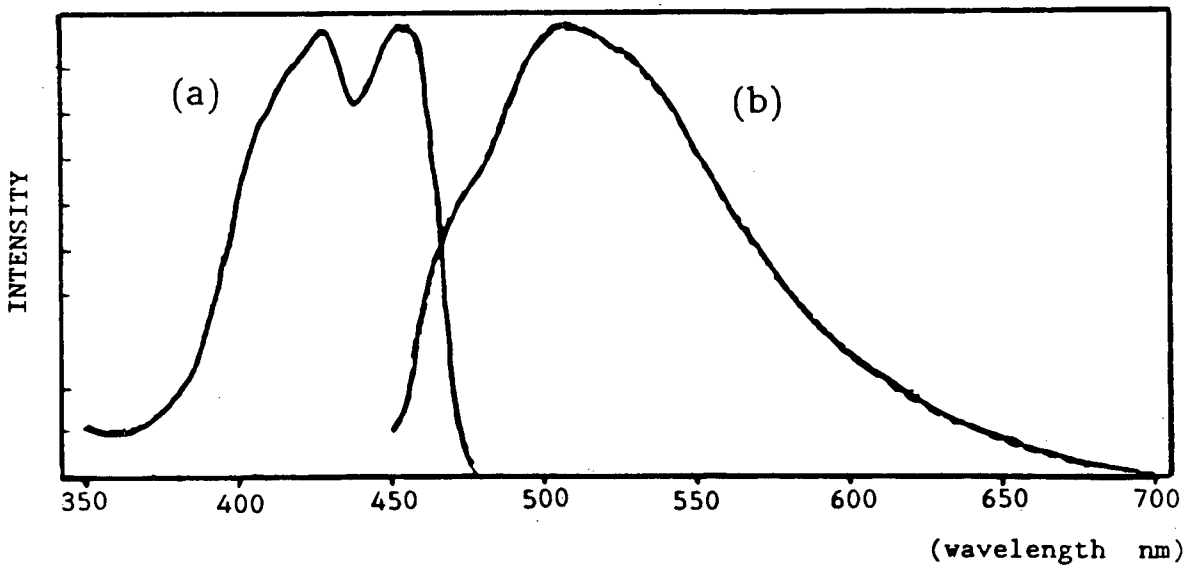

Figure 101. Luminescence Excitation (a) and Emission (b) Spectra of Species Y.

A correlation between the **RE** and the photochemical reactivity seems to be quite possible according to the above observations. Both the luminescence phenomena and the di-π-methane rearrangement are photochemically initiated and take place at the same time. Every time the reaction occurred in the solid state, the **RE** had also been present. Irradiation under conditions that cause no reaction did not generate the **RE** either. The formation of photoproducts and the **RE** can be prevented at (different) low temperatures indicating the existence of kinetic barriers for those two processes to occur.

If, as many of our observations seem to indicate, the **RE** and subsequent phenomena originate from light absorbed by molecules of diester **18**, the first question that should be answered concerns the excited state from which these transformations take place. In equation 1 of Figure 96, the involvement of the singlet excited state was indicated. Although no products other than **52** could be detected, either in solution or in the solid state, it is known that some dibenzobarrelenes can react from their singlet manifold.[66] The only singlet state reaction reported so far for this class of compounds is the formation of dibenzocyclooctatetraenes (**86**, Figure 102). This reaction has been postulated to occur by $2\pi + 2\pi$ addition of the vinylic double bond to a neighboring aromatic ring to produce an intermediate, **86-I**, which has never been detected.[66] This intermediate has been postulated to transform thermally by a retro $2\pi + 2\pi + 2\pi$ cycloaddition to form the final product **86**. Although a single intermediate, **86-I**, does not seem to account for our observations, other alternatives may be considered. For instance, it can be proposed that the conversion **86-I** to **86** occurs stepwise. One possibility would be a $4\pi + 2\pi$

retroaddition that would give a benzocyclobutane-orthoquinodimethane intermediate (**86-II**) before formation of **86**. Although the conjugation of this system is increased with respect to that of **86-I**, it appears that its spectroscopic properties may not justify our experimental observations. Ortho-quinodimethane, which is a singlet species,[167] is expected to be the

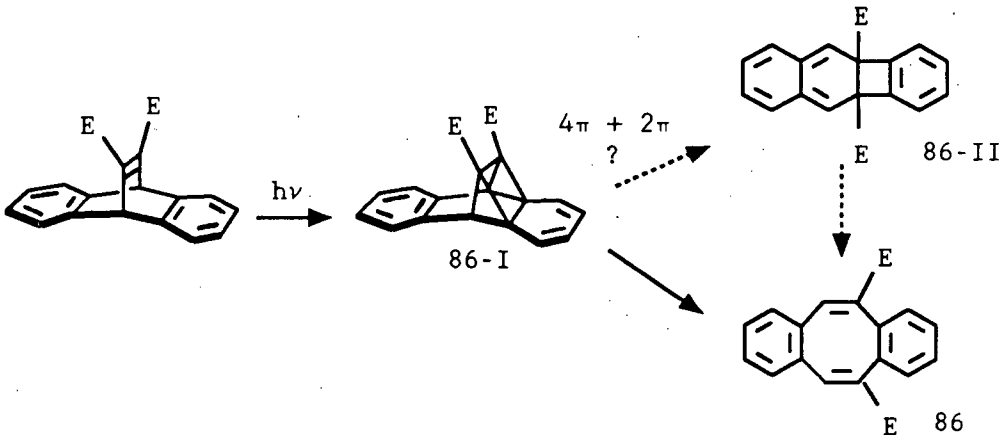

Figure 102. The singlet State Reactivity of Dibenzobarrelenes.

the lowest energy chromophore and is known to have the lowest absorption band around 370 nm,[167] which is still very far from the region in which both **X** and **Y** absorb (up to 580 and 475 nm respectively). Although we cannot discount the possibility that **X** and **Y** may originate from this or

another singlet state reaction, we have observed that dibenzobarrelene diesters that display simultaneous and sizeable singlet state reactivity in the solid state do not present the luminescence phenomena (see Part VI of the thesis). Probably the only way to exclude unambiguously the involvement of a luminescent intermediate from the singlet state of **18** would be by demonstrating its origin from the triplet state or from a different source. Although we cannot detect any additional products that would indicate its possible presence, it should be remembered that luminescence spectroscopy is a very sensitive technique that may detect very minute amounts of highly luminescent compounds.

The next alternative we have to consider is the possibility illustrated by equation 2 in Figure 96. The formation of **X** and **Y** from a triplet state reaction of **18** is a very interesting alternative. Similar to the case of the singlet state, there is apparently only one reaction available to the triplet excited state of dibenzobarrelene compounds, and that is the di-π-methane rearrangement. We will ignore the probability of any other triplet reaction and will analyze the probability of justifying the observed luminescence in terms of the di-π-methane rearrangement.

It should be recalled that two intermediates have been proposed to occur along the reaction pathway of the di-π-methane rearrangement.[46] It is interesting to note that we have found evidence for two transient intermediates, the red-emitting species **X** and its thermal product **Y**, which could be assigned to the species **BR-1** and **BR-2** shown in Figure 103 below.

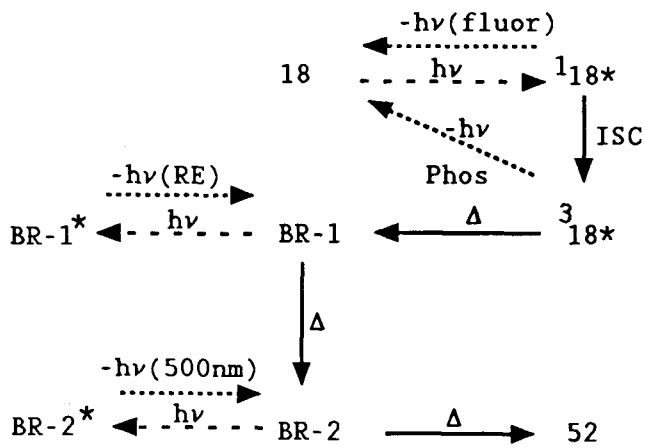

Figure 103. The Di-π-Methane Rearrangement as a Possible Explanation for the Luminescence of Crystalline Dibenzobarrelene Diesters.

The mechanism by which the photochemical reactivity could qualitatively explain the observed luminescence results can be described according to the above figure as follows:

1) A photon (λ < 340 nm) is absorbed by diester **18** in order to form its singlet excited state, ^{1}**18***.

2) ^{1}**18*** can revert to the ground state by fluorescence (λmax 412 nm), or,

3) ^{1}**18*** can intersystem cross to convert into its triplet excited state, ^{3}**18***.

4) ^{3}**18*** can revert to its ground state at low temperatures by phosphorescence (λmax 550 nm), or,

5) ^{3}**18*** can react photochemically to give the first, probably a

triplet state, di-π-methane biradical **BR-1**.

6) **BR-1** can now react at high temperatures to give the second di-π-methane biradical, **BR-2**, and,

7) **BR-1** can absorb a photon (335 nm > λ > 590) to form an excited state biradical **BR-1***.

8) The excited **BR-1*** can decay in a radiative manner to give the red luminescence observed (λmax 660 nm).

9) When **BR-2** is formed, it can either react thermally to form the final di-π-methane photoproduct **52**, or

10) **BR-2** can absorb a photon (480 nm > λ > 370 nm) to form an excited state **BR-2***.

11) **BR-2***, in turn, can revert back to its ground state (**BR-2**) by means of a radiative decay pathway (450 > λ > 700).

It should be noted that other alternatives, such as radiationless decay, are possible for each of the luminescent intermediates postulated between diester **18** and its photoproduct **52**. Decay of the biradicals to the ground state dibenzobarrelene reactant is also possible as has been demonstrated previously by Zimmerman[46] and Adam.[168]

The event where a reaction intermediate is formed and detected in rigid (usually glassy) media is a common analytical strategy known as matrix isolation.[169] The spectroscopic study of radicals and radical pairs in crystalline media has also been demonstrated by several authors including G. Closs,[170] A. Hutchison[171] and more recently M. McBride.[172] However, it should be pointed out that our observations are unique in that the proposed biradicals have discrete existences and relatively long

lifetimes even at ambient temperatures. In contrast, it seems that most studies on reactive intermediates up to now have been performed at temperatures around 77 K or below.

The Identity of Species X and Y.

Direct observation of the biradicals involved in the di-π-methane rearrangement of the naphthobarrelene **73** (Figure 67 on page 162 and Figure 104 below) has been reported in a glassy EPA (ether-isopentane-ethanol) matrix by K. Shaffner et al.[71] Flash photolytic analysis of compound **73** at 353 nm in the temperature range 88-200K resulted in the detection of a transient absorption shown to correspond to the triplet excited state ^{3}**73***(triplet-triplet absorption, λmax 380 and 430). At temperatures above 210 K in the flash photolytic experiment, the spectrum of ^{3}**73*** readily disappeared. In its place, a new sharp transient band grew in at λmax 380 nm. The lifetime of the new transient species was remarkably short at this temperature, with τ = 20$\pm$4 nsec in benzene, isopropanol and glycerol triacetate. It was shown that the species responsible for this transient could not be an excited state and it was assigned to the triplet biradical **BR-B**. Shaffner et al.[71] found further and convincing evidence for their assignment from ESR spectroscopic measurements that were consistent with the stepwise formation of two different triplet biradicals. The progress of the transformation **73--->BR-A--->BR-B--->PROD** could also be accounted for from infrared measurements. When the two latter analytical techniques were applied it could be observed that irradiation at 77 K gave ESR and IR

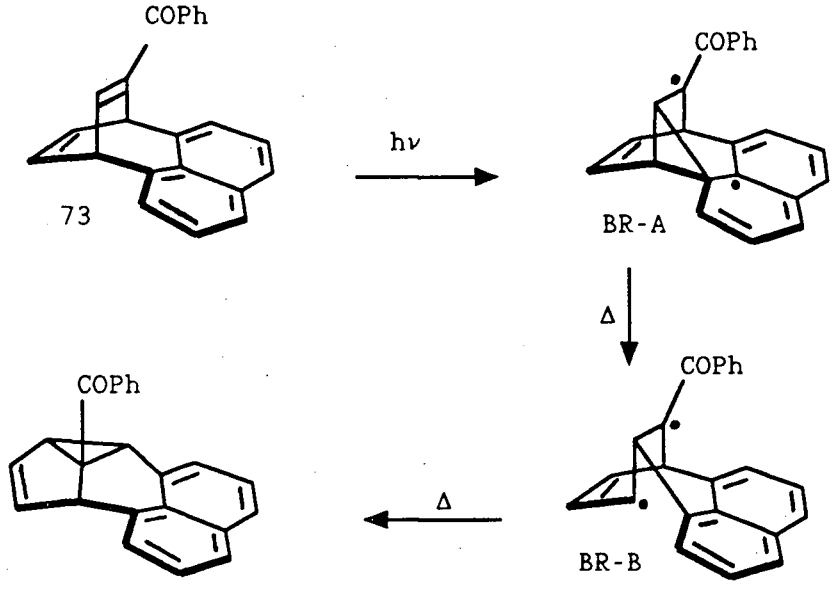

Figure 104. The Intermediates in the Di-π-methane Reaction of Naphthobarrelene 73.

transient bands corresponding to **BR-A** that persisted in the dark for at least two hours. When the samples were warmed from 77 to 94K without any further irradiation, the corresponding ESR and IR signals were slowly replaced by the signals of a new transient, **BR-B**. The second intermediate lasted without decrease in its intensity for two hours when it was re-cooled to 77 K, but had a significantly shorter lifetime of only a few minutes at 94K. It was also shown that the transformation of the first intermediate (**BR-A** ---> **BR-B**) was an irreversible process. Interestingly, the various steps of the photochemical transformation could also be followed by phosphorescence and fluorescence spectroscopy.[71] The most

striking observation related to the emission measurements was the fact that while compound **73** presented a strong phosphorescence, the emissive second biradical intermediate presented triplet-triplet fluorescence. By correlating the ESR signal intensities with the emission spectroscopic behavior, the authors concluded that it was only the second biradical, **BR-B**, that was emissive.

The reports by Shaffner et al. on the photochemistry of compound **73** add substantial credibility to the possibility that the two intermediate species observed here, **X** and **Y**, may belong to the biradical intermediates **BR-1** and **BR-2** shown in Figure 103 above. A possible concern may arise from the fact that our observations could be carried out without difficulty at ambient temperatures on biradicals that probably have nanosecond lifetimes in fluid solution at the same temperatures. However, Schaffner et al. also demonstrated that the stabilizing role of the solid matrix depended mostly on rigidity.[71] The lifetimes of the intermediates were recorded at different temperatures by flash spectroscopy in order to calculate their activation energies (Ea). Within the range studied (166-200 K), the Ea values obtained paralleled the changes in solvent viscosity as a function of temperature. This was shown to be true for three different solvents studied.

It seems possible that the viscosity and rigidity of a crystal at room temperature may be comparable to the viscosity and rigidity of a solvent glassy matrix around 200 K. If this were the case, the stability of the proposed biradicals in the crystalline medium can probably be well justified. It is interesting to note that indirect spectral evidence also supports our assignments of species **X** and **Y** as the biradicals

intermediates BR-1 and BR-2.

It has been suggested by J.C. Scaiano that biradicals generally show the same UV-spectral characteristics as analogous monoradicals.[173] In this manner, the spectrum of the photochemically generated Norrish type II biradical from valerphenone,[174] very closely resembles the spectrum of the ketyl radical[175] generated by photoreduction of acetophenone. Clearly, the lowest lying transitions in the 1,4-biradical are centered in its ketyl fragment and the interaction with the alkyl γ-radical center has a small effect on those transitions. Using similar logic, two different radical chromophores can be identified in the species BR-1. The lowest lying transition should probably be localized on the spirocyclooctadienyl moiety of the migrating aromatic ring (Figure 105) and not in the radical center that is next to the carboxylate ester group.

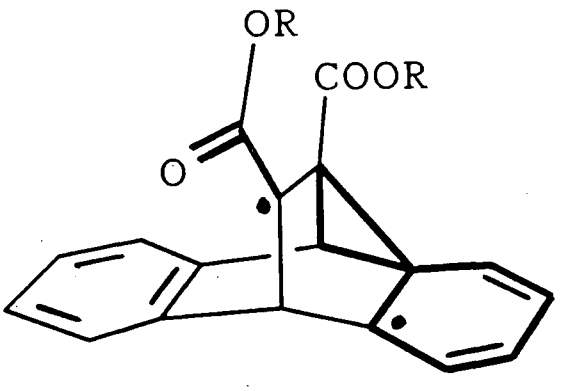

Figure 105. The Two Radical Centers of BR-1.

The absorption and fluorescence spectra for the spirocyclooctadienyl radical **87-R** have been determined recently in connection with studies on the neophyl rearrangement of the 2-phenylethyl radical shown in Figure 106.[176] Samples containing di-tert-butyl peroxide and the spirocycloctadiene **87** were irradiated at 347.1 nm. A transient absorption spectrum, consistent with the presence of previously known[177] cyclohexadienyl-like radicals, was observed. The spectrum, collected only in the vicinity of the visible range, was characterized by a weak absorption maximum around 560 nm. The location of this maximum, so far into the red, is not very common for aliphatic radicals but has been justified on experimental and theoretical grounds.[177] Studies on other cyclohexadienyl systems have shown that these species also have a very strong absorption in the ultraviolet (λmax 330 nm), in agreement with the strong (λmax ~360 nm) absorption of **X**. The fluorescence from the radical **87-R** was reported[176] to have an origin at 558 nm which was very similar to the one reported for the unsubstituted cyclohexadienyl radical.[177]

The resemblance between the spectral data from **X** and **87-R** is evident and supports the hypothesis that **X** may be identified with **BR-1**. It should be pointed out, however, that the absorption (fluorescence excitation) and emission of **X** are still substantially red shifted (~30-50 nm) with respect to those from **87-R** and other simple cyclohexadienyl radicals. Although this difference may possibly be justified from the additional substitution present in the case of **BR-1**, there is really not enough information available as to the effect of substituents on the spectral features of cyclohexadienyl radicals. The observed spectral differences could also arise from significant interaction between the two radical centers, which

we have ignored to this point.

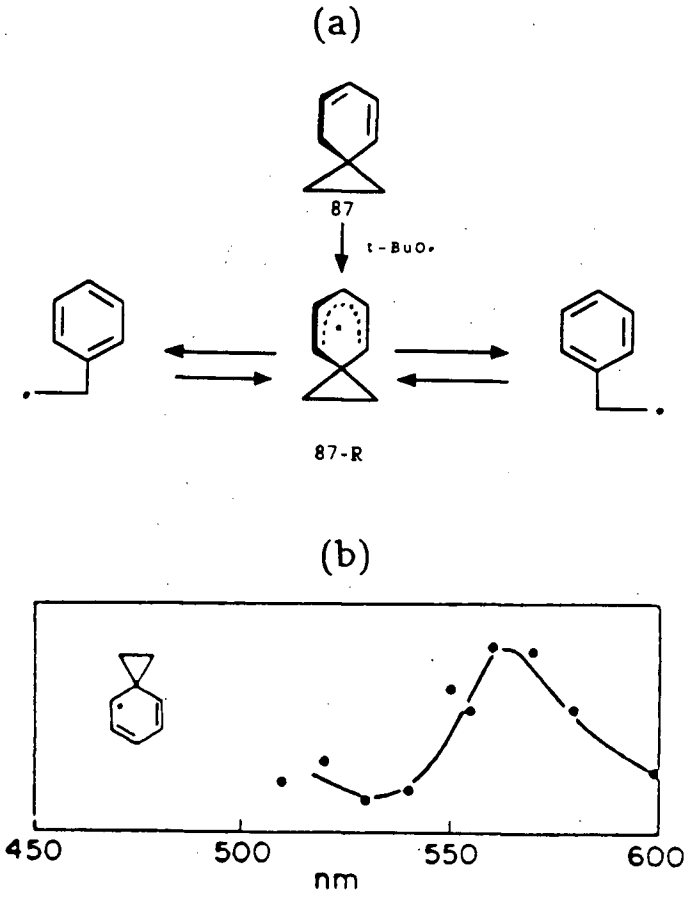

Figure 106. (a) The Neophyl Rearrangement of the Spirocyclooctadienyl Radical **87-R**, and, (b) Absorption Spectrum of **87-R**.

Turning our attention to the second luminescent species **Y**, which we have tentatively assigned as the second di-π-methane biradical **BR-2**, it can be appreciated that the lowest electronic transitions can probably be expected from the benzylic-localized radical center (Figure 107). The spectroscopic properties of benzylic radicals have also been studied by a number of workers and are relatively well documented.[178] It has been found that benzyl radicals exhibit a strong absorption band in the near ultraviolet region (λmax 305 and 318), and a very weak and structured band

in the visible region (360-460 nm) with two relatively sharp maxima at 435 and 450 nm.[178] The latter band is in good agreement with the fluorescence excitation band observed from the proposed species **BR-2**, which was also found to have two maxima in the visible range at approximately the same wavelengths (430 and 460 nm respectively). The fluorescence spectrum of the benzyl radical also compares remarkably well with the fluorescence of species **Y**. Presenting vibrational structure, the fluorescence spectrum of the benzyl radical covers the range between 460 and 600 nm, while the fluorescence of **Y** appears between 450 and 650 nm. Even though somewhat broader, the fluorescence of **Y** clearly presents vibrational structure consisting of at least three major bands which is in excellent agreement with the fluorescence of the benzyl radical.

It is apparent that the similarity between the spectra of benzyl and **Y** are closer than the similarities between the spirocyclooctadienyl radical, **87-R**, and the red-species **X**. While the spectral differences between the presumed **BR-1** and **87-R** may be difficult to explain, the similarities between **BR-2** (species **Y**) and benzyl have an experimental justification. This comes from an interesting but incomplete report given recently on the fluorescence of dibenzocycloheptanyl radical (**DBCH**) studied by Meisel et al[180] (Figure 107). The structural similarity that **BR-2** has with **DBCH** is evidently closer than the structural similarity between benzyl and **DBCH**. However, it was found that the emission spectrum of **DBCH** very closely resembles the spectrum of benzyl.

(a)

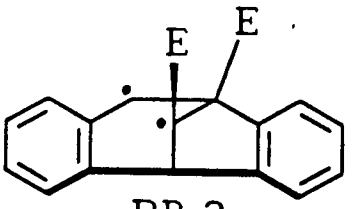

BR-2

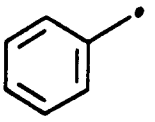

BENZYL

(b)

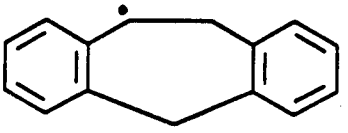

DBCH

(c)

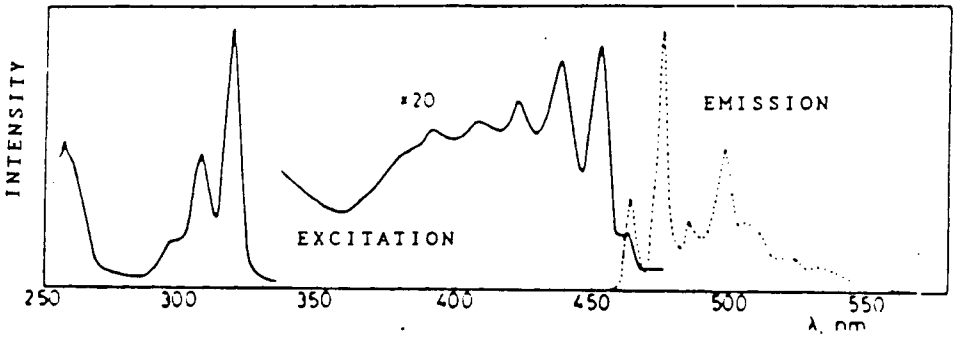

Figure 107. (a) Comparison Between **BR-2** and the Benzyl Radical, (b) Structure of the Dibenzocycloheptadienyl Radical **DBCH**, and, (c) Absorption and Emission Spectra of the Benzyl Radical.

We have presented strong evidence that indicates that the emitting species **X** and **Y**, formed in irradiated crystals of dibenzobarrelene diesters, may be the biradical intermediates evoked in the di-π-methane rearrangement. The study initiated here warrants further spectroscopic work including the use of ESR spectroscopy which should prove the triplet

nature of these species. Information obtained therefrom should be very valuable in the assignment of the emitting species and should be an important tool to help studying the detailed mechanism of the various processes involved in the transformation.[172] Spectroscopic studies at different temperatures (UV-VIS, IR and ESR) should help obtaining information regarding the thermal barriers observed as well as their possible nature.

PART VI. STUDIES ON 9-SUBSTITUTED DIBENZOBARRELENES

It was mentioned (Part III, page 149) that vinyl substituted dibenzobarrelene monoesters (**88**) rearrange with complete regioselectivity to give dibenzosemibullvalene products having the ester substituent at the C(8c) position[65] (**89**, Figure 108). This result has been interpreted in terms of the odd-electron center stabilization by the carbonyl group on the proposed biradical intermediates (page 150). The 9-carbomethoxy dibenzobarrelene **90**, on the other hand, was found to rearrange to a 67:33 mixture of the two alternative regioisomers, **91** and **92**[65] (Figure 109). This result was interpreted by Hixson et al.[44b] as arising from the reluctance of the rearranging molecule to position the electronegative carbomethoxy group at an incipient cyclopropyl site that is gaining substantial s character (92BR-I → 92BR-II). Both, vinyl- and 9-substituted dibenzobarrelenes were reported to undergo the triplet di-π-methane rearrangement as the only detectable photochemical reaction.

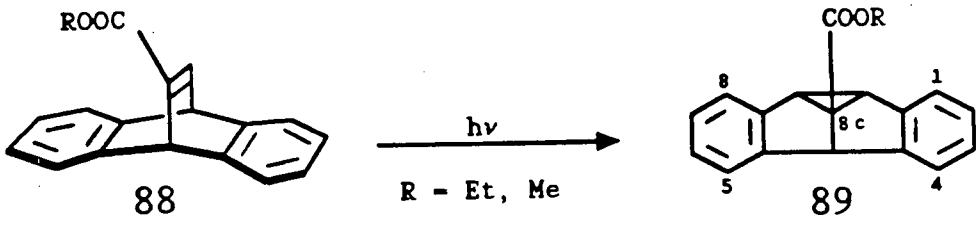

Figure 108. Photochemistry of Dibenzobarrelene Monoesters.

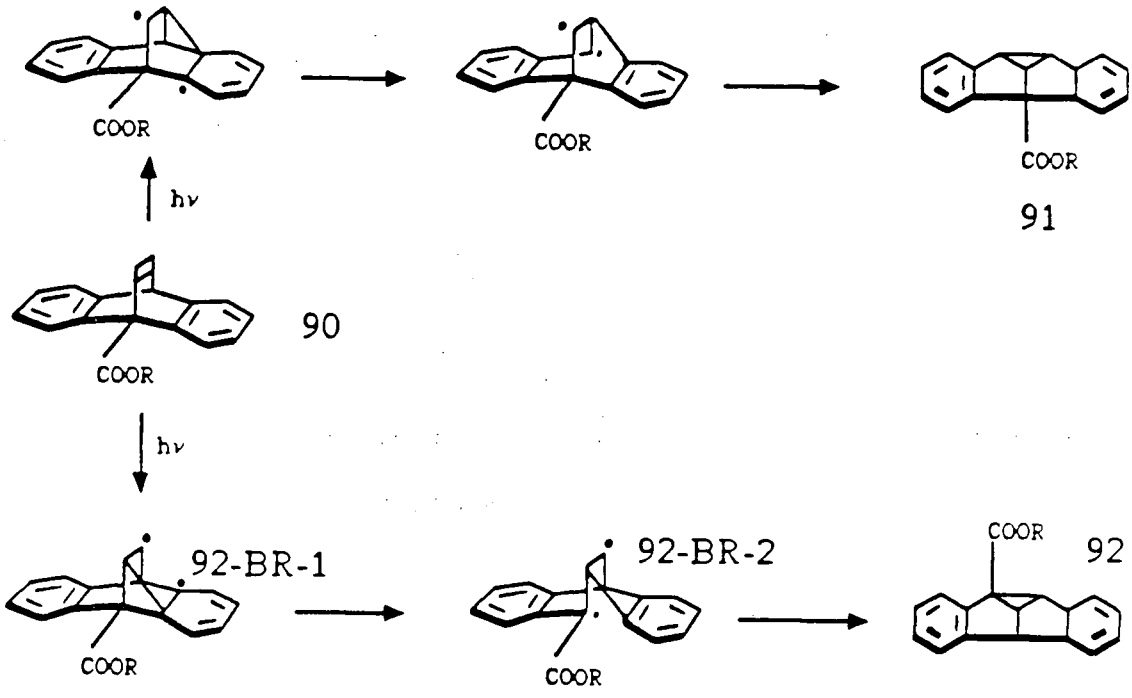

Figure 109. Photochemistry of 9-Carbomethoxy-Dibenozobarrelene.

The pronounced regioselectivity observed from compound **88** makes it an attractive model for the regioselective preparation of dibenzosemibullvalene derivatives where the position of the ester group may be predicted in a confident manner. Attachment of an isopropyl ester group to one of the bridgehead positions of compound **88** (R=Me), to give the 10,11- and 9,11-diesters **44** and **45** respectively, would not be expected to alter significantly the reaction regioselectivity in view of the moderate effect previously detected from the bridgehead substituent.[65] For instance, reaction of compounds **44** and **45** (Figure 110) would be expected to give mainly the dibenzosemibullvalenes **63A** and **96** respectively.

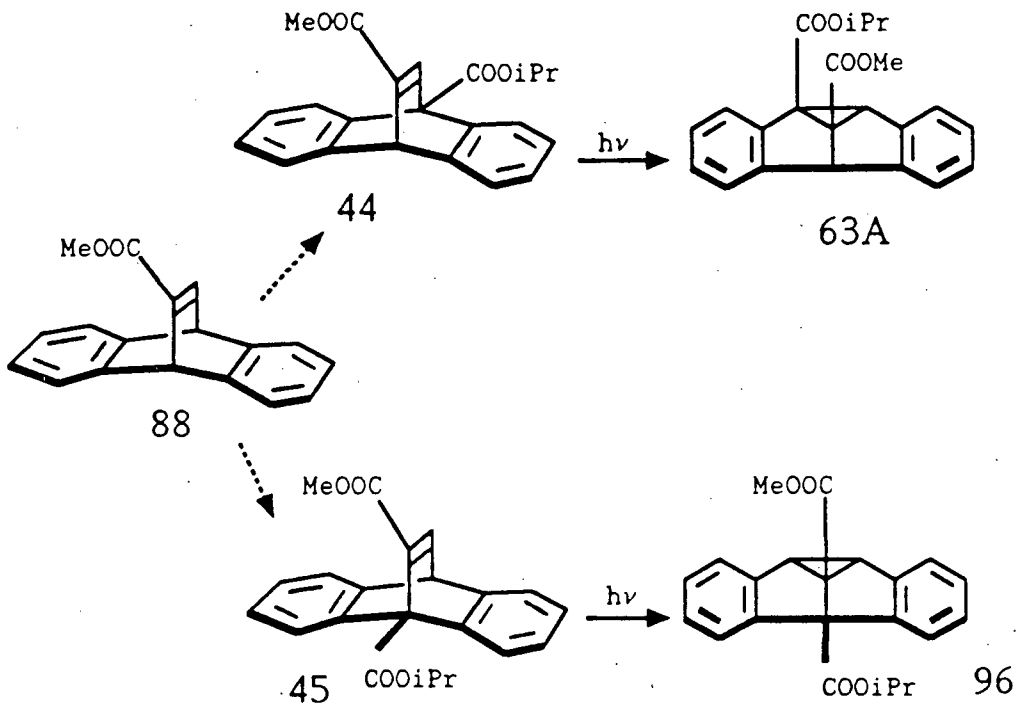

Figure 110. The 10,11- and 9-11-Dibenzobarrelene Diesters 44 and 45.

Photolysis of Diester 10-iPr/11-Me-44.

1) Photolysis in Solution.

Diester 44 was photolyzed first by sensitized irradiation in 0.01 M acetone solutions (Pyrex filter). A single photoproduct was formed cleanly and was identified as the expected dibenzosemibullvalene derivative 63A previously isolated from the photolysis mixture of diester Me/iPr-30 (Part III). In contrast to the 11,12-diesters studied before, 0.1 M benzene and acetonitrile solutions of diester 44 did not react upon direct irradiation with the nitrogen laser at 337.1 nm. It could be demonstrated that the UV

absorption spectrum of **44** was blue shifted by about 15 nm with respect to the absorption spectra of the 11,12-diesters. Photolysis at $\lambda \geq 290$ nm (Pyrex filter) gave two different products at low conversion values. One of the products in the photolysis mixture was identified as compound **63A** previously obtained by sensitized irradiation. The second product has been assigned the dibenzocyclooctatetraene structure **95** (Figure 111) based on its spectral properties and on previous literature reports on the formation of this type of compound[130,179] (vide infra). Because **95** proved to be unstable under the photolysis conditions, the ratio **63A**:**95** was highly dependent on the percent conversion. Although extrapolation to zero percent conversion gave a **63A**:**95** = 25:75 ratio, at 10% (glc) conversion the mixtures were found to contain almost identical amounts of the two products. Isolation of **95** for identification purposes was carried out by photolysis of 1 gram of diester **44** to only 10% conversion. Chromatography on silica gel removed the unreacted starting material and separation from **63A** was achieved by fractional recrystallization from diethyl ether. Mass spectral analysis of compound **95**, which is a crystalline solid (mp = 172-3°C), revealed its isomeric relationship with the starting material **44** and with the triplet state product **63A**.

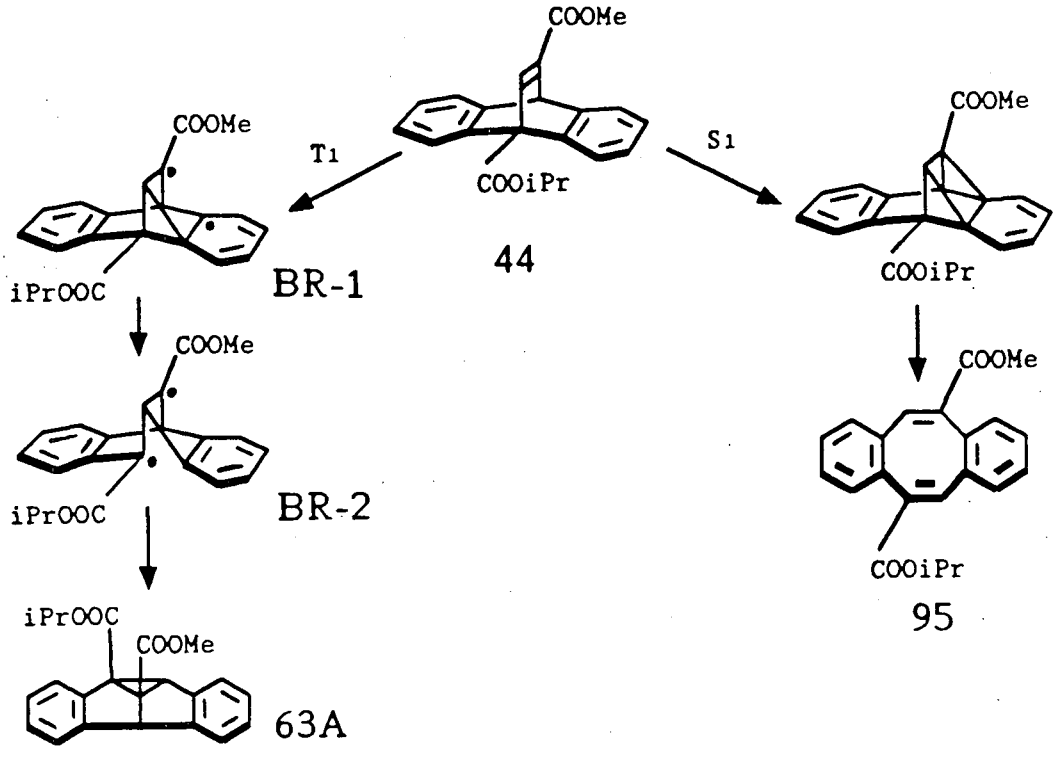

Figure 111. Photochemistry of Diester 44.

The presence of a dibenzocyclooctatetraene ring system could be confirmed by comparison of the spectral data obtained for compound **95** with the data reported in the literature for other similar compounds.[130,72] The ^{1}H NMR spectrum is characterized by the two vinylic protons in the cyclooctatetratene ring which were found at 8.07 and 8.01 ppm respectively (sharp singlets). The eight aromatic protons gave a non-symmetric group of signals in the region from 7.25 to 7.10 ppm. Resonances corresponding to the isopropyl ester group were found at 5.12 (1H, methine heptet) and 1.38 (6H, methyl groups doublet), while the carbomethoxy group appeared at 3.79 ppm (3H). The 18 sp^2 carbons required in the non-symmetric dibenzocyclooctatetraene diester skeleton were found in the ^{13}C NMR

spectrum. The infrared spectrum of compound **95** also supported our assignment as we found evidence for two ene-oate systems which are not expected in a dibenzosemibullvalene or any other product having the carbonyl groups on saturated carbons. The two carbonyl groups absorb at 1716 and 1710 cm^{-1} (shoulder) and the two vinyl absorptions occur at 1632 and 1640 cm^{-1}.

That compound **95** forms from a singlet state reaction while **63A** is a triplet-specific product was supported not only by the sensitization experiments but also from a Stern-Volmer analysis.[45] Using 1,3-cyclohexadiene as the triplet energy quencher, the quantum yields of formation of **95** (Φ_{95}) and **63A** (Φ_{63A}) were measured in benzene solution at 313 nm to conversions of ≤3%. The quantum yields of **95** and **63A** at zero quencher concentration were found to be 0.06 ± 0.005 and 0.023 ± 0.002 respectively. Samples containing 0.0, 0.2, 0.4, 0,6, 0.8 and up to 0.1 M quencher did not affect Φ_{95} but decreased Φ_{63A} significantly. This can be appreciated in Figure 112 where a Stern-Volmer plot of the results is shown. It should be pointed out that, according to the Stern-Volmer analysis,[139] the decrease in the quantum yield as a function of quencher concentration obeys the following linear relationship:

$$\Phi o/\Phi = 1 + k_q \tau [Q]$$

where Φ and Φo are the quantum yields with and without quencher, [Q] is the quencher concentration, k_q is the bimolecular quenching rate constant and τ is the lifetime of the excited state being quenched.

From the slope of the line in Figure 112 (0.8 M^{-1}), by assuming

diffusion controlled energy transfer from triplet 44 to the quencher, and by considering the rate of diffusion in benzene to be k_q = 5.0 x10^9 $mol^{-1}sec^{-1}$,[182] we arrive to the remarkably short triplet lifetime of 0.16 nsec (≈ 0.2 nsec).

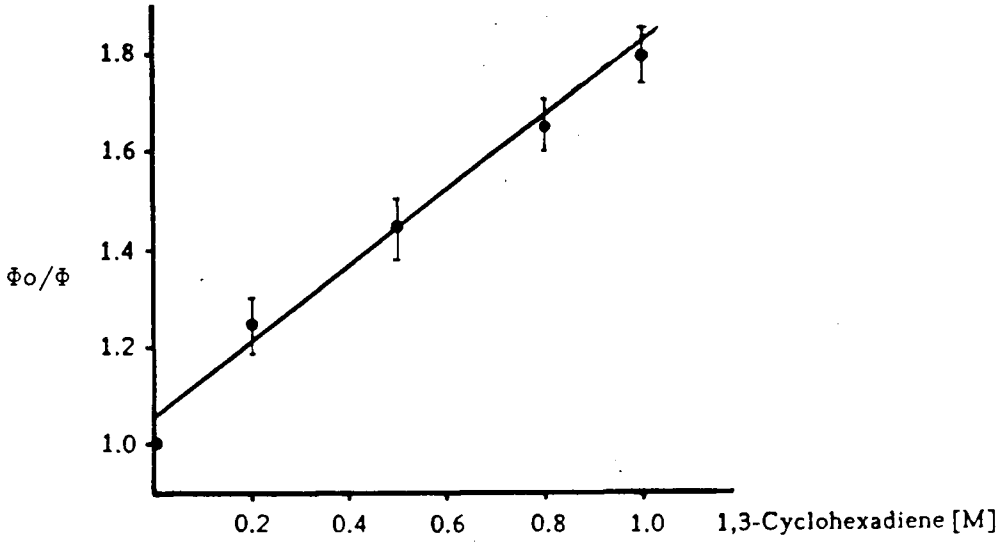

Figure 112. Stern-Volmer Plot for Formation of Dibenzosemibullvalene 63A from Diester 44.

It is interesting to compare the triplet lifetime and quantum yields for the vinyl monoester 88, the 11,12-diester Me/iPr-30 and the 10-11-diester 11-Me/10-iPr-44 (Figure 111). Compound 88 (R=Ethyl) was studied by S. Cristol[134] and compounds 30 and 44 have been analyzed in this thesis.

Dibenzobarrelene	Φ	τ(nsec)
11-Et-88	0.12	0.2
Me/iPr-30	0.20	1.0
11-Me/10-iPr-44	0.02	0.2

It can be seen that all three dibenzobarrelenes have approximately the same remarkably short triplet lifetime. Speculation as to the possible reasons for the ten-fold difference in the reaction quantum yields is not possible without knowing the intersystem crossing quantum yield of each of the above compounds.[45] It seems clear, however, that the triplet reactivity of the three substituted dibenzobarrelenes is very similar in spite of the large structural differences between all three compounds. This conclusion is based on the assumption that the di-π-methane rearrangement is the only process that deactivates the triplet excited state. This assumption is considered to be very reasonable in view of the fast decay rate of the triplet state, which would make it difficult for other processes to compete efficiently. It seems that addition of an ester group to the monoester **88**, whether on the vinyl or on the bridge position, does not cause any major changes on the chemical behavior of the triplet state. If the sensitized quantum yields of the three compounds were known, we could speculate about the differences in reactivity between the corresponding biradical intermediates. Very often a sensitized quantum yield of less than unity can be associated with reversion of the reaction intermediates to the ground state of the starting material.[180]

Interestingly, evidence of singlet state reactivity was only found in the case of the bridgehead substituted diester **44**. Although the reaction of dibenzobarrelene and other substituted derivatives to give the corresponding dibenzocyclooctatetraenes (DBCOT) has been well established as a singlet state process,[66,181] the factors that facilitate this reactivity are not known. After it was discovered that compounds such as the ester derivatives Me/Me-**18** and Et-**88**, do not react from their singlet

states, it was speculated that perhaps a very efficient intersystem crossing prevented these compounds from displaying singlet state reactivity.[66b] The "intersystem crossing" mechanism seemed to be supported by the observation that the alcohol derivative **97** yielded substantial amounts of the corresponding DBCOT[86b] (Figure 113). Compound **97** is not expected to have a large rate for intersystem crossing since it lacks a carbonyl group which is known to favor the required spin orbit coupling mechanism. We know now that the intersystem crossing quantum yields of **30** and **44** are less than unity because these compounds undergo relatively efficient room temperature fluorescence.

Another recent report on the formation of DBCOT from substituted dibenzobarrelenes was concerned with a series of bridgehead-substituted dibenzoyl dibenzobarrelenes **98a-f**[179] (Figure 113). From kinetic experiments based on the detection of the triplet excited states through flash photolytic experiments, the triplet lifetimes and the quantum yields of intersystem crossing were measured for all the compounds studied. It was found that the intersystem crossing quantum yields were very large for all of the compounds (0.7-1.0), and a striking ~100-fold variation on the triplet lifetimes was also reported.[179] Accompanying product analysis demonstrated that four of the six substrates (**98a-d**) undergo the triplet state di-π-methane rearrangement, and that two other compounds (**98e** and **98f**) gave the corresponding DBCOT's as the only detectable photoproducts. The authors proposed[179] that in the latter two cases the formation of products from the triplet state was largely impeded by the bulky substituent. It was speculated that the excited triplets should decay to some metastable intermediates that ultimately decays back to the starting

material. It seems that the observation of the singlet state reactivity in these cases was facilitated by the unreactive behavior of the triplet. There was no explanation offered, however, as to why steric hindrance would not impede the singlet state reaction, or why the singlet state reactivity should only be observed in those two cases and not at all in some of the other very similar compounds (i.e. the 9-cyclopentyl derivative **98d**).

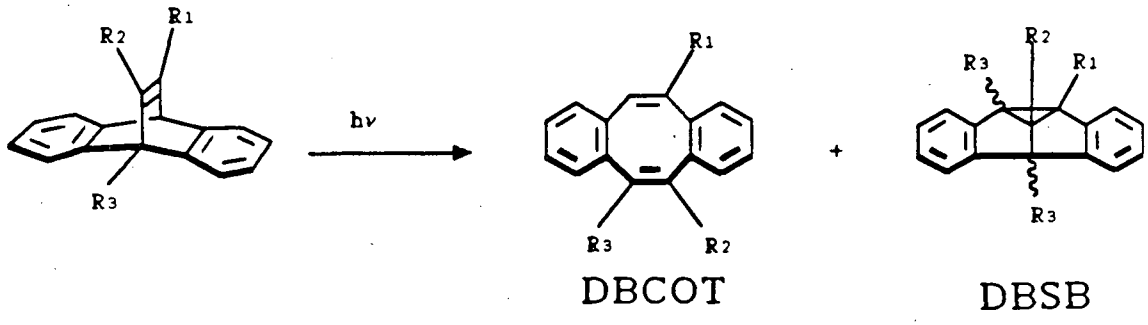

Compound	R_1	R_2	R_3	DBCOT	DBSB	Ref.
97	$C(OH)(CH_3)_2$	H	H	100	-	86b
98a	COPh	COPh	CH_2OH	-	64-82	179
98b	COPh	COPh	CH_2CH_3	-	75-86	"
98c	COPh	COPh	CH_2Ph	-	57	"
98d	COPh	COPh	C_5H_9	-	39-47	"
98e	COPh	COPh	$CH(CH_3)_2$	21-22	-	"
98f	COPh	COPh	C_6H_{11}	46-55	-	"
99	CO_2Me	CO_2Me	Me	77	13	72
100	CO_2Me	CO_2Me	NHOAc	15	85	130

Figure 113. Dibenzobarrelenes that Display Singlet State Reactivity.

With respect to the diesters studied this thesis, it should be pointed out that a singlet state reaction with $\Phi \geq 0.05$ could not have passed undetected in the case of diester **30**, or other 11,12-diesters, unless the corresponding DBCOT had rapidly isomerized into the dibenzosemibullvalenes **63A**, **63B** or into the starting material under the reaction conditions. In order to analyze this possibility, the photochemistry of DBCOT **95** was analyzed in dilute benzene, acetonitrile and acetone solutions. In all cases, up to 25 glc peaks were found, none of which had a retention time corresponding to any of the above dibenzosemibullvalenes or to dibenzobarrelenes **30** or **44**. Given the small amount of DBCOT **95** available, no attempt was made to identify the major reaction product which accounted for 30% of the total reaction mixture. The longer glc retention time and the mass of this material (glc-MS gave m/e = 694) indicates the possibility of a photochemical dimerization reaction.

While it is clear that a low quantum yield from the triplet state reaction would favor observation of singlet state reactivity, it is still not clear what the factors are that facilitate the latter. A very tentative correlation can be postulated, however, between dibenzobarrelene substitution at the 9-position and singlet state reactivity. Recent studies in this laboratory have shown that 9-methyl-dibenzobarrelene diester (**99**) reacts from its singlet state to give the corresponding dibenzocyclooctatetraene,[72] and a similar report on the corresponding 9-acetamido-derivative (**100**) has been published by Paddick et al.[130]

2) Photolysis in the Solid State.

Photolysis of single and powdered crystals of diester **44** was carried

out with the Pyrex filtered output of the Hanovia lamp. The reaction proceeded slowly and photolysis for as long as 40 h yielded only 10% of photoproducts. No trace of melting was detected in these samples (mp = 99-100°C).

In a manner similar to that observed as in solution photolysis, the product ratio was found to vary with the percent conversion. The **95**:**63A**=48:52 ratio obtained by extrapolation to zero percent conversion was substantially different from the ratio previously obtained in solution by direct irradiation (75:25). The fact that the solid state favors the triplet state reaction cannot be rigorously attributed to a different singlet:triplet excited state partitioning because of the relative inefficiency of the two reaction processes. An explanation that postulates that the di-π-methane rearrangement is a topochemically more favored process with respect to the reaction to form DBCOT is an equally viable alternative. The inefficiency of the two chemical processes can probably be attributed to the relatively tight crystal packing of compound 44 demonstrated from its X-ray crystal structure (see discussion below).[143]

The resonance stabilizing ability of the carbonyl group at the vinyl position on the biradical intermediates is expected to be close to ideal.[79] The methyl ester group has a torsion angle of 167.8°, which makes it close to the more stable s-trans conformation (180°).[80,136] The packing diagram of crystals of 44 (centrosymmetric space group $P2_1/a$) is shown in Figure 114. This diagram clearly demonstrates the congested environment at the two sides of the C(11)=C(12) vinylic double bond (see molecular structure and numbering also in Figure 114). It was also found that both carbonyl oxygens and a hydrogen atom have short intermolecular contacts

(interatomic distances under the sum of their Van der Waals radii of 2.72 Å for O...H and 2.40 Å for H...H)[151]: O(2)...H(2) 2.58 Å, O(4)...H(18b) 2.55Å and H(18)...H(18') 2.29 Å. While the congestion at both sides of the double bond is expected to slow the intramolecular $2\pi + 2\pi$ cycloaddition necessary for the singlet state reaction, the first step of the triplet reaction may not be so largely impeded. The H(12) attached to the vinyl carbon undergoing the benzo-vinyl bridging step is located in a relatively free environment. The steric interactions that could arise between H(12) and its lattice neighbors should not be very strong and they would not be expected to retard the first reaction step to give BR-1 (Figure 111, page 269). Even though the rearomatization step (to give BR-2) is expected to occur with relative ease, it seems that the final cyclopropyl ring-forming step could be a limiting factor. The final bond in the dibenzosemibullvalene product is formed between C(10) and C(11), which are found in the starting material at a non-bonded distance of 2.41 Å. Although changes in this distance at the stage of the two reaction intermediates are not known, it is expected that its magnitude should not change drastically until the single bond is to be formed. Here, the two carbons must come to a distance of approximately 1.54 Å and the steric interactions between the isopropyl ester group and the crystal lattice are expected to be considerable during this displacement. It seems possible that, in the event where this bonding process is frustrated by intermolecular steric interactions, the 1,3-biradical BR-2 could revert to starting material through BR-1, perhaps accounting for the low reaction efficiency. Attempts to detect any of the postulated biradical intermediates by luminescence spectroscopy have been unsuccessful. We do not know, however, whether our negative

results are due to low luminescence quantum yields, to low accumulation levels of BR-1 and BR-2, or to a lack of significant chemical reactivity altogether.

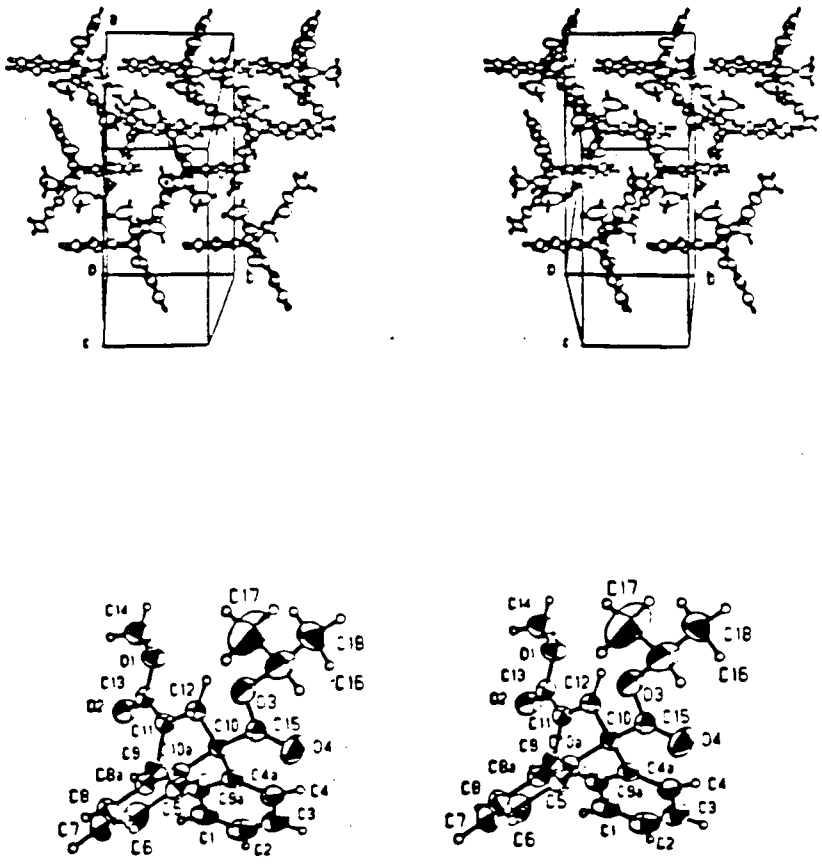

Figure 114. Stereoviews of the Packing Diagram and Molecular Structure of Diester 44.

Photolysis of Diester 11-Me/9-iPr-45.

1) In Solution.

The procedure used to photolyze diester **44** was repeated in the case of **45**. Similar results were discovered when acetone solutions gave a major product that accounted for 90% of the photoproduct mixture. The ^{1}H NMR, MS, and FTIR were in complete agreement with the structure of the expected dibenzosemibullvalene derivative **96**. The ^{1}H NMR spectrum of **96** consists of: (1) two symmetrical peak patterns between 7.25 and 7.00 ppm (8H) that were assigned to the aromatic protons, (2) the resonances of the isopropyl ester group appeared at 5.31 (1H, heptet, J=7Hz) and 1.30 ppm (6H, doublet, J=7Hz), (3) the two cyclopropyl protons that appeared at 3.82 ppm as a sharp singlet as expected for the mirror-symmetric dibenzosemibullvalene structure (this chemical shift compares well with the signal from the corresponding protons in the dibenzosemibullvalene **89** (page 265) studied by Ciganek, which appear at 3.77 ppm), and, (4) the methyl resonance of the other ester group appears at 3.65 ppm.

Although the minor component of the reaction mixture (5%) could not be isolated, some of its signals in the ^{1}H NMR spectrum of the reaction mixture are indicative of the alternative regioisomeric dibenzosemibullvalene structure **102**. This conclusion is based on the presence of two doublets at 4.25 and 4.69 (J = 8Hz), perhaps assignable to the vicinally coupled protons H(4b) and H(8c). This assignment is very uncertain and requires further proof.

Direct photolysis of Diester **45** in acetonitrile solution resulted in the formation of the two products observed before, although this time they

constituted only 15% of the reaction mixture (when extrapolated to zero percent conversion). The major (85%), singlet-specific photoproduct, was not isolated but in analogy with diester 44 it was assumed to be the dibenzocyclooctatetraene **101** (Figure 115).

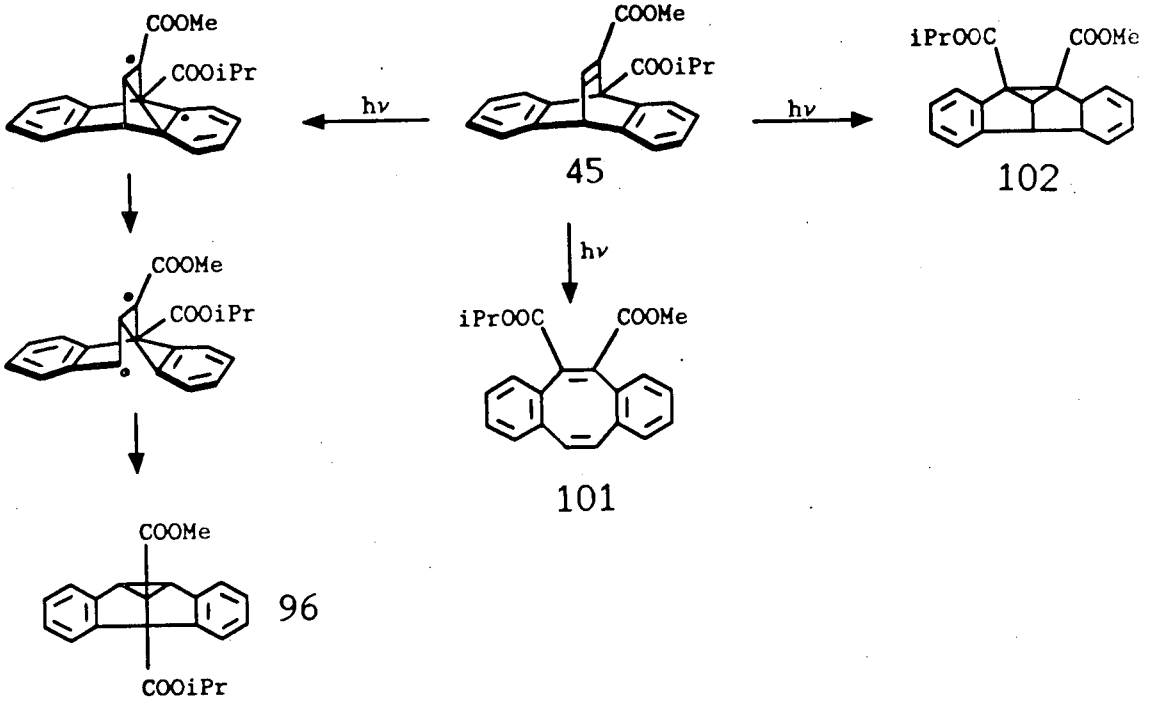

Figure 115. Photochemistry of Diester **45**.

The photoproduct ratio was remarkably altered in the solid state. After photolysis times of only 10 min the percent conversion detected by glc was within 2.5 and 4% and the **101**:**96** ratio was found to be 25:75 (compared to 85:15 in solution).

It was obvious that diester **45** has a remarkably greater solid state

reactivity compared to diester **44**. The photolysis time required to reach the same conversion under similar irradiation conditions was up to 15-20 times longer in the case of **44**. This interesting observation can be speculatively ascribed to the small size of the substituents attached to the atoms undergoing the larger displacements during the reaction (i.e. C(12) and C(10). The X-ray crystal structure of diester **45** was obtained (space group C2/c) and the packing diagram indicated that, in contrast to the packing of diester **44**, there are no unusually short contacts, and that the moving vinyl and bridghead carbons are relatively free (C(12) and C(10) in Figure 116). The motions of the methyl and isopropyl ester groups along the reaction are expected to be minimal in this case since they are in a position that is rather remote from the reaction centers (Figure 115).

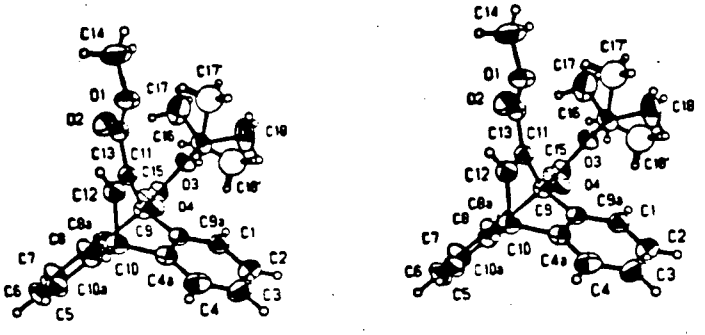

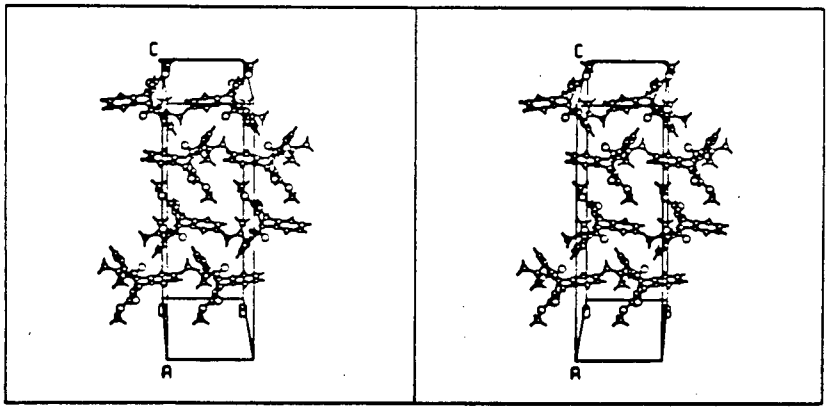

Figure 116. Stereoview of the Molecular and Packing Structures of Diester 45.

EXPERIMENTAL

General

Melting Points (mp). Melting points were determined on a Fisher-Johns hot stage apparatus and are uncorrected.

Infrared Spectra (IR). Infrared spectra were recorded on a Perkin Elmer 1710 Fourier transform spectrometer. The positions of the absorption maxima are reported in cm^{-1}. The spectra of liquid samples were recorded without solvent as thin films between two sodium chloride plates. Solid samples (2-5 mg) were ground in KBr (100-200 mg) and pelleted in an evacuated die (Perkin Elmer 186-0002) with a laboratory press (Carver, model B) at 20,000 psi.

Nuclear Magnetic Resonance Spectra. Proton nuclear magnetic resonance (^1H NMR) spectra, as indicated in each case, were recorded in deuterated chloroform, benzene, acetone or acetonitrile. The spectrometers used were a Bruker WP-80 (80 MHz), a Varian XL-300 (300 MHz) and a Bruker WP-400 (400 MHz). Signal positions are given in ppm (delta (δ), units) with tetramethyl silane as internal reference. The number of protons, signal multiplicity, coupling constants (in Hz) and assignments are given in parentheses following the signal position.

Carbon nuclear magnetic resonance (^{13}C NMR) spectra were recorded at 75.4 MHz on a Varian XL-300 instrument using deuterochloroform as a solvent and tetramethyl silane as the internal reference. Chemical shifts

observed under broad band proton decoupling $^{13}C-\{^{1}H\}$ are given in ppm (delta (δ), units) followed in some cases by their assignment.

Ultraviolet Spectra (UV). The UV spectra were recorded on a Lambda-4 Perkin Elmer spectrometer.

Mass Spectra (MS). Low and high resolution mass spectra were obtained on a Kratos MS 50 mass spectrometer. Coupled gas chromatography-mass spectral analysis (glc-MS) was performed on a Kratos MS 80 spectrometer attached to a Carlo-Erba gas chromatogram.

Microanalysis. Carbon, hydrogen and nitrogen elemental analysis were performed by the departmental microanalyst, Mr. P. Borda.

Gas Liquid Chromatography (glc). Gas chromatographic analyses were performed on a Hewlett-Packard 5890 A gas chromatograph. The signal from a flame ionization detector was integrated by a Hewlett-Packard 3392 A integrator. Helium was used as the carrier gas with a column head pressure of 15 psi. A 15 m x 0.25 mm fused silica capillary DB-1 column from J&W scientific Inc. was used for most analyses.

Thin Layer Chromatography (tlc). Analytical tlc was performed on commercial pre-coated silica gel plates (E. Merck, type 5554).

Optical Rotations ($[\alpha]_D$). The instrument used was a Perkin Elmer 141 polarimeter operated at the sodium D line (589 nm). Measurements were

realized at 20 °C on a 10 cm path length cell with a total volume of 1 ml. The optical rotation of a sample of (l)-(-)-menthol (Aldrich) in ethanol $[\alpha]_D$=50.1 (c=0.1) and pure chloroform $[\alpha]_D$=0 were used to calibrate the instrument readings.

Solvents and Reagents. Spectral grade solvents were further purified for spectroscopic and photochemical studies by methods reported in the literature. Optically active materials were used assuming the manufacturer's specifications to be correct.

Crystallizations. Crystallizations were systematically explored for most compounds in several solvents, solvent mixtures and from the melt. Crystallizations from solution were performed by slow solvent evaporation at ambient temperature and pressure. Crystallization from the melt were carried out by two methods: a) small scale crystallizations (less than 50 mg) were performed by slowly lowering the temperature of the sample contained in a sealed vial on the hot stage Fisher-Johns melting point apparatus. Polycrystalline material was obtained by this method and, b) larger scale crystallizations (up to 2 gr) were performed by slowly lowering the temperature of samples contained in a sealed vial inside a Kugelrohr oven. In some instances nucleation was induced by pricking the molten super-cooled sample with a flamed needle. The possibility of having polymorphic modifications was systematically monitored by solid state infrared spectroscopy.

X-Ray Analysis. All X-ray structures were determined by Dr. Fred

Wireko and Prof. James Trotter. The stereoscopic diagrams presented in this thesis were drawn with a locally modified version of the ORTEP program at a 50% probability level. Futher details and discussion on the crystallographic work (including the R-factors, standard deviations, thermal parameters, etc.) can be found in the Ph.D Thesis of Dr. Fred Wireko (University of British Columbia, 1988).

Synthesis of Starting Materials.

Dimethyl-9,10-dihydro-9,10-ethenoanthracene-11,12-dicarboxylate (18).[56]

A56 100 ml round bottom flask containing 5 g (28.1 mmol) of anthracene and 4.3 g (30 mmol) of dimethyl-2-butyne-1,4-dioate was attached to a reflux condenser and kept at 190°C for 2 h in an oil bath. The molten reaction mixture was allowed to cool down and solidify to a brown polycrystalline mass. The solid was dissolved in 30 ml of refluxing $CHCl_3$. Crystallization was then induced by scratching with a glass rod after addition of 50 ml of cold ethanol to yield 8.5 g of a pale yellow solid. After two recrystallizations from $CHCl_3$-EtOH, 8.1 g (25.3 mmol, 90% yield) of pure **18** were obtained as a white solid with mp = 160-161°C (lit:[65] 160-161°C). The spectroscopic properties of **18** which follow were in complete agreement with those reported in the literature.[65]

^1H NMR ($CDCl_3$, 80 MHz): δ 7.5-6.9 (8H, m, Ar-H), 5.5 (2H, s, bridgehead-H), 3.8 (6H, s, $-CO_2CH_3$).

^{13}C NMR ($CDCl_3$, 75 MHz): δ 165.8 (C=O); 146.9, 143.7, 125.3, 123.7 (Ar-C and Vinylic-C), 52.3 ($-CO_2CH_3$), 52.2 (Bridgehead-C).

IR (KBr) 1713, 1720 (2 C=O), 1632 (E-C=C-E), 1275 (C-O) cm^{-1}.

MS m/e (rel. intensity) 320 (M^+, 52.5), 260 (100), 202 (84), 178 (49).

UV (Cyclohexane) λ_{max}: 270 nm (ϵ 579,000) and 278 (ϵ 580,000) (π-π^*); 290 sh (ϵ 1,000) (n-π^*).

The structure of diester **18** was also confirmed by X-ray crystallographic analysis.

<u>9,10-Dihydro-9,10-ethenoanthracene-11,12-dicarboxylic acid (19)</u>.[56]

Eight grams (25 mmol) of the diester **18** were suspended in 50 ml of a 30% NaOH solution to which 30 ml of ethanol had been previously added. The mixture was refluxed until the suspended material was completely dissolved and then for two additional hours. The reaction mixture was cooled to room temperature and washed with diethyl ether to eliminate traces of unreacted starting material. The aqueous fraction containing the acid salt was acidified by dropwise addition of concentrated HCl while stirring in an ice-water bath. When the acid had completely precipitated it was extracted with diethyl ether (2 x 200 ml). The combined organic fractions were then dried over anhydrous Na_2SO_4 and evaporated to dryness. The diacid **19** (6.5 g, 22.3 mmol, 89 % yield) was obtained as a white solid. Recrystallization from acetone-hexane gave prisms with mp = 215-216°C (lit[64] mp =215-216°).

^{1}H NMR ($CDCl_3$, 80 MHz) δ 8.2 (2H, s. $-CO_2H$, exchanges with D_2O), 7.6-7.0 (8H, m, Ar-H), 6.0 (2H, s, bridgehead-H).

IR (KBr) 3400-3600 ($-CO_2$-H), 1700 (C=O) cm^{-1}.

MS m/e (rel. intensity) 292 (M^+, 0.4), 248 (21.5), 230 (56), 202 (100), 178 (5.3).

<u>9,10-Dihydro-9,10-ethenoanthracene-11-12-dicarboxylic acid anhydride</u>

(20).[56]

A suspension of 5 g (17 mmol) of diacid **19** in 50 ml of CH_2CL_2 and 4 gr (35 mmol) of oxalyl chloride was refluxed for 24 h. After this time the solvent and excess chloride were evaporated in vacuo and the resulting solid was recrystallized twice from ethyl acetate to give slightly yellow prisms with mp = 252-254°C (lit.[56] mp = 247°C).

^1H NMR ($CDCl_3$, 80 MHz) δ 7.5-7.0 (8H, m, Ar-H), 5.6 (2H, s, bridgehead-H).

IR (KBr) 1843 (C=O antisymmetric), 1787,1767 (C=O symmetric), 1637 (C=C) cm^{-1}.

MS m/e (rel. intensity) 274 (M^+, 67), 230 (59), 202 (100), 178 (57).

Diethyl-9,10-dihydro-9,10-ethenoanthracene-11,12-dicarboxylate (21).

A solution of the diester **18** (2 g, 6.5 mmol) in 100 ml of absolute ethanol was refluxed after addition of 1 ml of concentrated sulfuric acid. The reaction was followed by glc analysis (column DB-1, oven at 200°C) of 0.1 ml samples taken from the reaction mixture at different times (before injection the samples were diluted with diethyl ether, washed with saturated $NaHCO_3$, water and dried over Na_2SO_4). The reaction was stopped after the starting material and the product of partial transesterification (compound **28**, vide infra) had almost disappeared (10 days). The volume of ethanol was then reduced to 20 ml by evaporation in vacuo and 100 ml of diethyl ether were added. The resulting solution was washed successively with water (2 x 50 ml), a solution of 5% $NaHCO_3$ (2 x 50 ml) and water again (2 x 50 ml) and then dried over anhydrous Na_2SO_4. The solvent was

evaporated <u>in vacuo</u> and 2.2 g of crude product were obtained. Purification by column chromatography (silica gel, petroleum ether (bp = 35-60°C):ethyl acetate-96:4) gave 1.7 g (5.0 mmol, 80% yield) of **4**. Crystallization from several solvents including ethanol and cyclohexane yielded either plates or prisms but not both. The two samples were suitable for X-ray diffraction analysis and were confirmed to be dimorphic. The proposed structure is also supported by the following data.

mp: 93-94°C plates.

mp: 97-98°C prisms.

^{1}H NMR ($CDCl_3$, 300 MHz) δ 7.40-6.95 (8H, m, Ar-H), 5.42 (2H, s, bridgehead-H), 4.21 (4H, q, 7Hz, $-CO_2CH_2CH_3$), 1.27 (6H, t, 7Hz, $-CO_2CH_2CH_3$).

^{13}C NMR ($CDCl_3$, 75 MHz) δ 165.5 (C=O), 146.6, 143.8, 152.3, 123.7 (Ar-C and Vinylic-C), 61.36 ($-CO_2CH_2CH_3$), 52.4 (Bridgehead-C), 13.97 ($-CO_2CH_2CH_3$).

CPMAS ^{13}C NMR (45 MHz): $P2_12_12_1$ δ 166.7, 162.7, 152.4, 144.3, 143.9, 138.2, 125.8, 124.5, 123.4, 122.7, 60.1, 52.5, 50.5, 14.6, 14.2; $P2_1/c$ δ 166.8, 160.6, 155.4, 145.5, 144.2, 143.6, 142.9, 139.2, 138.8, 127.0, 125.3, 122.6, 121.7, 61.0, 59.4, 53.8, 50.5, 49.1, 15.5, 14.8, 13.2.

IR (KBr) (see figure 36) plates: 1716, 1717 (2 C=O), 1633 (E-C=C-E), 1259 (C-O); prisms: 1730, 1705 (2 C=O), 1640 (E-C=C-E), 1270 (C-O) cm^{-1}.

MS m/e (rel. intensity) 348(M^+, 44.4), 274(92.4), 202(100), 178(56); Calculated mass: 348.1362, found: 348.1365.

Analysis Calculated for $C_{22}H_{20}O_4$: C, 75.84; H, 5.79, found: C, 75.71; H, 5.70.

The structure of diester **21** was also supported by X-ray crystallo-

graphic analysis.

Di-1-propyl-9,10-dihydro-9,10-ethenoanthracene-11,12-dicarboxylate(22).

The procedure used for the preparation of the diethyl ester **21** was applied to 2 g of **18** (6.25 mmol), 100 ml of 1-propyl alcohol and 1 ml of concentrated H_2SO_4. The reaction time was 5 days and the yield after column chromatography (silica gel, petroleum ether (bp = 35-60°C):ethyl acetate-96:4) was 1.6 g (4.26 mmol, 68%). Crystallization from ethanol gave prisms with mp = 72°C.

^1H NMR ($CDCl_3$, 300 MHz) δ 7.40-6.95 (8H, m, Ar-H), 5.47 (2H, s, bridgehead-H), 4.15 (4H, t, 7Hz, $-CH_2-CH_2CH_3$), 1.68 (4H, m, $-CH_2-CH_2-CH_3$), 0.94 (6H, t, 7Hz, $-CH_2-CH_2-CH_3$).

IR (KBr) 1730, 1705 (2 C=O), 1640 (E-C=C-E), 1280 (C-O) cm^{-1}.

MS m/e (rel. intensity) 376 (M^+, 38), 288 (100), 202 (100), 178 (61); Calculated mass: 376.1675, found: 376.1685.

Analysis calculated for $C_{24}H_{24}O_4$: C, 76.57; H, 6.43, found: C, 76.37; H, 6.37 .

The structure of diester **22** was also confirmed by X-ray crystallographic analysis.

Di-2-propyl-9,10-dihydro-9,10-ethenoanthracene-11,12-dicarboxylate (23).

The procedure used for the preparation of the diester **21** was applied to 5 g (15.6 mmol) of **18**, 200 ml of 2-propanol and 2 ml of concentrated H_2SO_4. The reaction time was 10 days. The yield after chromatography

(silica gel, petroleum ether (bp = 35=-60°C):ethyl acetate- 95:5) was 4.9 g (13.1 mmol, 84%). Crystallization from cyclohexane gave prisms of two different crystallographic modifications with indistinguishable morphologies but considerably different solid state IR and CPMAS ^{13}C NMR spectra. Selective crystallization was possible from ethanol and the melt to give crystals with space groups determined as Pbca and $P2_12_12_1$ respectively. No difference could be found in their melting points of 145-146°C.

^1H NMR ($CDCl_3$, 300 MHz) δ 7.4-6.9 (8H, m, Ar-H), 5.7 (2H, s, bridgehead-H), 5.1 (2H, hept, J=6Hz, $-CH(CH_3)_2$), 1.28 (12H, d, 6Hz, $-CH(CH_3)_2$)

^{13}C NMR ($CDCl_3$, 75.4 MHz) δ 164.74 (C=O), 146.24, 146.73, 125.03, 123.43 (Ar-C and vinylic-C), 68.85 ($-OC(CH_3)_2$), 52.26 (bridgehead-C), 21.42 ($-OC(CH_3)_2$).

CPMAS ^{13}C NMR (45 MHz): $P2_12_12_1$: δ 165.79, 163.63, 151.66, 144,86, 143.24, 141.84, 127.06, 125.02, 122.75, 69.47, 68.71, 54.26, 51.67, 23.08, 21.90, 20.82, 19.09; Pbca: δ 166.87, 163.63, 148.96, 146.80, 145.94, 144.11, 143.35, 142.71, 127.50, 125.23, 123.83, 122.86, 69.90,68.49, 54.04, 51.88, 22.54, 21.90, 18.66.

IR (KBr, see figure 38) ($P2_12_12_1$): 1724,1704 (2 C=O), 1636 (E-C=C-E), 1270 (C-O); Pbca: 1720 (2 C=O), 1640 (E-C=C-E), 1262 (C-O) cm^{-1}.

MS m/e (rel. intensity) 376 (M^+, 41), 247 (100), 202 (100), 178 (72); Calculated mass: 376.1675, found: 376.1668.

Analysis calculated for $C_{24}H_{24}O_4$: C, 76.57; H, 6.43, found: C, 76.62; H, 6.38.

The structure of Diester **23** was also confirmed by X-ray crystallographic analysis.

Di-[(R,S)-2-butyl]-9,10-dihydro-9,10-ethenoanthracene-11,12-dicarboxylate (24).

The procedure used for the preparation of the diester **21** was modified by using (R,S)-2-butanol and a refluxing time of 6 days. The yield obtained was 72% and upon crystallization from ethanol slightly opaque prisms were obtained with mp = 95-96°C.

^{1}H NMR ($CDCl_3$, 300 MHz) δ 7.45-6.98 (8H, m, Ar-H), 5.42 (2H, s, bridgehead-H), 4.95 (2H, m, -CH(CH_3)CH_2CH_3), 1.62 (4H, m, -CH(CH_3)CH_2CH_3), 1.26 (6H, d, 7Hz, CH(CH_3)CH_2CH_3), 0.95 (6H, t, 7Hz, CH(CH_3)CH_2CH_3).

IR (KBr) 1724, 1699 (2 C=O), 1634 (E-C=C-E), 1266 (C-O) cm^{-1}.

MS m/e (rel. intensity) 404 (M^+, 23), 248 (91), 202 (93), 178 (55), 57 (100).

Analysis calculated for $C_{26}H_{28}O_4$: C, 77.20; H, 6.98, found: C, 77.00; H, 6.84.

Di-(R,S)-2-octyl-9,10-dihydro-9,10-ethenoanthracene-11,12-dicarboxylate (25).

The procedure used for the preparation of the diester **21** was modified by using (R,S)-2-octanol. After a reflux time of 24 h and normal workup procedure and chromatographic separation, compound **25** was obtained in 69 % yield as an oil at room temperature.

^{1}H NMR ($CDCl_3$, 300 MHz) δ 7.41-7.33 (4H, m, Ar-H), 5.44 (2H, s, bridgehead-H), 5.00 (2H, m, -CH(CH_3)R), 1.70-1.20 (H, m), 1.12 (6H, d, 7Hz, -CH(CH_3)R), 0.90 (9H, m).

IR (neat) 1730, 1700 (2 C=O), 1630 (E-C=C-E), 1255 (C-O) cm^{-1}.

MS m/e (rel. intensity) 516 (M^+, 12), 248 (100), 202 (53), 178 (34); Calculated mass: 516.3240, found: 516.3239.

Di-[(l)-(-)-menthyl]-9,10-dihydro-9,10-ethenoanthracene-11,12-dicarboxylate (26).

(a) Preparation of di-(l)-(-)-menthyl-2-butyne-1,4-dicarboxylate (27).[57]

A mixture of 1 g (8.8 mmol) of 2-butyne-1,4-dicarboxylic acid and 5 g (32.1 mmol) of (l)-(-)-menthol were heated together in a reflux apparatus by using an oil bath at 150°C. The formation of the product was monitored by tlc (silica gel, petroleum ether (bp = 35-60°C):ethyl acetate,19:1). After 24 h the reaction mixture was allowed to cool to room temperature, dissolved in 50 ml of diethyl ether and washed with 5% aq $NaHCO_3$ (2 x 50 ml) and pure water (1 x 50 ml). The resulting product was purified by column chromatography (same conditions as in tlc above) to yield 2.75 g (7.05 mmol, 80% yield) of pure **27**. Recrystallization from ethanol gave prisms with mp = 134-5°C (lit.[57] mp = 135-6°C).

^1H NMR ($CDCl_3$, 400 MHz) δ 4.84 (2H, td, J=6.5 and J=4Hz), 2.02 (2H, m), 1.90 (2H, qd, J=7 and J=4Hz), 1.69 (2H, m), 1.45 (2H, m), 1.05 (2H, m), 0.92 (6H, d, J=6.5Hz), 0.90 (3H, d, J=7Hz), 0.76 (3H, d, J=6.5Hz).

^{13}C NMR ($CDCl_3$, 100 MHz) δ 151 (2 C=O), 77.0 (C≡C), 74.4, 46.4, 40.1, 33.6, 31.0, 25.7, 22.9, 21.5, 20.3 and 15.7 (aliphatic menthyl carbons)

IR (KBr) 1713 (C=O), 1258 (C-O) cm^{-1}.

MS m/e (rel. intensity) No molecular ion at 390, 375 (0.35), 347 (0.30), 206 (3.79), 138 (97), 95 (100).

Analysis calculated for $C_{24}H_{38}O_4$: C, 73.81; H, 9.81, found: C, 73.81; H, 9.75.

(b) Diels-Alder Reaction Between Acetylene Diester 27 and Anthracene to Yield Dibenzobarrelene 26.

Compound **26** was prepared in a similar manner as the diester **18**. Purification was carried out by column chromatography (silica gel, petroleum ether (bp = 35-60°C)-ethyl acetate, 95:5). Fine small plates with mp = 168°C were obtained by crystallization from several solvents including ethanol. The identification of **26** followed from its spectral properties.

^{1}H NMR ($CDCl_3$, 300 MHz) δ 7.40-6.95 (8H, m, Ar-H), 5.40 (2H, s, bridgehead-H), 4.78 (2H, td, J=10Hz and J=4.8 Hz, menthyl methine), 2.15-0.75 (18H, m, menthyl-H).

IR (KBr) 1723, 1698 (2 C=O), 1638 (E-C=C-E), 1272, 1255 (2 C-O) cm^{-1}.

MS m/e (rel. intensity): 568 (M^+, 1), 248 (100), 203 (18), 178 (14). Calculated Mass: 568.3554, found: 568.3560.

<u>11-Ethyl-12-methyl-9,10-dihydro-9,10-ethenoanthracene-11-12-dicarboxylate (28).</u>

Four grams of diester **18** (12.5 mmol) were dissolved in 100 ml of freshly distilled ethanol and 1 ml of concentrated sulfuric acid was added. The mixture was refluxed and the formation of products monitored by tlc (silica gel, petroleum ether (bp = 35-60°C):ethyl acetate, 19:1). When

the two spots attributed to the expected products (larger reference factor than **18**) reached the same intensity as the spot of the starting material, the reaction was stopped (48 h). The ethanol volume was reduced to about 20 ml by evaporation in vacuo and 150 ml of diethyl ether were added. The reaction mixture was washed successively with water (2 x 100 ml), saturated $NaHCO_3$ (2 x 100 ml) and water again. The organic fraction was dried over anhydrous Na_2SO_4 and then evaporated to dryness. The three components found in the crude reaction mixture were separated by column chromatography using the same conditions employed in the tlc analysis. The separation was poor and required up to three passes to isolate 0.76 g of diester **28**, the compound with intermediate polarity. Recrystallization from ethanol yielded prisms with mp = 104-106°C.

^{1}H NMR ($CDCl_3$, 300 MHz) δ 7.41-6.98 (8H, m, Ar-H), 5.50, 5.48 (2H, 2s, bridgehead-H), 4.31 (2H, q, J=7.2Hz, $CO_2CH_2CH_3$), 3.78 (3H, s, CO_2CH_3), 1.27 (3H, t, J=7.2Hz, $CO_2CH_2CH_3$).

IR (KBr) 1728, 1703 (2 C=O), 1639 (E-C=C-E'), 1269 (C-O) cm^{-1}.

MS m/e (rel. intensity) 334 (M^+, 38), 274 (52), 260 (47), 202 (100), 178 (48). Calculated mass: 334.1205, found: 334.1208

Analysis calculated for $C_{21}H_{18}O_4$: C, 75.43; H, 5.43, found: C, 75.31; H, 5.35.

11-Methyl-12-(1-propyl)-9,10-ethenoanthracene-11,12-dicarboxylate (29).

A solution of 2 g (7.3 mmol) of the anhydride **20** and 50 ml of methanol contained in a 100 ml round bottom flask was refluxed for 2 h. The excess alcohol was evaporated in vacuo and the flask containing the resulting

acid was attached to a reflux apparatus. The solid was re-dissolved upon addition of a mixture of 20 ml of dry CH_2Cl_2 and 2 ml of oxalyl chloride causing instantaneous evolution of gaseous HCl. The solution was refluxed for 1 h after the bubbling had stopped and then the solvent was evaporated in vacuo to yield a viscous oil. This was refluxed for 2 h after addition of 20 ml of 1-propanol that had been freshly distilled over CaH_2. After this time the expected product (**29**) was obtained as a yellow viscous oil. Purification by column chromatography (silica gel, petroleum ether (bp = 35-60°C):ethyl acetate, 19:1) gave 2.27 g (6.6 mmol, 91% yield) of (**29**) as a white solid. Crystallization from ethanol gave colorless needles.

mp = 103-4°C.

^{1}H NMR ($CDCl_3$, 300 MHz) δ 7.43-7.02 (8H, m Ar-H), 5.56 and 5.52 (2H, 2s, bridgehead-H), 4.18 (2H, t, J=7Hz, $-CO_2CH_2CH_2CH_3$), 3.80 (3H, s, $-CO_2CH_3$), 1.70 (2H, m, $-CO_2CH_2CH_2CH_3$), 0.97 (3H, t, J=7Hz, $-CO_2CH_2CH_2CH_3$).

IR (KBr) 1737, 1720 (2 C=O), 1645 (E-C=C-E'), 1273 (C-O) cm^{-1}.

MS m/e (rel. intensity) 348 (M^+, 39), 288 (43), 261 (37), 202 (100), 178 (45).

Analysis Calculated for $C_{22}H_{20}O_4$: C, 75.84; H, 5.79, found: C, 75.59; H, 5.74 .

11-Methyl-12-(2-Propyl)-9,10-ethenoanthracene-11,12-dicarboxylate (30).

The procedure used to prepare **28** was modified by using 5 g (14.6 mmol) of diester **1**, 200 ml of freshly distilled 2-propanol and allowing a reaction time of 48 h. Similar workup and purification procedure yielded 1.8 g of pure **13**. Crystallization from ethanol gave needles with mp =

124-5°C.

^{1}H NMR ($CDCl_3$, 80 MHz) δ 7.40-6.90 (8H, m, Ar-H), 5,95 and 5.90 (2H, 2s, bridgehead-H), 5.1 (1H, hept, J=6Hz, $-CO_2CH(CH_3)_2$), 3.7 (3H, s, $-CO_2CH_3$), 1.2 (6H, d, J=6Hz, $-CO_2CH(CH_3)_2$).

IR (KBr) 1729, 1701 (2C=O), 1633 (E-C=C-E'), 1264 (C-O) cm^{-1}.

MS m/e (rel. intensity) 348 (M^+, 15.8), 202 (100), 178 (64.8).

Analysis calculated for $C_{22}H_{20}O_4$: C, 75.84; H, 5.79, found: C, 75.61; H, 5.70 .

The structure of compound **30** was also confirmed by X-ray crystallographic analysis.

<u>11-(2-Butyl)-12-methyl-9,10-dihydro-9,10-ethenoanthracene-11,12-dicarboxylate (31).</u>

a) Racemic.

The procedure used to prepare **28** was modified by using 5 g (14.6 mmol) of **18**, 200 ml of (R,S)-2-butanol and allowing a reaction time of 56 h. Similar workup and purification yielded 1.2 g (3.3 mmol, 23% yield) of **31**. Crystallization from ethanol gave colorless needles.

mp = 94-95°C.

^{1}H NMR ($CDCl_3$, 400 MHz) δ 7.40-6.90 (8H, m, Ar-H), 5.45 (2H, s, bridgehead-H), 4.95 (1H, m, $-CO_2CH(CH_3)CH_2CH_3$), 3.76 (3H, s, CO_2CH_3), 1.58 (2H, m, $CO_2CH(CH_3)CH_2CH_3$), 1.24 (3H, d, J=7Hz, $CO_2CH(CH_3)CH_2CH_3$), 0.91 (3H, t, J=7Hz, $CO_2CH(CH_3)CH_2CH_3$).

IR (KBr) 1729, 1703 (2 C=O), 1633 (E-C=C-E'), 1254 (C-O) cm^{-1}.

MS m/e (rel. intensity) 362 (M^+, 27), 306 (33), 202 (100), 178 (89).

Calculated mass: 362.1518, found: 362.1519.

b) Optically pure.

The procedure used for the preparation of **29** was modified by using (S)-(+)-2-butanol instead of 1-propanol. The yield after chromatographic purification was 43%. Crystallization from ethanol gave needles with mp = 91-92°C. The spectroscopic and analytical data of **(+)-31** resulted identical in all respects to that of **(±)-31**. The solid state IR spectra showed only minimal differences. The optical rotation was $[\alpha]_D$ = 16.6° ($CHCl_3$, c=0.3).

<u>11-(1,1-Dimethyl-1-ethyl)-12-methyl-9,10-dihydro-9,10-ethenoanthracene-11-12-dicarboxylate (32).</u>

The procedure used to prepare the diester **29** was modified by using 1,1-dimethyl-1-ethanol (tert-butanol) instead of 1-propanol. The yield after chromatographic purification was 67%. Crystallization from ethanol and many other solvents gave very fine plates with mp = 128-129°C.

^1H NMR ($CDCl_3$, 80 MHz) δ 7.45-6.85 (8H, m, Ar-H), 5.45 and 5.40 (2H, 2s, bridgehead-H), 3.75 (3H, s, $-CO_2CH_3$), 1.45 (12H, s, $-CO_2C(CH_3)_4$).

IR (KBr) 1740, 1698 (2 C=O), 1635 (E-C=C-E'), 1111 (C-O) cm^{-1}.

MS m/e (rel. intensity) 362 (M^+, 9), 306 (34), 262 (45), 202 (100), 178 (43).

Analysis calculated for $C_{23}H_{22}O_4$: C, 76.22; H, 6.12, found: C, 76.06; H, 6.26 .

11-Methyl-12-(1-pentyl)-9,10-dihydro-9,10-ethenoanthracene-11-12-dicarboxylate (33).

The procedure used to prepare the diester **29** was modified by using 1-pentanol instead of 1-propanol. Compound **33** is a viscous oil at room temperature.

^1H NMR ($CDCl_3$, 300 MHz) δ 7.42-6.98 (8H, m, Ar-H), 5.51 and 5.47 (2H, 2s, bridgehead-H), 4.18 (2H, t, J=6.8Hz, $-CO_2CH_2(CH_2)_3CH_3$), 3.78 (3H, s, $-CO_2CH_3$), 1.70-1.20 (6H, m, $-CO_2CH_2(CH_2)_3CH_3$), 0.92 (3H, t, J=7Hz, $-CO_2CH_2(CH_2)_3CH_3$).

IR (neat) 1714 (2 C=O), 1635 (E-C=C-E'), 1266, 1214 (C-O) cm^{-1}.

MS m/e (rel. intensity) 376 (M^+, 54), 316 (53), 260 (57), 202 (100), 178 (47).

Analysis Calculated for $C_{24}H_{24}O_4$: C, 76.57; H, 6.43, found: C, 76.39; H, 6.36 .

11-[(S)-(-)-2-Methyl-1-butyl]-12-methyl-9,10-dihydro-9,10-etheno anthracene-11-12-dicarboxylate (34).

The procedure used to prepare **29** was modified by using (S)-(-)-2-methyl-1-butanol (Aldrich) instead of 1-propanol. The yield after chromatographic purification was 69%. Crystallization occurred spontaneously after ~12 months and recrystallization from ethanol-ether yielded very fine plates.

mp = 63-65°C.

^1H NMR ($CDCl_3$, 300 MHz) δ 7.45-7.00 (8H, m, Ar-H), 5.51, 5.46 (2H, 2s, bridgehead-H), 4.04 (2H, m, $-CO_2CH_2CH(CH_3)CH_2CH_3$), 3.79 (3H, s,

$-CO_2(CH_3)$), 1.75 (1H, m, $-CO_2CH_2CH(CH_3)CH_2CH_3$), 1.4-1.1 (2H, m, $-CO_2CH_2CH(CH_3)CH_2CH_3$), 0.95 (3H, d, J=7.5Hz, $-CO_2CH_2CH(CH_3)CH_2CH_3$), 0.91 (3H, t, J=7.5Hz, $-CO_2CH_2CH(CH_3)CH_2CH_3$).

IR (KBr) 1731, 1703 (2 C=O), 1633 (E-C=C-E'), 1263 (C-O) cm^{-1}.

MS m/e (rel. intensity) 376 (M^+, 32), 316 (32), 260 (60), 202 (100), 178 (61).

Analysis calculated for $C_{24}H_{24}O_4$: C, 76.57; H, 6.43, found: C, 76.35; H, 6.61 .

11-(2,2-Dimethyl-1-propyl)-12-methyl-9,10-dihydro-9,10-ethenoanthracene-11-12-dicarboxylate (35).

The procedure used to prepare **29** was modified by using 2,2-dimethyl-1-propanol instead of 1-propanol. Crystallization occurred spontaneously after ~20 months. Recrystallization from ethanol-diethyl ether gave an apparently amorphous solid with mp = 75-80°C.

^1H NMR ($CDCl_3$, 400 MHz) δ 7.40-6.90 (8H, m, Ar-H), 5.43, 5.42 (2H, 2s, bridgehead-H), 3.77 (3H, s, $-CO_2CH_3$), 1.80 (2H, q, 7Hz, $-CO_2C(CH_3)_2CH_2CH_3$), 1.45 (6H, s, $-CO_2C(CH_3)_2CH_2CH_3$), 0.86 (3H, t, J=7Hz, $-CO_2C(CH_3)_2CH_2CH_3$).

IR (KBr) 1737, 1703 (2 C=O), 1635 (E-C=C-E'), 1269 (C-O) cm^{-1}.

MS m/e (rel. intensity) 376 (M^+, 32), 344 (7), 316 (32), 306 (17), 260 (60), 202 (100), 178 (61). Calculated mass: 376.1675, found: 376.1684.

11-[(1)-(-)-Menthyl]-12-methyl-9,10-dihydro-9,10-ethenoanthracene-11-12-dicarboxylate (36).

The procedure used to prepare **28** was modified by using 0.30 g (0.5 mmol) of the diester **26**, 50 ml of freshly distilled methanol and allowing a reaction time of 30 h. Similar work up and chromatographic separation gave 0.10 g (0.23 mmol, 46% yield) of pure **19** obtained as a viscous oil.

^{1}H NMR ($CDCl_3$, 300 MHz) δ 7.40-6.90 (8H, m, Ar-H), 5.48 and 5.41 (2H, 2s, bridgehead-H), 4.70 (1H, td, J=10, J=4.5Hz, -CO_2CH-menthyl), 3.72 (3H, s, -CO_2CH_3), 2.1-0.75 (18 H, m, menthyl group).

IR (neat) : 1716 (2 C=O), 1635 (E-C=C-E), 1260 (C-O) cm^{-1}.

MS m/e (rel. intensity): 444 (M^+, 8), 412 (1), 306 (55), 262 (100), 202 (86), 178 (48). Calculated mass: 444.2302, found: 444.2299.

<u>11-Phenyl-12-methyl-9,10-dihydro-9,10-ethenoanthracene-11,12-dicarboxylate 37.</u>

The procedure used to prepare **29** was modified by using a 20% molar of excess of phenol dissolved in benzene instead of using neat 1-propanol. Crystallization from acetonitrile gave needles with mp = 180-1°C.

^{1}H NMR ($CDCl_3$, 300 MHz) δ 7.50-7.00 (13H, m. Ar-H), 5.65 (2H, s, bridgehead-H), 3.70 (3H, s, -CO_2CH_3).

IR (KBr) 1720 (C=O), 1625 or 1590 (E-C=C-E'), 1270, (C-O) cm^{-1}.

MS m/e (rel. intensity) 382 ($M,^+$ 4), 350 (5), 289 (88), 261 (100), 202 (36), 178 (40).

Analysis calculated for $C_{25}H_{18}O_4$: C, 78.52; H, 4.74, found: C, 79.31; H, 4.82.

The structure of diester **37** was also confirmed by X-ray crystallographic studies.

11-Ethyl-12-(2-propyl)-9,10-dihydro-9,10-ethenoanthracene-11,12-dicarboxylate (38).

The procedure used to prepare **29** was modified by using 5 g (13.3 mmol) of diester **23**, 200 ml of ethanol and allowing a reaction time of 60 h. Similar work up and purification procedures gave 1.05 g (2.9 mmol, 22% yield) of pure **38**. Crystallization from ethanol gave prisms.

mp = 104-105°C.

^{1}H NMR ($CDCl_3$, 300 MHz) δ 7.40-6.90 (8H, m, Ar-H), 5.47 and 5.45 (2H, 2s, bridgehead-H), 5.09 (1H, hept, J=7.3Hz, $-CO_2CH(CH_3)_2$), 4.23 (2H, q, J=7.1 Hz, $-CO_2CH_2CH_3$), 1.28 (3H, t, J=7.1 Hz, $-CO_2CH_2CH_3$), 1.26 (6H, d, J=7.3 Hz, $-CO_2CH(CH_3)_2$).

IR (KBr) 1699 (2 C=O), 1627 (E-C=C-E'), 1274 (C-O) cm^{-1}.

MS m/e (rel. intensity) 362 (M^+, 35), 274 (61), 202 (100), 178 (51).

Analysis calculated for $C_{23}H_{22}O_4$: C, 76.22; H, 6.12, found: C, 76.36; H, 6.21 .

11-Ethyl-12-[(S)-(+)-2-butyl]-9,10-ethenoanthracene-11,12-dicarboxylate (39).

The procedure used to prepare **29** was modified by using ethanol and (S)-(+)-2-butanol instead of methanol and 1-propanol respectively. Crystallization from ethanol gave colorless needles.

mp = 72-73°C.

^{1}H NMR ($CDCl_3$, 300 MHz) δ 7.43-6.90 (8H, m, Ar-H), 5.49 and 5.48 (2H, 2s, bridgehead-H), 4.97 (1H, m, $-CO_2CH(CH_3)CH_2CH_3$), 4.26 (2H, q, J=7Hz,

$-CO_2CH_2CH_3$), 1.61 (2H, m, $-CO_2CH(CH_3)CH_2CH_3$), 1.27 (6H, 2t, $-CO_2CH_2CH_3$ and $-CO_2CH(CH_3)CH_2CH_3$), 0.94 (3H, t, J=7Hz, $-CO_2CH(CH_3)CH_2CH_3$).

IR (KBr) 1740, 1730 and 1715 (2 C=O), 1640 (E-C=C-E'), 1273 (C-O) cm^{-1}.

MS m/e (rel. intensity) 376 (M^+, 28), 274 (63), 247 (48), 202 (100), 178 (48).

Analysis Calculated. for $C_{24}H_{24}O_4$: C, 76.57; H, 6.43, found: C, 76.36; H, 6.38.

<u>(2-Propyl)-9,10-ethenoanthracene-11-carboxylate-12-carboxylic acid (41).</u>

A suspension of 5 g (18.2 mmol) of the anhydride **20** in 50 ml of 2-propanol (freshly distilled over CaH_2) was refluxed for two hours after which it completely dissolved. The reflux was continued for a three additional hours. The excess alcohol was evaporated <u>in vacuo</u> and the resulting solid was recrystallized from an acetonitrile-petroleum ether (bp = 35-60°C) mixture to yield 6.05 g (99% yield) of plate-like crystals.

mp = 176-177°C.

^1H NMR ($CDCl_3$, 300 MHz) δ 7.50-6.90 (8H, m Ar-H), 6.15 and 5.78 (2H, 2s, bridgehead-H), 5.20 (1H, hep, J=7Hz, $-CO_2CH_2(CH_3)_2$), 1.4 (6H, d, J=7Hz, $-CO_2CH_2(CH_3)_2$)

IR (KBr) 3400-2200 ($R-CO_2-H$), 1724 (R-C(OH)=O), 1680 (R-C(OR)=O), 1626 (E-C=-E'), 1202 (C-O) cm^{-1}.

MS m/e (rel. intensity) 334 (M^+, 1), 290 (21), 203 (100), 178 (41); Calculated mass: 334.1205, found: 334.1204.

Analysis Calculated for $C_{21}H_{18}O_4$: C, 75.43; H, 5.43, found: C, 73.19;

H, 5.40.

[(R,S)-2-Butyl]-9,10-ethenoanthracene-11-carboxylate-12-carboxylic acid (40).

The procedure used to prepare the monoacid **41** was modified by using 0.65 g (3.37 mmol) of the anhydride **20** and 20 ml of (R,S)-2-butanol. The product was purified by column chromatography (silica gel, acetone:$CHCl_3$, 1:1) to yield a viscous oil in 32% yield.

^1H NMR (CD_3CN, 80 MHz) δ 10.0 (1H, s, $-CO_2H$), 7.5-6.9 (8H, m Ar-H), 5.8 and 5.7 (2H, 2s, bridgehead-H), 5.0 (1H, m, $-CO_2CH(CH_3)CH_2CH_3$), 1.6 (2H, m, $-CO_2CH(CH_3)CH_2CH_3$), 1.3 (3H, d, J=7Hz, $-CO_2CH(CH_3)CH_2CH_3$), 0.95 (3H, t, J=7Hz, $-CO_2CH(CH_3)CH_2CH_3$).

IR (neat) 3420-2300 ($R-CO_2-H$), 1730 (R-C(OH)=O), 1700 (R-C(OR)=O), 1640 (E-C=C-E') cm^{-1}.

MS m/e (rel. intensity) 348 (M^+, 9), 304 (15), 248 (67), 203 (100), 178 (40); Calculated mass: 326.1362 found: 326.1363.

11-(2-Butyl)-12-(2-propyl)-9,10-ethenoanthracene-11,12-dicarboxylate (42).

a) Racemic:

A solution containing 2 g (5.99 mmol) of the acid **40**, 20 ml of dry CH_2Cl_2 and 5 ml of oxalyl chloride was placed in a reflux apparatus. The solution was refluxed for 4 h total and the solvent was evaporated *in vacuo* to yield a viscous oil which was assumed to be the corresponding acyl chloride. This was immediately refluxed for two hours after addition

of 20 ml of freshly distilled (R,S)-2-butanol. Rotatory evaporation of the unreacted alcohol gave the desired product (42) as a yellow viscous oil. Purification by column chromatography (silica gel, petroleum ether (bp = 35-60°C):ethyl acetate, 19:1) gave 2.27 g (5.81 mmol, 97% yield) of (42) as a white solid. Crystallization from ethanol gave colorless prisms.

mp = 122-4°C.

^{1}H NMR ($CDCl_3$, 300 MHz) δ 7.4-7.0 (8H, m Ar-H), 5.43 and 5.41 (2H, 2s, bridgehead-H), 5.06 (1H, hep, J=7Hz, $-CO_2CH(CH_3)2$), 4.88 (1H, m, $-CO_2CH(CH_3)CH_2CH_3$), 1.6 (2H, m, $-CO_2CH(CH_3)CH_2CH_3$), 1.25 (9H, 2d, $-CO_2CH(CH_3)CH_2CH_3$ and $-CO_2CH(CH_3)_2$, 0.97 (3H, t, J=7Hz, $-CO_2CH(CH_3)CH_2CH_3$).

IR (KBr) 1724, 1703 (2 C=O), 1636 (E-C=C-E'), 1220 (C-O) cm^{-1}.

MS m/e (rel. intensity) 390 (M^+, 19), 247 (95), 202 (100), 178 (70). Calculated mass: 390.1831, found: 390.1831.

Analysis Calculated for $C_{25}H_{26}O_4$: C, 76.90; H, 6.71, found: C, 76.98; H, 6.74 .

b) Optically active:

The procedure used to prepare racemic 42 was modified by using optically pure (S)-(+)-2-butanol. The chemical yield and the spectroscopic and analytical data of this material were very similar to those from the racemate. Crystallization from ethanol gave prisms with mp = 133-5°C. The solid state FTIR spectra of the optically active sample and the racemate are shown in Figure 80. The optical activity of this compound was measured in chloroform: $[\alpha]_D$ = 11.0° ($CHCl_3$, c = 0.05).

Diels-Alder Reaction Between (2-Propyl)-9-anthracenecarboxylate and Methyl-2-propyne-1-carboxylate (Methyl Propiolate).

(a) Preparation of (2-Propyl)-9-anthracenecarboxylate (43).[60]

A suspension of 1.019 g (4.59 mmol) of 9-anthracenecarboxylic acid in 10 ml of $CHCl_3$ and 1 ml of oxalyl chloride was refluxed for 2 h after which the solid completely dissolved and the initially vigorous evolution of CO_2 had stopped. The solvent and excess oxalyl chloride were evaporated *in vacuo* to yield a yellow solid assumed to be the corresponding acyl chloride. The flask was then re-attached to the reflux system and 3 ml of freshly distilled 2-propanol were added dissolved in 10 ml of $CHCl_3$. The solid dissolved and started to evolve HCl gas instantaneously. The reflux was initiated and maintained until 1 h after the gas evolution had stopped. After this time (3 h) the resulting solution was evaporated to dryness, dissolved in diethyl ether and washed successively with water, saturated $NaHCO_3$ and water. Evaporation of the ethereal solution gave 1.132 g (4.29 mmol, 93% yield) of a yellow solid which after crystallization from diethyl ether-hexane mixtures gave yellow prisms with mp = 92-3°C (lit[60] mp = 93-4°C)

^1H NMR ($CDCl_3$, 300 MHz) δ 8.50 (1H, s, H-10), 8.10-7.45 (8H, m, Ar-H), 5.64 (1H, hept, J=7Hz, $CO_2CH(CH_3)_2$), 1.53 (6H, d, J=7Hz, $CO_2CH(CH_3)_2$).

IR (KBr) 1718 (C=O), 1215 (C-O) cm^{-1}.

MS m/e (rel. intensity) 264 (M^+, 66), 222 (100), 205 (41), 177 (28).

Analysis Calculated for $C_{18}H_{16}O_4$: C, 81.79; H, 6.10, found: C, 81.50; H, 6.10 .

(b) Diels-Alder Reaction:

A Carius tube containing 1.33 g (5.04 mmol) of (2-propyl)-9-anthracenecarboxylate (from **(a)**) and 0.25 ml (6.3 mmol) of methyl propiolate was sealed and heated in an oven at 190°C for 4 h. The components of the resulting brown viscous oil were separated by column chromatography (silica gel, petroleum ether (bp = 35-60°C)-ethyl acetate 95:5). After the first fractions containing 0.040 g of the unreacted anthracene derivative, two Diels-Alder addition products were obtained without elution overlap. The first was obtained in 1.134 g (3.32 mmol, 66% yield) and was crystallized from ethanol as thin colorless plates with mp = 102-103°C. The second product, obtained in 0.403 g (1.18 mmol, 23.4% yield) was crystallized also from ethanol as prisms with a mp = 165-166°C. The stereoisomeric nature of the expected Diels-Alder addition products was supported by MS analysis, but their identification was primarily based on the ^1H NMR coupling difference between the H_{10}-H_{11} (1,3 coupling, J = 2.1Hz) and the H_{10}-H_{12} (1,2 coupling, J = 15Hz) protons (see Figure 24, page 48).

a) Major Product.

<u>9-(2-Propyl)-12-methyl-9,10-dihydro-9,10-ethenoanthracene-9,12 dicarboxylate (44).</u>

^1H NMR ($CDCl_3$, 300 MHz) δ 8.15 (1H, d, J=2.1Hz, H-10), 7.5-6.98 (8H, m, Ar-H), 5.63 [1H, d, J=2.1Hz, H(11)], 5.59 (1H, hept, J=6Hz, $-CH(CH_3)_2$), 3.76 (3H, s, CO_2CH_3), 1.55 (6H, d, J=6Hz, $-CH(CH_3)_2$).

IR (KBr) 1727, 1709 (2 C=O), 1623 (E-C=C-H), 1228, 1216 (2 C-O) cm^{-1}.

MS m/e (rel. intensity) 348 (M^+, 49), 306 (23), 260 (60), 202 (100).

Analysis Calculated for $C_{22}H_{20}O_4$: C, 75.84; H, 5.79, found: C, 75.86; H, 5.90 .

The structure of diester 44 was also supported by X-ray crystallographic analysis.

b) Minor Product.

<u>9-(2-Propyl)-11-methyl-9,10-dihydro-9,10-ethenoanthracene-9,12-dicarboxylate (45).</u>

^{1}H NMR ($CDCl_3$, 300 MHz) δ 7.90 (2H, m, Ar-H), 7.71 (1H, d, J=8Hz, H-10), 7.29 (2H, m, Ar-H), 7.03 (4H, m, Ar-H), 5.46 (1H, hept, J=7Hz, $-CH(CH_3)_2$), 5.14 [1H, d, J=8Hz, H(12)], 3.70 (3H, s, CO_2CH_3), 1.42 (6H, d, J=7Hz, $-CH(CH_3)_2$).

IR (KBr) 1736, 1723 (2 C=O), 1616 (E-C=C-H), 1269, 1255 (2 C-O) cm^{-1}.

MS m/e (rel. intensity) 348 (M^+, 32), 288 (18), 261 (26), 233 (27), 202 (100).

Analysis calculated for: $C_{22}H_{20}O_4$: C, 75.84; H, 5.79, found: C, 75.57; H, 5.93 .

The structure of diester 45 was also supported by X-ray crystallographic analysis.

<u>Photochemical Procedures.</u>

General.

Photolyses for analytical purposes were carried out with a Molectron UV 22 Nitrogen laser (λ = 337.1 nm, 330 mW average power) and a 450 W medium pressure Hanovia lamp. Solution photolyses were systematically

explored in 0.1 M benzene and acetonitrile, for direct irradiations, and in acetone for triplet sensitization studies. Before irradiation the samples were degassed by several freeze-pump-thaw cycles and sealed with paraffin film under a nitrogen atmosphere. Solid samples were photolyzed in 0.4 ml Pyrex or quartz tubes as single crystals and powders after the air of the containers was exchanged by nitrogen. The photolyzed samples were routinely analyzed by glc, glc-MS and ^{1}H NMR. In some cases solid compounds were also irradiated in KBr matrices prepared in the same manner as for infrared spectroscopy.

For preparative photolysis a sample of 0.2 to 1.0 g of the corresponding compound was dissolved in 250 ml of spectral grade acetone and placed in a 250 ml Pyrex immersion well. The samples were deoxygenated for 30 minutes before irradiation by using a steady flow of nitrogen gas through the stirred solutions. The nitrogen flow was continued during the irradiation, which was performed with the Pyrex filtered output ($\lambda > 290$ nm) of the 450 W medium pressure Hanovia lamp. Samples taken at different intervals were analyzed by glc in order to check for the reaction progress. When there was less then 3% of starting material remaining the irradiation was stopped and the solvent evaporated under reduced pressure. Before attempting any separation or purification treatment, the samples were analyzed by ^{1}H NMR spectroscopy and the results observed were correlated with those obtained by capillary glc. Purification of the products was carried out by column chromatography and recrystallization in the case of solid materials.

Low temperature photolyses were performed by maintaining the sample in a slurry bath prepared with a suitable solvent and liquid nitrogen, or by

using a bath controlled from a Cryocool CC-100-II immersion cooling system from Neslab Instruments Inc. The temperature in either case was maintained within ±1°C and the irradiations were performed with the nitrogen laser.

Photochemical Studies on 11,12-Dimethyl-9,10-dihydro-9,10-etheno-anthracene-11,12-dicarboxylate (18)

Preparative irradiation of **18** (1.0 g) gave a single product. This was obtained as a slightly yellow oil which was purified by chromatography using a short silica gel column and using CH_2Cl_2 as the eluent. Crystallization from ethanol yielded colorless prisms (0.940 mg) which were used for the spectroscopic characterization of:

Dimethyl-4b,8b,8c,8d-tetrahydro-dibenzo[a,f]cyclopropa[cd]pentalene-8c,8d-dicarboxylate (52).

mp = 94-95°C (lit.[65] mp = 98-99°C).

^{1}H NMR ($CDCl_3$, 80 MHz) δ 7.4-6.9 (8H, m, Ar-H), 5.05 [1H, s, H(8d)], 4.50 [1H, s, H(4b)], 3.85 [3H, s, $-CO_2CH_3$(8b)], 3.65 [3H, s, $-CO_2CH_3$(8c)].

IR (KBr) 1737, 1717 (2 C=O), 1250 (C-O) cm^{-1}.

MS m/e (rel. intensity) 320 (M^+, 33), 260 (94), 202 (100).

Analytical Solution and Solid State Photolysis.

Single crystals and powders of **18** (typically 2-5 mg per experiment) were exposed at various temperatures to the light from the nitrogen laser (λ = 337.1 nm) and from the Pyrex (λ >290 nm) or quartz (λ > 200 nm)

filtered output of the Hanovia mercury lamp. Irradiations for different lengths of time were first explored and the results compared with those obtained from parallel solution irradiations (Table II, page 54). After the desired irradiation period the appearance of the solids was analyzed under a microscope and the percent conversion determined by glc. A single product, with retention time and mass spectrum identical to the solution product, was observed in all cases.

Preparative Photolysis of 18 in the Solid State.

A sample consisting of 600 mg of polycrystalline **18** in a 5 ml Pyrex test tube was sealed after the air was exchanged by nitrogen gas and irradiated with the Hanovia lamp. The tube was kept in a horizontal position and the sample dispersed over the maximum surface area. The reaction progress was monitored by glc analysis of small samples taken every two hours. The irradiation was stopped at 28% conversion, after which the rate of the reaction had become very slow. The solid was then dissolved and the product enriched to up to 80% by separating some of the starting material by fractional recrystallization in ethanol. ^{1}H NMR and IR spectroscopic analysis of this sample established its identity with the solution product.

Derivatization of 18 to Perform Purification of Photoproduct 52.

Since chromatographic separation of **52** from its starting material was unsuccessful under a variety of conditions employed a derivatization method was devised. This could be achieved easily by treatment of the reaction mixture with ethereal diazomethane:[67]

Addition Product Between 1 and Diazomethane.

An excess of freshly distilled diazomethane was added to 20 ml of an ethereal solution containing a mixture of **18** and **52**. The solution was left overnight in the fume hood. After this time the diazomethane yellow color had disappeared and the solvent was rotatory evaporated to give a clear oil which was chromatographed (silica gel, petroleum ether (bp = 35-60°C):ethyl acetate 19:1). The derivatization product was found to elute first and it was identified as the pyrazoline cycloaddition product **53**. The dibenzosemibullvalene **52** obtained after this treatment was found to be 100% pure by glc.

11,12-Dimethyl-9,10-dihydro-9,10-[3',4']pyrazolidinoanthracene-11,12-dicarboxylate (53).

mp = 153-154 °C (lit.[67] mp = 146-148 °C)

^{1}H NMR ($CDCl_3$, 300MHz) δ 7.6-7.1 (8H, m, Ar-H), 5.4 [1H, s(br), H(9) or H(10)], 4.85 (1H, d, J=18Hz, $-CH_2-N=N-$), 4.55 (1H, d, J=18Hz, $-CH_2-N=N-$), 4.35 [1H, s, H(9) or H(10)], 3.6 (3H, s, $-CO_2CH_3$), 3.47 (3H, s, $-CO_2CH_3$).

IR (KBr) 1747, 1732 (2 C=O) cm^{-1}.

MS m/e (rel. intensity) No M^+ at 376, 334 (3), 302 (12), 274 (38), 215 (95), 178 (100),

Analysis Calculated for $C_{21}H_{18}O_4N_2$: C, 69.60; H, 5.01; N, 7.73, found: C, 69.54; H, 4.98; N, 7.80.

Relative Solid State Quantum Yields of Diester 18.

Relative solid state quantum yields were measured by photolyzing

crystals of 18 in the form of KBr pellets (5% by weight). The homogeneity of the pellets was determined by focussing the infrared laser beam of the FTIR spectrometer on different regions of the pellet and measuring the intensity of a selected absorption band. Pellets showing fluctuations larger than 3% in the intensity readings were discarded. The pellets selected were irradiated at 20°C and 15 cm from the laser aperture. With the laser working at a repetition rate of 20 Hz, irradiations were performed for periods of 30 and 60 seconds and the IR spectrum of the samples was recorded before and after each photolysis. The disappearance of the vinyl diester absorption of the starting material at 1632 cm^{-1} was used to quantify the extent of reaction. After a total irradiation time of 10 minutes, the contents of the pellets were extracted with diethyl ether and water and the organic fraction was analyzed by glc. The final FTIR and glc results were found to agree to 5% or better. The same results were obtained in duplicate runs and are shown as a plot of log (percent product) vs. irradiation time in Figure 29 (page 66).

<u>Photolysis of 9,10-Dihydro-9,10-ethenoanthracene-11,12-dicarboxylic-acid (19).</u>

Compound 19 (1.0 g) was preparatively photolyzed in acetone solution using the procedure described in the General Experimental Section. The reaction progress in this case was monitored by ^{1}H NMR. The product was obtained as a white crystalline solid with prism like morphology. The diacid 54 was also converted into the dimethyl compound 52 by treatment with ethereal diazomethane.

4b,8b,8c,8d-Tetrahydro-dibenzo[a,f]cyclopropa[cd]pentalene-8c,8d-dicarboxylic acid (54).

mp = 235-240 °C (bubbles on melting).

^{1}H NMR (Acetone-d_6, 300 MHz) δ 7.45-7.00 (8H, m, Ar-H), 5.10 [1H, s, H(4b)], 4.45 [1H, s, H(8b)], 4.2-3.5 (2H, s(br), -CO_2H).

IR (KBr) 3400-2300 (CO_2-H), 1700 (C=O) cm^{-1}.

MS m/e (rel. intensity) 292 (M^+, 0.2), 248 (43), 203 (100), 178 (3).

<u>Photochemical Studies on 11,12-Diethyl-9,10-dihydro-9,10-etheno-anthracene-11,12-dicarboxylate (21).</u>

The diester **21** was photolyzed in solution and in the solid state in the same manner as **18**. A single and identical product was obtained in the solution media and in the two solid state modifications. The isolated product was crystallized as small prisms from ethanol and was identified as:

Diethyl-4b,8b,8c,8d-tetrahydro-dibenzo[a,f]cyclopropa[cd]pentalene-8c,8d-dicarboxylate (55).

mp = 78°C.

^{1}H NMR ($CDCl_3$, 300 MHz) δ 7.35-7.0 (8H, m, Ar-H), 5.02 [1H, s, H(8d)], 4.45 [1H, s, H(4b)], 4.32 [2H, m, -$CO_2CH_2CH_3$(8b)], 4.15 [2H, q, J=6.8 Hz, -$CO_2CH_2CH_3$(8c)], 1.32 (3H, t, J=6.8 Hz, -$CO_2CH_2CH_3$), 1.25 (3H, t, 6.8 Hz, -$CO_2CH_2CH_3$).

IR (KBr) 1733, 1719 (2 C=O), 1244 (C-O) cm^{-1}.

MS m/e (rel. intensity) 348 (M^+, 42), 303 (13), 274 (100), 202 (90), 178 (5.1).

Analysis calculated for $C_{22}H_{20}O_4$: C, 75.84; H, 5.79, found: C, 75.71; H, 5.70.

Relative Solid State Quantum Yields Between Dimorphs of Compounds 21.

The quantum yields of the dimorphic diester **21** were measured relative to the quantum yields of diester **18** and **23** (the latter was also studied in two solid state modifications) by photolyzing crystals of the $P2_12_12_1$ and $P2_1/c$ modifications in the form of KBr pellets. The irradiations were carried out in the same manner as for diester **18** and the disappearance of the vinyl diester absorptions of the starting materials at 1640 ($P2_12_12_1$) and 1633 ($P2_1/c$) were used to quantify the extent of reaction. The results obtained are presented in Table IV (page 96).

Stereoselectivity Differences Between the Dimorphic Modifications of 21.

Single Crystals of the $P2_12_12_1$ and $P2_1/c$ modifications of **21** were irradiated at room temperature with the nitrogen laser for 20 min. After photolysis, the crystals were then dissolved in exactly 1.0 ml of $CHCl_3$ and their optical rotation measured along with that of a sample photolyzed in solution. The percent conversion was measured by glc and the specific optical rotations calculated according to the following formula:

$[\alpha]_D = \alpha / Ws \times C$ where: $[\alpha]$ = Specific Rotation

α = Optical Rotation

Ws = Weight of sample in g

C = Fraction of photoproduct (% conversion / 100) determined by glc.

The results from the above measurements are shown in Table V (page 109).

Photolysis of 11,12-Di-(1-propyl)-9,10-dihydro-9,10-ethenoanthracene-11,12-dicarboxylate 22.

Compound **22** was photolyzed in solution and in the solid state in a similar manner as **18** to give:

Di-(1-propyl)-4b,8b,8c,8d-tetrahydro-dibenzo[a,f]cyclopropa[cd]pentalene -8c,8d-dicarboxylate (56).

Compound **56** crystallizes by slow evaporation from ethanol solutions.

mp = 62-75°C.

^{1}H NMR ($CDCl_3$, 300 MHz) δ 7.50-7.00 (8H, m, Ar-H), 5.05 [1H, s, H(4b)], 4.46 [1H, s, H(8d)], 4.15 (4H, m, $-CO_2CH_2CH_2CH_3$), 1.7 (4H, m, $-CO_2CH_2CH_2CH_3$), 0.95 (6H, m, two $-CO_2CH_2CH_2CH_3$).

IR (neat) 1729 (2 C=O), 1244 (C-O).

MS m/e (rel. intensity) 376 (M^+, 21), 316 (13), 288 (100), 247 (33), 202 (91), 178 (6). Calculated mass: 376.1675, found: 376.1673.

Photolysis of 11,12-Di-(2-propyl)-9,10-dihydro-9,10-ethenoanthracene-11,12-dicarboxylate (23).

Compound **23** was photolyzed in solution and in the solid state in a similar manner as **18**. A single product was observed in solution and in the two crystal modifications. This was identified as:

Di-(2-propyl)-4b,8b,8c,8d-tetrahydro-dibenzo[a,f]cyclopropa[cd]-pentalene-8c,8d-dicarboxylate (57).

mp = 111-112°C.

^1H NMR ($CDCl_3$, 300 MHz) 7.4-7.0 (8H, m, Ar-H), 5.20 [1H, m, $-CO_2CH(CH_3)_2$(8d)], 5.0 [1H, s, H(4b)], 5.0 [1H, m, $-CO_2CH(CH_3)_2$(8c)], 1.5-1.2 [12H, m, $-CO_2CH(CH_3)_2$ (8c and 8d)].

^{13}C NMR ($CDCl_3$, 75.4 MHz) 167.80 and 166.73 (2 C=O); 149.67, 149.48, 134.42, 133.48, 127.15, 126.95, 126.29, 126.21, 125.16, 124.86, 120.98 and 120.85 (Aromatic-C); 68.69 and 68.32 (two $-CH(CH_3)_2$); 67.11 [C(8d)]; 57.33 [C(8d)]; 55.14 [C(4b)], 48.30 [C(8b)], 21.33, 21.25 and 21,22 ($-CH(CH_3)_2$).

IR (KBr) 1728, 1712 (2 C=O), 1256, 1236 (2 C-O) cm^{-1}.

MS m/e (rel. intensity) 376 (M^+, 23), 334 (3), 316 (13), 288 (35), 247 (86), 202 (100), 178 (6).

Analysis calculated for $C_{24}H_{24}O_4$: C, 76.57; H, 6.43, found: C, 76.86; H, 6.41 .

Differences in Reactivity Between the two Crystalline Modifications of Compound 23.

The relative quantum yields of the $P2_12_12_1$ and Pbca modifications of **23** were determined in the same manner as for compound **21**. The results are also shown in Table IV.

Differences in stereoselectivity were also explored for dimorphic **23** in a similar manner as for compound **21**. Several experiments were done in order to establish three principal aspects: 1) Generation of optical activity in chiral crystals ($P2_12_12_1$) of **23**, 2) Extent of asymmetric induction and 3) Correlation between the reactant and product absolute

stereochemistry.

1) Generation of Optical Activity in Crystals of Diester iPr/iPr-23.

Crystals of the $P2_12_12_1$ and Pbca modifications of diester **23** were photolyzed and analyzed for the generation of optical activity in the same manner as crystals of diester **21**. Several crystal batches were used as described in the text (Part II of this thesis). The results obtained here are shown in Tables VI-X (pages 112, 122-124 and 126).

2. Determination of the Enantiomeric Excess from Solid State Photolysis of Chiral Crystals of 23.

A sample consisting of 44.1 mg of 65.4% levorotatory **57** was obtained when four of the crystals from batch 2 whose photolysis results are shown in Table VI were combined, and ten fractional crystallizations were carried out from petroleum ether. The enantiomeric composition of the product was not altered by the crystallizations as shown by the specific rotation of the sample ($[\alpha]_D$ = -24°). The enriched sample and one consisting of a photolyzed single crystal (20.9% product, $[\alpha]_D$ = 24.5°, not recrystallized) were then analyzed by ^1H NMR at 300 MHz after successive additions of the chiral shift reagent [3-(heptafluoropropyl hydroxymethylene)-d-camphorato]europium (III), $Eu(hfc)_3$. The enantiomeric resonances of a racemic sample had been previously shown to resolve satisfactorily after addition of 0.2 eq of the chiral lanthanide reagent.

Spectra corresponding to the racemate and optically active samples after addition of $Eu(hfc)_3$ are shown in Figure 46 (page 114). The enantiomeric excess estimated within the limits of the NMR method is

considered to be ≥97%.

Correlation of the Absolute Stereochemistry between Dibenzobarrelene 23 in Pro-(-)-23 Crystals and its Optically Pure Product (-)-57.

A single chiral crystal of **pro-(-)-23** with well developed faces and edges and weighing 55 mg was grown by slow evaporation of a saturated cyclohexane solution previously seeded with a small crystal obtained from batch 2 (see Table VI, page 112). A small fragment was separated in order to obtain X-ray diffraction data to determine the structure and absolute configuration of **pro-(-)-23** by applying the method of anomalous dispersion. When this analysis successfully revealed a 11M, 12P absolute configuration (conformational chirality formalism, see Figure 48 on page 118), the remaining 53.2 mg of the original single crystal were photolyzed for 30 min with the nitrogen laser. The optical rotation of the reacted crystal and its percent conversion were then obtained to calculate the specific optical rotation which was consistent with all the previous results, $[\alpha]_D$= -25.3° ($CHCl_3$, c= 0.053).

In order to determine the absolute configuration of the photoproduct **(-)-57**, the technique of anomalous X-ray dispersion was applied to a sample of the optically pure material obtained in the following manner. Three samples of **23** previously photolyzed in the solid state (0.3347 g) and shown to give levorotatory material were selected for enrichment of the product by crystallization of the starting material. An oily mother liquor containing 45 mg of 56% product was obtained after four fractional crystallizations. The chiral product **(-)-57** (20 mg, 98% pure by glc) could be purified easily by column chromatography (silica gel, petroleum

ether (bp = 35-60°C):ethyl acetate 19:1) after the remaining starting material was converted to the pyrazoline cycloadduct by treatment of the mixture with diazomethane. Crystallization of **(-)-57** from diethyl ether and ethanol gave square crystals suitable for X-ray anomalous dispersion analysis. This analysis showed **(-)-57** to have the (S)-4b,(S)-8b,(S)-8c, (S)-8d, configuration (see page 118).

(-)-Di-(2-propyl)-(S)-4b,(S)-8b,(S)-8c,(S)-8d-tetrahydro-dibenzo[a,f]-cyclopropa[cd]pentalene-8c,8d-dicarboxylate (-)-57.

mp = 124-5°C (prisms from diethyl ether-ethanol)

The solution spectroscopic properties of this samples were identical to those from the racemate previously isolated from solution photolysis of diester **23**.

IR (KBr) 1732, 1712, (2 C=O), 1251, 1231 (2 C-O) cm^{-1}.

The structure of diester **(-)-57** was also confirmed by X-ray crystallographic analysis.

<u>Photolysis of</u>

<u>11,12-Di-[(R,S)-2-butyl]-9,10-dihydro-9,10-ethenoanthracene-11,12-dicarboxylate (24).</u>

Compound **24** was photolyzed in solution and in the solid state in a similar manner as the dimethyl diester **18** to give:

Di-[(R,S)-2-butyl]-4b,8b,8c,8d-tetrahydro-dibenzo[a,f]cyclopropa[cd]-pentalene-8c,8d-dicarboxylate (58).

Compound **58** was obtained as mixture of diastereomers (two glc peaks). The mixture was found to be a viscous liquid at 20°C. The spectroscopic data that follows were obtained on the photoproduct mixture.

^{1}H NMR (acetone-d_6, 300 MHz) δ 7.45-7.05 (8H, m, Ar-H), 5.12 [1H, s, H(8b)], 5.05 [1H, m, -$CO_2CH(CH_3)CH_2CH_3$), 4.45, 4.43, 4.41 (total 1H, 3s, H(8c)], 1.65 (4H, m, -$CO_2CH(CH_3)CH_2CH_3$), 1.40-1.20 (6H, m, -$CO_2CH(CH_3)CH_2CH_3$), 1.05-0.85 (6H, m, -$CO_2CH(CH_3)CH_2CH_3$).

IR (neat) 1733 (C=O), 1290 (C-O) cm^{-1}.

MS m/e (rel. intensity) 400 (M^+, 22), 348 (10), 330 (13), 302 (26), 275 (23), 247 (100), 202 (81), 178 (4). Calculated mass: 404.1988, found 404.1990.

<u>Photolysis of 11-(2-Propyl)-12-methyl-9,10-ethenoanthracene-11,12-dicarboxylate (30).</u>

1) Solution Photolysis and Identification of the Photoproducts.

Samples of compound **30** were photolyzed in solution and found to give two products (glc analysis) in a 55:45 ratio. The product ratio was found to be independent of the solvent used (benzene, acetonitrile and acetone). Preparative photolysis (100 mg) was carried out in the same manner as for compound Me/Me-**18**. After a ^{1}H NMR and a glc-MS spectra of the reaction mixture were obtained, several unsuccessful attempts were made to perform chromatographic separation of the reaction mixture. The two products turned out to be isomeric with the starting material and had ^{1}H NMR spectra that strongly suggested the two expected di-π-methane products.

The identity of the two photoproducts could be established by spectroscopic analysis and confirmed by X-ray diffraction analysis. The

major product, the dibenzosemibullvalene diester **63A**, could be separated after it was discovered that it can be selectively crystallized (colorless prisms) in low yield from methylcyclohexane. The mother liquor after this crystallization was found to have an equimolar composition of the two products. This solution was found suitable for fractional crystallization using diethyl ether as the solvent. The minor product, dibenzosemibullvallene diester **63B**, could be separated (colorless prisms) 97% pure in low yield after 7 fractional crystallizations. This compound only started to crystallize preferentially after it was present in more than 70% in the mother liquor.

8c-Methyl-8b-(2-propyl)-4b,8b,8c,8d-tetrahydro-dibenzo[a,f]cyclopropa[cd]-pentalene-8c,8b-dicarboxylate (63A).

mp = 139-141°C.

^{1}H NMR ($CDCl_3$, 300 MHz) δ 7.35-7.05 (8H, m, AR-H), 5.24 (1H, m, C(8b)-$CO_2CH(CH_3)_2$), 5.05 (1H, s, C(8b)-H), 4.45 (1H, s, C(4b)-H), 3.70 (3H, s, -CO_2CH_3), 1.30,1.32 (6H, 2d, J=7Hz, -$CO_2CH(CH_3)_2$).

IR (KBr) 1735 (C=O), 1253 (C-O) cm^{-1}.

MS m/e (rel. intensity) 348 (M^+, 35), 306 (30), 260 (70), 202 (100).

Analysis Calculated for $C_{22}H_{20}O_4$*: C, 75.84; H, 5.79, found: C, 75.90; H, 5.93 .

8b-Methyl-8c-(2-propyl)-4b,8b,8c,8d-tetrahydro-dibenzo[a,f]cyclopropa[cd]-pentalene-8c,8b-dicarboxylate (63B).

mp = 110-112°C.

^{1}H NMR ($CDCl_3$, 300 MHz) δ 7.35-7.05 (8H, m, Ar-H), 5.05 (1H, m,

C(8c)-$CO_2CH(CH_3)_2$), 5.07 (1H, s, C(8b)-H), 4.49 (1H, s, C(4b)-H), 3.88 (3H, s, -CO_2CH_3), 1.22, 120 (6H, 2d, J=7Hz, -$CO_2CH(CH_3)_2$).

IR (KBr) 1737, 1717 (C=O), 1248 (C-O) cm^{-1}.

MS m/e (rel. intensity) 348 (M^+, 25), 316 (15), 261 (100), 202 (75).

Analysis Calculated for $C_{22}H_{20}O_4$*: C, 75.84; H, 5.79, found: C, 75.90; H, 5.93 .

* The elemental analysis was performed on the **63A/63B** mixture.

2) Solid State Photolysis.

Compound 30 was photolyzed in the solid state in the same manner as **18**. The product ratio was obtained by glc and found to be **63A:63B** = 93:7. The dependence of the product ratio was studied as a function of temperature and found to be invariant from -70 to 20°C. The product ratio was also found to be constant to up to a conversion of 30% after which the crystals became largely unreactive.

Photolysis of Dibenzosemibullvalene 63A.

Dilute (0.001 M) benzene, acetonitrile and acetone solutions of the photoproduct **63A** were photolyzed with the Hanovia lamp through a Pyrex filter. Analysis of these samples by glc revealed no trace of reaction.

Photolysis of Compounds 28, 29 and 32 to 39.

These compounds were photolyzed in solution and in the solid state in a similar manner as diester 30. Two regioisomeric photoproducts were observed in each case, both in solution and in the solid state. No product

separation could be achieved and the mixtures were analyzed by glc, glc-MS, FTIR and ^{1}H NMR. The chromatographic and spectroscopic results of each mixture were correlated with those of **63A** and **63B** which had been assigned unambiguously (vide supra). The $-CO_2CH_3$ proton resonances (the ethyl ester methylene resonances in the cases of Et/iPr-**38** and Et/sBu-**39**), the glc retention times and the respective integrated areas from the regioisomeric products **A** and **B** as obtained in solution and in the solid state are shown in Table XI (page 132) and in Figure 56 (page 141). In all cases the spectral data were in complete agreement with the two expected dibenzosemibullvalene diester structures. It was also found that the mass spectral fragmentation pattern of the regioisomeric structures **A** and **B** follows a regular trend. The pertinent ions and their relative abundances are shown in Table XII (page 139). The detailed ^{1}H NMR spectroscopic information deduced from the photolysis mixtures is presented below.

Photolysis Mixture of Me/Et-28.

Major Regioisomer (A):

8c-Methyl-8b-(ethyl)-4b,8b,8c,8d-tetrahydro-dibenzo[a,f]cyclopropa[cd] pentalene-8c,8b-dicarboxylate (61A).

^{1}H NMR ($CDCl_3$, 400 MHz) δ 7.40-7.00 (8H, m, Ar-H), 5.06 [1H, s, H(4b)], 4.47 [1H, s, H(8d)], 4.35 (2H, q, J=7Hz, $-CO_2CH_2CH_3$), 3.70 (3H, s, $-CO_2CH_3$), 1.34 (3H, t, J=7Hz, $-CO_2CH_2CH_3$).

IR of mixture (KBr): 1726 and 1702 (C=O), 1461, 1294 and 1215 (C-O), 1061, 754 cm^{-1}.

MS of mixture m/e (rel. Intensity) 334 (M^+, 100), 302 (11), 289 (13),

275 (50), 274 (60), 261 (64), 202 (82); Calculated mass: 334.1205, found: 334.1202.

Minor Regioisomer (B):

8d-Methyl-8c-(ethyl)-4b,8b,8c,8d-tetrahydro-dibenzo[a,f]cylopropa[cd]-pentalene-8c,8b-dicarboxylate (61B).

^{1}H NMR ($CDCl_3$, 400 MHz) δ 7.40-7.00 (8H, m, Ar-H), 5.05 [1H, s, H(4b)], 4.49 [1H, s, H(8d)], 4.17 (2H, q, J=7Hz, $-CO_2CH_2CH_3$), 3.86 (3H, s, $-CO_2CH_3$), 1.24 (3h, t, J=7Hz, $-CO_2CH_2CH_3$).

Photolysis Mixture of Me/nPr-29.

Major regioisomer (A).

8c-Methyl-8b-(1-Propyl)-4b,8b,8c,8d-tetrahydro-dibenzo[a,f]cyclopropa[cd]-pentalene-8c,8b-dicarboxylate (62A).

^{1}H NMR (C_6D_6, 300 MHz) δ 7.4-6.7 (8H, m, Ar-H), 5.1 [1H, s, H(4b)], 4.7 [1H, s, H(8d)], 4.1 (2H, m, $-CO_2CH_2CH_2CH_3$), 3.3 (3H, s, $-CO_2CH_3$), 1.4 (2H, m, $-CO_2CH_2CH_2CH_3$) , 0.7 (3H, m, $-CO_2CH_2CH_2CH_3$).

IR of mixture (neat) 2967 (C-H), 1729 (C=O), 1474, 1438, 1291, 1246 (C-O), 1088, 1043, 741 cm^{-1}.

MS of mixture m/e (rel. intensity) 348 (M^+, 41), 316 (7), 288 (58), 261 (64), 202 (100). Calculated mass: 348.1362, found: 348.1362.

Minor regioisomer (B).

8d-Methyl-8c-(1-propyl)-4b,8b,8c,8d-tetrahydro-dibenzo[a,f]cylopropa[cd]-pentalene-8c,8b-dicarboxylate (62B).

^{1}H NMR (C_6D_6, 300 MHz) δ 7.4-6.7 (8H, m, Ar-H), 5.0 [1H, s, H(4b)], 4.7 [1H, s, H(8d)], 3.9 (2H, m $-CO_2CH_2CH_2CH_3$), 3.5 (3H, s, $-CO_2CH_3$), 1.3

(2H, m, $-CO_2CH_2CH_2CH_3$) , 0.7 (3H, m, $-CO_2CH_2CH_2CH_3$).

Photolysis Mixture of Me/sBu-31.

Major Regioisomer (A):

8c-Methyl-8b-(2-butyl)-4b,8b,8c,8d-tetrahydro-dibenzo[a,f]cyclopropa[cd]-pentalene-8c,8b-dicarboxylate (64A)

^1H NMR ($CDCl_3$, 400 MHz) δ 7.35-7.02 (8H, m, Ar-H), 5.05 [1H, s, H(4b)], 5.05 (1H, m, $-CO_2CH(CH_3)CH_2CH_3$), 4.47 [1H, s, H(8d)], 3.70 (3H, s, $-CO_2CH_3$), 1.60 (2H, m, $-CO_2CH(CH_3)CH_2CH_3$), 1.31 and 1.25 (3H*, d, J=7Hz, $-CO_2CH(CH_3)CH_2CH_3$, 0.95 and 0.91 (3H*, t, J=7Hz, $-CO_2CH(CH_3)CH_2CH_3$).

*Resolution of two diastereomeric signals.

IR of mixture (neat) 1729 (C=O), 1474, 1461, 1438, 1380, 1336, 1291, 1249 and 1088 (C-O), 1042, 758 cm^{-1}.

Glc-MS m/e (rel. intensity) peak A-I: 362 (M^+, 9), 306 (58), 289 (11), 278 (15), 262 (14), 261 (31), 260 (94), 247 (65), 246 (54), 233 (19), 230 (15), 219 (21), 203 (44), 202 (100); peak A-II 362 (M^+, 11), 306 (49), 289 (13), 278 (12), 262 (26), 261 (28), 260 (92), 247 (56), 246 (68), 233 (17), 230 (10), 219 (20), 203 (35), 202 (100); .

Analysis calculated for: $C_{23}H_{22}O_4$: C, 76.22; H, 6.12, found (in photolysis mixture): C, 76.50; H, 6.35.

Minor Regioisomer (B):

8b-Methyl-8c-(2-butyl)-4b,8b,8c,8d-tetrahydro-dibenzo[a,f]cyclopropa[cd]-pentalene-8c,8b-dicarboxylate (64B).

^1H NMR ($CDCl_3$, 400 MHz) δ 7.35-7.02 (8H, m, Ar-H), 5.05 [1H, s, H(4b)], 4.89 (1H, m, $-CO_2CH(CH_3)CH_2CH_3$), 4.44 and 4.43 [1H*, s, H(8d)], 3.86 (3H, s, $-CO_2CH_3$), 1.60 (2H, m, $-CO_2CH(CH_3)CH_2CH_3$), 1.18 and 1.17

(3H*, d, J=7Hz, $-CO_2CH(CH_3)CH_2CH_3$), 0.87 and 0.86 (3H*, t, J=7Hz, $-CO_2CH(CH_3)CH_2CH_3$).

(* = resolution of two diastereomeric signals)

Glc-MS m/e (rel. intensity) peak B: 362 (M^+, 8), 330 (9), 302 (8), 289 (11), 262 (50), 261 (92), 260 (22), 247 (14), 246 (17), 202 (76), 41 (100).

Photolysis Mixture of Me/tBu-32.

Major Regioisomer (A):

8c-Methyl-8b-(1,1-dimethyl-1-ethyl)-4b,8b,8c,8d-tetrahydro-dibenzo-[a,f]cyclopropa[cd]pentalene-8c,8b-dicarboxylate (65A)

^1H NMR ($CDCl_3$, 80 MHz) δ 7.4-7.0 (8H, m, Ar-H), 5.0 [1H, s, H(4b)], 4.4 [1H, s, H(8d)], 3.70 (3H, s, $-CO_2CH_3$), 1.50 (9H, s, $-CO_2(CH_3)_3$).

IR of mixture (neat) 2981 (C-H), 1729 (C=O), 1474, 1458, 1438, 1369, 1340, 1295, 1252 and 1154 (C-O), 1046, 758 cm^{-1}.

Glc-MS m/e (rel. intensity) 362 (M^+, trace), 306 (100), 289 (16), 278 (17), 260 (96), 247 (68), 246 (68), 233(20), 202 (99), 189 (16).

Analysis calculated for: $C_{23}H_{22}O_4$: C, 76.22; H, 6.,26, found (in photolysis mixture): C, 76.08; H, 6.16.

Minor Regioisomer (B):

8b-Methyl-8c-(1,1-dimethyl-1-ethyl)-4b,8b,8c,8d-tetrahydro-dibenzo-[a,f]cyclopropa[cd]pentalene-8c,8b-dicarboxylate (65B).

^1H NMR ($CDCl_3$, 80 MHz) δ 7.4-7.0 (8H, m, Ar-H), 5.0 [1H, s, H(4b)], 4.4 [1H, s, H(8d)], 3.85 (3H, s, $-CO_2CH_3$), 1.40 (9H, s, $-CO_2(CH_3)_3$).

Glc-MS m/e (rel. intensity) 362 (M^+, 3), 306 (6), 289 (11), 262 (100), 260 (5), 247 (19), 246 (8), 202 (82), 189 (9).

Photolysis Mixture of Me/nPent-33.

Major Regioisomer (A):

8c-Methyl-8b-(1-pentyl)-4b,8b,8c,8d-tetrahydro-dibenzo[a,f]cyclopropa[cd]-pentalene-8c,8b-dicarboxylate (66A)

^{1}H NMR ($CDCl_3$, 300 MHz) δ 7.35-7.00 (8H, m, Ar-H), 5.08 [1H, s, H(4b)], 4.49 [1H, s, H(8d)], 4.10 (2H, m, $-CO_2CH_2(CH_2)_3CH_3$), 3.70 (3H, s, $-CO_2CH_3$), 1.80-1.40 (6H, m, $-CO_2CH_2(CH_2)_3CH_3$), 0.95 (3H, m, $-CO_2CH_2(CH_2)_3CH_3$).

IR of mixture (neat) 2954 (C-H), 1729 (C=O), 1437, 1292, 1246 and 1088 (C-O), 1046, 741 cm^{-1}.

Glc-MS m/e (rel. intensity) 376 (M^+, 10), 317 (3), 275 (2), 260 (25), 247 (12), 233 (20), 218 (20), 202 (100).

Analysis calculated for $C_{24}H_{24})_4$: C, 76.57; H, 6.43, found (in photolysis mixture): C, 76.45; H, 6.29.

Minor Regioisomer (B):

8b-Methyl-8c-(1-pentyl)-4b,8b,8c,8d-tetrahydro-dibenzo[a,f]cyclopropa-[cd]pentalene-8c,8b-dicarboxylate (66B).

^{1}H NMR ($CDCl_3$, 300 MHz) δ 7.35-7.00 (8H, m, Ar-H), 5.06 [1H, s, H(4b)], 4.46 [1H, s, H(8d)], 4.30 (2H, m, $-CO_2CH_2(CH_2)_3CH_3$) 3.86 (3H, s, $-CO_2CH_3$), 1.80-1.40 (6H, m, $-CO_2CH_2(CH_2)_3CH_3$), 0.95 (3H, m, $-CO_2CH_2(CH_2)_3CH_3$).

Glc-MS m/e (rel. intensity) 376 (M^+, 5), 316 (20), 261 (35), 246 (15), 229 (25), 218 (30), 202 (100).

Photolysis Mixture of Me/iPen-34.

Major Regioisomer (A):

8c-Methyl-8b-(2-methyl-1-butyl)-4b,8b,8c,8d-tetrahydro-dibenzo[a,f]-cyclopropa[cd]pentalene-8c,8b-dicarboxylate (67A)

^{1}H NMR ($CDCl_3$, 300 MHz) δ 7.40-7.00 (8H, m, Ar-H), 5.08 [1H, s, H(4b)], 4.02 [1H, s, H(8d)], 4.01 (2H, m, $-CO_2CH_2CH(CH_3)CH_2CH_3$), 3.70 (3H, s, $-CO_2CH_3$), 1.70 (1H, m, $-CO_2CH_2CH(CH_3)CH_2CH_3$), 1.40 (2H, m, $-CO_2CH_2CH(CH_3)CH_2CH_3$), 1.20 (3H, m, $-CO_2CH_2CH(CH_3)CH_2CH_3$), 0.95 (3H, m, $-CO_2CH_2CH(CH_3)CH_2CH_3$).

IR of mixture (neat): 1729 (C=O), 1474, 1760, 1090.

Glc-MS m/e (rel. intensity) 376 (M^+, 9), 348 (1), 317 (41), 306 (14), 289 (4), 262 (15), 261 (21), 260 (66), 247 (44), 246 (43), 202 (100).

Analysis calculated for $C_{24}H_{24}O_4$: C, 76.57; H, 6.43, found (in photolysis mixture): C, 76.65; H, 6.58.

Minor Regioisomer (B):

8b-Methyl-8c-(2-methyl-1-butyl)-4b,8b,8c,8d-tetrahydro-dibenzo[a,f]-cyclopropa[cd]pentalene-8c,8b-dicarboxylate (67B).

^{1}H NMR ($CDCl_3$, 300 MHz) δ 7.40-7.00 (8H, m, Ar-H), 5.10 [1H, s, H(4b)], 4.05 [1H, s, H(8d)], 4.01 (2H, m, $-CO_2CH_2CH(CH_3)CH_2CH_3$), 3.84 (3H, s, $-CO_2CH_3$), 1.70 (1H, m, $-CO_2CH_2CH(CH_3)CH_2CH_3$), 1.40 (2H, m, $-CO_2CH_2CH(CH_3)CH_2CH_3$), 1.20 (3H, m, $-CO_2CH_2CH(CH_3)CH_2CH_3$), 0.95 (3H, m, $-CO_2CH_2CH(CH_3)CH_2CH_3$).

Glc-MS m/e (rel. intensity) 376 (M^+, 6), 344 (3), 316 (21), 306 (2), 289 (3), 262 (24), 261 (53), 260 (25), 247 (13), 246 (18), 202 (100).

Photolysis Mixture of Me/neoPen-35.

Major Regioisomer (A):

8c-Methyl-8b-(2,2-dimethyl-1-proyl)-4b,8b,8c,8d-tetrahydro-dibenzo[a,f]-cyclopropa[cd]pentalene-8c,8b-dicarboxylate (68A)

^{1}H NMR ($CDCl_3$, 300 MHz) δ 7.40-7.00 (8H, m, Ar-H), 5.03 [1H, s, H(4b)], 4.38 [1H, s, H(8d)], 3.70 (3H, s, $-CO_2CH_3$), 1.82 (2H, q, J=6Hz, $-CO_2C(CH_3)_2CH_2CH_3$), 1.52 and 1.49 (6H, 2s, $-CO_2C(CH_3)_2CH_2CH_3$), 0.91 (3H, t, J=6Hz, $-CO_2C(CH_3)_2CH_2CH_3$).

IR of mixture (neat) 1729 (C=O), 1474, 1461, 1438, 1384, 1341, 1292, 1243 and 1152 (C-O), 1088, 759 cm^{-1}.

Glc-MS m/e (rel. intensity) 376 (M^+, 2), 306 (15), 261 (15) 260 (10), 247 (10), 230 (20), 219 (25), 202 (100); Calculated mass: 376.1675, found: 376.1672.

Minor Regioisomer (B):

8b-Methyl-8c-(2,2-dimethyl-1-propyl)-4b,8b,8c,8d-tetrahydro-dibenzo[a,f]-cyclopropa[cd]pentalene-8b,8c-dicarboxylate (68B).

^{1}H NMR ($CDCl_3$, 300 MHz) δ 7.40-7.00 (8H, m, Ar-H), 5.01 [1H, s, H(4b)], 4.41 [1H, s, H(8d)], 3.85 (3H, s, $-CO_2CH_3$), 1.78 (2H, q, J=6Hz, $-CO_2C(CH_3)_2CH_2CH_3$), 1.42 and 1.41 (6H, 2s, $-CO_2C(CH_3)_2CH_2CH_3$), 0.87 (3H, t, J=6Hz, $-CO_2C(CH_3)_2CH_2CH_3$).

Glc-MS m/e (rel. intensity) No M^+ at 376, 261 (30), 246 (20), 218 (10), 202 (100), 189 (40).

Photolysis Mixture of Me/Menth-36.

Major Regioisomer (A):

8c-Methyl-8b-[(1)-(-)-menthyl]-4b,8b,8c,8d-tetrahydro-dibenzo[a,f]-

cyclopropa[cd]pentalene-8c,8b-dicarboxylate (69A)

^{1}H NMR ($CDCl_3$, 300 MHz) δ 7.36-7.00 (8H, m, Ar-H), 5.06 and 5.05 [1H*, s, H(4b)], 4.90 (1H, m, menthyl methine), 4.46 and 4.39 [1H*, s, H(8d)], 3.70 and 3.69 (3H*, s, $-CO_2CH_3$), 2.20-0.70 (18H, m, menthyl group).

IR of mixture (neat) 2954 and 1870 (strong C-H), 1733 (C=O), 1457, 1388, 1292 and 1248 (C-O), 1088, 1038, 757 cm^{-1}.

Glc-MS m/e (rel. intensity): 444 (M^+, 13), 262 (78), 246 (20), 229 (10), 202 (100), 189 (11), 176 (19).

Analysis calculated for $C_{29}H_{32}O_4$: C, 78.35; H, 7.26, found (in photolysis mixture): C, 78.10; H, 7.40.

Minor Regioisomer (B):

8b-Methyl-8c-[(1)-(-)-menthyl]-4b,8b,8c,8d-tetrahydro-dibenzo[a,f]-cyclopropa[cd]pentalene-8c,8b-dicarboxylate (69B).

^{1}H NMR ($CDCl_3$, 300 MHz) δ 7.36-7.00 (8H, m, Ar-H), 5.06 and 5.05 [1H*, s, H(4b)], 4.80 (1H, m, menthyl methine), 4.46 [1H, s, H(8d)], 3.86 and 3.85 (3H*, s, $-CO_2CH_3$), 2.20-0.70 (18H, m, menthyl group).

Glc-MS m/e (rel. intensity): No M^+ at 444, 306 (44), 260 (46), 247 (43), 229 (21), 218 (26), 202 (100), 189 (28).

Photolysis Mixture of Me/Ph-37.

Major Regioisomer (B).

8b-Methyl-8c-Phenyl-4b,8b,8c,8d-tetrahydro-dibenzo[a,f]cyclopropa-[cd]pentalene-8c,8b-dicarboxylate (69A)

^{1}H NMR ($CDCl_3$, 300 MHz) δ 7.50-7.05 (13H, m, Ar-H), 5.25 [1H, s, H(4b)], 4.72 [1H, s, H(8d)], 3.91 (3H, s, $-CO_2CH_3$).

IR of mixture (neat) 3025, 2953 (C-H), 1738 (C=O), 1592 (C=C phenyl),

1493, 1457, 1436, 1292 and 1199 (C-O), 1068, 740 cm^{-1}.

MS of mixture m/e (rel. intensity) 382 (M^+, 25), 289 (21), 261 (45), 230 (23), 202 (100), 94 (52); Calculated mass: 382.1205, found: 382.1205.

Minor Regioisomer (A).

8c-Methyl-8b-phenyl-4b,8b,8c,8d-tetrahydro-dibenzo[a,f]cyclopropa[cd]-pentalene-8c,8b-dicarboxylate (69B).

^1H NMR ($CDCl_3$, 300 MHz) δ 7.50-7.05 (13H, m, Ar-H), 5.17 [1H, s, H(4b)], 4.65 [1H, s, H(8d)], 3.80 (3H, s, $-CO_2CH_3$).

Photolysis Mixture of Et/iPr-38.

Major Regioisomer (A).

8c-Ethyl-8b-(2-propyl)-4b,8b,8c,8d-tetrahydro-dibenzo[a,f]cyclopropa[cd]-pentalene-8c,8d-dicarboxylate (71A).

^1H NMR ($CDCl_3$, 400 MHz) δ 7.35-7.03 (8H, m, Ar-H), 5.23 (1H, m, $-CO_2CH(CH_3)_2$), 5.05 [1H, s, H(4b)], 4.44 [1H, s, H(8d)], 4.18 (2H, m, $-CO_2CH_2CH_3$) , 1.35-1.20 (9H, $-CO_2CH_2CH_3$ and $-CO_2CH(CH_3)_2$).

IR of mixture (neat) 1982 (C-H), 1727 (C=O), 1462, 1375, 1291, 1249 and 1102 (C-O), 1046, 762 cm^{-1}.

MS of mixture m/e (rel. intensity) 362 (M^+, 35), 320 (12), 303 (10), 302 (8), 288 (22), 264 (61), 202 (100).

Analysis Calculated for: $C_{23}H_{22}O_4$: C, 76.22; H, 6.12, found (in photolysis mixture): C, 76.24; H, 6.30.

Minor Regioisomer (B).

8d-Ethyl-8c-(2-propyl)-4b,8b,8c,8d-tetrahydro-dibenzo[a,f]cyclopropa[cd]-pentalene-8c,8d-dicarboxylate (71B).

^1H NMR ($CDCl_3$, 400 MHz) δ 7.35-7.03 (8H, m, Ar-H), 5.04 (1H, m,

$-CO_2CH(CH_3)_2$), 5.05 [1H, s, H(4b)], 4.46 [1H, s, H(8d)], 4.35 (2H, m, $-CO_2CH_2CH_3$) , 1.35-1.20 (9H, $-CO_2CH_2CH_3$ and $-CO_2CH(CH_3)_2$).

Photolysis Mixture of Et/sBu-39.

Regioisomer (A).

8c-Ethyl-8b-[(S)-(+)-2-butyl)-4b,8b,8c,8d-tetrahydro-dibenzo[a,f]-cyclopropa[cd]pentalene-8c,8d-dicarboxylate (72A).

^1H NMR (C_6D_6, 300 MHz) δ 7.35-6.70 (8H, m, Ar-H), 5.20 [1H, ss, H(8d)], 5.15 (1H, m, $-CO_2CH(CH_3)CH_2CH_3$), 4.75 [1H, ss, H(8b)], 4.18 (2H, m, $-CO_2CH_2CH_3$), 1.6-0.7 (11H, m, $-CO_2CH(CH_3)CH_2CH_3$ and $-CO_2CH_2CH_3$).

IR of mixture (neat) 1982 (C-H), 1727 (C=O), 1462, 1375, 1291, 1249 and 1102 (C-O), 1046, 762 cm^{-1}.

Glc-MS m/e (rel. intensity) peak AI: 376 (M^+, 11), 320 (11), 303 (15), 274 (83), 247 (52), 230 (15), 219 (21), 202 (100), 178 (32); peak AII: 376 (M^+, 10), 320 (13), 303 (13), 274 (88), 247 (54), 230 (19), 219 (27), 202 (100), 178 (28); Calculated mass: 376.1675, found: 376.1670.

Regioisomer (B).

8d-Ethyl-8c-[(S)-(+)-2-butyl)-4b,8b,8c,8d-tetrahydro-dibenzo[a,f]-cyclopropa[cd]pentalene-8c,8d-dicarboxylate (72B).

^1H NMR (C_6D_6, 300 MHz) δ 7.35-6.70 (8H, m, Ar-H), 5.10 [1H, s, H(8d)], 4.95 (1H, m, $-CO_2CH(CH_3)CH_2CH_3$), 4.75 [1H, ss, H(8b)], 3.95 (2H, m, $-CO_2CH_2CH_3$), 1.6-0.7 (11H, m, $-CO_2CH(CH_3)CH_2CH_3$ and $-CO_2CH_2CH_3$).

Glc-MS m/e (rel. intensity) peak B: 376 (M^+, 5), 330 (11), 303 (8), 302 (7), 275 (80), 247 (33), 230 (11), 219 (14), 202 (77), 56 (100).

Photochemical Studies on 11-(2-Propyl)-9,10-ethenoanthracene-11-carboxylate-12-carboxylic acid (41).

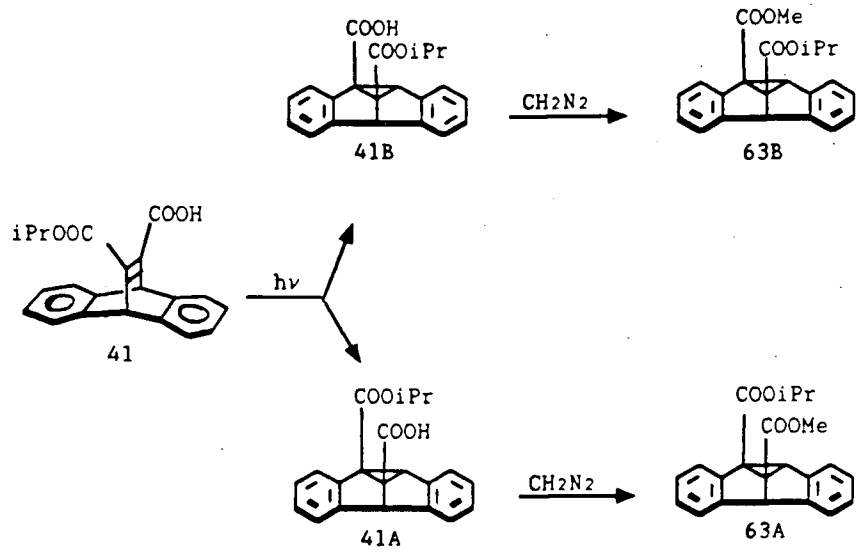

The solution photochemistry of the acid 41 was explored in different solvents and at different concentrations. Solid state photolyses were explored parallel to the solution irradiations. Analytical photolyses were performed as outlined in the General Experimental Section. Two products were observed in all cases and were shown to correspond to the regioisomeric dibenzosemibullvalene monoacids **41A** and **41B** by converting them into their corresponding methyl esters **63A** and **63B**. This conversion was achieved through two esterification procedures.

1) Esterification via the Acyl Chloride.

A solution of 15 mg of monoacid **40** that had been previously photolyzed in acetonitrile was evaporated in vacuo and the residue refluxed for two hours after addition of 2 ml of CH_2Cl_2 and 1 ml of oxalyl chloride. The solvent and excess oxalyl chloride were eliminated by rotatory evaporation under reduced pressure and then by vacuum pumping at about 1.0 torr for 30

min. The resulting oil, assumed to be the corresponding acyl chloride, was not identified but immediately set to reflux with 2 ml of methanol. After two hours the excess alcohol was evaporated and the residue dissolved in 10 ml of diethyl ether in order to wash it with water, $NaHCO_3$ and water again. The ether solution was dried over $MgSO_4$ and then the solvent evaporated to dryness. The resulting product (6 mg, 40% yield) was analyzed by glc and two peaks were found in a 90:10 ratio. The retention times of these signals were identical to those from the dibenzosemibull-valenes **63A** and **63B** respectively as shown by coinjection analysis. The structure assignment of these products was confirmed by ^1H NMR analysis of the mixture.

2) Esterification with Diazomethane.

A sample of 5 mg of the monoacid **41** that had been photolyzed previously as a 0.1 M acetonitrile solution was evaporated to dryness. An ethereal solution containing a large excess of diazomethane was added and the mixture left overnight in the fume hood. After the solvent was evaporated the sample was analyzed by glc and found to contain a 50:50 mixture of dibenzosemibullvalenes **63A** and **63B** in quantitative yield. Other samples were analyzed by the same method and the results obtained from duplicate photolyses in several solvents and concentrations are shown below along with the solid state results. An entry including the results from the acid anion formed in aqueous $NaHCO_3$ solution are also included.

Medium and Concentration Dependent Photochemistry of Acid 41.

Entry	Solvent	Conc. (M)	63A*(%)	63B*(%)
1	t-BuOH	0.005	47	53
2	"	0.010	47	53
3	"	0.05	49	51
4	"	0.10	49	51
5	CH_3CN	0.01	51	49
6	"	0.05	50	50
7	"	0.10	49	51
8	Acetone	0.01	52	48
9	"	0.10	49	51
10	Benzene	0.001	81	19
11	"	0.003	80	20
12	"	0.006	78	22
13	"	0.010	76	24
14	"	0.03	68	32
15	"	0.06	60	40
16	"	0.10	55	45
17	Crystal	--	25	75
18	$NaHCO_3$aq	0.01	91	9

* Ratio determined after the acid mixture was converted into the corresponding methyl ester by treatment with CH_2N_2.

Photochemical Studies on 11-(2-Butyl)-12-(2-propyl)-9,10-etheno-anthracene-11,12-dicarboxylate (42).

The racemic and optically active forms of the diester 42 were photolyzed in solution and in the solid state as described in the General Experimental Section. Three peaks were observed by glc analysis of the reaction mixtures. The integrated areas of these peaks, at 16.30, 16.60 and 17.90 min (Column DB-1, oven at 200°C and column head pressure of 12.5 psi), are shown in Table XII (page 179). The results shown were obtained over a large number of experiments and were reproducible to ±5%.

^1H NMR of the photolysis mixture (acetone-d_6, 300 MHz) δ 7.40-7.00 (total 8H, m, Ar-H), 5.16 [1H, m, $-CO_2CH(CH_3)_2$ at C(8b)], 5.08 and 5.07

[1H*, s, H(4b)], 4.98 (1H, m, $-CO_2CH(CH_3)_2$ and $-CO_2CH(CH_3)CH_2CH_3$) at C(8c) and C(8b) respectively], 4.85 [1H, m, $-CO_2CH(CH_3)CH_2CH_3$ at C(8c)], 4.39, 4.37 and 4.05 [1H*, s, H(8d)], 1.75-1.50 (2H, m, $-CO_2CH(CH_3)CH_2CH_3$), 1.35-1.25 (9H, m, $-CO_2CH(CH_3)_2$ and $-CO_2CH(CH_3)CH_2CH_3$), 1.00-0.80 (3H, m, $-CO_2CH(CH_3)CH_2CH_3$).

(* = Resolution of diastereomeric signals).

IR of the photolysis mixture (neat) 2977 and 2935 (C-H), 1729 (C=O), 1462, 1385, 1290, 1248 and 1106 (C-O), 1036, 758 cm^{-1}.

Glc-MS m/e (rel. intensity) Peak AI: 390 (M^+, 10), 334 (7), 316 (11), 303 (5), 302 (2), 289 (4), 288 (19), 247 (100), 202 (73); Peak AII: 390 (M^+, 9), 334 (10), 316 (12), 303 (4), 302 (1), 289 (5), 288 (22), 247 (100), 202 (70); Peak B: 390 (M^+, 15), 330 (9), 303 (4), 302 (14), 289 (23), 288 (6), 247 (100), 202 (80); Calculated mass: 390.1831, found: 390.1836.

The assignment of the ions pertinent to the identification of the corresponding products are included in Table XIV (page 181). The mass spectral results from racemic or optically active **24** turned out to be identical whether photolyzed in solution or in the solid state.

Independent preparation of

(±)-4b(R),8b(R),8c(R),8d(R)-8c-(2-propyl)-8b-[(R)-2-butyl]-4b,8b,8c,8d--tetrahydro-dibenzo[a,f]cyclopropa[cd]pentalene-8c,8b-dicarboxylate (74I) and of

(±)-4b(R),8b(R),8c(R),8d(R)-8c-(2-propyl)-8b-[(S)-2-butyl]-4b,8b,8c,8d-tetrahydro-dibenzo[a,f]cyclopropa[cd]pentalene-8c,8b-dicarboxylate (74II).

A sample of 0.750 g of the sec-butyl monoacid **40** was photolyzed in 200 ml of acetonitrile as described in the General Experimental Section. The solvent was evaporated <u>in vacuo</u> and the residue refluxed for two hours after addition of 30 ml of CH_2Cl_2 and 5 ml of oxalyl chloride. The solvent and excess oxalyl chloride were eliminated by rotatory evaporation under reduced pressure and then by vacuum pumping at 1.0 torr for 30 min. The resulting viscous oil, assumed to be the corresponding acyl chloride, was not identified but immediately set to reflux with 20 ml of 2-propanol. After two hours the excess alcohol was evaporated and the residue dissolved in 30 ml of diethyl in order to wash it with water, $NaHCO_3$ and water again. The ether solution was dried over $MgSO_4$ and then the solvent evaporated to dryness. The crude reaction mixture was subjected to column chromatography (silica gel, petroleum ether (bp = 35-60°C):ethyl acetate, 19:1). The combined fractions corresponding to the expected diastereoisomeric products (62.3 mg, 92% pure by glc) were identified by glc (two peaks AI and AII) and confirmed by glc-MS and ^1H NMR (measured in acetone-d_6).

^1H NMR (acetone-d_6, 300 MHz) δ 7.4-7.0 (8H, m, Ar-H), 5.16 (1H, m, $-CO_2CH(CH_3)_2$), 5.08 [1H, s, H(4b)], 4.86 (1H, $-CO_2CH(CH_3)CH_2CH_3$), 4.37 and 4.39 [1H*, s, H(8d)], 1.70-1.50 (2H, m, $-CO_2CH(CH_3)CH_2CH_3$), 1.35-1.15 (9H, m, $-CO_2CH(CH_3)_2$) and $-CO_2CH(CH_3)CH_2CH_3$), 0.80-0.75 (3H, m, $-CO_2CH(CH_3)CH_2CH_3$).

(* = Resolution of diastereomeric signals).

IR of the mixture (neat) 2977 and 2935 (C-H), 1729 (C=O), 1462, 1385, 1290, 1248 and 1106 (C-O), 1036, 758 cm^{-1}.

Glc-MS m/e (relative intensity) Peaks AI and AII identical to those obtained from photolysis of iPr/sBu-42.

Independent preparation of

(±)-4b(R),8b(R),8c(R),8d(R)-8c-[(R)-2-butyl)-8b-(2-propyl]-4b,8b,8c,8d-tetrahydro-dibenzo[a,f]cyclopropa[cd]pentalene-8c,8b-dicarboxylate (75I) and of

(±)-4b(R),8b(R),8c(R),8d(R)-8c-[(S)-2-butyl)-8b-(2-propyl)-4b,8b,8c,8d-tetrahydro-dibenzo[a,f]cyclopropa[cd]pentalene-8c,8b-dicarboxylate (75II)

The procedure outlined above was applied to a sample of the isopropyl monoacid 41. (R,S)-Sec-butanol was used in the final esterification step. The expected products were obtained in similar manner and yields and identified by glc (one peak only, peak-B), glc-MS and ^{1}H NMR.

^{1}H NMR (acetone-d_6, 300 MHz) δ 7.4-7.0 (8H, m, Ar-H), 5.10 [1H, s, H(4b)], 5.01 (2H, m, $-CO_2CH(CH_3)_2$ and $-CO_2CH(CH_3)CH_2CH_3$), 4.37 and 4.35 [1H*, ss, H(8d)], 1.70-1.50 (2H, m, $-CO_2CH(CH_3)CH_2CH_3$), 1.40-1.20 (9H, m, $-CO_2CH(CH_3)_2$) and $-CO_2CH(CH_3)CH_2CH_3$), 1.00-0.80 (3H, m, $-CO_2CH(CH_3)CH_2CH_3$).

(* = Resolution of diastereomeric signals)

IR of the mixture (neat) 2977 and 2935 (C-H), 1729 (C=O), 1462, 1385, 1290, 1248 and 1106 (C-O), 1036, 758 cm^{-1}.

The identity of these products was further confirmed by coinjection with the photolysis mixture of iPr/sBu-42.

Solvent Dependence of the ^{1}H NMR Shifts of the Photolysis Products from Diester iPr/sbu-42.

In order to obtain more information needed to establish the identity and relative amounts of the different products, a series of ^{1}H NMR spectra

of the total solution reaction mixture were run in several solvents. The goal of this study was to find a signal from each diastereomer that could be resolved in order to quantify their relative amounts in the photolysis mixture. It was found that the protons attached to C(8b) were sharp singlets isolated from all the other proton resonances. The chemical shifts of the signals corresponding to this proton and to the one attached to C(4b) are shown in Table XV (page 183).

Asymmetric Synthesis in Chiral Crystals of Racemic iPr/sBu-42.

A series of single crystals from several crystallization batches of racemic 42 were photolyzed at 0°C with the nitrogen laser. The weight, the percent conversion and the optical rotation of each crystal were accurately measured after photolysis in order to observe the extent of optical activity induced in each experiment. The results obtained are shown in Table XXI (page 208).

Determination of the Asymmetric Induction in $P2_12_12_1$ Crystals of the Resolved 2-Butyl Compound (S)-(+)-42.

a) Preparative Photolysis of (S)-(+)-42 in the Solid State.

A sample of 0.110 g of polycrystalline (S)-(+)-42 was photolyzed for 1 h in the solid state at 0°C with the nitrogen laser. In order to separate the products from the unreacted starting material, the whole reaction mixture was treated with an ethereal solution containing an excess of diazomethane. The starting material was converted to a mixture of diazomethane addition compounds (no characterization of these compounds

was attempted) that were chromatographically separable from the photoproducts. The separation of 30.4 mg (28% yield) of the photoproduct mixture was achieved by using silica gel chromatography with petroleum ether (bp = 35-60°C):ethyl acetate 19:1 as the eluent.

b) Hydrolysis of the Total Reaction Mixture.

A solution containing 15.7 mg of the photoproduct mixture obtained above {$[\alpha]_D$= 20.6° (c = 0.016, $CHCl_3$)}, 10 ml of ethanol and 5 ml of 10% NaOH was refluxed for 2 h. After this period, the solvent volume was reduced to 5 ml under reduced pressure. The solution was then acidified by dropwise addition of conc. HCl and the precipitated diacid was extracted with 2 x 30 ml portions of diethyl ether. The combined organic extracts were dried over $MgSO_4$ and evaporated to dryness to give a solid residue (11.3 mg 96% yield). The above residue was dissolved in 5 ml of diethyl ether and added to 5 ml of a solution containing a large excess of ethereal diazomethane distilled immediately before. The yellow solution was left overnight causing evaporation of the solvent to give a clear oil that was easily crystallized from ethanol to give 12.4 mg of dibenzosemibullvalene **52**. This sample was then dissolved in exactly 1.0 ml of $CHCl_3$ and its optical rotation measured: $[\alpha]_D$= 14.5° (c = 0.012, $CHCl_3$).

c) Chiral Shift Reagent Studies.

The 300 MHz ^1H NMR spectrum of the sample prepared above and one of racemic **52** were recorded before and after addition of the chiral shift reagent [3-(heptafluoropropyl hydroxymethylene)-d-camphorato]europium (III), $Eu(hfc)_3$. Successive additions of 0.2 eq of $Eu(hfc)_3$ to the racemic sample showed that the optimum shift was achieved after the first addition. The two methyl ester resonances originally at 3.71 and 3.89

split into two at 3.75, 3.78 and 3.96, 4.01 respectively (see Figure 84, page 210). The integrated area of these signals was used to determine an enantiomeric excess of 80% in the optically active sample.

Determination of the Asymmetric Induction in $P2_12_12_1$ Crystals of Racemic 2-Butyl Compound [(R,S)-42].

The procedure used to determine the asymmetric induction of crystals of optically active 42 was modified by using a large (0.1606 g) single crystal instead of polycrystalline material. A large single crystal was used in order ensure a homogeneous composition of the solid used (only one enantiomorphous phase). Before performing the solid state photolysis, the crystal was finely crushed and 43.4 mg were saved in order to measure the optical activity and the enantiomeric excess of the starting material {$[a]_D$ = -0.9°, (c = 0.043, $CHCl_3$, ee = 8%).

The photolysis was taken to 15% conversion (α_D = -0.430°, (c = 0.012, $CHCl_3$) and the crude reaction mixture was treated with excess diazomethane in order to separate 0.0154 mg of di-π-methane products {$[\alpha]_D$= -14.4° (c = 0.015, $CHCl_3$)} and 0.1047 g of pyrazoline adducts {$[\alpha]_D$ = -1.58° (c = 0.1, $CHCl_3$), ee = 12.7%}. A sample of optically active 42 was also reacted with CH_2N_2 in order to have the information necessary to determine the approximate specific rotation of the mixture of the cycloaddition products {$[\alpha]_D$max = 12.44°, (c = 0.01, $CHCl_3$)}.

The separated photoproduct mixture was hydrolyzed, reesterified with CH_2N_2 to give a sample of diester 52, and then analyzed by ^1H NMR after addition of $Eu(hfc)_3$. An enantiomeric excess of approximately 80% was measured in this manner by integration of the enantiomerically resolved

methyl ester signals.

Determination of the Asymmetric Induction by the 2-Butyl Group on the Solution Photolysis of Optically Active 42.

The procedure used above to determine the solid state asymmetric inductions were applied to 0.0305 g of the photoproduct mixture ($[\alpha]_D$= 8.07° (c = 0.03, $CHCl_3$) obtained from solution photolysis of (S)-(+)-42. An enantiomeric excess of 1.5 ± 1 was calculated from the specific rotation of a sample of Me/Me-52 obtained after the photolysis mixture from (S)-(+)-42 was hydrolyzed and esterified with diazomethane.

Determination of the Asymmetric Induction by the 2-Butyl Group on the Solution Photolysis of Racemic 42.

No optical activity was observed from the solution photoproducts mixture of racemic 42.

<u>Photochemical Studies on 10-(2-Propyl)-11-methyl-9,10-dihydro-9,10-etheno anthracene-9,12-dicarboxylate (44).</u>

Compound 44 was photolyzed in solution and in the solid state in a similar manner as the diester Me/iPr-30. Triplet sensitization was performed in acetone (0.01 M solution, Pyrex filter) and resulted in the formation of only one product that was characterized as the dibenzosemibullvalene **63A** previously obtained from photolysis of diester 30. The triplet product was found to form also on direct irradiation along with a singlet specific product in a ratio that turned out to be very dependent on the percent conversion. The singlet photoproduct could be isolated in

very low yield when 1 g of 44 was photolyzed to only 10% conversion. The unreacted starting material was separated by column chromatography (silica gel, petroleum ether (bp = 35-60°C)-ethyl acetate 96:4) and the desired product obtained by fractional recrystallization from diethyl ether. In analogy to previous literature reports this product has been identified as:

5-(2-Propyl)-11-methyl-dibenzo[a,e]cyclooctatetraene-5,11-dicarboxylate 47.

mp = 172-3°C (colorless prisms)

^{1}H NMR ($CDCl_3$, 400 MHz) 8.07 and 8.01 [2H, 2s, H(6) and H(12)], 5.12 [1H, hept, J=6.5 Hz, $-CO_2CH(CH_3)$], 3.79 (3H, s, $-CO_2CH_3$), 1.28 (6H, d, J=6.5 Hz, $-CO_2CH(CH_3)_2$).

^{13}C NMR (25.4 MHz, $CDCl_3$) d 167.13 and 166.12 (2 C=O), 142.83, 141.80, 136.40, 136.14, 135.80, 135.06, 134.00, 133.82, 130.23, 130.09, 127.54, 127.42, 127.26, 127.20, 127.16 and 127.05 (Aromatic and olefinic-C), 68.91 (2-propyl-CH), 52.39 (CO_2CH_3), 21.85 and 21.77 (2-propyl-CH_3).

IR (KBr) 1716 and 1710sh (C=O), 1632 and 1640 (E-C=C-H), 1280 and 1247 (2 C-O) cm^{-1}.

MS m/e (rel. intensity) 348 (M^+, 29), 306 (21), 289 (6), 262 (35), 202 (100). Calculated Mass 348.1362; found: 348.1362.

<u>Photochemical Studies on 9-(2-Propyl)-11-methyl-9,10-dihydro-9,10-ethenoanthracene-9,12-dicarboxylate 45.</u>

Compound 45 was photolyzed in a similar manner as 44. Two products were obtained in acetone in a ratio of 95:5. Irradiation in acetonitrile

to low conversion values gave the same two products in 15% plus a third product which was not isolated. The relative amounts of the third (singlet specific) product decreased rapidly with conversion in analogy with the dibenzocyclooctatetraene **95** previously isolated from diester **44**. An attempt to establish the structural identity of the major product obtained in acetone was based on the spectroscopic analysis of the reaction mixture:

a) Major product:

4b-(2-Propyl)-8c-methyl-4b,8b,8c,8d-tetrahydro-dibenzo[a,f]cyclopropa-[cd]pentalene-4b,8c-dicarboxylate (95).

^{1}H NMR ($CDCl_3$, 300 MHz) δ 7.25-7.02 (8H, m, Ar-H), 5.31 (1H, hept, J=7 Hz, $-CO_2CH(CH_3)_2$), 3.84 [2H, s, H(8b) and H(8d)], 3.70 (3H, s, $-CO_2CH_3$), 1.30 (6H, d, J=7 Hz, $-CO_2CH(CH_3)_2$).

IR (KBr) 3045 and 2982 (C-H), 1729 and 1725 (C=O), 1435, 1293, 1278 and 1236 (C-O), 1195, 1109, 1096, 740 cm^{-1}.

MS m/e (relative intensity) 348 (M^+, 31), 289 (15), 288 (18), 261 (26), 233 (26), 229 (19), 202 (100); Calculated mass: 348.1362, found: 368.1364.

Quantum Yields and Quenching Studies.

Quantum yields were measured for compounds Me/Me-**18**, Me/iPr-**30**, and Me/iPr-**44** using valerophenone actinometry in a merry-go-round apparatus. Benzene was used as the solvent in all cases after it was freed from thiophene by a procedure described in the literature. All the solutions were prepared in benzene containing 3 x 10^{-3}M tetracosane (n-$C_{24}H_{50}$), which was used as internal standard for accurate glc quantification of the

amount of photoproducts being formed. The relative detector response of the internal standard and of the photoproduct whose quantum yield of formation was under study, was determined prior to photolysis. The samples (3 ml of 0.1 M solution) were photolyzed by duplicate in Pyrex tubes after they were degassed by three freeze-pump-thaw cycles and sealed with paraffin film. All the solutions were optically opaque at 313 nm. The temperature of the merry-go-around apparatus was kept at at 16-19°C by circulating water through a large water bath in which it was immersed. The 331 nm line of the medium pressure 450 W Hanovia Lamp was isolated by circulating a 0.002 M potassium chromate solution containing 5% potassium carbonate (wt/wt) and by placing 7-54 Corning filters in the filter holders. The number of quanta was calculated by taking the quantum yield of acetophenone formation (from 0.1 M valerophenone in benzene) as Φ=0.3.[184] The number of moles of acetophenone was also calculated by glc using 5 x 10^{-3} M tetradecane as the internal standard. The number of moles of product formation was calculated relative to the alkane internal standard by triplicate glc analysis of each sample. The percent conversion of valerophenone and the diester under study were monitored by glc and kept under 5%. In the quenching experiments 0.1 M solutions of the diesters **30** and **44** were prepared containing the appropriate amount of 1,3-cyclohexadiene. The concentration of the latter was explored in test trials from 10^{-3} to 1.2 M. The quantum yields and quenching experiments (where appropriate) were carried out at least twice for every sample.

Luminescence Measurements.

All measurements were carried out using a Perkin-Elmer LS-5 spectrofluorimeter interfaced with a Perkin-Elmer computer. A pulsed Xenon discharge lamp (8.3 W) was the instrument light source. The instrument was normally operated with slit widths giving 2.5-5 nm bandpasses and scan speeds of 60 nm/min. Fluorescence measurements in solution were carried out in 10 x 10 mm quartz cells with illumination at 90°. Studies in the solid state were carried out by front surface excitation and detection. Ambient temperature studies were carried out on samples contained in a cell consisting of a circular (0.5 cm diameter) quartz plate pressed against a black metallic holder. The sample orientation was adjusted such that most specular reflections missed the emission monochromator entrance. Low temperature measurements were carried out on powdered and polycrystalline samples contained in a 0.4 ml quartz tube (3 mm i.d.) placed in the cell compartment of a Perkin-Elmer low temperature luminescence accessory. Excitation and detection were also carried out at the front face of the cell. A 340 nm cut-off Corning glass filter was used at the emission filter holder in order to eliminate the second harmonic of the commonly used 337 nm excitation wavelength. Some small and relative sharp peaks were detected in some emission spectra in the region between 400-500 nm. These were identified as originating from scattered light. The intensity of these peaks, however, turned out to be relative small compared with the luminescence intensity being measured and, besides optimizing the cell geometry, no attempts were made to correct the spectra obtained.

REFERENCES.

1. The following is a partial list of some of the most recent review articles on the field of solid state chemistry: (a) Schmidt, G.M.J.,"Solid State Photochemistry", Ginsburgh, D., Ed., Verlag Chemie, New York, **1976**; (b) Ramamurthy, V. and Venkatesan, K., Chem. Rev., **1987**, 87, 433-481; (c) Ramamurthy, V., Tetrahedron, **1986**, 42, 5753; (d) Desiraju, G.R., Endeavour, **1984**, 8, 201; (e) Hasegawa, M., Chem. Rev. **1983**, 83, 507; (f) Thomas, J.M., Morsi, S.E. and Desvergne, J.P., Adv. Phys. Org. Chem., **1977**, 15, 63; (g) Addadi, L., Ariel, S., Lahav, M., Leiserowitz, L., Popovitz-Biro, R. and Tang, C.P. in "Chemical Physics of Solids and their Surfaces", Roberts, M.W., Eds., The Royal Society of Chemistry, London, 1980, Vol. 8, Ch. 7; (h) Gavezzoti, A. and Simmoneta, M., Chem. Rev., **1982**, 82, 1; (i) Cohen, M.D., Angew. Chem. Int. Ed. Engl., **1975**, 14, 386; (j) Scheffer, J.R., Acc. Chem. Res., **1980**, 13, 283; (k) Paul, I.C. and Curtin, D.Y., Acc. Chem. Res., **1973**, 6, 217; (l) McBride, J.M., Acc. Chem. Res., **1983**, 16, 304; (m) Byrn, S.R., "The Solid State Chemistry of Drugs," Academic Press, New York, 1982; (n) Trotter, J., Acta Crys., **1983**, B39, 373.

2. Matsuura, T., Sata, Y. and Ogura, K., Tetrahedron Lett., **1968**, 4627.

3. Appel, W.K., Greenhough, T.J., Scheffer, J.R. and Trotter, J., J. Am. Chem. Soc., **1979**, 101, 213.

4. (a) Quinkert, G., Opitz, K., Wiersdorff, W.W. and Winlich, J., Tetrahedron Lett., **1963**, 1863; (b) Quinkert, G., Tabata, T., Hickman, E.A.J. and Dobrat, W., Angew. Chem., Int. Ed. Engl., **1971**, 10, 199.

5. Wohler, F., Pogg. Ann., **1828**, 12, 253.

6. (a) Markwald, W., Z. Phys. Chem., **1899**, 30, 140; (b) Ciamician, G. and Silber, P., Chem. Ber., **1901**, 34, 2040; (c) Bacher, H. in "Handbucher der Biologishen Arbeitsmethoden," Abderhaldenm E., Ed.,, Urban und Schwarzenberg: Berlin-Vienna, **1929**, Abt. I, Teil 2, p. 1828; (d) For a review accounting for work up to 1952 see: Mustafa, A., Chem. Rev., **1952**, 51, 1.

7. Dunitz, J.D. in "Solid State Photochemistry," Ginsburgh, D., Ed., Verlag Chemie, New York, 1976, p. 255.

8. Kohlshutter, H.W., Z. Anorg. Allg. Chem., **1918**, 105, 121.

9. Cohen, M.D. and Schmidt, G.M.J., J. Chem. Soc., **1964**, 1996-2000.

10. (a) Cohen, M.D., Schmidt, G.M.J. and Sonntag, F.I., ibid., 2000-2013; (b) Schmidt, G.M.J., ibid, 2014-2021; (c) Bregman, J., Osaki, K., Schmidt, G.M.J. and Sonntag, F.I., ibid., 2021-2030.
11. See comment in: Hammett, L.P., "Physical Organic Chemistry," McGraw Hill, New York, 1970, p. 243.

12. March, J., "Advanced Organic Chemistry," John Wiley and Sons, New York, 1985, Ch. 6.

13. Kitaigorodsky, A.I., "Mixed Crystals," Springer Verlag, Berlin, 1984.

14. (a) Hagan, M., "Clathrate Inclusion Compounds," Reinhold, New York, 1962; (b) Tsoucaris, G. in "Organic Solid State Chemistry," Desiraju, G.R., Ed., Elsevier, Amsterdam, 1987, ch. 7.

15. Mandelcorn, L., Ed., "Non-Stoichiometric Compounds," Academic Press, New York, 1964.

16. Atwood, J.L., Davies, J.E.D. and MacNicol, D.D., Eds., "Inclusion Compounds," Academic Press, London, 1984, Vols. 1-3.

17. Cohen, M.D., Tetrahedron, **1987**, 43, 1211.

18. Wegner, G., Pure Appl. Chem., **1977**, 49, 443.

19. (a) Thomas, J.M., Nature, **1981**, 289, 633; (b) Jones, W., Nakanishi, H. and Thomas, J.M., J. Chem. Soc. Chem. Comm., **1980**, 610; (c) Theocharis, C.R. and Jones, W. in "Organic Solid State Chemistry," Desiraju, G.R., Ed., Elsevier, Amsterdam, 1987.

20. Weisinger-Lewin, Y., Vaida, M., Popovitz-Biro, R., Chang, H.C., Manning, F., Frolow, F., Lahav, M. and Leiserowitz, L., Tetrahedron, **1987**, 43, 1449-1475.

21. (a) Paul, I.C. and Curtin, D.Y. in "Organic Solid State Chemistry," Desiraju, G.R., Ed., Elsevier, Amsterdam, 1987; (b) Paul, I.C. and Curtin, D.Y., Science, **1975**, 187, 19-26.

22. Lamartine, R., Bertholon, G., Vincent-Falquet, M.-F. and Perrin, R., Ann. Chim., **1976**, 131-147.

23. Somorjai, A.G., "Chemistry in two Dimensions," Cornell University Press, Ithaca, N.Y., 1981.

24. (a) Holland, H.L. and Richardson, M.F., Mol. Cryst. Liq. Cryst., **1980**, 58, 311; (b) Chenchaiah, P.C., Holland, H.L. and Richardson, M.F., J. Chem. Soc. Chem. Comm., **1982**, 436.

25. (a) Toda, F., Tanaka, K. and Sekikawa, A., J. Chem. Soc. Chem. Comm. **1987**, 279; (b) Patil, A.O., Curtin, D.Y. and Paul, I.C., J.

Am. Chem. Soc., 1984, 106, 348.

26. Miller, R.D., Curtin, D.Y. and Paul, I.C., J. Am. Chem. Soc., 1974, 96, 6340.

27. Parker, R.P. and Smith, J.M., U.S. Patent 2,644,011 (1953).

28. (a) Lamartine, R., Perrin, R., Bertholon, G. and Vincent-Falquet, M.-F., J. Am. Chem. Soc., 1977, 99, 5436-38; (b) Lamartine, R., Perrin, R., Bertholon, G. and Vincent-Falquet, M.-F., Mol. Cryst. Liq. Cryst., 1976, 32, 131-6.

29. Kearsley, S.K. in "Organic Solid State Chemistry," Desiraju, G.R., Ed., Elsevier, Amsterdam, 1987, Ch. 3.

30. Kitaigorodsky, A.I., "Molecular Crystals and Molecules," Academic Press, New York, 1973.

31. Dunitz, J.D., "X-ray Analysis and the Structure of Organic Molecules," Cornell University Press, Ithaca, N.Y., 1979, p. 312-318.

32. Baughman, R.H., J. Chem. Phys., 1978, 68, 3110.

33. (a) McBride J.M., Segmuller, B.E., Hollingsworth, M.D., Mills, D.E. and Weber, B.A., Science, 1986, 234, 830-835; (b) Hollingsworth, M.D. and McBride, J.M., J. Am. Chem. Soc., 1985, 107, 1792-1793; (c) McBride, J.M., Acc. Chem. Res., 1983, 16, 304.

34. Sherwood, J.N. and Thomson, S.J. Trans. Faraday Soc., 1960, 56, 1443. 35. Lazar, M. in "The Chemistry of Peroxides," Patai, S., Ed., John Wiley and Sons, New York, 1983.

36. Ariel, S., Askari, S.H., Scheffer, J.R., Trotter, J. and Walsh, L. in "Organic Phototransformations in Non-Homogeneous Media," Fox, M.A., Ed., ACS Symposium Series No. 278, 1985.

37. Gavezzotti, A., J. Am. Chem. Soc., 1983, 105, 5220-5225.

38. Windsor, M.W. in "Physics and Chemistry of the Organic Solid State," Fox, D., Labes, M.M. and Weissberger, A., Eds., John Wiley, New York, 1965.

39. Birks, J.B., "Photophysics of Aromatic Molecules," Wiley, New York, 1970.

40. Craig, D.P. and Walmsley, S.H., "Excitons in Molecular Crystals," Benjamin, New York, 1968.

41. Powell, R.C. and Soos, Z.G., Luminescence, 1975, 11, 1.

42. (a) Ferguson, J. and Mau, W.-H., Molecular Physics, **1974**, 27, 377-87; (b) Doetschman, D.C. and Hutchison, C.A., J. Chem. Phys., **1972**, 56, 3964-3982.

43. Turro, N.J., "Modern Molecular Photochemistry," Benjamin/Cummins, Menlo Park, Ca., 1978.

44. Lakowics, J.R., "Principles of Fluorescence Spectroscopy," Plennum Press, New York, 1983.

45. Wagner. P.J. in "Creation and Detection of the Excited State," Lamola, A.A., Ed., Marcel Dekker, New York, 1971.

46. (a) Zimmerman, H.E. in "rearrangements in Ground and Excited States," de Mayo, P., Ed., Wiley Interscience, New York, 1980, Ch. 16; (b) Hixson, S.S., Mariano. P.S. and Zimmerman, H.E., Chem. Rev., **1973**, 73, 531-555.

47. Zimmerman, H.E. and Grunewald, G.L., J. Am. Chem. Soc., **1966**, 88, 123 (b) Zimmerman, H.E., Binkley, R.W., Givens, R.S. and Sherwin, M.A., J. Am. Chem. Soc., **1967**, 89, 3932.

48. Paquette, L.A. and Bay, E., J. Am. Chem. Soc., **1984**, 106, 6693-6701; (b) Paquette, L.A., Varadarajan, A. and Burke, L., J. Am. Chem. Soc., **1986**, 108, 8032-39; (c) Paquette, L.A. and Burke, L., J. Org. Chem., **1989**, 52, 2674-2679.

49. (a) Srinivasan, R., in "Advances in Photochemistry," John Wiley, New York, 1966, Vol. 4., p. 113-42; (b) Mousseron, M. in "Advances in Photochemistry," John Wiley, New York, 1966, Vol. 4., p. 195-224.

50. Woodward, R.B. and Hoffman, R., "The Conservation of Orbital Symmetry," Verlag Chemie, Wienheim, 1970.

51. Saltiel, J., D'Agostino, J. Megarity, E.D., Metts, L. Neuberger, K.R., Wrighton, M. and Zefiriov, O.C. in "Organic Photochemistry," Chapman, O.L., Ed., Marcel Dekker, New York, 1973, Vol. 3.

52. (a) Zimmerman, H.E. and Epling, G.A., J. Am. Chem. Soc., **1970**, 92, 1406; (b) Swenton, J.S., Crumrine, A.L. and Walker, T.S., J. Am. Chem. Soc., **1970**, 1406.

53. Zimmerman, H.E. and Pratt, A.C., J. Am. Chem. Soc., **1970**, 92, 1409 and 6259.

54. Zimmerman, H.E. and Samuelson, G.E., J. Am. Chem. Soc., **1969**, 91, 5307; ibid, **1967**, 89, 5971.

55. (a) Griffin, G.W., Marcantonio, A.F. Kristinsson, H., Tetrahedron Lett., **1965**, 2951; (b) Zimmerman, H.E. and Klun, R.T., Tetrahedron, **1978**, 34, 1775; (c) Zimmerman, H.E., Gruenbaum, W.T., Klun, R.T., Steinmetz, M.G. and Welter, T.R. J. Chem. Soc. Chem. Comm., **1978**, 228.

56. Diels, O. and Alder, K., Justus Liebigs Ann. Chem., **1931**, 486, 191-202.

57. (a) Hilditch, T.P., Proc. Chem. Soc., **1904**, 27, 6; (b) Hilditch, T.P., J. Chem. Soc., **1904**, 99, 224-39.

58. Lauer, W.M. and Gensler, W.J., J. Am. Chem. Soc., **1945**, 67, 1171.

59. Wilcox, F.C. and Craig, A.C., J. Org. Chem., **1961**, 26, 1491-4.

60. Heller, E. and Schmidt, G.M.J., Isr. J. Chem., **1971**, 9, 449.

61. Bart, J.C.J. and Schmidt, G.M.J., Isr. J. Chem., **1971**, 9, 429-48.

62. Silverstein, R.M., Bassler, G.C. and Morril, T.C., "Spectrometric Identification of Organic Compounds," 4th Ed., John Wiley & Sons, New York, 1981.

63. Wireko, F. and Trotter, J., Unpublished Results.

64. Figueys, H.P. and Dralanis, A., Tetrahedron, **1972**, 28, 3031.

65. Ciganek, E., J. Am. Chem. Soc., **1966**, 88, 2882-2883.

66. (a) Brewer, J. and Heaney, H., J. Chem. Soc. Chem. Comm., **1967**, 811; (b) Rabideau, P.W., Hamilton, J.B. and Friedman, L., J. Am. Chem. Soc., **1968**, 90, 4466.

67. Hemetzberger, H., Holstein, W. and Werres, F., Tetrahedron, **1983**, 39, 1151-1160.

68. Chang, H.C., Popovitz-Biro, R., Lahav, M. and Leiserowitz, L., J. Am. Chem. Soc., **1987**, 109, 3883-3893.

69. (a) Scheffer, J.R. and Trotter, J., Rev. Chem. Intermed., **1988**, 9, 271-305; (b) Scheffer, J.R. in "Organic Solid State Chemistry," Desiraju. G.R., Ed. Elsevier, Amsterdam, 1987.

70. Quenemoen, K., Borden, W.T., Davidson, E.R. and Feller, D., J. Am. Chem. Soc., **1985**, 107, 5054-5059.

71. Demuth, M., Amrein, W., Bender, C.O., Braslavsky, S.E., Burger, U., George, M.V., Lemmer, D. and Shaffner, K., Tetrahedron, **1981**, 19, 3245-3261.

72. Pokkuluri, P., M. Sc. Thesis, University of British Columbia.

73. (a) Bowen, E.J., Nature, **1944**, 153, 653; Ferguson, J., Aust. J. Chem., **1956**, 9, 160.

74. Frenkel, J.I., Phys. rev., **1931**, 37, 1276.

75. Johns, H.E. in "Creation and Detection of the Excited State," Lamola, A.A., Ed., Marcel Dekker, New York, 1971, Ch. 3.

76. Wan, J.K.S., McCormick, E.J., Baum. E.J. and Pitts, J.N., J. Am. Chem. Soc., 1965, 87, 4409-5515.

77. McCrone, W.C. in "Physics and Chemistry of the Organic Solid State," Fox, D., Labes, M.M. and Weissberger, A., Eds., John Wiley, New York, 1965.

78. Eliel, E., "Stereochemistry of Carbon Compounds," McGrow-Hill, New York, 1962.

79. Dewar, M.J.S., J. Am. Chem. Soc., **1952**, 74, 3341.

80. (a) George, W.O., Hassid, D.V., Harris, W.C. and Maddams, W.F., J. Chem. Soc. Perkins II, **1974**, 392-396; (b) Compton, D.A.C, George, W.O. and Porter, A.J., J. Chem. Soc. Perkins II, **1974**, 400-404.

81. Schweizer, W.B. and Dunitz, J.D., Helv. Chim. Acta, **1982**, 65, 1547.

82. Bernstein, J. in "Organic Solid State Chemistry," Desiraju, G.R., Ed., Elsevier, Amsterdam, 1987.

83. Corradini, P., Chim. Ind., **1973**, 55, 122.

84. (a) Gaultier, J., Hauw, C. and Bouas-Laurent, H., Acta Cryst., **1976**, B32, 1220; (b) Becker, H.-D., Hall, S.R., Skelton, B.W. and White, H.H., Aust. J. Chem., **1984**, 37, 1313.

85. Kitaigorodsky, A.I., "Organic Chemical Crystallography," Consultants Bureau, New York, 1961.

86. Fletton, R.A., Lancaster, R.W., Harris, R.K., Kenwright, A.M., Packer, K.J., Waters, D.N. and Yeadon, A., J. Chem. Soc., Perkins II, **1986**, 1705-1709.

87. (a) Ferguson, L.N. "Organic Molecular Structure," Willard Grant Press, Boston, 1975; (b) Ingraham, L.L. in "Steric Effects in Organic Chemistry," Newman, M.S., Ed., John Wiley and Sons, New York, 1956.

88. Ariel, S., Scheffer, J.R., Trotter, J. and Wong, Y.-F., Tetrahe-

dron Lett., 1893, 42, 4555-4558.

89. Harris, K.R., "Nuclear Magnetic Resonance Spectroscopy," Pitman Publishing Co., London, **1983**, Ch. 6.

90. (a) Evans, S.V., Omkaram, N., Scheffer, J.R. and Trotter, J., Tetrahedron Lett., **1986**, 27, 1419; (b) Nakanishi, H., Veno, K. and Sasada, Y., Acta Cryst., **1976**, B32, 3352; (c) Lewis, T.W., Curtin, D.Y. and Paul, I.C., J. Am. Chem. Soc., **1979**, 101, 5717-5726.

91. Jaffe, A.B., Skinner, K.J. and McBride, J.M., J. Am. Chem. Soc., **1972**, 94, 8510.

92. (a) Scheffer, J.R. and Garcia-Garibay, M. in "Photochemistry on Solid Surfaces," Matsura, T. and Anpo, M., Eds., Elsevier, Amsterdam, in Press; (b) Green, B.S., Lahav, M. and Ravinobich, D., Acc. Chem. Res., **1979**, 12, 191-197; (c) Green, B.S. and Lahav, M., J. Mol. Evol., **1975**, 6, 99-115.

93. Jacques, J., Collet, A. and Wilen, S.H., "Enantiomers Racemates and Resolutions," Wiley Interscience, New York, 1983.

94. Buerger, M.J., "Elementary Crystallography," Wiley, New York, 1963, p. 199-457.

95. Mighell, A.D. and Himes, V.L., Acta Cryst., **1983**, 39A, 737-740.

96. (a) Pincock, R.E. and Wilson, K.R., J. Am. Chem. Soc., **1971**, 93, 1291-1292; (b) Pincock, R.E., Perkins, R.R., Ma, A.S. and Wilson, K.R., Science, **1971**, 174, 1018-1020.

97. Havinga, E., Biochim. Biophys. Acta, **1954**, 13, 171-164.

98. Newman, A.C.D. and Powell, H.M., J. Chem. Soc., **1952**, 3747-3751.

99. Markwald, W., Ber., **1904**, 37, 1368.

100. (a) Morrison, J.D. and Mosher, H.S., "Asymmetric Organic Reactions," American Chemical Society, Washington, D.C., 1976; (b) Morrison, J.D., Ed., "Asymmetric Synthesis," Academic Press, New York, 1983, Vol. 1-5; (c) Kagan, H.B. and Fiaud, J.C., Top. Stereochem., **1978**, 10, 175-285.

101. Seebach, D., Imwinkelried, R. and Weber, T. in "Modern Synthetic Methods 1986," Scheffold, R., Ed., Springer-Verlag, Berlin, 1986.

102. Izumi, Y. and Tai, A., "Stereo-Differentiating Organic Reactions," Academic Press, New York, 1977.

103. Horner, L., Siegel, H., Buthe, H., Angew. Chem. Int. Ed. Engl.,

1968, **7**, 942.

104. (a) Seebach, D., Dorr, H., Bastani, B. and Ehrig, V., Angew. Chem. Int. Ed. Engl., **1975**, 14, 634-636; (Seebach, D. and Oei, H.-A., Angew. Chem. Int. Ed. Engl., **1975**, 14, 634-636.

105. (a) Gerdil, R. "Tri-o-Thymothide Clathrates," Topics in Current Chemistry, Vol. 140, Springer-Verlag, Heidelberg, 1987, p.71-105; (b) Toda, F., Tanaka, K. and Oda, M., Tetrahedron Lett., **1988**, 29, 653-654; (c) Toda, F., Tanaka, K. and Yagi, M., Tetrahedron, **1987**, 43, 1495.

106. Rau, H., Chem. Rev., **1986**, 83, 175-185.

107. (a) Barron, L.D., Chem Soc. Rev., **1986**, 16, 189-223; (b) Barron, L.D., J. Am. Chem. Soc., **1986**, 108, 5539-5542.

108. Ostromisslensky, I., Chem. Ber., **1908**, 41, 3035-3046.

109. Farina, M., Audisio, G. and Natta, G., J. Am. Chem. Soc., **1967**, 89, 5071.

110. Penzien, K. and Schmidt, G.M.J., Angew. Chem., Int. Ed. Engl., **1969**, 8, 608-609.

111. Green, B.S., Lahav, M. and Schmidt, G.M.J., Mol. Cryst. Liq. Cryst., **1975**, 29, 187-200.

112. (a) Elgavi, A., Green, B.S. and Schmidt, G.M.J, J. Am. Chem. Soc., **1973**, 85, 2058-59; (b) Addadi, L. and Lahav, M., Pure Appl. Chem., **1979**, 51, 1269-1284; (c) Addadi, L., Van Mil, J. and Lahav, M., J. Am. Chem. Soc., **1982**, 104, 3422-3427; (d) Addadi, L., Ariel, S., Lahav, M., Leiserowitz, L., Popovitz-Biro, R. and Tang, C.P. in "Chemical Physics of Solids and their Surfaces," Roberts, M.W. and Thomas, J.M., Eds., The Royal Society of Chemistry, London, 1980, Specialist Periodical Reports, Vol. 8., Ch. 7.

113. Sullivan, G.R., Topics in Stereochem., **1978**, 10, 287-329.

114. It is known that optical purity, which is measured by polarimetry, is not always identical to the enantiomeric purity measured by some other analytical techniques: Horeau, A., Tetrahedron Lett., **1961**, 3132.

115. Evans, S.V., Garcia-Garibay, M., Omkaram, N., Scheffer, J.R., Trotter, J.R. and Wireko, F., J. Am. Chem. Soc., **1986**, 108, 5648-5650.

116. Scheffer, J.R., Trotter, J., Garcia-Garibay, M. and Wireko, F., Mol. Cryst. Liq. Cryst., **1988**, 156, 63-84.

117. Cahn, R.S., Ingold, C. and Prelog, V., Angew. Chem., Int. Ed. Engl., **1966**, 5, 385-415.

118. Bijvoet, J.M., Peederman, A.F. and Van Bommel, J.A., Nature, **1951**, 168, 271-272.

119. (a) Allen, F.H., Acta Cryst., **1981**, B37, 890; (b) Allen, F.H., Acta Cryst., **1980**, B36, 81.

120. (a) Walker, D.C., Ed., "Origins of Optical Activity in Nature," Elsevier, New York, 1979; (b) Brewster, J.H., J. Chem. Ed., **1986**, 63, 667-70; (c) Ellias, W.E., J. Chem. Ed., **1972**, 49, 448-454; (d) Albernethy, J.L., J. Chem. Ed., **1972**, 49, 455-461.

121. See references 96a and 112c.

122. (a) Havinga, E., Chem. Weekblad., **1941**, 38, 642 (C.A. **1942**, 36, 5790); (b) Fock, A., Z. Kryst., **1902**, 35, 399.

123. For an excellent discussion of Pasteur's work with sodium ammonium tartrate see: Fieser, L. and Fieser, M., "Advanced Organic Chemistry," Reinhold, New York, 1961, p. 69.

124. Iwamura, M., Takada, H. and Iwamura, H., Tetrahedron Lett., **1980**, 4865.

125. Hemetsberger, H. and Nobbe, M., Tetrahedron, **1988**, 44, 67-80.

126. (a) Winnik, M.A., Org. Mass. Spectrom., **1974**, 9, 920-951; (b) Tam, S.W. in "The Chemistry of Acid Derivatives," Supplement B, Part I, Patai, S., Ed., John Wiley & Sons, New York, 1979, Ch. 4.

127. Deutsh, J. and Mandelbaum, A., J. Am. Chem. Soc., **1970**, 92, 4288.

128. Taft, R.W. in "Steric Effects in Organic Chemistry," Newman, M.S., Ed., Wiley, New York, 1956, Ch. 13.

129. Gray, G.W., Ed., "Steric Effects in Conjugated Systems," Butterworths Scientific, London, 1958.

130. Paddick, R.G., Richards, R.G. and Wright, G.J., Aust. J. Chem., **1976**, 29, 1005-15.

131. A recent example of this approach can be found in: Baldwin, S.W. and Mazzuckelli, T.J., Tetrahedron Lett., **1986**, 27, 5975-5978.

132. See reference 87.

133. Jarvis, B.B., Gavoni, J.P. and Zell, P.J., J. Am. Chem. Soc., **1971**, 93, 913-918.

134. Cristol, S.J. and Hager, J.W., J. Org. Chem., **1983**, 48, 2005-2007.

135. (a) Dhami, K.S. and Stothers, J.B., Tetrahedron Lett., **1964**, 12, 631-639; (b) Dhani, K.S. and Stothers, J.B., Can. J. Chem., **1965**, 43, 479-497.

136. (a) Delseth, C., Nguyen, T.-T. and Kintzinger, J.-P., Helv. Chim. Acta, **1980**, 63, 498-475; (b) Baumstark, A.L., Balakrishan, P., Dotrong, M., McCloseky, C.J., Oakley, M.G. and Boyikin, D.W., J. Am. Chem. Soc., **1987**, 109, 1059-1062.

137. (a) Burket, U. and Allinger, N.L., "Molecular Mechanics," American Chemical Society: Washington, 1982; (b) Osawa, E. and Musso, H. in "Topics in Stereochemistry," Allinger, N.L., Eliel, E.L. and Wilen, S.H., Eds., Wiley, New York, 1982, p. 117; (c) The program used was MMPMI by Gilbert, K.E. and Gajewski, J.J., Serena Software, Bloomington, Indiana.

138. (a) Seeman, J.J., Chem. Rev., **1983**, 83, 83-133; (b) Lewis, F.D., Johnson, R.W., J. Am. Chem. Soc., **1972**, 94, 8914-16.

139. Stern, O. and Volmer, M., Physik. Z., **1919**, 20, 183.

140. Ingraham, L.L. in "Steric Effects in Organic Chemisytry," Newman, M.S., Ed., John Wiley and Sons, New York, 1956, Ch. 11.

141. von Rague Schleyer, P., Pure Appl. Chem., **1987**, 1647-1660.

142. Shorter, J., Quart. Rev., **1970**, 24, 433-453.

143. Trotter, J. and Wireko, F., Unpublished Results.

144. (a) Gavezzotti, A. in "Organic Solid State Chemistry," Desiraju, G.R., Ed., Elsevier, Amsterdam, 1987.

145. (a) Meyer, A.Y., J. Chem. Soc., Perkins II, **1985**, 1161-1169; (b) Meyer, A.Y., J. Chem. Soc., Perkins II, **1986**, 1567-1572.

146. Allinger, N.L., Adv. Phys. Org. Chem., **1976**, 13, 1.

147. Hagler, A.T., Huler, E. and Lifson, S., J. Am. Chem. Soc., **1974**, 96, 5319-5327.

148. Craig, D.P., Lindsay, R.N., Mallet, C.P., Markey, B.R., Chem. Phys., **1983**, 79, 9.

149. Roozeboom, H.W.B., Z. Phys. Chem., **1899**, 28, 494.

150. Simpson, H.J. and March, R.E, Acta Cryst., **1966**, 20, 550.

151. Bondi, A., J. Phys. Chem., **1964**, 68, 441.

152. Garcia-Garibay, M., Scheffer, J.R., Trotter, J. and Wireko, F., Tetrahedron Lett., **1987**, 41, 4789-4792.

153. Green, B.S., Arad-Yellin, R. and Cohen, M., Topics in Sterochem., **1986**, 16, 131-218.

154. Hadjoudis, E., Vittorakis, M. and Moustakali-Mavridis, I., Tetrahedron, 43, 2345-2360.

155. (a) Porter, G. and West, M.A. in "Investigation of the Rates Mechanisms of Reaction," Techniques of Chemistry, Vol. 6, Part II, Ch. 10, Wiley Intersinece, New York, 1974: (b) Bensasson, R.V., Land, E.J. and Truscott, T.G., "Flash Photolysis and Pulse Radiolysis; Contributions to the Chemistry of Biology and Medicine," Pergamon Press, Oxford, 1983. 156. Small, R.D. and Scaiano, J.C., J. Phys. Chem., **1977**, 81, 828.

157. Trozzolo, A.M. and Gibbons, W.A., J. Am. Chem. Soc., **1967**, 89, 239-243.

158. Wilkinson, F. and Willsher, C.J., Tetrahedron, **1987**, 43, 1197-1210.

159. Rabeck, J.F. in "Experimental Methods in Photochemistry and Photophysics," Part 2, Ch. 23, Wiley, New York, 1982.

160. Longworth, J.W. in "Creation ans Detection of the Excited State," Lamola, A.A., Ed., Marcel Dekker, New York, 1971, Vol. I, Part A, Ch. 7. p. 343-374.

161. See Reference 43.

162. (a) Birks, J.B., Rep. Prog. Phys., **1975**, 38, 903; (b) Stevens, B. Adv. Photochem., **1971**, 8, 161.

163. Cohen, M.D., Ludmer, Z. and Yakhot, V., Phys. Status Solidi, **1975**, B67, 57.

164. Chandross, E.A. and Ferguson, J., J. Chem. Phys., **1966**, 45, 3554-3564 and 3564-3567.

165. Cohen, M.D., Ludmer, A. and Yakhot, V., Chem. Phys. Lett., **1976**, 38, 398-400.

166. Ferguson, J. and Mau, A.W.-H., Molecular Physics, **1974**, 27, 377-387.

167. Platz, M.S. in "Diradicals," Borden, W.T., Ed., John Wiley and Sons, New York, 1982, Ch. 5, p. 195-258.

168. Adam, W., De Lucchi, O., Peters, K., Peters, E.-M. and von Schnering, H.G., J. Am. Chem. Soc., **1982**, 194, 5747-5753.

169. Sheridan, R.S. in "Organic Photochemistry," Padwa, A., Ed., Marcel Dekker, New York, 1987, Vol. 8., 159-248.

170. Closs, G., Hutchison, C.A. and Kohler, B.E., J. Chem. Phys., **1966**, 44, 413.

171. Hutchison, C.A. and Doetschman, D.C., J. Chem. Phys., **1972**, 56, 3964-3982.

172. (a) Walter, D.W. and McBride, J.M., J. Am. Chem. Soc., **1981**, 103, 7069-7073; (b) Walter, D.W. and McBride, J.M., J. Am. Chem. Soc., **1981**, 103, 7074-7084.

173. Johnston, L. and Scaiano, J.C., J. Am. Chem. Soc., **1986**, 108, 2349-2353.

174. Small, R.D. and Scaiano, J.C., Chem. Phys. Lett., **1977**, 50, 431-434.

175. Lutz, H., Breheret, E. and Lindqvist, L., J. Phys. Chem., **1973**, 77, 1758-1762.

176. Effio, A., Griller, D., Ingold, K.U, Scaiano, J.C. and Sheng, S.J., J. Am. Chem. Soc., **1980**, 102, 6063-6068.

177. Sheng, S.J., J. Phys. Chem., **1978**, 82, 442-444.

178. Ono, Y, Ikeshoji, T. and Mizuno, T., Chem. Phys. Lett., **1975**, 451-454.

179. Hiratzuka, H., Okamura, T, Tanaka, I. and Tanizaki, Y., J. Phys. Chem., **1980**, 84, 285-289.

180. Bromberg, A. and Meisel, D., J. Phys. Chem., **1985**, 89, 2507-2513.

181. Cristol, S.J., Kaufman, R.L., Opitz, S.M., Szalecki, W. and Bindel, T.H, J. Am. Chem. Soc., **1983**, 105, 3226-34.

182. Wagner, P.J., J. Am. Chem. Soc., **1967**, 89, 5898-5901.

183. Perrin, D.D., Armarego, W.L.F., Perrin, D.R., "Purification of Laboratory Chemicals," Pergamon Press, Oxford, 1980.

184. Encina, M.V., Lissi, E.A., Lemp, E., Zanocco, A. and Scaiano, J.C., J. Am. Chem. Soc., **1983**, 105, 1856-1860.

PUBLICATIONS

1. S.V. Evans, M. Garcia-Garibay, N. Omkaram, J.R. Scheffer, J. Trotter, and F. Wireko. Use of Chiral Single Crystals to Convert Achiral Reactants to Chiral Products in High Optical Yield: Applications to the Di-π-Methane and Norrish Type II Photorearrangements. J. Am. Chem. Soc., 108, 5648 (1986).

2. M. Garcia-Garibay, J.R. Scheffer, J. Trotter, and F. Wireko. Triplet Energy Sensitization of a Crystalline Phase Photorearrangement. Tetrahedron Lett., 28, 1741 (1987).

3. J.R. Scheffer, M. Garcia-Garibay, and O. Nalamasu. The Influence of the Molecular Crystalline Environment on Organic Photorearrangements. Organic Photochemistry, A. Padwa, Ed., Marcel Dekker, Inc., Vol. 8., Ch. 4 (1987)

4. M. Garcia-Garibay, J.R. Scheffer, J. Trotter, and Fred Wireko. Generation of Optical Activity Through Solid Reaction of a Racemic Mixture that Crystallizes in a Chiral Space Group. Tetrahedron Lett. 28, 4789 (1987).

5. M. Garcia-Garibay, J.R. Scheffer, J. Trotter, and F. Wireko. Addition of Bromine Gas to Crystalline Dibenzobarrelene: An Enantioselective Carbocation Rearrangement in the Solid State. Tetrahedron Lett. 29, 1485 (1988).

6. M. Garcia-Garibay, J.R. Scheffer, J. Trotter and F. Wireko. Intermolecular Steric Effects on Unimlecular Rearrangements in Crystalline Media. Tertahedron Lett. 29, 2041 (1988).

7. J.R. Scheffer, J. Trotter, M. Garcia-Garibay and F. Wireko. Studies on the Di-π-Methane Photorearrangement in the Solid Sate. Mol. Cryst. Liq. Cryst. Inc. Nonlin. Opt. 156, 63 (1988).

8. S. Ariel, S. Evans, M. Garcia-Garibay, B.R. Harkness, N. Omkaram, J.R. Scheffer, and J. Trotter. The Generation of 1,3-Biradicals in Rigid Media: Crystal Structure-Solid State Reactivity Correlations. J. Am. Chem. Soc. 110, 5591 (1988).

9. J.R. Scheffer and M. Garcia-Garibay. Absolute Asymmtric Synthesis via Photochemical Reactions in Chiral Crystals. Photochemistry on Solid Surfaces. T. Matsuura and M. Anpo, Eds. Elsevier, Amsterdam, in Press.

10. S. Ariel, M. Garcia-Garibay, J.R. Scheffer, and J. Trotter. Crystal Structure of A Cyclization Product of 1-(4-Chlorophenyl)-2-Cyclooctyl-ethanone and Reaction Pathway in Norrish Type II Cyclization. Acta Crystallog., in Press.